ISSN 0236-2945

LIGHT & ENGINEERING

Volume 27, Number 2, 2019

Editorial of Journal
"Light & Engineering" (Svetotekhnika), Moscow

Lou Bedocs

March 1942 – February 2019

After a serious illness at the age of 77, a distinguished lighting technician, the largest figure in international standardization in the field of lighting engineering, Mr. Lou Bedocs died. Lou was a former Technical Director of Thorn Lighting Limited and the manager of the Thorn Lighting Technology Centre (Spennymoor, England). He was also a permanent active member of the international editorial board of our journal Light & Engineering (since 1993).

Lou (his real name is Lajos) was born in Hungary and after the long twists and turns of the post-war period and the events of the year 1956 in Hungary, he landed in England, where he finished his education and graduated from Malvern Chase Secondary School. Thanks to exceptional energy, inexhaustible optimism and great curiosity, he found work at the leading lighting company Thorn Lighting Limited (from 1957).

Since then, he has been interested in lighting engineering which became the work of his life, 60 years of which Lou gave to successful work at Thorn Lighting Limited. Mr. Lou Bedocs creatively and actively collaborated with many international organizations (ISO, CEN, BSI, CIE, CLL, Lux-Europe). He was awarded a number of Gold and Silver medals for research work. He also led the work on the preparation of a number of important European standards.

Not only a great specialist and public figure has left us, a wonderful, open and kind person has gone, whose memory will remain forever in our hearts and souls.

The members of the editorial board of the Svetotekhnika/ Light & Engineering Journal, including the ones who knew the deceased well, and Julian Aizenberg, Peter Thorns, and Raisa Stolyarevskaya who communicated and collaborated with him for many years

Journal “Light & Engineering” had been founded by Prof. Julian B. Aizenberg in 1993

LIGHT & ENGINEERING

СВЕТО ТЕХНИКА

Editorial of Journal “Light & Engineering/Svetotekhnika”

Moscow, 2019

Editorial Office:

Russia, VNISI, Rooms 327 and 334
106 Prospekt Mira, Moscow 129626

Tel: +7.495.682.26.54
Tel./Fax: +7.495.682.58.46
E-mail: lights-nr@inbox.ru
http://www.l-e-journal.com

Light & Engineering" is an international scientific Journal subscribed to by readers in many different countries. It is the English edition of the journal "Svetotekhnika" the oldest scientific publication in Russia, established in 1932.

Establishing the English edition "Light and Engineering" in 1993 allowed Russian illumination science to be presented the colleagues abroad. It attracted the attention of experts and a new generation of scientists from different countries to Russian domestic achievements in light and engineering science. It also introduced the results of international research and their industrial application on the Russian lighting market.

The scope of our publication is to present the most current results of fundamental research in the field of illumination science. This includes theoretical bases of light source development, physiological optics, lighting technology, photometry, colorimetry, radiometry and metrology, visual perception, health and hazard, energy efficiency, semiconductor sources of light and many others related directions. The journal also aims to cover the application illumination science in technology of light sources, lighting devices, lighting installations, control systems, standards, lighting art and design, and so on.

"Light & Engineering" is well known by its brand and design in the field of light and illumination. Each annual volume has six issues, with about 80–120 pages per issue. Each paper is reviewed by recognized world experts.

To promote the work of the Journal, the editorial staff is in active communication with Thomson Scientific (Citation index) and other international publishing houses and agencies, such as Elsevier and EBSCO Publishing.

CONTENTS

VOLUME 27 **NUMBER 2** **2019**

LIGHT & ENGINEERING

Light & Engineering
Vol. 27, No. 2, pp. 4–22, 2019 *https://doi.org/10.33383/2019-011*

REVIEW OF THE CURRENT STATE AND FUTURE DEVELOPMENT IN STANDARDISING ARTIFICIAL LIGHTING

Peter Thorns

Thorn Lighting Ltd.
E-mail: Peter.Thorns@zumtobelgroup.com

"It is with gratitude that I dedicate this paper to the memory of Lou Bedocs. Lou was a mentor throughout much of my professional life and also a good friend. He helped me write my first ever research report and collaborated with me on a number of research projects. He encouraged my involvement in the world of standards and regulations and was always ready to give help or guidance."

ABSTRACT

This paper discusses the organisations involved in the development of application standards, European regulations and best practice guides, their scope of work and internal structures. It considers their respective visions for the requirements for future standardisation work and considers in more detail those areas where these overlap, namely human centric or integrative lighting, connectivity and the Internet of Things, inclusivity and sustainability.

Keywords: artificial lighting, standardisation, application requirements, regulatory body, IoT

1. INTRODUCTION

When considering artificial lighting there are two main areas of standardisation, product requirements and application requirements. Product requirements are predominantly concerned with safety and performance whilst application requirements consider what criteria need to be satisfied when using a product within a lighting installation. This paper shall predominantly focus on the work of standardisation of application requirements.

As the development of standards may be performed to address specific regulatory requirements from an individual state such as the United Kingdom or Russia, or from a wider political body such as the European Union, there can also be close links between standards organisations and regulatory bodies. For instance the documents EN15193–1:2017 [1] and PD CEN TR15193–2:2017 [2] were developed under a European Union Mandate to support the European Energy Performance of Buildings Directive [3].

Professional and trade associations can also help drive the standardisation process as they develop concepts regarding best practice and solutions that provide more functions. They also tend to provide a large number of the experts working within standards development.

Fig. 1. Inter-relationships and inputs to standardisation

However standards need a solid scientific basis, and therefore make use of papers presented in academic journals and technical conferences. The academic input in terms of new research helps guide standards development to define/refine established best practice.

Therefore the standardisation landscape can be quite complex and confusing when viewed from the outside, Fig. 1.

Who works within these structures and organisations in developing standards and who they represent can be difficult to appreciate and can change depending upon the organisation they are a member of and their role within the organisation.

However within this arena, much valued work is produced to help guide lighting professionals in best practice.

2. STRUCTURES AND REPRESENTATIVES

At an international level standardisation is generally performed within the International Electrotechnical Commission (IEC) for product standards and the International Organization for standardisation (ISO) for application standards. Within Europe these equate to CENELEC for product standards, the European Committee for Electrotechnical Standardisation, and CEN for application standards, the European Committee for Standardisation.

International standards may also be produced by other organisations such as the International Commission on Illumination (CIE) or less formally by various industry consortia such as Zhaga, a global lighting-industry organisation that aims to standardise components of LED luminaires.

These organisations can roughly be split into four categories;

- Professional societies which generally concern a specific discipline and further the interests of professionalism within that discipline and their members.
- Trade associations and industry consortia which generally represent the interests of a specific industry with respect to standards and regulations and may also develop the market potential for that industry.
- Standards bodies, which develop technical standards giving requirements based upon good practice and acceptance.
- Law making or regulatory bodies such as governments who enact laws to enforce safety and standards and protect consumers.

When working across these organisations a person may be representing themselves, their employers or their country as shown in Fig. 2.

So within professional societies a person generally acts as an individual, unless they have a formally appointed position, in which case they tend to represent the society; within industry associations a person tends to represent a company; and within standards bodies they tend to represent a country. It is difficult for a person from academia or industry to be directly involved in law-making although they can influence the process through lobbying and informing politicians and government organisations on what is good practice and practicably achievable.

	Societies	Associations	Standards	Laws and directives
World	CIE	WTO	ISO, IEC	UN
Continents	IESNA, CIEChina, IESAustralia	NEMA CCI AMF	ANSI, ASTM CCC ASI..	Federal Governments
European	(Lux Europa)	LightingEurope	CEN, CENELEC	EU
National, in each country, f.e.	LiTG, SLL, ILP, LTG, SLG, AFE, NsVV, ...	ZVEI, FEEI, LIA, SdIE	DIN, BSI, ON, AFNOR, SNI,	National laws f.e. Building regulations, EnEV, ...
Representation	Dedicated lighting experts	Companies lighting experts	Appointed national delegates	Politicans, lobbyists

Fig. 2. National and International organisations and representation

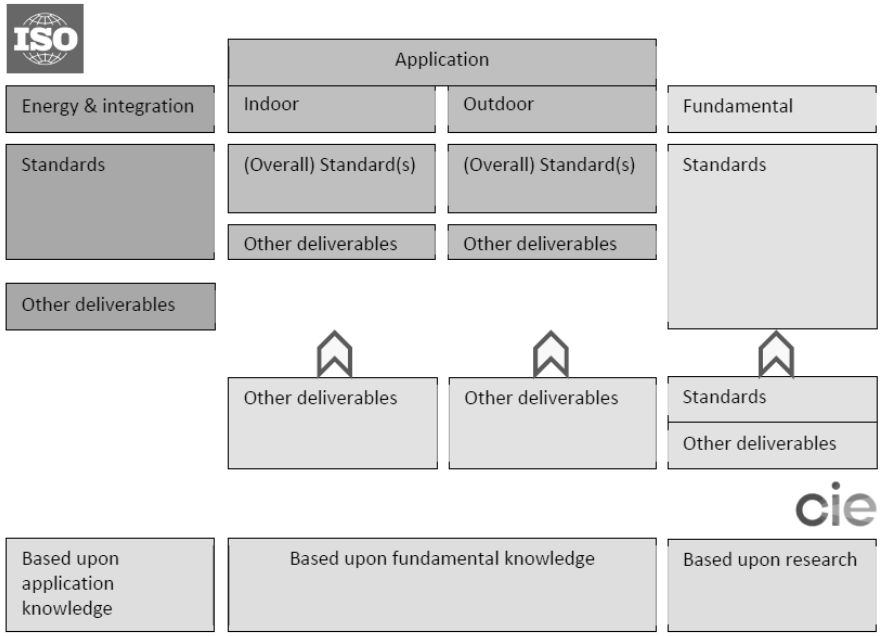

Fig. 3. Visualisation of horizontal cooperation between ISO/TC274 and CIE in lighting [36]

To help coordinate work between committees and organisations formal liaison arrangements may be agreed, and in this case a person will represent the organisation they are liaising for. So, for example, a liaison officer for ISO/TC274 to the CIE would represent ISO/TC274 within the CIE.

National standards bodies, such as BSI, will shadow the standards work, being performed at an international level, propose national experts to help in the work and submit comments on proposed work items and draft documents. They will also vote on the acceptance of documents submitted for approval and publication. For example, BSI shadows the work being performed within CEN/CENELEC and also ISO/IEC.

Each of these categories and their component organisations are considered below.

3. STANDARDS ORGANISATIONS

3.1. ISO/TC274: Light and Lighting

At the level of international standardisation ISO/TC274 is the main technical committee with a scope of standardisation in the field of application of lighting. It is a relatively new technical committee, previously at ISO level lighting was considered as a factor within a diverse set of technical committees producing non lighting specific standards. For example, lighting was considered within the work of ergonomics standardisation committees. To ensure lighting was considered correctly by dedicated lighting experts, and that the chain of national shadow committees commenting and voting on lighting related standards corresponded correctly, the topic of lighting was centralised within ISO/TC274. It works closely with the International Commission on Illumination (CIE) and coordinates work programs. This cooperation results in three possible routes for new work items depending upon the level of cooperation that is considered relevant:

- Informative relation – One organization is fully entrusted with a specific work item and keeps the other fully informed of all progress.
- Collaborative relation – One organization takes the lead in the activities, but the work sessions and meetings may receive delegates from the other organisation who have observer status and who ensure the technical liaison with the other organization. These delegates may also make written contributions were considered appropriate during the progress of this work.
- Integrated liaison – Joint Working Groups ensure integrated meetings for handling the realisation of standards under a principle of total equality of participation.

This is visualised in Fig. 3, taken from the Strategic Business plan of ISO/TC274, where the work of CIE is identified as concerning fundamental knowledge and based upon research whereas the work of

ISO/TC274 is based upon application knowledge. Joint standards use both of these areas of expertise in their development.

ISO/TC274 is responsible for the existing standards:

- ISO 8995–1:2002 Lighting of work places – Part 1: Indoor;
- ISO/CIE 8995–3:2018 Lighting of work places – Part 3: Lighting requirements for safety and security of outdoor work places;
- ISO 30061:2007 Emergency lighting.

At the time of writing this paper ISO/TC274 has four standards, technical specifications or reports under development as work items:

- *ISO/CIE FDIS20086* Light and lighting – Energy performance of lighting in buildings. This draft standard specifies the methodology for evaluating the energy performance of lighting systems for providing general illumination inside non-residential buildings and for calculating or measuring the amount of energy required or used for lighting inside buildings. It is closely related to EN15193–1:2017[1];
- *ISO/WD TR21783* Light and lighting – Integrative lighting – Non-visual effects. This draft Technical Report shall include a summary of the published scientific studies on non-visual effects of light on humans, plus an evaluation of related material that is suitable for use in practice or an indication where more knowledge and validation is necessary for safe and beneficial lighting applications;
- *ISO/CIE PRF TS22012* Light and lighting – Maintenance factor determination – Way of working. This draft Technical Specification specifies a standardised way of working for determining the maintenance factor for both outdoor and indoor lighting installations using the methodologies as described in CIE154:2003 [37] and CIE097:2005 [38];
- *ISO/TC274 WG2* Commissioning process of lighting systems. This technical specification will give requirements on the commissioning of lighting systems.

The requirements will include procedures, methods, and documentation for the commissioning of the functionality of lighting systems. It will present details on the commissioning of lighting systems without focusing on technical characteristics of specific components.

One further working group is also active but currently has not raised their work to a formal work item.

- *ISO/TC274 JWG5* Lighting for work places.

This joint working group is to update the existing standard *ISO 8995–1:2002 Lighting of work places – Part 1: Indoor*.

When developing standards a view to possible future technologies and applications is always necessary to ensure relevant standards are available in a timely manner. ISO/TC274 identifies the path of technological development as shown in Fig. 4, where:

- Adaptive lighting is defined as lighting responding to circumstances or according to predefined conditions, while maintaining the lighting quality within the specified requirements for these circumstances or conditions [39];
- Integrative lighting is defined as lighting specifically designed to produce a beneficial physiological and/or psychological effect upon humans [39].

Additional key considerations identified are the aging population within society and energy performance, especially with respect to environmental concerns and global climate change. Climate

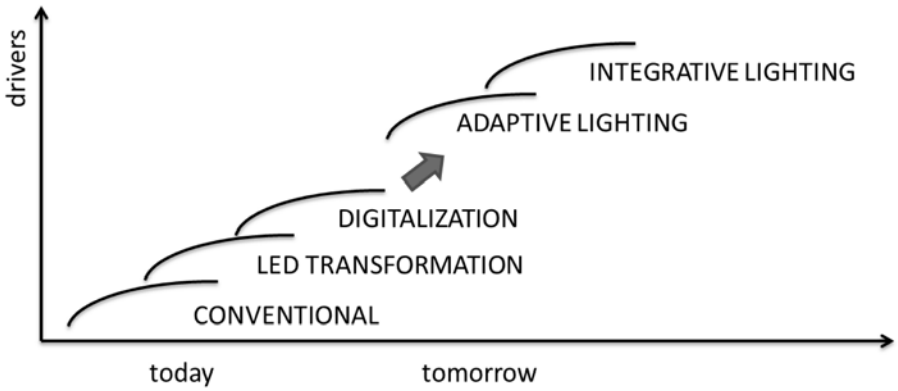

Fig. 4. Relevant technological developments and their evolution over time [36]

change is becoming an important regulatory driver within the lighting industry, as it is within all aspects of life, and this is reflected in its increased importance in standardisation. However, the lighting needs for an increasingly aging yet active population needs careful consideration within this energy aware scenario. The growth of digitalisation and the Internet of Things (IoT) should help lighting meet these requirements by efficiently providing light when needed and ensuring it is the correct light for the individual as opposed to purely lighting for the task.

3.2. CEN/TC169 LIGHT AND LIGHTING

At the level of European standardisation for lighting application CEN/TC169 is the main technical committee with a scope of standardisation in the field of vision, photometry and colorimetry, involving natural and man-made optical radiation over the UV, the visible and the IR regions of the spectrum, and application subjects covering all usages of light, indoors and outdoors, including environmental, energy and sustainability requirements and aesthetic and non-image forming biological aspects.

As such, it is responsible for many standards, technical specifications (TS) and technical reports (TR) (Table).

To manage the development and maintenance of such a list of documents covering a diverse set of subjects requires careful organisation. To help with this CEN/TC169 contains many working groups. Each working group is responsible for one or more of the standards given in the table:

WG 1 Basic terms and criteria;
WG 2 Lighting of work places;
WG 3 Emergency lighting in buildings;
WG 4 Sports lighting;
WG 6 Tunnel lighting;
WG 7 Photometry;
WG 8 Photobiology;
WG 9 Energy performance of buildings;
WG 11 Daylight;
WG 12 Joint Working Group with CEN/TC226 – Road lighting;
WG 13 Non-visual effects of light on human beings;
WG 14 ErP Lighting Mandate Management Group.

Each working group has a convenor who organises and acts as a facilitator for the work of the group and reports back to CEN/TC169 on progress a minimum of twice a year at the annual plenary meeting and also at a mid-term convenors meeting.

At the time of writing this paper, CEN/TC169 has seven work items in progress, updates to EN1837, EN13032–1, EN13032–4, EN12464–1 and EN15193–1, and also two new work items concerning "BIM Attributes for Luminaires and Sensors" and "Guidance Notes on the use of dynamic signage systems".

Again, similar to ISO/TC274, when developing standards a view to possible future technologies and applications is always necessary to ensure relevant standards are available in a timely manner. CEN/TC169 identifies the external factors that will influence lighting and therefore standards development work as:

- Urbanisation – the trend towards increased urban living and more densely populated urban areas;
- Sustainability – the need to reduce energy usage and preserve natural resources;
- Aging populations – the need for proper design of both indoor and outdoor spaces including lighting, to cater for aging occupants or those with reduced visual capacity;
- Connectivity / Internet of things – the increasing trend to link products and services;
- Glazing technologies – developments in window and shading technologies helping the move to near zero-energy buildings;
- Building Information Modelling – the requirement for data-rich virtual models to help throughout the entire building and components life cycles.

4. PROFESSIONAL SOCIETIES

4.1. CIE

The International Commission on Illumination (CIE) is a professional organisation that advances knowledge on topics concerning the science and art of light and lighting, colour and vision, photobiology and image technology. It has a strong tradition of technical and scientific excellence and is recognized by ISO as an international standardisation body (see section 3.1 and Fig. 3).

The work of the CIE is split between six divisions and each division may establish a technical committee (TC) to carry out a specific work item, such as producing or updating a technical report or standard. When the work item is complete the TC

Table

EN1837	Safety of machinery – Integral lighting of machines;
EN1838	Lighting applications – Emergency lighting;
EN12193	Light and lighting – Sports lighting;
EN12464	Light and lighting – Lighting of work places
	Part 1: Indoor work places
	Part 2: Outdoor work places;
EN12665	Light and lighting – Basic terms and criteria for specifying lighting requirements;
EN13032	Light and lighting – Measurement and presentation of photometric data of lamps and luminaires
	Part 1: Measurement and file format
	Part 2: Presentation of data for indoor and outdoor work places
	Part 3: Presentation of data for emergency lighting of work places
	Part 4: LED lamps, modules and luminaires
	Part 5: Presentation of data for luminaires used for road lighting;
CEN/TR13201–1	Road lighting – Part 1: Guidelines on selection of lighting classes
EN13201	Part 2: Performance requirements
	Part 3: Calculation of performance
	Part 4: Methods of measuring lighting performance
	Part 5: Energy performance indicators;
EN14255	Measurement and assessment of personal exposures to incoherent optical radiation
	Part 1: Ultraviolet radiation emitted by artificial sources in the workplace
	Part 2: Visible and infrared radiation emitted by artificial sources in the workplace
	Part 3: UV-Radiation emitted by the sun
	Part 4: Terminology and quantities used in UV-, visible and IR-exposure measurements;
CR14380	Lighting applications – Tunnel lighting;
EN15193–1	Energy performance of buildings – Energy requirements for lighting – Part 1: Specifications, Module M9;
CEN/TR15193–2	Energy performance of buildings – Energy requirements for lighting – Part 2: Explanation and justification of EN15193–1, Module M9;
EN16237	Classification of non-electrical sources of incoherent optical radiation;
EN16268	Performance of reflecting surfaces for luminaires;
EN16276	Evacuation Lighting in Road Tunnels;
CEN/TR16791	Quantifying irradiance for eye-mediated non-image-forming effects of light in humans;
EN17037	Daylight in buildings;
CEN/TS17165	Light and lighting – Lighting system design process.

is closed, unlike, for example, CEN/TC169 where the working group still exists after a particular work item is completed. The divisions cover:

Division 1 Vision and Colour;
Division 2 Physical Measurement of Light and Radiation;
Division 3 Interior Environment and Lighting Design;
Division 4 Transportation and Exterior Applications;
Division 6 Photobiology and Photochemistry;
Division 8 Image Technology.

Each division has a division director, division secretary, division editor and a number of associate directors who ensure the divisional work program continues.

The CIE has a vast range of technical reports and standards, many of which contain the fundamental knowledge that is used to define requirements within standards and regulations. It is continually striving to understand the next key issues and

uses this to define a research strategy which currently include:

– Recommendations for Healthful Lighting and Non-Visual Effects of Light;

– Colour Quality of Light Sources Related to Perception and Preference;

– Integrated Glare Metric;

– Adaptive, Intelligent and Dynamic Lighting;

– Visual Appearance: Perception, Measurement and Metrics;

– Support for Tailored Lighting Recommendations;

and other fundamental issues including those concerning photometry and colorimetry.

4.2. Lux-Europa

Lux-Europa is the European Lighting Society and its members are representatives from national European lighting societies.

Lux-Europa does not give professional status or produce codes of practice but it has importance in standards work in that every 4 years it hosts the Lux-Europa Conference. This provides an arena for the presentation of much research and also Euro-centric topics such as new or upcoming legislation and standards.

4.3. Society of Light and Lighting and Institution of Lighting Professionals (UK)

Many countries have their own professional organisations and these organisations produce best practice guides on many aspects of lighting. Within the UK the two main professional organisations for lighting are the Society of Light and Lighting (part of the Chartered Institute of Building Services Engineers) and the Institution of Lighting Professionals.

The Society of Light and Lighting (SLL) is the descendant of the UK Illuminating Engineering Society that was formed in 1909. The Institute of Lighting Professional has its origins in the Association of Public Lighting Engineers, founded in 1924. The organisations to a large extent complement each other with relatively little overlap in work. They aim to promote the benefits of good lighting, good practice in lighting design, and the development of lighting as an integral part of a low-energy and sustainable future. They also liaise with the UK Government on lighting matters and provide members with a recognised professional standing.

Both organisations produce a range of publications covering individual application areas, relevant legislation and information on the technology of light. In general the content of these documents is driven by lighting standards but on occasions the content may drive standards work. An example is the guidance on obtrusive light that is found in CIE150 [4]. For a period the requirements specified by the Institution of Lighting Professionals [5] was more proscriptive than those in the CIE150 document but with the latest edition of CIE150 they have become harmonised again.

It should be noted that The Society of Light and Lighting is the UK member of Lux-Europa.

5. INDUSTRY ASSOCIATIONS

5.1. LightingEurope

LightingEurope is the industry association that represents the lighting industry within Europe. Its mission is to advocate and defend the lighting industry in Brussels, working with European agencies and the European Commission to reconcile EU policy with lighting best practice. It aims to promote efficient lighting practices for the benefit of the global environment, human comfort and the health and safety of users.

To help in this, LightingEurope brings together industry experts with local and European policy experts in Working Groups covering specific areas of lighting policy. The Working Groups are:

– LEDification – LEDs have enabled energy efficient solutions, which allow more ambitious energy targets to be written into legislation. It is, however, important to preserve the balance between energy efficiency and lighting best practice and to protect the basic quality requirements for LED luminaires;

– Intelligent Lighting Systems – As buildings become smarter lighting will become the backbone of an intelligent building, and through increasing use of sensors and controls intelligent lighting systems will provide users and building owners more control over the quality, flexibility, and scalability of a lighting system. Similarly, the development of smart city concepts based upon intelligent systems will provide a city-wide matrix of network points for data gathering and control;

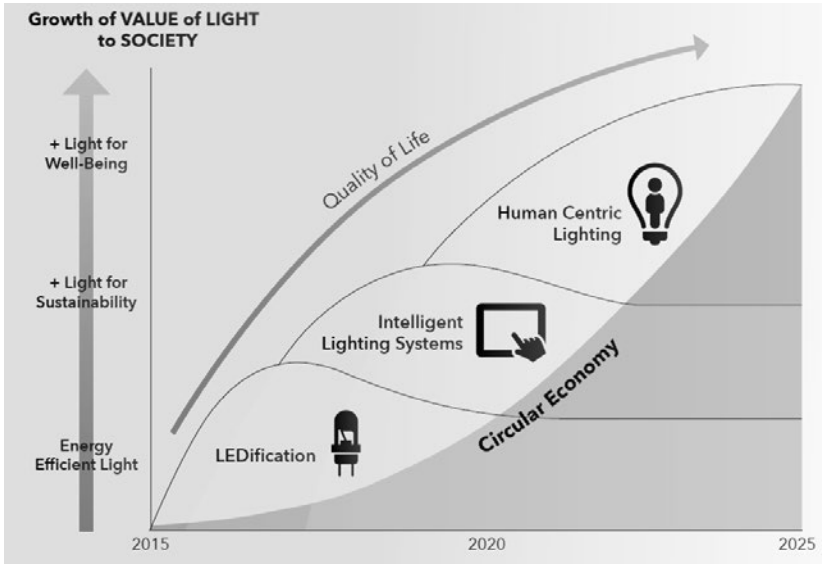

Fig. 5. Developments in the lighting market [35]

– Human Centric Lighting – Light has the power to energize, to relax, to increase alertness, cognitive performance and mood, and to improve the sleep-wake cycle of people. This WG aims to promote the idea of human centric lighting by making information available, initiating scientific studies and organizing events targeted at legislative and business decision makers. Note in this sense, the term human centric lighting is equivalent to the term integrative lighting used by CIE and ISO;

– Circular Economy – The principle of the circular economy is to minimize the ecological footprint of products that means elements of circular economy include refurbishment, remanufacture and reuse, and re-distribution.

Industry associations need a view to the future to ensure relevant standards are available in a timely manner, to educate legislators and the market in the potential new markets and to prevent legislation from inadvertently interfering with new ideas and applications. LightingEurope has a strategic roadmap showing how it expects the lighting market will develop and how this will add to the value of light and the quality of installations (Fig. 5).

This shows that LEDification, the adoption of LED technology, is considered well established, allowing increased use of controls. The digital nature of solid-state lighting technology will aid in the growth of intelligent lighting systems and the IoT which in turn will open the way to human centric solutions. All the while sustainability in terms of the circular economy will increase in importance.

Fig. 4, showing the vision of ISO/TC274, and Fig. 5 show obvious parallels, so both organisations see lighting application and technology developing in a similar way.

5.2. Lighting Industry Association (UK) and ZVEI (Germany)

National trade associations aim to represent their trade within the country to the marketplace and to legislators. A fundamental difference between the LIA and ZVEI is that the LIA is purely concerned with lighting whereas ZVEI represents the German electrical and electronics industry, and therefore has much wider concerns. However, within ZVEI different divisions address different industry sectors and there is a division dedicated to lighting.

Both, the LIA and the lighting division of ZVEI are members of LightingEurope, representing their member's rights in the European arena and they are heavily involved in standards committees, both nationally and worldwide.

The LIA and the lighting division of ZVEI have a number of working groups made up of experts from member companies. These tend to monitor any relevant legislation and liaise with and submit comments to legislators, and also address technical topics to provide a resource of technical information and guidance that members may use to develop the lighting market. Therefore, to an extent national trade associations mirror LightingEurope, although on a national level. However national associations may identify key issues and these may be developed at a national level, promoted up to LightingEurope for a more European approach, or both as is considered appropriate.

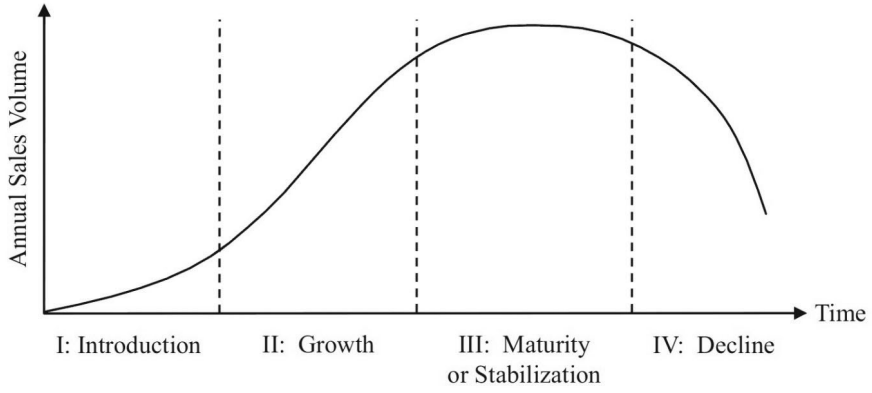

Fig. 6. A typical technology life-cycle curve

6. STANDARDS INTO THE FUTURE

Lighting is in a time of change, not just in terms of technologies such as light sources and solid-state devices but from the practice of lighting for the task to now lighting for people and individuals, from lighting purely for vision to lighting for vision, wellbeing and communication, and into the world of connected devices and the Internet of Things where lighting moves from being a source of light to being a data point.

This is a challenge for standards. Standards are not guides or research documents but factual documents based upon evidence and proven fact. They give established best practice metrics and criteria without necessarily defining how these criteria should be achieved. This creates a problem as radically new concepts and techniques need researching and proving before they are likely to be incorporated into a standard. In addition, to develop a standard normally takes at least three years. This means that standards can lag the development of new products and application techniques, at times significantly. In terms of a typical technology life-cycle, such as shown in Fig. 6, this means that a standard on the application of a technology might only be published during the growth phase of the technology life-cycle and the introduction phase is used to gain enough experience with the technology to define standard criteria. An example of this could be human-centric lighting, where products and applications have been produced but recommendations and design criteria within standards are still very limited.

However, as has been shown above, each organisation within lighting standardisation has a view to the future, be it a standards body, trade association or professional organisation. These viewpoints show a large amount of overlap and in terms of lighting application they cover: – Human centric or integrative lighting; – Connectivity and the Internet of Things; – Inclusivity, in terms of visual capabilities; – Sustainability.

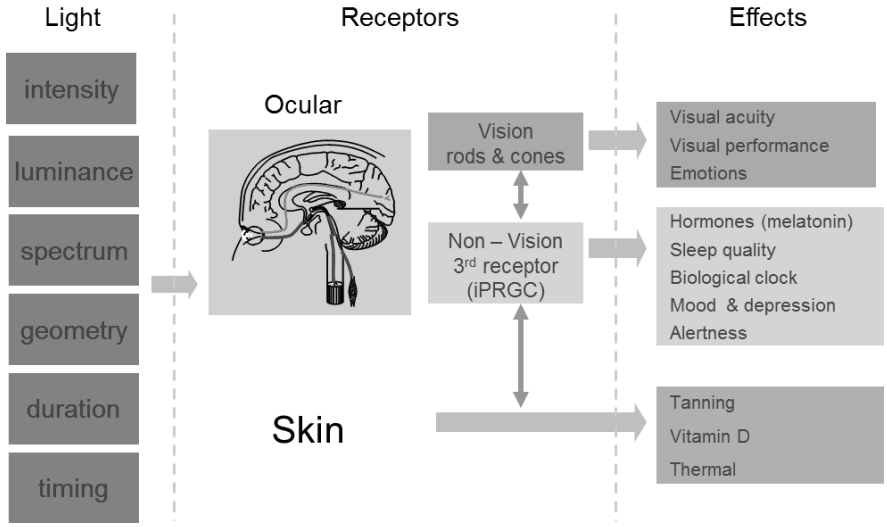

Fig. 7. Simplified overview of impacts of light on humans

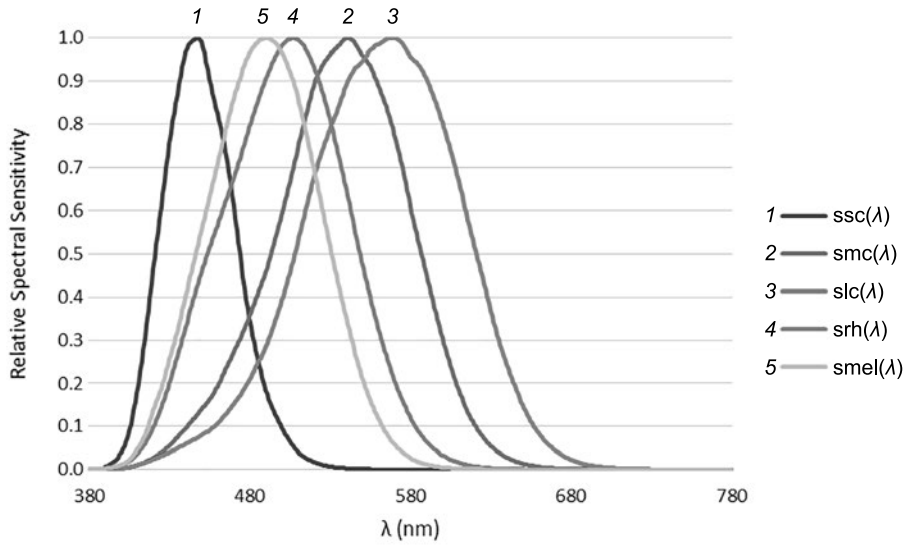

Fig. 8. The α-opic action spectra [6]

These topics provide challenges in terms of practice, metrics and usage and can lead into discussion about additional topics such as colour.

6.1. Human-centric/Integrative Lighting

As shown in Fig. 7, humans interact in many complex ways with light. Light itself has many properties and these create the visual scene, the emotional response and also the biological response. These different responses require new metrics as existing units no longer reflect what is being measured. The units of lumen, candela and lx are visual metrics based upon the eye photopic response curve, which itself is a compromise whose validity is openly questioned due to it not correctly accounting for the S-cone response (amongst other issues). These metrics are not really valid for a photo-biological response based upon both visual and non-visual receptors.

In Fig. 8 the melanopic sensitivity function is shown as a function of wavelength (smel), as defined by Lucas et al [7]. It is significantly different to the 3 CIE short (ssc), medium (smc) and long (slc) cone sensitivity functions for the 10° observer, nor does it correspond to the CIE scotopic rod sensitivity function (srh). Therefore any measure using conventional cone-based (photopic) or rod-based (scotopic) metrics cannot correctly account for the human biological response to light. Fig. 8 does demonstrate that the circadian effect will be impacted by spectral content in addition to flux density, or in very simplistic terms the light level and colour temperature.

A number of proposals have been made for metrics to measure this non-visual impact from lighting.

The WELL Building Standard [8] uses the unit of Equivalent Melanopic Lux (*EML*). This is calculated from the visual illuminance within a space (*L*) and the melanopic ratio (*R*), a weighting factor based upon the light source. The visual illuminance is measured vertically 1.2m above floor level.

The WELL Building Standard provides a spreadsheet to calculate this based upon the melanopic action spectrum given in CIE S026.E:2018 and the CIE $V(\lambda)$ curve, the spectral luminous efficiency function for photopic vision (https://www.wellcertified.com/en). Based upon the spectral content of the light source the melanopic response and spectral response is calculated and then the total melanopic response is divided by the total visual response and this value is then multiplied by 1.218.

Then

$$EML = L \times R \text{ (unit: equivalent melanopic lx).} \quad (1)$$

A second proposal came from the Lighting Research Centre, Rensselaer Polytechnic Institute.

M.S. Rea et. al. [9] proposed the metric Circadian Light which is the irradiance at the cornea weighted to reflect the spectral sensitivity of the human circadian system as measured by acute melatonin suppression after a one-hour exposure. A second metric, the Circadian Stimulus (CS) is the effectiveness of the spectrally weighted irradiance at the cornea from threshold (CS = 0.1) to saturation (CS = 0.7).

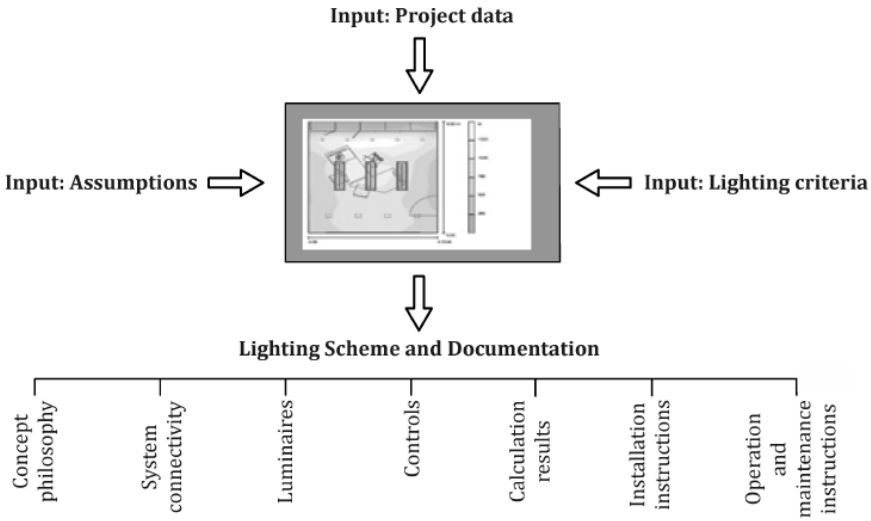

Fig. 9. Lighting system design process and documentation [11]

Similar to EML a spreadsheet is freely available to download and calculate these values or a web-based on-line tool may be used (https://www.lrc.rpi.edu/cscalculator/).

This demonstrates that there is no universally accepted measure to allow human centric design, let alone accepted limits.

Even assuming accepted metrics and limits are agreed upon there is then the question of timing. When discussing biological rhythms we have to understand these are not the same as the physical day/night rhythms of our planets 24 hour cycle. The wake/sleep cycle of an individual may be removed from the natural cycle of day and night to a greater or lesser extent due to work patterns, social habits, and age, gender or chrono-biological traits. There is no universal clock that people are in time with; everyone has their own personal clock which is synchronised to their own wake/sleep cycle.

The implication of this is that human-centric design involves not only some measure of circadian flux but also biological time and light history. Therefore, unless a relatively uniform population exists with complimentary needs, such as a care home for Alzheimer's patients, or at least relatively uniform day/night timings, such as an office with single shift fixed working hours or a factory which may have multiple shift patterns but with only 1 shift in operation at any one time, human-centric design will potentially require a careful approach to avoid penalising some occupants in preference to others.

The WELL Building Standard provides an attempt at accounting for this by stipulating the required level of 200 EML should be present at least between the hours of 9:00 until 13:00. However, this makes the assumption that a person is working a normal daytime shift pattern synchronised with the natural day/night cycle. This is not valid in many situations and could result in applying a circadian lighting design out of step with the occupant biological time.

Therefore without effective lighting controls, human-centric lighting can only be applied with a broad brush on a generic level.

6.2. Connectivity and the Internet of Things

Whilst we discuss the benefits of increased connectivity and the Internet of Things it must be accepted that despite lighting sensors and controls being widely available for many years many lighting installations, both old and new, still do not use any but the more basic control techniques, generally a manual switch.

The European Commission highlighted this in their "Preparatory study of lighting systems Lot 37", produced by consultants VITO [10]. This concluded that:

- The maximum EU-28 total savings for optimised lighting system designs with controls are depending on the reference light source scenario;
- The maximum EU-28 total annual electricity savings due to lighting system measures are 20–29 TWh/a in 2030 and 48–56 TWh/a in 2050;
- This is approximately 10 % (2030) or 20 % (2050) of the total EU-28 electricity consump-

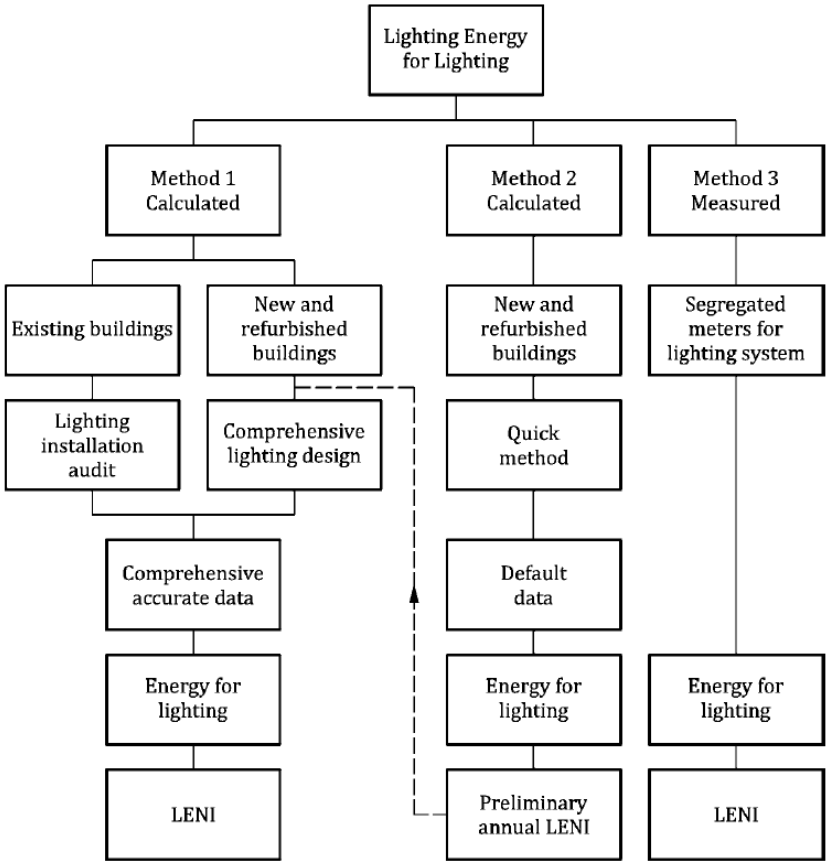

Fig. 10. Flow chart illustrating methods to determine energy for lighting [1]

tion for non-residential lighting in the BAU-scenario for light sources[1].

To support this, CEN produced a new technical specification PD CEN/TS17165:2018 [11] which sets out the general framework of a lighting system design process that can be applied to lighting of any project including smart buildings. It describes the expected inputs into producing a lighting system design and the expected outputs, as shown in Fig. 9.

To produce energy efficient lighting systems and to support the use of lighting controls it is necessary to demonstrate energy savings. Standards exist for both: for buildings and roads. EN15193–1:2017 [1] details the calculation for *LENI*, the Lighting Energy Numeric Indicator. This calculation is shown in equation 2 below.

$$LENI = \left. \begin{array}{l} \{(F_c \times \dfrac{P_i}{1000} \times F_o[(t_D \times F_D) + t_{N]}]\} + \\ +\{[t_y - (t_D + t_N)] \times (P_{ci} + P_{em})\} \end{array} \right/ A, \quad (2)$$

where

LENI is the lighting energy numeric indicator (kWh/(m² year)),

F_c is the savings from constant illuminance controls for the area,

P_j is the power density of the area (W/m²),

F_O is the savings from occupancy controls for the area,

t_D are the daylight operating hours for the area (h),

F_D is the savings from daylight controls for the area,

t_N are the night time (non-daylight) operating hours for the area (h),

ty are the annual operating hours for the area (h),

P_{ci} is the total luminaire control standby power,

P_{em} is the total emergency standby power,

A is the room area (m²).

Techniques for calculating the savings from control technologies are given within the standard. A LENI value may also be produced for existing lighting installations either through metering of the electrical supply to the lighting or by estimation based upon a lighting installation audit. The 3 methods are shown in Fig. 10.

[1] Note: BAU means “Business as Usual” or in effect we continue as we are.

An equivalent energy calculation exists for road lighting, as specified within EN13201–5:2015 [12]. This defines the Annual Energy Consumption Indicator (AECI), which is given in equation 3 below.

$$D_E = \frac{\sum_{j=1}^{m} \left(P_j \times t_j \right)}{A}, \tag{3}$$

where

D_E is the annual energy consumption indicator for a road lighting installation (Wh/m²),

P_j is the operational power associated with the j^{th} period of operation (W),

t_j is the duration of the j^{th} period of operation (h),

A is the size of the area lit by the same lighting arrangement (m²),

m is the number of different operational periods.

When lighting controls are in use an operational period would also include the period during daylight hours when the lighting was not active to account for the controls standby power. When presence detection is used it is necessary to assume the probability for each of the lighting levels.

Given that we can calculate energy usage and the impact of lighting controls, more widespread use of control technologies is required. There is much additional help and advice available for the use of lighting controls. CIE222 [13] provides guidelines in order to balance lighting quality, user comfort and energy efficiency in lighting controls solutions for lighting in non-residential building. It describes the background to lighting control strategies, contains an extensive literature study on application of controls and 12 tables that evaluate the influence of controls in applications. The report allows an appropriate control strategy to be chosen either starting from the application and working forward to predicted outcomes, or starting with desired outcomes and working back to the required control strategies to achieve these.

An alternative resource is the Lighting Control Guide from the UK Lighting Industry Association [14] which provides an appreciation of the benefits of lighting controls, helps match lighting controls and light sources with application and provides a decision tree to assist in the selection of the most suitable lighting controls.

A major consideration with the use of a more advanced control systems is commissioning, ensuring that the system operates correctly. This is where the work of standards committees such as ISO/TC274 WG2 Commissioning process of lighting systems is very important to give a good practice yardstick to work to.

With the development of more advanced concepts such as the IoT and smart cities many more possibilities are being developed and considered. For a smart city this could include aspects such as social profiling of application spaces, for example in terms of:

- Expected age profile of users across time of day and time of week;
- Expected social activities across time of day and time of week;
- Expected transportation modes;
- Prevalence and type of any crime;
- Area category, such as inner-city/urban/rural, retail/entertainment/residential, etc.

As the usage and occupant profile changes within a space so should the lighting.

Similarly for buildings a profile may be developed on space or energy usage. Sensors and system software can detect when rooms or single desks are occupied and this data can be visualised, allowing space usage to be optimised. In addition utilising daylight, presence and time-based controls allows energy usage to be minimised. So lighting within buildings should complement the people performing a task, and not just consider the task requirements as if they were being performed by a "standard" person with "standard" visual capacity and no emotional needs.

Another potential application of advanced control techniques is in emergency lighting. Current practice provides lighting to allow the evacuation of a building but has no knowledge of the state of the building and escape routes. Therefore it is up to individual occupants to ascertain if an escape route is safe to use, the lighting and signage is constant irrespective of the true condition. Linking the emergency lighting to other building services such as smoke or heat detection systems, would allow occupants to be directed around areas of potential danger, whilst the use of monitors that can detect occupant density within spaces and escape routes could allow routing around congested areas, smoothing the evacuation process in the quickest possible time. However these systems have their own particular considerations and concerns.

Testing the functionality of the intelligent emergency lighting system through life becomes more complex with numerous interdependencies and

links with external systems. Automatic testing would be essential and would require careful configuration. Security of communications would be essential. Loss of communication with internal or external system components would compromise the system ability to direct occupants safely, of especial concern when these types of systems become established and people start to rely on them to keep them safe. Cybersecurity will also be an issue as any connected system introduces security risks. These are not just at the level of the emergency lighting system, although a third-party being able to activate evacuation alarms whilst simultaneously disabling evacuation systems is a concern, but any connected system is a potential gateway into more sensitive areas of an IT network. Therefore parts of the functionality of lighting systems may become under the remit of IT departments and specialists.

In recognition of the increased risks posed by the IoT and enhanced connectivity a new document being prepared is the EU Cybersecurity Act [15] which will provide schemes to certify products for Cybersecurity. Certification will be to either basic, substantial or high levels where:

- Basic – minimises known basic risk;
- Substantial – minimises known security threats from actors with limited skills and resources;
- High – minimises state of the art attacks by actors with significant skills and resources.

National governments and organisations are also developing guidance, for example a publication from the UK CIBSE [16], a white paper from the German ZVEI [17] and the UK Department for Digital, Culture, media and Sport [18].

However, as data collection and usage increases through the IoT and intelligent lighting systems, individual rights are in danger of being compromised. Therefore developments both in technology and in standards and application are tempered by legal regulation. In the European Union this is principally covered by the General Data Protection Regulation (GDPR) [19]. This covers the processing of personal data in the context of the activities of an establishment of a controller or a processor in the European Union, regardless of whether the processing takes place in the European Union or not, and it covers the monitoring of the behaviour of individuals within the EU. Key definitions include:

– Personal data – any information relating to an identified or identifiable natural person;.

An identifiable natural person – A person who can be identified, directly or indirectly, in particular by reference to an identifier such as a name, an identification number, location data, an online identifier or to one or more factors specific to the physical, physiological, genetic, mental, economic, cultural or social identity of that natural person.

Therefore any information that allows a specific identifiable occupant to be located, and even more so if this allows information to be gathered about their current mental state (think personalised human-centric lighting concepts) is covered. This will extend to areas such as smart phone applications that allow users to move through a smart city or building easier, permissions on data gathering and usage and how they are granted and accepted must be very carefully considered.

6.3. INCLUSIVITY

The concept of a standard person has existed for a long time. Leonardo da Vinci's painting of Vitruvian Man (1490) showed a standardised representation of the proportions of a human body but this was based upon the much earlier work of an architect from Ancient Rome, Vitruvius, who published a correlation of ideal human proportions with geometry in book III of his treatise "De architectura" [20]. A standard person is important because it allows the principle of "one size fits all", in workplaces, homes, public buildings, furniture, appliances, transport and lighting. Chairs, desks, stairs, doors, etc. all benefit from the availability of a standard person to design around. However the standard person also indirectly promotes discrimination in that those who do not conform to the norm are either forced to comply or disadvantaged.

And this exists in lighting as much as in any other profession. Lighting installations are designed to provide the correct lighting condition for the majority of the population, but those with particular physical, mental or visual requirements are generally not considered.

Inclusive design (alternatively termed as universal design) ensures all people are included by quality of design, irrespective of their capabilities, and designers have to accept responsibility for the impact of their designs. This quality of design should consider multiple impacts from the relatively obvious, such as wheelchair users have a different eye-height and therefore experience glare differently,

to issues requiring more consideration. If we explore sight loss there are three main generic types of sight loss, such as:

- Residual sight users is the group, which makes up the majority of people with sight loss; typically their sight will be bad enough to be registered blind or partially sighted but still of considerable use;
- Long cane users when long canes are a mobility aid used primarily by people with very little useable sight and allow changes in levels and texture to be perceived as well as detection and identification of obstacles;
- Guide dog users group represents a small fraction of the sight loss population; they are often amongst the most mobile.

Inclusivity is not just how we light a space but also where we position lighting fixtures and fittings. For example, if we consider how these people move through a space and how the siting of lighting fixtures will impact this (based upon Sight Line [21]).

- Residual sight users

Tonal contrast is the most important source of information. Residual sight users feel more comfortable on wide, spacious, uncluttered footways and pedestrian areas.

Sight, and therefore light, is still is a major factor.

For lighting, fixtures that have little contrast with the background can render them almost invisible.

- Long cane users

Rely predominantly on tactile and audible sources, and will usually attempt to walk along the building line.

Careful siting of lighting furniture away from the building line can aid these users

- Guide dog users

Guide dogs are trained to walk down the centre of a footway or corridor and avoid obstacles. They are also trained to locate crossings and entrances. If a guide dog cannot detect a space big enough to fit through it will just stop, leaving its owner stranded.Careful siting of lighting fixtures and furniture at key points such as crossing areas and building entrances helps the guide dog navigate these spaces

Lighting standards frequently only address these issues with relatively basic comments. The European Standard EN12464–1 [22] states that lighting levels may be increased when "the visual capacity of the worker is below normal". However, like most standards, it gives little advice on what this means in application. For more in-depth information publications such as CIE227:2017 [23] gives valuable advice, both on the causes of reduced visual capacity and what this means and also lighting requirements to help counteract these issues. This includes recommendations on lighting requirements for older occupants to move through escape routes, a safety issue that is frequently forgotten. It also discusses some applications of integrative / human-centric lighting in a section on the non-visual effects of light on older people and people with low vision.

Lighting not only has an impact based upon the visual capacity of an observers eye, it also has a mental impact based upon the ability of an observer to decode the visual scene. Observers with dementia may have good eyesight but their ability to understand common features and effects that we take for granted may not function correctly. Shadows become holes in the ground, or giant spiders, etc., the direction of shadows may be disturbing, for example light from below an object, and glare sources disorientate and confuse. Sources of information for this include papers by Torrington et al [24]

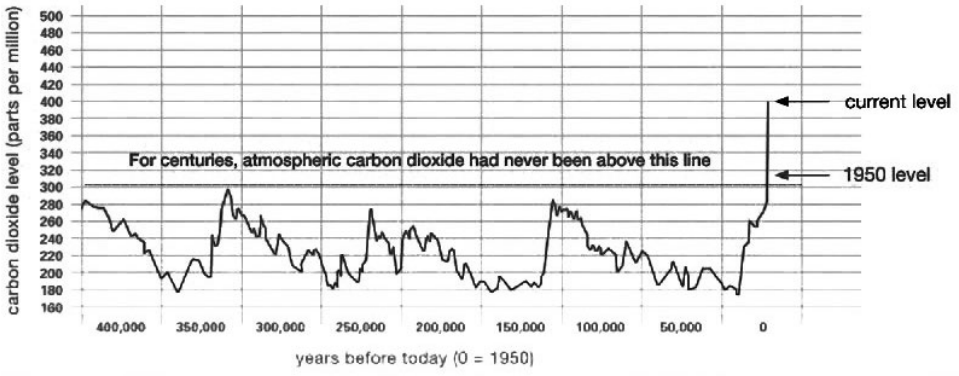

Fig. 11. Atmospheric CO_2 levels through time (source: NASA https://climate.nasa.gov/evidence/)

and Sloane et al [25], IES CG-1–09 [26], or the University of Stirling [27].

6.4. SUSTAINABILITY

Lighting performs a balance in that people need lighting to live, however lighting has a global impact on our climate. Fig. 11 shows the levels of CO_2 in the atmosphere through a period of time and it is obvious that levels have increased and are still increasing dramatically.

In a 2013 report [28], the United Nations Environment Programme (UNEP) stated

"*Electricity for lighting accounts for almost 20 % of electricity consumption and 6 % of CO_2 emissions worldwide. According to the International Energy Agency, approximately 3 % of global oil demand can be attributed to lighting. If not addressed immediately, global energy consumption for lighting will grow by 60 % by the year 2030.*"

In addition in a report from the Organisation for Economic Co-operation and Development (OECD) [29] Angel Gurria, OECD Secretary-General stated

"*Growth in materials use, coupled with the environmental consequences of material extraction, processing and waste, is likely to increase the pressure on the resource bases of our economies and jeopardise future gains in well-being.*"

These facts are driving regulation and legislation to push for more energy efficient and sustainable solutions and a move to a circular economy as shown in Fig. 12.

After collection as we push the product, its components or its materials back into the manufacturing chain we can see that the further up the chain we go the greater the environmental impact. So we can see that the preferred options at product end-of-life are to reuse or to refurbish the product or its individual components. Recycling has a larger environmental impact as more processes are required to turn the waste into a new usable product.

Fig. 12. Principle of the circular economy [35]

However, as identified by UNEP and illustrated in Fig.13, whilst the end-of-life phase is important to preserve the environmental investment in the existing product, the in-use phase before this is critical. Fig.13, from an environmental product declaration produced according to EN ISO 14025 [30] and EN15804 [31], shows that 99 % of the global warming potential for this product is in the use phase. Therefore it is critical that the product is as efficient in use as possible, and is also used as efficiently as possible.

Within Europe eco-design regulations exist to remove less efficient products and components from the market. Current regulations are

- Regulation (EC) No 244/2009 with regard to ecodesign requirements for nondirectional household lamps [32].
- Regulation (EC) No 245/2009 with regard to ecodesign requirements for fluorescent lamps without integrated ballast, for high intensity discharge lamps, and for ballasts and luminaires able to operate such lamps [33].

Assessment parameter	Unit	Production Stage	Construction Process Stage	Use-stage	End-of-Life Stage	Benefits and loads beyond the system boundary
		A1-A3	A4, A5	B4, B6	C2-C4	D
Acidification Potential (AP)	[kg SO_2 eq]	6,02E-02	1,33E-03	1,45E+00	2,95E-03	-2,91E-02
Eutrophication Potential (EP)	[kg PO_4^{3-} eq]	5,90E-03	2,66E-04	1,30E-01	3,69E-04	-2,06E-03
Global Warming Potential (GWP100)	[kg CO_2 eq]	2,08E+01	1,23E+00	5,22E+02	5,35E+00	-7,83E+00
Primary energy, renewable	[MJ]	4,75E+01	8,25E-01	2,55E+03	3,52E+00	-1,56E+01
Primary energy, non renewable	[MJ]	3,48E+02	7,41E+00	9,10E+03	1,36E+01	-9,78E+01

Fig.13. Extract from Environmental Product Declaration (source: Thorn Lighting Ltd, Product code 96628133)

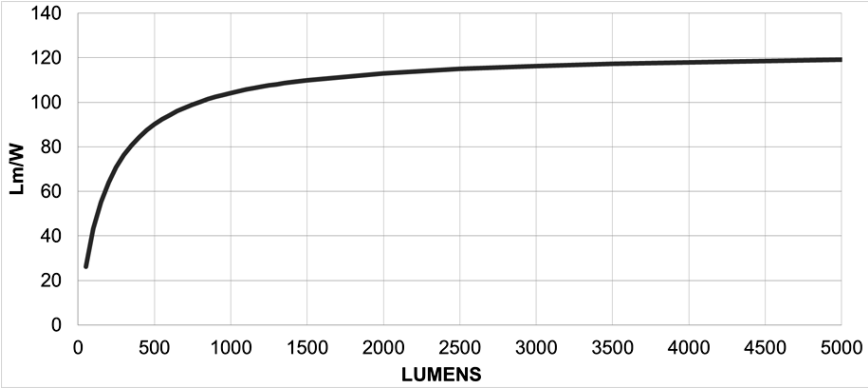

Fig. 14. Graphical representation of efficacy limits based upon equation 4

• Regulation (EU) No 1194/2012 with regard to ecodesign requirements for directional lamps, light emitting diode lamps and related equipment [34].

However these are in the process of being replaced by a single regulation which will come into effect on 1st September 2021. Efficiency limits will be calculated using equation 4.

$$P_{onmax} = C \times \left(L + \frac{\Phi_{use}}{F \times \eta} \right) \times R, \qquad (4)$$

where

P_{onmax} is the maximum on-mode power (in W);

η is the threshold efficacy (in lm/W, light source type dependant);

L is the end loss factor (in W, light source type dependant);

C is the correction factor for light source characteristic;

F is the efficacy factor (1.0 for Non-Directional Light Sources, 0.85 for Directional Light Sources);

R is the CRI factor (0.65 for CRI≤25, (CRI+80)/160 for CRI>25).

Equation 4 results are shown in Fig. 14 with light source efficacy limits approximately between (100–120) lm/W.

It must be recognised that increasing the efficiency limits for lighting sources and luminaires will have diminishing returns. As more high-efficiency luminaires are installed, less significant gains will be made by more efficient product replacing already efficient product. Therefore the focus will move towards lighting systems as opposed to individual lighting products. This is demonstrated by a document produced by consultants VITO [10] that concluded:

"*The maximum EU-28 total savings for optimised lighting system designs with controls are depending on the reference light source scenario and the maximum EU-28 total annual electricity savings due to lighting system measures are 20–29 TWh/a in 2030 and 48–56 TWh/a in 2050. This is approximately 10 % (2030) or 20 % (2050) of the total EU-28 electricity consumption for non-residential lighting in the BAU-scenario for light sources.*"

So efficiency will move towards the regulation of full lighting systems with sensors and controls and sustainability will move towards maintainable luminaires with replaceable LED light sources and reusable components.

7. CONCLUSIONS

As has been described the world of standards and regulations is complex and attempts to address the needs of changing and evolving markets and technologies. They aim to provide a measure against which solutions may be compared for suitability but increasingly also address issues such as environmental and security concerns.

As our world changes in the future, automation increases along with connectivity, social demographics and expectations change, tasks and functions develop to meet the requirements of a 21st Century society, so will standards and regulations have to evolve to meet the needs of new generations. Research will be required to understand possibilities and impacts and the results will have to be embodied into documents that describe codes of practice.

As our predecessors in lighting struggled with how to quantify and codify basic principles so will the next generation of lighting professionals in an ever changing and exciting environment where boundaries between professions blurs and vision becomes only one aspect of design.

REFERENCES

1. EN15193–1:2017, Energy performance of buildings. Energy requirements for lighting. Specifications, Module M9.

2. PD CEN/TR15193–2:2017, Energy performance of buildings. Energy requirements for lighting. Explanation and justification of EN15193–1, Module M9.

3. DIRECTIVE2010/31/EU OF THE EUROPEAN PARLIAMENT AND OF THE COUNCIL of 19 May 2010 on the energy performance of buildings. https://eur-lex.europa.eu/legal-content/EN/ALL/; ELX_SESSIONID=FZMjThLLzfxmmMCQGp2Y1s2d3TjwtD8QS3pqdkhXZbwqGwlgY9KN%212064651424?uri=CELEX:32010L0031

4. CIE150:2017. Guide on the limitation of the effects of obtrusive light from outdoor lighting installations. Vienna, Central Bureau CIE, 2017.

5. Guidance for the reduction of obtrusive light. Institution of Lighting Professionals, Rugby. https://www.theilp.org.uk/documents/obtrusive-light/

6. CIE S026/E:2018. CIE System for Metrology of Optical Radiation for ipRGC–Influenced Responses to Light. Vienna, Central Bureau CIE, 2018.

7. Lucas, R.J., Peirson, S.N., Berson, D.M., Brown, T.M., Cooper, H.M., Czeisler, C.A., Figueiro, M.G., Gamlin, P.D., Lockley, S.W., O'Hagan, J.B., Price, L.L.A., Provencio, I., Skene, D.J., Briainard, G.C. Measuring and using light in the melanopsin age. Trends in Neurosciences, January 2014, Vol. 37, No1.

8. The WELL Buildings Standard v1 with Q42018 addenda, International WELL Building Institute, New York, 2018.

9. Rea, M.S., Figueiro, M.G., Bierman, A., Hammer, R. Modelling the spectral sensitivity of the human circadian system. Lighting Research and Technology, Vol. 44, No4, 2012.

10. van Tichelen, P., Lam, W.C., Waide, P., Kemna, R., Vanhooydonck, L., Wierda, L. Preparatory study on lighting systems 'Lot 37'. European Commission, 2016. http://ecodesign-lightingsystems.eu/sites/ecodesign-lightingsystems.eu/files/attachments/2016Preparatory_study_on_lighting_systemsTasks0_4_7final2.pdf

11. PD CEN/TS17165:2018. Light and lighting – Lighting system design process.

12. EN13201–5:2015. Road lighting Part 5: Energy performance indicators.

13. CIE222:2017. Decision Scheme for Lighting controls in Non-Residential Buildings. Vienna, Central Bureau CIE, 2017.

14. Lighting Control Guide. LIA, Telford, 2018. https://www.thelia.org.uk/sites/default/files/resources/20181010 %20LIA%20Lighting%20Control%20Guide%20October%202018 %20issue.pdf

15. Proposal for a REGULATION OF THE EUROPEAN PARLIAMENT AND OF THE COUNCIL on ENISA, the "EU Cybersecurity Agency", and repealing Regulation (EU) 526/2013, and on Information and Communication Technology cybersecurity certification (''Cybersecurity Act''). European Commission, 2017. https://eur-lex.europa.eu/legal-content/EN/TXT/?uri=COM:2017:477:FIN

16. DE6.1 Cyber security in building service design. CIBSE, Balham. 2018. ISBN978–1–912034–06–2.

17. Horizontal Product Regulation for Cybersecurity. ZVEI, Frankfurt am Main. 2018. https://www.zvei.org/fileadmin/user_upload/Presse_und_Medien/Publikationen/2018/November/Horizontale_Produktregulierung_fuer_Cybersicherheit_Whitepaper/ZVEI-Whitepaper_Horizontal_Product_Regulation_for_Cybersecurity_english.pdf

18. Code of Practice for Consumer IoT security. UK Department for Digital, Culture, media and Sport. 2018. https://www.gov.uk/government/publications/secure-by-design/code-of-practice-for-consumer-iot-security

19. REGULATION (EU) 2016/679 OF THE EUROPEAN PARLIAMENT AND OF THE COUNCIL of 27 April 2016 on the protection of natural persons with regard to the processing of personal data and on the free movement of such data, and repealing Directive 95/46/EC (General Data Protection Regulation). European Commission. 2016. https://eur-lex.europa.eu/legal-content/EN/TXT/?qid=1549027470773&uri=CELEX:32016R0679

20. Vitruvius (translated Morgan, M.H.). Vitruvius: The Ten Books on Architecture. Dover Publications Inc, 1998. ISBN978–0486206455.

21. Atkin, A. Sight Line: Designing Better Streets for People with Low Vision. Helen Hamelyn Centre. 2010. ISBN978–1–907342–28–8.

22. EN12464–1:2011. Light and lighting – Lighting of work places Part 1: Indoor work places.

23. CIE227:2017. Lighting for Older People and People with Visual Impairment in Buildings. Vienna, Central Bureau CIE, 2017.

24. Torrington, J.M., Tregenza, P.R. Lighting for people with dementia. Lighting Research and Technology, Vol. 39, No1, 2007.

25. Sloane, P.D., Figueiro, M., Garg, S., Cohen, L.W., Reed, D., Williams, C.S., Preisser, J., Zimmerman, S. Effect of home-based light treatment on persons with de-

mentia and caregivers. Lighting Research and Technology, Vol. 47, No2, 2015.

26. Illuminating Engineering Society. Lighting your way to better vision. IES CG-1–09. New York: Illuminating Engineering Society of North America. 2009.

27. McNair, D., Cunningham, C., Pollock, R. Light and lighting design for people with dementia. University of Stirling. 2010. ISBN978 185769250 1.

28. THE RAPID TRANSITION TO ENERGY EFFICIENT LIGHTING: AN INTEGRATED POLICY APPROACH. The United Nations Environment Programme/ Global Environment Facility. 2013.

29. Global Material Resources Outlook to 2060 Economic drivers and environmental consequences. OECD. 2018.

30. EN ISO 14025:2010. Environmental labels and declarations. Type III environmental declarations. Principles and procedures.

31. EN15804:2012+A1:2013. Sustainability of construction works. Environmental product declarations. Core rules for the product category of construction products.

32. COMMISSION REGULATION (EC) No 244/2009 of 18 March 2009 implementing Directive 2005/32/EC of the European Parliament and of the Council with regard to ecodesign requirements for non-directional household lamps. European Commission. 2009. https://eur-lex.europa.eu/legal-content/EN/TXT/?qid=1549030304631&uri=CELEX:32009R0244

33. COMMISSION REGULATION (EC) No 245/2009 of 18 March 2009 implementing Directive 2005/32/EC of the European Parliament and of the Council with regard to ecodesign requirements for fluorescent lamps without integrated ballast, for high intensity discharge lamps, and for ballasts and luminaires able to operate such lamps, and repealing Directive 2000/55/EC of the European Parliament and of the Council. European Commission. 2009. https://eur-lex.europa.eu/legal-content/EN/TXT/?qid=1549030396228&uri=CELEX:32009R0245

34. COMMISSION REGULATION (EU) No 1194/2012 of 12 December 2012 implementing Directive 2009/125/EC of the European Parliament and of the Council with regard to ecodesign requirements for directional lamps, light emitting diode lamps and related equipment. European Commission. 2012. https://eur-lex.europa.eu/legal-content/EN/TXT/?qid=1549030464785&uri=CELEX:32012R1194

35. LightingEurope Strategic Roadmap 2025 of the European Lighting Industry. LightingEurope. 2016. https://www.lightingeurope.org/images/160404-LightingEurope_Roadmap—-final-version.pdf

36. STRATEGIC BUSINESS PLAN ISO/TC274. ISO. 2018. https://isotc.iso.org/livelink/livelink/fetch/2000/2122/687806/ISO_TC_274__Light_and_lighting_.pdf?nodeid=16594506&vernum= –2

37. CIE154:2003. The maintenance of outdoor lighting systems. Vienna, Central Bureau CIE, 2003.

38. CIE097:2005. Guide on the maintenance of indoor electric lighting systems. Vienna, Central Bureau CIE, 2005.

39. CIE DIS017:2016 ILV: International Lighting Vocabulary 2nd Edition. Vienna, Central Bureau CIE, 2016.

Peter Thorns
graduated from Sunderland Polytechnic with an honours degree in Electrical and Electronic Engineering. He is very active in ISO, CEN and CIE Division 3, UK and European trade associations and is a fellow of CIBSE and the SLL. His fields of interest include the application of light, human-centric lighting, environmental concerns and energy efficiency

Light & Engineering
Vol. 27, No. 2, pp. 23–31, 2019 *https://doi.org/10.33383/2018-030*

INNOVATIVE CONCEPTIONS OF NATURAL LIGHT USING AS AN ESSENTIAL COMPONENT OF THE FORMAION OF ARCHITECTURAL SPACE

Natalia A. Saprykina

Moscow Architectural Institute (State Academy, MARKHI)
E-mail: nas@markhi.ru

ABSTRACT

The purpose of the article is identification of the innovative conceptions of using natural light properties to form architectural space interactively associated with the habitable environment. It is noted that the natural light, being an extremely powerful tool for the organization of architectural objects, attracts attention of many scientists and designers working in different fields of architecture. The results of the review of their architectural researches and developments are presented in connection with the considered problem. It is established that the innovative conceptions of the natural light modelling can be used to create the appropriate objects of architecture. The obtained results can be useful for the theory and practice of habitat formation opening up completely new opportunities in architecture.

Keywords: light environment, artificial sunlight, energy potential, natural light

1. INTRODUCTION

Relevance and Actuality

It is known, that natural light not only provides visual perception of a person, but also performs psychological, biological and aesthetic functions. It plays a major role in the habitable space, changing architectonics, proportions, and the nature of the emotional impact. Depending on its quality, impressions can be very diverse and have a profound effect on the perception and enrichment of our understanding of the environment. The features of light for spatial organization and optimization of the light environment of architectural objects are very important. The shape formation and space in architecture appear only in the presence of light. It should be noted the environmental aspect of natural lighting due to its significantly higher energy efficiency compared to artificial lighting, what may be a decisive indicator of the optimization of future possibilities of the architecture. The problem of inhabited space organization by means of the natural light use always was in the architectures interests. Suffice it to recall such masterpieces of architectural creativity as the building of the Central city library of Vyborg town in Russia, built in 1933–1935 by the Finnish architect A. Aalto. In the main hall of the library there are no traditional windows (the surface of the walls was left for hanging bookshelves). Natural diffused light, which not makes shadows, enters in the room through the round window on the roof. Another well-known example is the building of the headquarters of the company "Johnson wax "(1936–1939), in Racine (Wisconsin, USA), in which the constructive basis of the Central hall of the company is designed in the form of "tree" expanding upward columns by the American architect F.L. Wright. Light is carried out through transparent glass tubes, giving a smooth soothing lighting throughout the room. Later, 13 years later, a research complex was built, and there is the outer glazing of the laboratory tower was made of bent glass tubes giving an extremely pleasant aesthetic effect of diffused soft light. In this regard, the purpose of the article is to identify innovative ways of

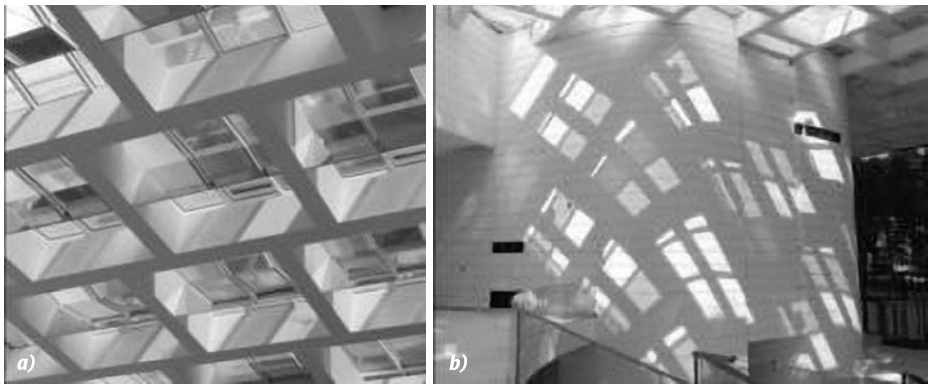

Fig. 1. Trap of light in the lobby of the tower " Eqho "(Paris): a – lattice structure of mirror ceiling panels; b – coloured light spots on the inner wall facing North placed in direct, in which sunlight never gets

using natural light as an important component of the architectural space lighting interactively associated with the environment. This is due to the fact that the versatility and complexity of using of natural light as well as the breadth of its "manifestation" techniques requires consideration of the relevant concepts in some aspects. In connection with the relevance of this problem, a review of existing architectural solutions for the use of natural light in the formation of the architectural environment was carried out in different areas.

2. CONCENTRATION AND TRANSPORTATION OF THE NATURAL LIGHT

In accordance with present time requirements to the shaping of spatial habitat in the practice of design and construction of the architectural objects there are a variety of proposals for the use of the natural light to change the perception of space during the day and the season's changes.

Among the examples there are the modernization of the facade of the 130-meter tower "Eqho", built in 1988 in the business district Defance (Paris), and the reconstruction of its lobby, that allowed the natural light penetration to it.

Development of the project of transformation of day and night appearance of the lobby was carried out by the architectural Studio Hubert & Roy with the participation of Studio Concepto specializing in the field of lighting design [1]. The architecture of the lobby, due to the presence of a glass roof, allows incoming natural light to change the perception of its space during the day by projection on the walls and the floor of shadows from the special elements located at the top (Fig. 1).

The use of dichroic glass allows painting the light passing through it, changing its colour within the specified limits depending on the angle of incidence of sunlight. This is provided by the deflection of certain rays of light with the help of mirror panels suspended inside the metal lattice structure, which allows coloured rays directing to the inner wall. The proposed lighting system as a "trap"

Fig.2. Trap of light in the transport interchange hub "Fulton Center"(New York): a – general view of the building node; b – internal space with a mesh structure of the dome

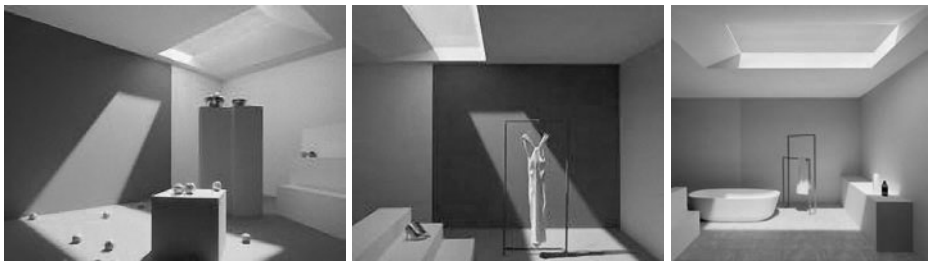

Fig.3 Device simulating sunlight "CoeLux": examples of interior solutions

of light allows you to enhance the impression of the perceived space of the lobby and to control natural light for 24 hours a day, as long as you want. The ability to transport natural light for its delivery to the subway platform is provided in a large transport interchange hub "Fulton Centre" in the heart of lower Manhattan, which combines 11 subway lines (the authors of the project – Grimshaw Architects Bureau together with engineering and design company Arup). The glazed rectangular volume of the interchange unit is about 34000 m**²**. It has a spacious atrium with a height of about 34 m with a waiting room in the centre and outlets at the edges. The steel dome with an angled light aperture, under which the lift surrounded by a ladder stand is located, completes the construction (Fig. 2).

On the inner walls of the dome, complex mesh structure is fixed on the crisscrossing steel cables with a height of over 21 meters and a diameter of about 15m (developed by the office of James Carpenter Design Associates). In this case, the process of creating a mobile design by engineers who needed to first understand how it will work depending on pressure, air temperature, air conditioning system and other factors is of professional interest. At the same time, the behaviour of the object in 815 situations, both standard (heat, cold, time changes) and force majeure, as well as in case of fire, was simulated using special software. Having thus determined the optimal form of the structure, the engineers studied and calculated the distribution of the levels of natural and artificial lighting depending on the external conditions. It should be noted that the electric lighting in the interchange unit is used only in pedestrian crossings, where a kind of grid of fluorescent lamps is also used [2]. An example of the creation of "artificial sunlight" to simulate realistic natural lighting in enclosed spaces (rooms without Windows, museums, metro stations) is the unique device "CoeLux" developed by Professor Paolo Trapani from the University of Insabria (Italy). It looks like an ordinary skylight and is designed to recreate realistic "sunlight" in enclosed spaces. A complex optical system that accurately simulates the sun and its rays uses LEDs with high colour quality. A special visualization mechanism has an interface designed to simulate the sky and sunlight falling into the windows (Fig. 3) [3]. "CoeLux" not only delivers artificial daylight in enclosed spaces, but can be programmed to emulate three lighting scenarios depending on geographical location (for example, providing warm light, typical for Northern regions, or Equatorial, vertical type lighting, cool shades and more dramatic shadows). The device has a small thickness and can be built into any suspended ceiling. The usual methods of using and transformation of natural light, scientists try to complement by the new ways. For example, physicists from Chile and Germany have developed a two-dimensional optical trap of light using mutu-

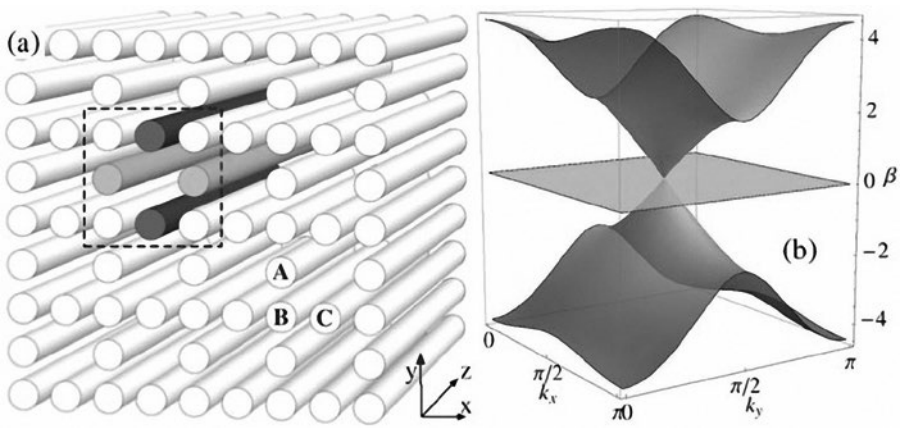

Fig. 4 Model and diagram of natural light blocking in two-dimensional trap

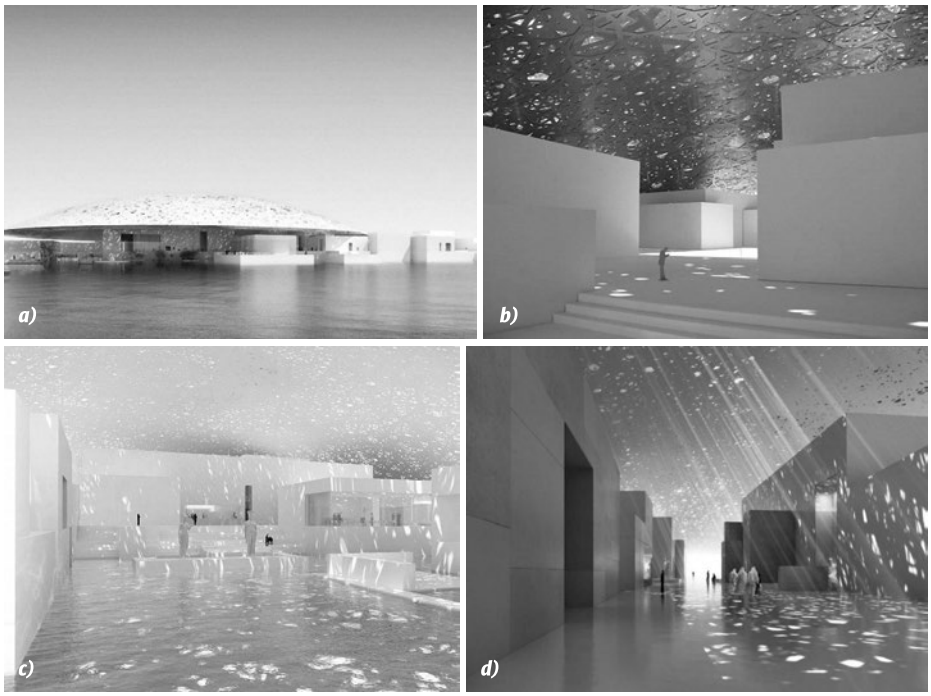

Fig. 5 Complex "Louvre Abu Dhabi" (UAE) a – general view; b, c, d – options for solving of the interior space

al interference of electromagnetic oscillations. It is a two-dimensional version of the crystal structure of perovskite – one of the hardest materials on Earth. The method, where light is blocked on the two coordinate axes and can freely spread in the third one, has advantages over other methods. It is much simpler and requires materials with a small refractive index (Fig. 4) [4].

It is absolutely obvious that the considered tendency of concentration and transportation of natural light would be absolutely impossible without the using of parametric approach to the formation of architectural space as a system of conceptual, technological and aesthetic components.

3. PROTECTION FROM SOLAR RADIATION AND CONTROL OF NATURAL LIGHT

Another aspect of natural light modelling is protection from solar radiation.

This problem is widely described in publications about practical and theoretical developments in the field of shadow systems of sun protection [5–6], etc.

The developments using new methods of working with light, using innovative approaches, manifested in two forms: static and dynamic, are of interest.

An example of a static approach is the complex "Louvre Abu Dhabi" which was opened in November 2017 (UAE) and had been developed by the winner of the Pritzker prize architect J. Nouvel. In this complex city with exhibition area about 8000m^2, 55 Museum buildings are covered with a floating dome.

The complex pattern of the dome, as a result of geometric design repeated in different volumes and angles, is formed by eight layers, which are arranged in a certain order (four outer one and four inner one), which gives the dome an exquisite mesh structure, which realizes the constant struggle of shadow and light expressing the nature of this country. The geometric lace dome of "Louvre Abu Dhabi" creates the impression of intertwined palm leaves traditionally used in this country as a roofing material producing the effect of "rain of light" (Fig. (5) [7]. Inside the huge "floating" dome, the rain of light patterns illuminates the micro-city small galleries, lakes and landscapes.

The dome covers two-thirds of the Museum, creating shading and reducing energy consumption. In addition, the Museum complex passes light through the underground water channel, turning the space into a refreshing oasis. An example of dynamic reception in natural light control is the al Bahr office towers in Abu Dhabi, which also have a sun protection system. Fully glazed buildings have a movable facade consisting of 2000 dynamic panels, which can completely close or open the facade areas. The panels are equipped with photovoltaic cells, which react to sunlight and accumulate solar energy (Fig. 6),8]. This allows you to reduce

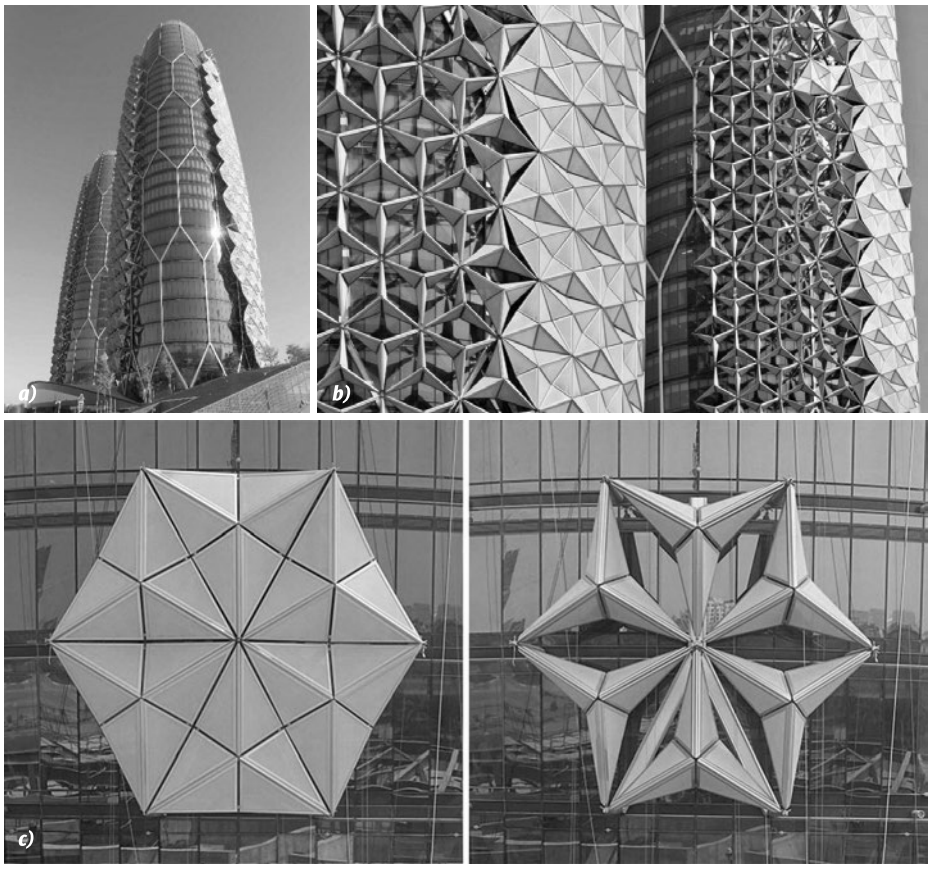

Fig. 6. The system of sun protection in the office towers "Al Bahr" in Abu Dhabi:
a – general view;
b – modification of sun protection devices;
c – transformation scheme panels

the temperature of the rooms and supply buildings with electricity.

The art centre in Shanghai also has a movable façade built by the Foster + Partners Bureau and the Heatherwick Studio [9]. A feature of the complex is a constantly changing, dynamic facade, which, in accordance with the required lighting of the interior space, can be transformed and significantly changes building view by moving a set of bronze pipes arranged in three rows and covering the main volume of the building, Fig. 7, [9].

Protection from solar radiation and control the fluorescent light causes the necessity of development and implementation in the development of kinematic methods of formation and functioning of architectural objects. This is due to the fact that natural changes and the nature of human activity determine the contradiction between the static and dynamic components of the environment under the influence of constantly changing factors of socio-cultural and natural environment.

4. ORGANIZATION OF LIGHT ENVIRONMENT OF ARCHITECTURAL OBJECTS

Innovative approaches to the formation of habitat are directly related to the modelling of natural light in the organization of the light environment of architectural objects.

This is manifested in the creative pursuits of the Swiss architect P. Zumthor. In 2010, the architect

Fig. 7. Dynamic facade of the art centre in Shanghai (China): general view (transformation options)

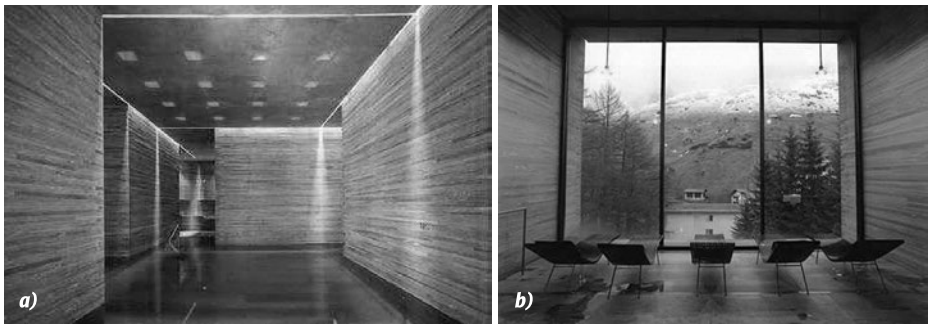

Fig. 8. Baths in Vals (Switzerland): a – the interior of the pool; b – the interior of the restroom

P. Zumthor won first prize at the prestigious competition "Daylight – Award" (in the category "Architecture")[1] for the project term in the Vals.

The thermal baths in the Vals, according to experts, gave reasons to take in attention the relationship of properties of water and stone, light and shadow (Fig. 8) [11]. At the same time, the light in the building of the Museum "Columbus" of the Cologne diocese plays a crucial role – "it snatches out space in time and broadcasts it to people, offering them to decide on the time." (P. Zumthor). Significant for P. Zumthor the construction of the chapel of St. Benedict in Sumvitg (Graubünden, Switzerland) (Fig. 9), [10, 11] may be attributed to an analogical case.

The trend of using bionic methods of consumption of the maximum amount of solar energy throughout the day is manifested in the project "solar cycle", developed by the architectural Studio "Paolo Venturella & Meno Meno Piu Architects" for the amusement Park "Freshkills park " (New York, USA). The object is both a large-scale solar battery and a multi-purpose pavilion for concerts, sports events, lectures, etc. The shape of the building structure aimed at the trajectory of the sun collects its rays at all angles (Fig. 10) [12]. The "solar cycle" has two surfaces. The first one, the photoelectric surface, looks always to the Sun, and the second one, the mirror, reflects everything around and multiplies the entertainment of the landscape distributing natural light under the closed part of the pavilion. In addition to the well-known and sufficiently detailed methods of collecting and concentration of natural light, the most effective solution is guaranteed by light-water systems [13, 14]. Such systems collect natural light through light intakes, installed on the roof and walls, and transmit it into the interior through hollow pipes with mirror surfaces.

The application in architecture of methods using biologically useful structures are the subject of research and design of architectural objects by many creative groups of architects, using in their activities, the methods of computational design.

[1] It should be noted that the idea of evaluating architectural works in the context of modelling light belongs to the Swiss foundation VELUX STIFTUNG, since 1980 supporting and financing projects related to the study of natural light and optimal possibilities for its use in medicine and architecture [10].

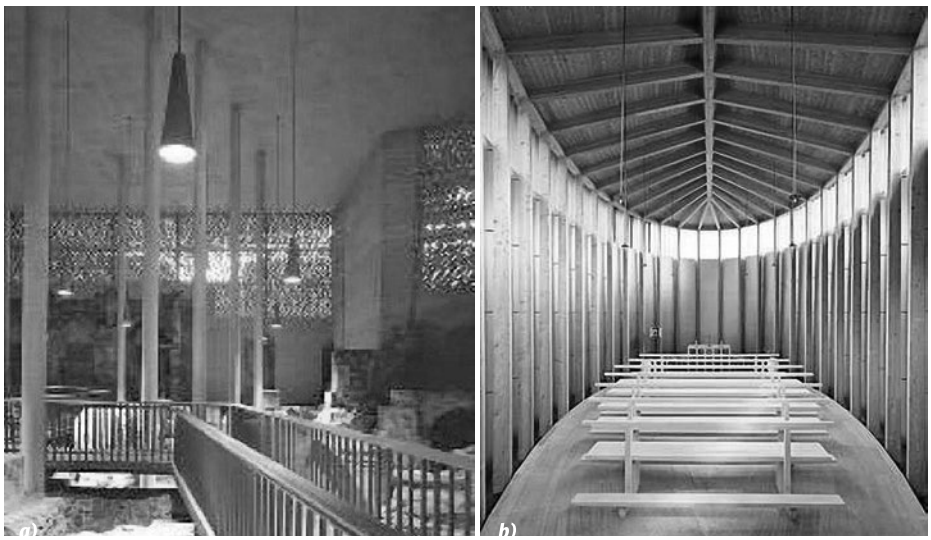

Fig. 9. Architecture of natural light by Peter Zumthor:
a – Museum, Cologne diocese of Columbus;
b – St. Benedict chapel in Sumvitg

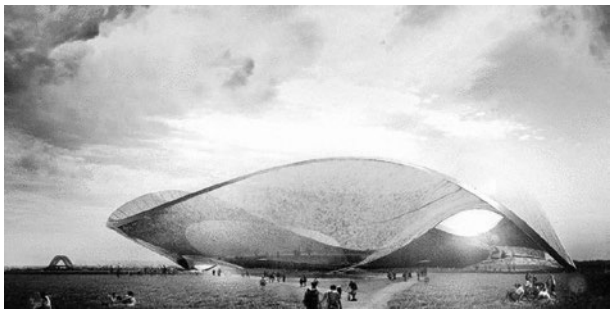

Fig. 10. Pavilion " Solar cycle"

The progressive direction in the development of architecture, using new environmentally friendly technologies in the creation of project proposals, is associated with a new attitude to the importance of maintaining of the environment and to the conservation of energy.

5. ENERGY POTENTIAL OF NATURAL LIGHT

Alongside with the considered methods of natural light modelling, the potential possibilities of solar radiation energy management arouse professional interest now. So, according to a well-known legend, Archimedes almost completely burned the Roman fleet, which attacked in 212 BC his native Syracuse in Ancient Greece to do this, he used an array of concave mirrors made of polished copper [15]. On the other hand, architects have always considered and took into account the power of solar lighting of buildings. And it is fraught with failure to account for force majeure situations. So, the new skyscraper, "Walkie-Toki", in the financial district of London, thanks to its configuration, reflects sunlight so intensely that it is able to melt the plastic parts of cars parked nearby (Fig. 11) [16]. The correct using of solar energy was demonstrated in 1970, in the creation of the solar furnace in Von ROM-Odeyo (Eastern Pyrenees, France) as an ecological source of high temperatures. The mirror structure has a diameter of 54 m and consists of 10,000 concave mirrors that reflect and focus the Sun's rays on a size measuring 40 cm diagonally. The group of mirrors acts as a parabolic reflector, which concentrates light in its focus. The furnace power is 1 MW. While on the contrary a parabolic mirror set a heliostat is a special mirror 63 plate with 180 partitions. The array of mirrors acts as a parabolic reflector, concentrating light in its focus. Each heliostat has a parabola sector, which reflects the collected light. On the concave mirror the Sun's rays gather at the point of focus, where the temperature reaches 3500 °C, and the temperature in the huge solar furnace can be adjusted by installing mirrors at different angles. Heliostats move after the Sun to maximize the collection of solar energy (Fig. 12) [17]. An illustration of the potential use of solar energy is the Solar Ark, the largest solar energy monument in Gifu (Japan) created by the company Sanyo, which is connected with the 50-year history of human relations with clean energy. A large photovoltaic system (declared maximum power of 630 kW) is combined with a modern scientific centre. The building has a "Solar energy Museum" and "Solar laboratory", which hold symposiums and forums to discuss problems and exchange ideas (in cooperation with the science Foundation of Japan and international organizations). The total length of the structure-315 m, height is the 31.6 m in the centre and 37.1 m at the edges, width is the 13.7 m at the bottom and 4.6 m at the top, weight is the 3000 tons.

Fig. 11. The skyscraper "Walkie-talkie", (London)

Fig. 12. Solar furnace in the Pyrenees (France)

Fig. 13. Solar energy monument "Solar Ark" (Japan):
a – facade; b – general view

The number of photovoltaic cells is equal to 5046, in the dark time on the façade 77200 cells of red, blue and green LEDs, controlled from a computer, are switching on.

The complex has water and air purification systems (95 tons of carbon per year).

"Sunny ark" is surrounded by a kind of Aqua Park, which includes fountains and two ponds, each of which has a waterfall (Fig. 13) [18]. The interior lighting of the complex is carried out by "Solight" lamps (unique products equipped with a compact engine controlled by a small solar battery), which automatically change the direction of radiation in accordance with the movement of the Sun in the sky, which is used as a source of natural light due to the lack of Windows in restaurants and other rooms.

In this regard, it is important to note the need to revise the usual means of architecture, taking into account the achievements in other fields of science and technology, especially to improve the comfort and safety of the environment, as well as to save financial costs and energy resources.

6. CONCLUSION

The typology of architecture is updated today with new types of architectural objects, which are the scientific and technological denominators of our epoch. Innovative ways of using natural light as an important component of the environment are presented in this article-review in the context of the conceptions considered in it.

The concentration and transportation of natural light change the perception of the surrounding space during the day and as the seasons change.

There is a possibility of natural lighting of underground spaces. More and more new ways of collecting of the natural light and creating "artificial sunlight" for the device to simulate realistic natural lighting in enclosed spaces are being invented.

Modern methods of working with light in different areas of man's activity are manifested in the sun and natural light control, which are associated with the use of new kinematic techniques of formation and functioning of architectural objects, using innovative approaches to working with light and manifested in two forms: static and dynamic. This indicates the need to revise the usual means of architecture and to expand the use of achievements in other areas of science and technology. Alternative approaches to the organization of the light environment of architectural objects are manifested in the creative researches of modern architects-researchers of light, sound and space. The emergence of the concept of "living light" and the trend of using bionic methods of consumption of the maximum amount of solar energy during a day is manifested in the developments of architectural objects, which is associated with a new attitude to the value of the environment, conservation of energy, increase comfort and safety of the people habitat. The energy potential of natural light (p. 5) and control of the latter are of the professional interest. A competent attitude to the use of natural radiation would be impossible without appropriate technical means and the development of high technologies, without the application of environmental principles in architecture.

The considered directions in the use of natural light, as an important component of existence, indicate the breadth of methods of its manifestation, and the variety of means of its transformation and regulation. In this regard, it should be noted that these examples of the use of natural light in the formation of the architectural environment arose due to many areas of knowledge, which are developing very actively.

The obtained results can be useful for the theory and practice of habitat formation, opening up completely new opportunities in architecture. This sets the task of further research of completely new methods of work in this direction.

REFERENCES

1. R. Narboni, V. Nicholas "A Light Trap in the Lobby of the "Eqho Tower" in the Quarters of the Défense (Paris)" // Light & Engineering, 2015, V. 23, № 1. pp. 25–32.

2. Starostina A. Trap for light. / http://www.archplatforma.ru/?act=1&nwid=3587 (date of access: 28.02.2018).

3. The designer has developed an artificial "sunlight". CoeLux, URL: http://www.sveto-tekhnika.ru/ru/businessnews-3/pages/business/coelux (date accessed: 11.03.2018).

4. Two-dimensional trap for light is created.

URL: http://www.nanonewsnet.ru/news/2015/sozdana-dvumernaya-lovushka-dlya-sveta (date accessed: 09.03.2018).

5. Zemtsov V.A., Soloviev A.K., Shmarov I.A. Brightness parameters of the standard sky of MKO in calculations of natural lighting of rooms and their application in various light-climatic conditions of Russia// Light & Engineering, 2017, V.25, № 1, pp. 106–114.

6. Dvoretskiy A T., Morgunova M.A., Serghey-chuk O.V., Spiridonov A.V.

Methods of designing of fixed shading devices // Light & Engineering, 2017, V.25, № 1, pp. 115–120.

7. "Rain of light" under the dome of the Louvre Abu-Dhabi //. URL: http://green-buildings.ru/ru/dozhd-sveta-pod-kupolom-luvra-abu-dabi (date accessed: 11.03.2018).

8. Buildings Shield Themselves From Sunlight In The Most Unusual Way. URL: http://corevertical.com/Page/Buildings_Shield_Themselves_From_Sunlight_ In_The_Most_Unusual_Way (date accessed:: 13.03.2018).

10. Tsekhmister T.I., Peter Zumthor

URL: http://book.uraic.ru/project/conf/txt/005/arch-vuz22_pril/33/template_article-ar=K41–60-k49.htm (date accessed: 12.03.2018)/

11. Yurkina O. Architecture as poetry of light. URL: http://nashagazeta.ch/node/8419 (date accessed: 11.03.2018).

12. Solar Loop-energy self-supporting pavilion in a New York Park URL: https://econet.kz/articles/2975-solar-loop-energeticheski-samoobespechivayuschiysya-pavilon-v-nyu-yorkskom-parke Oh? (circulation date 10.03.2018)

13. Aizenberg Ju. B., Bukhman G.B., Korobko A.A., Pyatigorsk V.M. Several Unrealized Constructive Solutions of Optical Schemes and Lighting Systems with Hollow Light Guides// Light & Engineering, 2016, V24, № 4, pp. 4–13.

14. Aladov A.V., Biryuchinskiy S.B., Waluchow V.P., Saglam A.L., Taleisnik N.A. Chernyakov A.E. Dynamically controlled lighting system with LEDs with wide range of color temperatures (2800–10000) K and a high colour quality (Ra > 90) // Light & Engineering, 2017, V.25, № 1, pp. 65–74.

15. Deadly Sun: Mirror of the Third Reich / / URL: http://paranormal-news.ru/news/ubijstvennoe_solnce_zerkalo_tretego_rejkha/2013–04–03–6568?from=mirtesen (date of circulation: 11.03.2018).

16. Architecture sunlight // URL: http://turupupu.ru/?p=23942 (date accessed: 13.03.2018).

17. Solar furnace in the Pyrenees. Green source of high temperature // URL: http://greenevolution.ru/multimedia/solnechnaya-pech-v-pireneyax-zelenyj-istochnik-vysokix-temperatur/ (accessed: 11.03.2018).

18. Sanyo Solar Ark.(the world's largest solar energy monument) / / URL: http://www.membrana.ru/articles/technic/2004/02/27/213200.html (circulation date 11.03.2018)

Natalia A. Saprykina,
Prof., Dr. of Architecture, graduated from the Moscow Institute of Architecture (MARKHI) in 1970. At present, she is a Leader of the chair "Fundamentals of Architectural Design" of the Moscow Architectural Institute (MARKHI), Honoured architect of the Russian Federation, a member of the Moscow Union of Architects

Light & Engineering
Vol. 27, No. 2, pp. 32–41, 2019 *https://doi.org/10.33383/2018-069*

THE SUN RAY AS A TOOL TO DESIGN AN ARCHITECTURAL FORM

Nicolai L. Pavlov

Moscow Architectural Institute (State Academy, MARKHI)
E-mail: pavlovnl@mail.ru

ABSTRACT

The regularities of constructing crucial architectural forms are shown based on the architecture of Ancient Egypt, Western Europe, and Russia: obelisks, pyramids, statues, tents, and spires. It is shown that the source of projection for these and some other architectural forms was the Sun[1] or its image in the shape of a golden ball. The sun ray is serving as a tool for solar elevation.

Keywords: sun ray, solar projection, projection angle

1. INTRODUCTION

The topic of the sun, its light, the sun ray as the physical phenomena and the source of life on the Earth is studied by almost all natural sciences: astronomy, physics, chemistry, biology, etc. Its influence on the structure and properties of living and non-living matter, climate, life of animal and vegetable worlds, and, of course, on humans is being studied. It turns out that, under conditions of our recently formed industrial civilization, different kinds of solar emission influence functioning of most engineering systems.

The Sun and sunlight have formed a set of pre-scientific and religious understandings in the traditional cultures that were developing for thousands of years. These understandings have determined the evolution of the human culture in many ways.

The role of the sun and sunlight in relation to architecture, built environment, structures, and their complexes, is analysed in sufficient detail. In some instances, this role is determined by respective technical and medical standards regarding orientation, solar exposure, etc. The role of the sun in the professional architectural environment is usually considered a presentation of general and detailed appearance of buildings, which creates the best conditions for perceiving their architecture. We can talk from that perspective about the influence of the sun and sunlight on modern architectural form-making.

Apart from other obvious technical, biological, and utility factors, the role of the sun in traditional cultures for constructing any architecture was determined by a notional setting based on the natural role of the sun in the world. During many thousands of years, the system of common and religious images of a godly and creative role of the Sun was created based on that setting. The key to revealing the meaning and setting of the wide range of architectural approaches which determined the form-making from extreme antiquity to our times may be a typical image of the Sun as the creator of everything in traditional cultures.

2. THE OBELISKS, PYRAMIDS, AND STATUES IN ANCIENT EGYPT

When talking about the role of the sun in architecture-setting, it is essential to look at the architecture of Ancient Egypt where the cult of the Sun prevailed for almost 3,000 years. The beginning of the solar cult dominance is already noted in the age of *the Old Kingdom* in the days of *Pharaoh Djoser*

[1] By request of the author, *the Sun* in a number of cases is capitalized (ed. note).

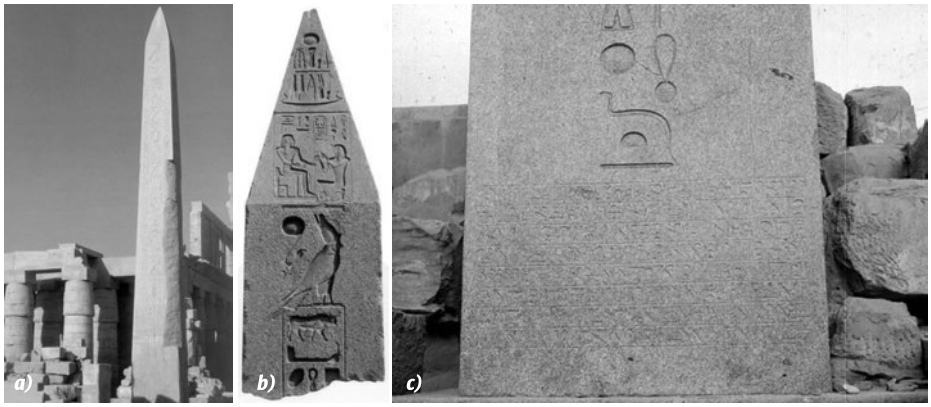

Fig. 1. The obelisks:
a – Thutmose III;
b – Ramesses II;
c – Hatshepsut

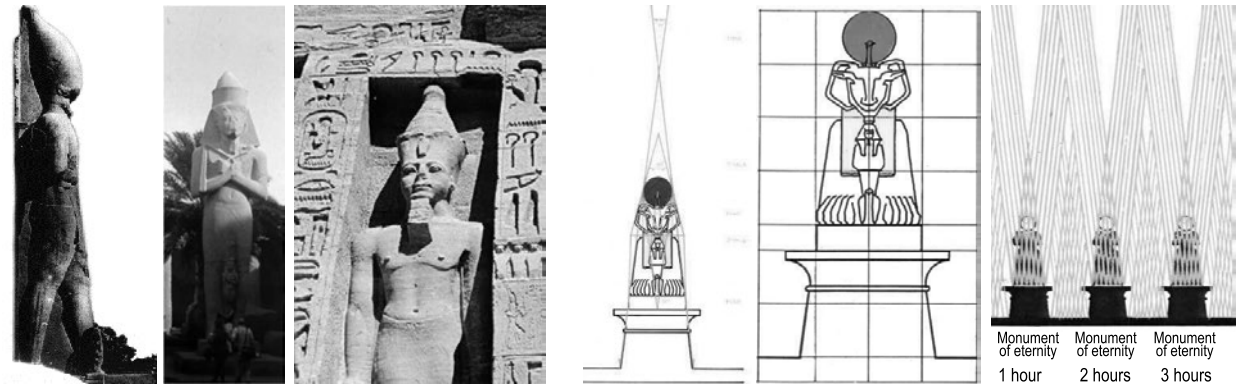

Fig. 2. *a* – the statues of Ramesses II in the Ipet-isut[1] Temple [1] and Abu Simbel; *b* – the radial and modular arrangements of the sphinxes in front of the western pylon of the Ipet-isut Temple

[1] The temple that we know as *the Amun-Ra Temple* in Karnak was called *Ipet-isut* in Ancient Egypt, i.e. the chosen place for the residence of the god. The temple that we know as *the Luxor Temple* was called *ipet resyt* in Ancient Egypt, i.e. the harem of the god.

known for his funerary complex with a first big step pyramid (28th c. B. C.)[2].

Let us start with the construction of an obelisk. This theme has received little attention in terms of the aspect covered by us. *Herodotus* noted an obelisk as the ray of the sun on the earth. *Marie-Henri Stendhal*, a faithful soldier of *Napoleon* and a future writer, noted that in his Egyptian diary.

Our goal is to show the architectural means that allowed to reach that effect. Let us start with the shape of an obelisk. Its tetrahedral pillar has a face widening from top downward from 1.5 to 0.5°. The classic obelisk of *Queen Hatshepsut* almost definitely has 35' which is equal to a visible angular scale of the high sun. The pyramid-shaped top of the same obelisk called *pyramidion* by the Greeks has a 30° top forming angle which is equal to 2 hours of solar motion on the horizon[3]. The upper part of pillar ribs was covered with white gold or *electrum* (green gold) as early Greeks called it[4]. The pyramidion was covered with similar gold.

The top of the obelisk, ribs framed with white gold in some cases, had literally represented a vertical sun ray. It was always possible to find the bearing point of the ray reflected from the pyramidion in the field. The pyramidion faces were made

[2] There are differences of opinion among scholars concerning dating from the 28th to 27th c. B. C. [1, p. 265; 2, p. IX; 3, p. 12].

[3] Daylight time in the Ancient times and the Middle Ages was calculated with 12 hours similar to a solar year that had 12 lunar months. Daylight time had different length in different seasons before invention of a water clock in the Hellenistic period and with invention of a mechanical clock in the Middle Ages. However, it was enough to determine the mean angle of a sun dial with a sun clock which was knows in Egypt in the age of the Old Kingdom, as well as with special surveys of solar motions on the horizon. There are indications of a 24-hour daytime notion appearing in Egypt in the 19th c. B. C.

[4] So called *white gold* is still very widespread in Egypt.

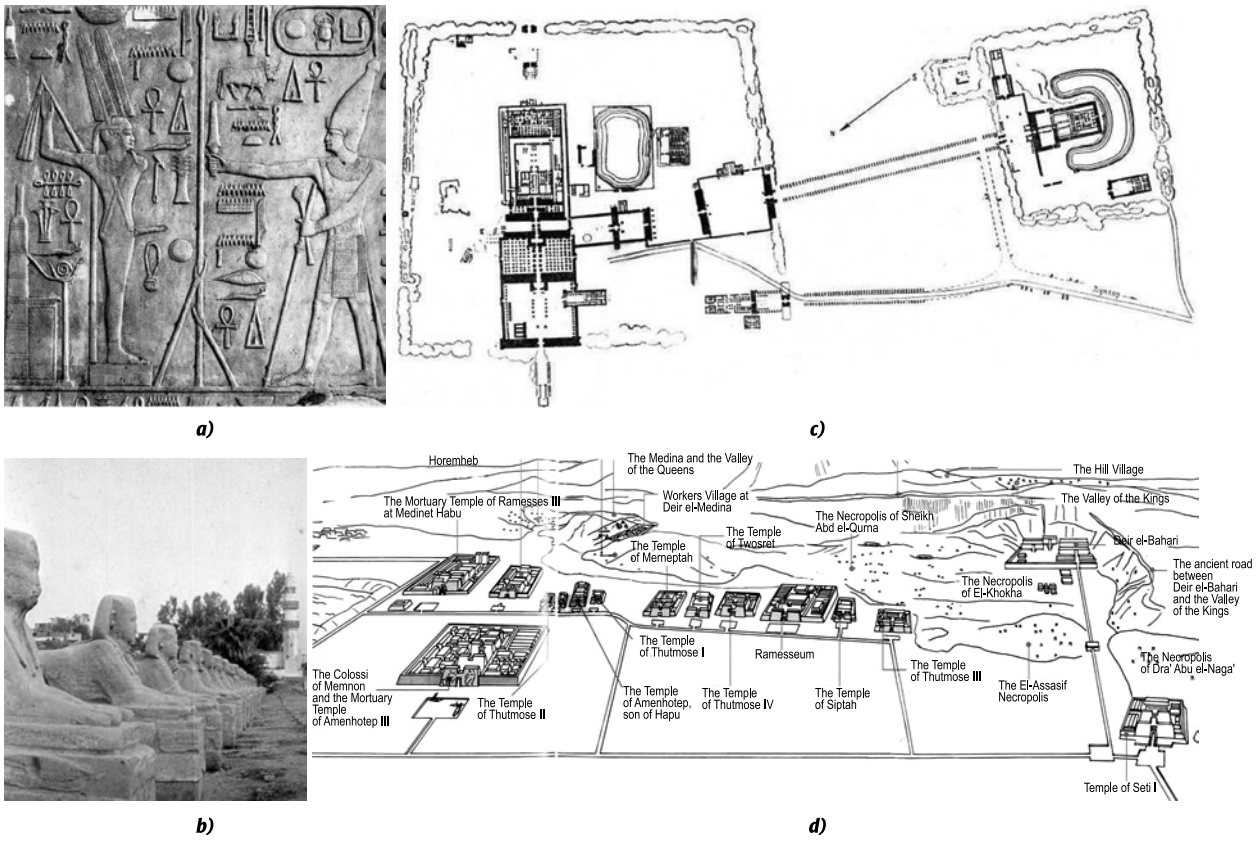

Fig. 3. Luxor: *a*, *b* – Amun-Ra as ithyphallic Min gives birth to the Pharaoh-headed sphinxes, his children, with his semen ray; *c, d* – the avenues of the sphinxes confirm the ritual path of the god, the giver of life, in the temple system of the eastern and western banks of the Nile

a bit out-bowed (curved) in early obelisks. As a result, the ray reflection from curved gilded face was visible almost for the whole daylight time. The obelisks at the entrance pillars of the temple created a special effect at the sunrise. They were taller than temple walls. Their tops were illuminated first by rays of the rising sun. It is not a coincidence that *Hatshepsut* wrote this at the pedestal of her obelisks: *"Their rays illuminate Both Lands when our Father rises between them."*

The images and texts on granite faces of the obelisks are a whole new topic. The faces show the Pharaoh kneeling down in front of the throne of his Father, the god of the Sun. There is a *serekh* – a conventional design of a palace with falcon-headed *Horus* – at the top of pillar faces. The divine text flows from this palace to the pedestal of the obelisk. The Ancient Egyptians, similar to people that possessed scientific knowledge of the 20th century, considered the sun ray to contain some sort of information. It was a text of a divine and solar origin in their case. The text ended with *zet* that means eternity (Fig. 1).

The sun ray falls on the earth, petrifies, and becomes a granite pillar and the monument to eternity. This is how the Ancient Egyptians called their sacral constructions: pyramids, temples, obelisks, steles, and statues[5].

The son of the Sun – the Pharaoh – represented in different forms such as walking, standing, sitting, and lying statues (sphinxes) has been the obelisk in its initial form. They all fit into the contour of the obelisk, the top forming angle of which is around 30°. Many walking statues are literally coming out from the obelisk, presented in a form of a stele behind their back. The sun ray which falls on the earth gives birth to children of the Sun – Pharaohs. The sun ray demonstrably burns into the rock, and the figure of *Ramesses II* appears in the famous *Abu Simbel Temple* (Fig. 2a).

The momentum of posture usually correlates with its proximity to the sanctuary. The closer to the sanctuary: the more powerful is the creating ability of the god of the Sun and the holier is the land where it falls. The god and the Pharaoh are shown walking

[5] Cf. generally accepted modern terms as *historical landmark*, *cultural landmark*, *architectural monument*, *ancient manuscript*, etc.

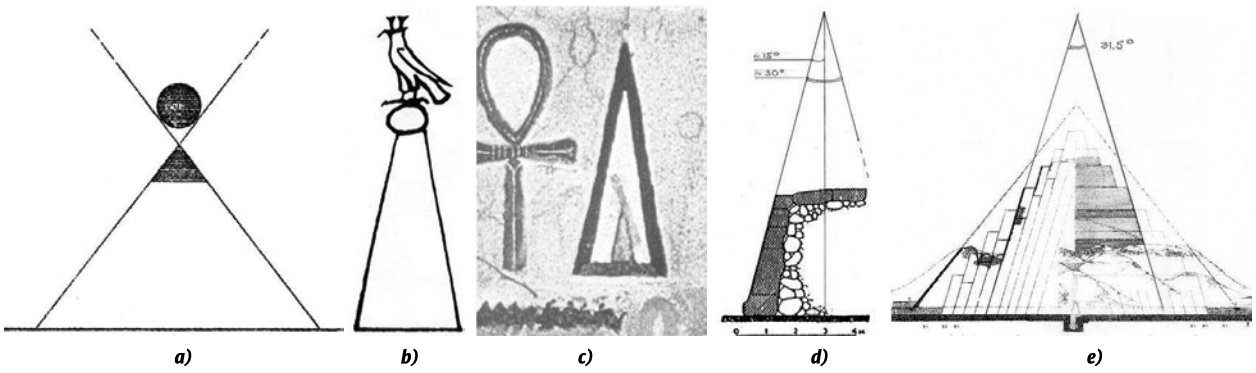

Fig. 4. The Ancient Egyptians imagined and built pyramids from the Sun, with an angle of about 30°: *a* – the scheme of from-the-Sun projection of the outer contour of the pyramid; *b* – the Ancient Egyptian images of the pyramid; *c* – the construction of the traditional tombstone, mastaba; *d* – the construction of the inner structure of the pyramid for Sneferu, the 1st Pharaoh of the Dynasty IV, 27th-26th c. B. C.

both in and before the sanctuary. The throne statue of the Pharaoh, the son of the god and the king on the earth, is put before the pylon of the temple. The Pharaoh begotten by the sun ray in the body of a lion – the king of animals – is shown at the avenue of sphinxes.

The contour of the sphinx is projected from the Sun with an angle of 15°, i.e. through hourly motion of the Sun on the horizon. The 15° contour of the solar sphinx with the head of a ram is completed with a demonstrable image of the contour of the obelisk with a top forming angle of 30°. The stone disk covered with white gold between the horns of the ram used to serve as the upper base of the contour. This golden disk demonstrably represented the Sun as the source of projection, the divine creator of the ram-headed sphinx, the patron of the image of the Pharaoh under its beard.

The sphinx was a procreation of the Sun, a solar projection, for both the architect and the worshipper of *Amun-Ra*. The golden disk was a sacral block equal to the ell of the king, 52.5 cm, for stonecutters who cut the sphinx out of the stone block using a modular grid.

The altar pedestal of the sphinx at the avenue before the western entrance to the temple, from the side of the Nile (Egypt), which shows the cosmic journey of *Amun-Ra* from east to west, is projected with a 15° top angle. The sun ray gave birth to the ram-headed sphinx when it fell on the altar pedestal, the monument to eternity. The hourly shift of the sun ray with a 15° angle was focused by 2 cornices between the pedestals. The sun ray measured 1 hour of real time, 1 hour of life, with the 15° angle between the sphinxes. One of the hymns to the god of the Sun says:

"You are far away, but your rays are on the earth. You are in front of the people, your motion."

Amun-Ra was shown as *Min*, the giver of life, in the avenue of the sphinxes. He walked south in an ithyphallic form to the female temple: first to the temple of his spouse, *Mut*, and then to his own harem temple in Luxor (Egypt). It is interesting that, upon exiting from his own temple, *Amun-Ra* was turning left, to the South, "answering the call of his heart", and walking down the avenue of the sphinxes to the temple of his spouse. When exiting the temple of the spouse and heading to the harem temple, he was turning left again. He was walking down the avenue of the sphinxes, passing the temple of his son, *Khonsu*, all the way to the temple in Luxor (Egypt). He was dropping not just a ray, but a seed ray, along the way. An hour-long sun ray with the 15° angle was falling there on the altar pedestal and giving birth to the Pharaoh-headed sphinx. The sun ray gave birth to real vegetation: fruit trees planted in ditches between the sphinxes. The motion of *Amun-Min*, the giver of life, was shown with a huge system of sacral avenues on both sides of the Nile (Fig. 3):

"You are walking like father, giving birth to children, bringing heirs into the world, pristine for your children. ...His spouse is the earth, which he inseminates" (*Leyden Papyrus*). *"The semen of the god is good, coming in front of him,"* said architect *Ineni* about *Queen Hatshepsut* ([5, p. 330], [8. p. 56], [6, p. 59]).

The West European Egyptology studies architectural monuments based on translated texts and archaeological data including excavations data, i.e. from the ground. The same from-the-ground approach is used when dealing with the issue of build-

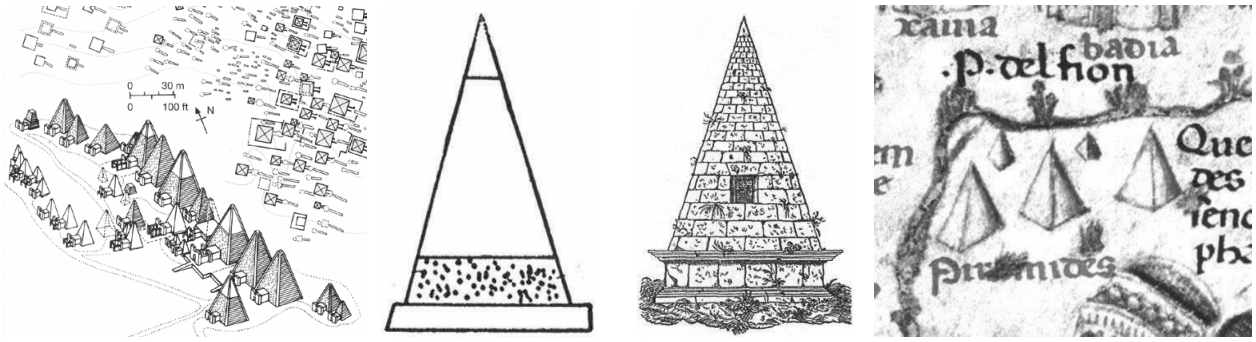

a) *b)* *c)* *d)*

Fig. 5: *a* – the small pyramids in Meroë, first centuries; *b, c*, *d* – a pyramid drawn by an Ancient Egyptian artist (*b*) and by a Western European artist of the 15th c. (*c, d*)

ing pyramids: the parameters of the base and the angle of the face slope to the foundation are meticulously measured.

The obvious fact that the Egyptians thought about building a pyramid not from the ground but from the Sun as their main deity is somehow lost in this approach. With that approach, the top of the pyramid should be considered as a starting point of the projection, and it is necessary to calculate not the angle between the face and the base, but the forming apex angle, the angle of a solar projection that creates the pyramid.

The top of the pyramid and the top of the obelisk were ornamented with gold-covered stone, a shining pyramidion. The faces of the pyramid were coated with white limestone from stone mines in Tora located opposite of Giza, upstream of the Nile (Egypt). The top of the pyramid and the top of the obelisk shone with sunlight reflected by white gold.

It is important to note the fact which is usually addressed only through the constructive point of view when describing pyramids: the pyramid had not one but two apex forming angles.

The angle that shaped the outer contour of the pyramid is evident to everybody. This angle – the projection angle of the outer contour faces for the big pyramids of the Old Kingdom and the Middle Kingdom – oscillated about 52° within 45 to 70°.

The other angle, hidden in the body of the pyramid and forming its inner structure, usually is about 30°. This angle is evident in memorial tombs, *mastaba*, since the first dynasties. It is also important that this angle and its solar projection exist in different representations of pyramids. The life-bearing role of the sun is shown with green colour, the colour of vegetation, both inside and along the outline of the pyramid. This proves that the ancient Egyptians built a pyramid and thought about it as a construction with an apex forming angle close to 30°.

The Egyptians could not build a big pyramid with apex forming angle close to 30° and a 200-meter foot side. The height of the pyramid would be more than doubled with such size of the base. Limestone and sandstone blocks in the base would also break down under the pressure. When there was no necessity to build huge pyramids, small pyramids with an about 30° apex forming angle and a chalkstone top were built on a massive scale (Figs. 4, 5).

3. THE TENTS AND SPIRES IN WESTERN EUROPE

The Europeans that visited Egypt in the middle of the 15th century depicted the pyramids with an approximately 30° apex forming angle, just like the ancient Egyptians designed them. Mediaeval Christian Europe did not save such a developed cult of the Sun as Ancient Egypt. But the image of a deity of the Sun that creates life with its ray lived deep inside the traditional folk-life culture from the earliest times. It is natural that tents crowned with a golden ball above the temples were seen as the sun ray which blesses the land, the church, and the man. The world perceived the European cities as the magnificence of dozens of tents and spires. There were tents with an apex forming angle close to 30°.

It is obvious that the obelisks taken out of Egypt by the Roman Caesars and *Napoleon* were naturally but not always consciously perceived by the Europeans as the procreation of the Sun. The obelisks were put up in front of the churches in Ancient Rome and later in Papal Italy. There are much fewer sunny days in Europe and even in Italy

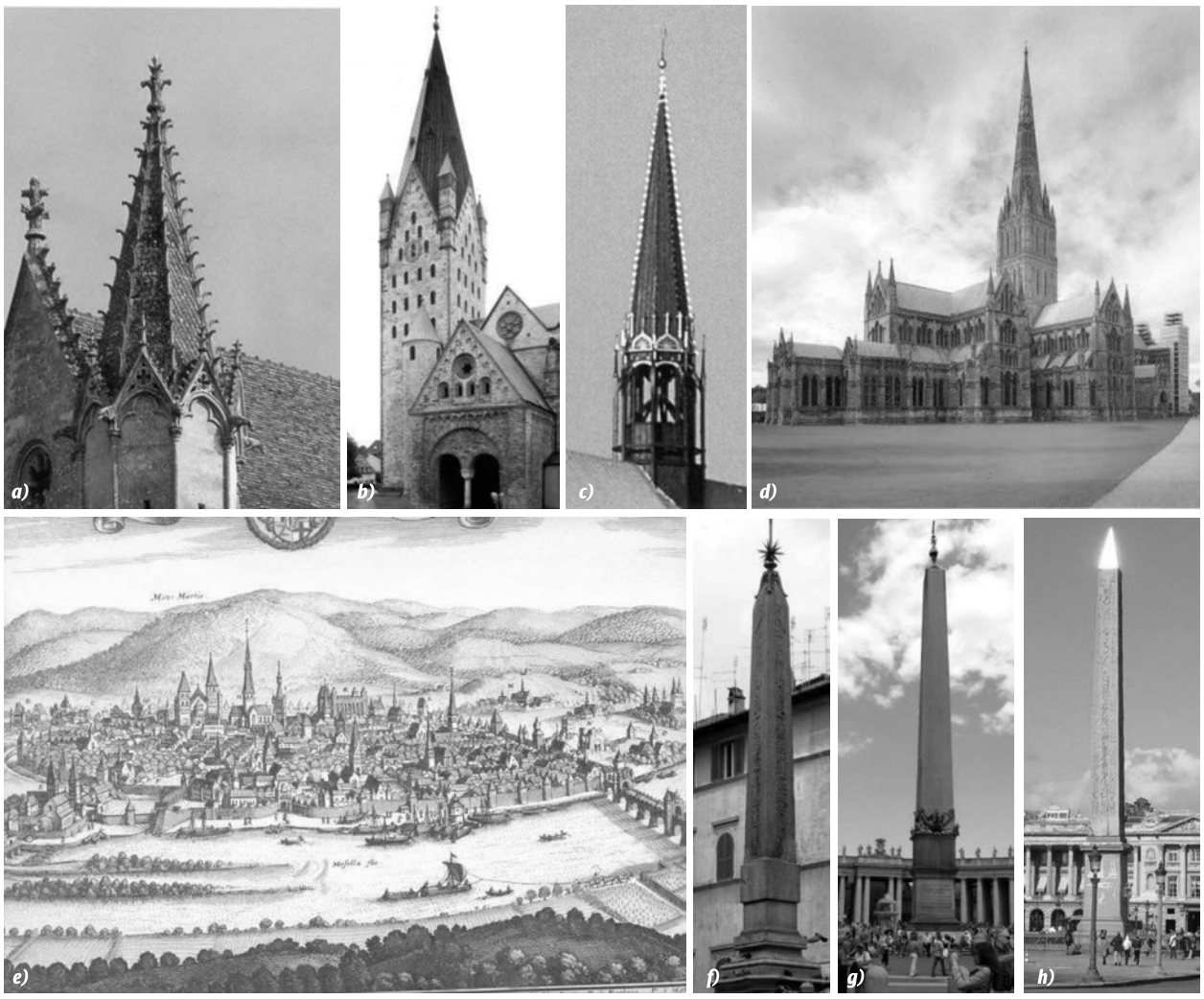

Fig. 6: *a* – the Church in Saint-Germer-de-Fly Abbey (France, 13th c.); *b* – the Church of Saint Patrokli, Soest (Germany, early 13th c.); *c* – the Saint Mary's Church, Lübeck (Germany, early 14th c.); *d* – the Cathedral Church of the Blessed Virgin Mary, Salisbury (England, 13th-14th c.); *e* – the tents and the spires in Trier (Germany); *f* – the Egyptian obelisk in front of the City Church, Rome (Italy); *g* – the Egyptian obelisk in the square in front of the Saint Peter's Basilica, Rome (Italy); *h* – the Egyptian obelisk in Place de la Concorde, Paris (France)

than in Egypt. The obelisks and church tents were crowned for more clarity with a golden ball or a depiction of the Sun with outgoing rays. The Egyptian obelisk was put in a place in *Paris* (France) where, during the French Revolution, stood the guillotine that executed thousands of people, and the square was renamed to *Place de la Concorde*. The pyramidion of the obelisk was made in modern time as shiny as it was in Ancient Egypt (Fig. 6).

4. THE TENTS, SPIRES, AND OBELISKS IN RUSSIA

Temples, royal mansions, and fort towers in Russia were crowned with tents from the earliest times. Russia had no white gold but aspen. Simple-shaped roofs were covered with aspen boards, and complex-shaped roofs were covered with an aspen shingle. Aspen is a hydrophobic wood. The aspen roofing turns silvery after 2–3 years. The aspen roofing looks silver against the background of a cold northern sky and in a cold northern sun.

With stone construction, tent churches became more widespread. An apex forming angle was around 30° even more often in Russia than in Western Europe. A copper or gilded ball was put up instead of a wooden ball at the upper base of the tent. The tent was projected from that golden solar ball. It is not a coincidence that the height of the temple in texts describing the construction order and later in reports on measurements was set as *up to the apple*. The ball may have been combined with a gold-

Fig. 7. The tents in the Russian architecture: *a* – the Trinity Church in Nyonoksa (early 18th c.); *b* – the Saints Zosima and Savvaty Church, the Trinity Lavra of Saint Sergius (early 17th c.); *c* – the Church of Ilya the Prophet, Yaroslavl (middle 17th c.); *d* – the Spasskaya Tower, Moscow (Kremlin); *e* – the tents on the Palace of Tsar Alexei Mikhailovich in Kolomenskoye near Moscow (middle 17th c.), watercolour by G. Quarenghi (18th c.); *f* – the tents on the Kremlin (engraving, 18th c.)

en onion dome that shone in the sun and visibly represented the celestial body in a grey sky. The golden ball under the cross was put up not only above the tents but also above the domes.

Foreign architects who worked in Russia were brought up according to the European traditions of tents and spires and perceived the Russian tent traditions as quite natural [9, p. 140–141]. *Christopher Galloway* from Scotland built a tent over *the Spasskaya Tower* at *the Moscow Kremlin* (Russia). He put up the same golden ball in the upper base of the tent. From the golden ball down the ribs of the 8-faced tent, *Galloway* stretched a chain of outbowed tiles which are alternating on yellow and green colours. The sparkling light ran down the ribs of the tent. This theme was now developed, and trichromatic illuminations are stretched over the tiles. It can be seen that the ruby star with golden strips may be perceived as a form of a golden ray star that the Catholics put up on the Egyptian obelisks.

The Russian cities were reaching to the sky towards the Sun with many tents crowned with a golden ball as representation of the sun up until the 1930s (Fig. 7).

Peter the Great built Saint Petersburg (Russia), imitating traditions of Northern Europe where spires were preferred over tents. The desire to pierce the grey sky with the sun ray can be understood since there are just over 60 sunny days in Saint Petersburg just as in Northern Europe. The crowning of spires for *the Saints Peter and Paul Cathedral* and the *Admiralty Building* with a golden ball and their projection from top downwards, from the sun, even unconscious, is also understandable. The golden ball also appeared under the royal eagle at the top of the obelisk that was put up in honour of victories by *Count Rumyantsev* over the Turks. Spires found their own perception in Russia. Commoners viewed them as a peculiar form of a tent.

The spire fashion reached the outlying north provinces in the first half of 18th century. The architect put up 3 copper spires on the top of *the Saint Gate of the Archangel Michael Monastery* in Veliki Ustyug (Russia). Copper acidifies and turns green

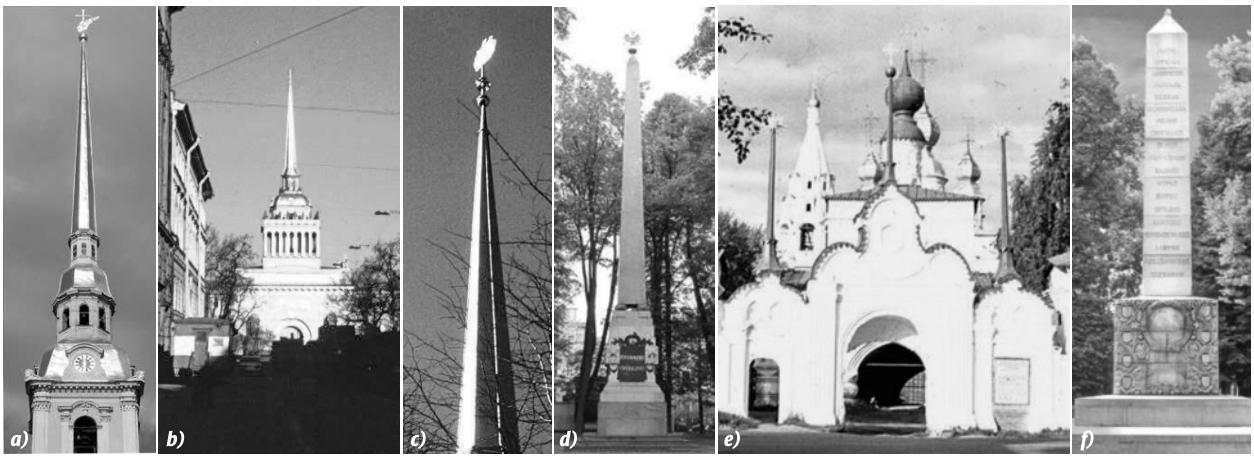

Fig. 8. The spires and obelisks in the Russian architecture: *a* – the spire over the Saints Peter and Paul Cathedral, St. Petersburg (early 18th c.); *b, c* – the spire over the Admiralty Building, St. Petersburg (early 19th c.); *d* – the Obelisk in Honour of the Victories by Count Rumyantsev-Zadunaisky, St. Petersburg (late 18th c.); *e* – the Saint Gate of the Archangel Michael Monastery in Veliki Ustyug (early 18th c.); *f* – the Obelisk in Honour of the 300th Anniversary of the House of Romanovs, Moscow (early 20th c.)

with time, and the sound keeper paints it green with no extra thought. The spire was crowned with a copper ball and a cross above the central span. The ray celestial bodies, the same as on the Egyptian obelisks in front of the Roman churches, are still shining above the side entrances even after their restoration (Fig. 8).

The obelisks were put up as monuments in honour of heroes and important historical events in Russia of the 19th and 20th centuries. Even the weird-shaped *Obelisk in Honour of the 300th Anniversary of the House of Romanovs* is crowned with some sort of a stone ball. The plywood obelisks were put up as tombstones for fallen soldiers during and shortly after the World War II. They were often crowned with a plywood star that was hastily sawed-out. They were eventually substituted with concrete obelisks crowned with a gilded star. The grave of the hero fallen for his nation should be illuminated by the sun ray (Fig. 9).

The only thing left to understand is why an apex forming angle of an obelisk, a pyramid, and a tent was tilting to 30° in Ancient Egypt, Medieval Europe, and Russia. There is one fundamental regularity that exists not only in the architecture. This mathematical regularity is usually called the golden ratio. The golden ratio is simply represented with a bisected line segment where the small part is related to the big part as well as the big part is related to the whole segment. This correlation is numeri-

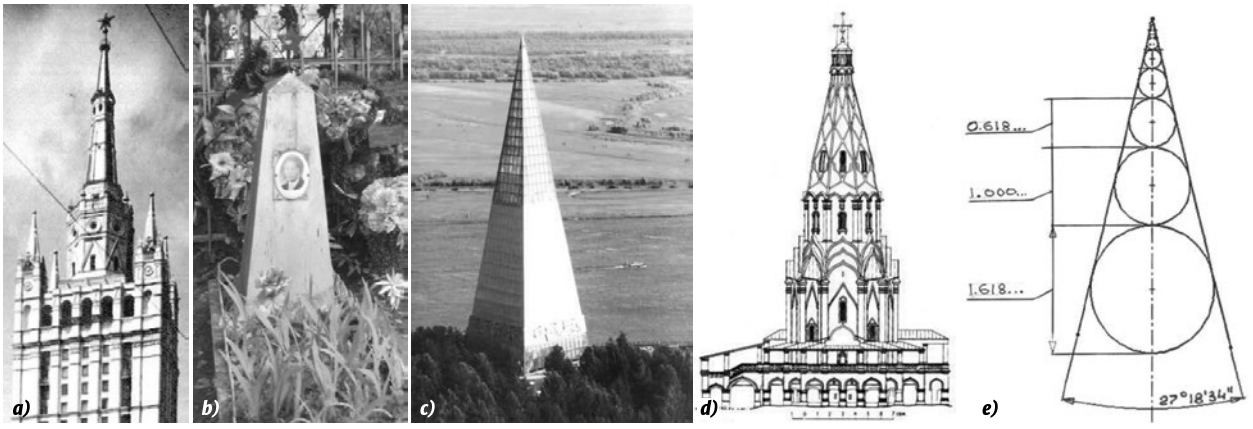

Fig. 9. The spires, the obelisks, and the tents in Russia (from the latter half of the 20th c. to the early 21st c.): *a* – the Kudrinskaya Square Building, Moscow (middle 20th c.); *b* – the obelisk on the grave of a country policeman, Vologda Region (early 21st c.); *c* – the Memorial to Yugra Oilers, Western Siberia (late 20th c.); *d, e* – the upper corner of the projection in the tent construction from the golden apple: the tent of the Church of the Ascension, Kolomenskoye, Moscow, (middle 16th c.) (*d*) and the scheme of the projection angle of the golden ratio (*e*)

cally represented as 0.618…: 1.00: 1.618… The Ancient Greeks knew about this harmonious correlation, and it was empirically used even before that. The theoreticians of the Renaissance in the 19th and 20th centuries perceived the golden ratio either mono-dimensionally – by a linear series – or bi-dimensionally – by a dimensional ratio of rectangles.

This proportional regularity was constantly found outside of the architecture and art in the construction of natural bodies: crystals, plants, animals, and human. This regularity is now found in the structure of the planetary orbits in the Solar System [4, p. 256–284]. *Pavel Florensky*, a great Russian scientist and a philosopher, wrote in 1916: *"... the golden ratio is an ONTOLOGICAL LAW; as understood before, it expresses the construction of a WHOLE BODY as such"* [7, p. 485].

When imagining a three-dimensional correlation of the golden ratio, one will get an infinitive series of spheres in the same common axis with their radii correlating as… 0.618…: 1.00: 1.618…: … (Fig. 9e). The apex forming angle for such a series of spheres will be about 27° 18' 34", i.e. 30° in rough approximation. This is one of the ontological aspects of this topic. The other aspect is determined by the construction of our eyeball, an optimum sight angle which has approximately the same angular dimensions. The whole perception of the outer world by the human is determined with these parameters. The human system of the land navigation and the choice of the motion path are based thereon. If that assumption is correct, it means that the nature created its ontological construction in the course of evolution, including the construction of people which determines their space impression of the outer world. That explains the universal human tendency to projecting architectural forms from the universal human celestial body, the Sun, with an apex forming angle of about 30°.

5. CONCLUSION

The presented set of observations allows to make some generalisations since it is based on the broad spectrum of cases from different cultural traditions related to different historical eras.

We see two factors in terms of the universal history – similar perception of natural events and their representation in human culture, including the architecture, – are naturally created by the universal essential living bases and the similarity of human reasoning. Many scientific and technical discoveries were made almost simultaneously and totally independently from each other in different countries, as we know from the recent history.

One can say in terms of a specific subject of research that the human felt a life-giving role of the Sun from the very beginning and perceived it as the source of life. This ancient belief which created a simple and natural solar cult in some historical situations and a well-developed religious system in other situations is fully proven by the modern science. It is natural that the sun ray was perceived as the bearer of the prizes of life, first unconsciously and then consciously, in some cases as the bearer of the celestial information and, of course, as a divine weapon that can give life, warm, or burn, and that can also create. There is no better example of the universal creating natural phenomena expressed in culture than the Sun and its rays.

Plutarch, a famous Greek historian of the 1st and 2nd centuries, said: *"There is only one sky above all nations, and one god has many names."*

REFERENCES

1. Dieter, A. The Encyclopaedia of Ancient Egyptian Architecture. The American University in Cairo Press, 2003, 274 p.

2. Smith, W.S. The Art and Architecture of Ancient Egypt. Yale University Press, 1998, 297 p.

3. Montet, P. Eternal Egypt: The Civilization of Ancient Egypt from Earliest Times to Conquest by Alexander the Great. Phoenix Press, 2005, 338 p.

4. Ochinskiy, V.V. Revisiting the Golden Proportion Conception in Natural Sciences // Metaphysics. 21st Century. Moscow: BINOM, Laboratoriya znaniy, 2006, 285 p.

4. Ochinskiy, V. V. K kontseptsii zolotoy proportsii v yestestvoznanii // Metafizika. Vek XXI. M.: BINOM, Laboratoriya znaniy, 2006, 285 p.

5. Turaev, B.A. The History of the Ancient East, Vol. 1. Leningrad: OGIZ-SOTSEKGIZ, 1936, 361 p.

5. Turaev, B.A. Istoriya Drevnego Vostoka, Vol. I. L: OGIZ-SOTSEKGIZ, 1936, 361 p.

6. Turaev, B.A. The Story of Sinuhe and the Samples of Egyptian Documentary Autobiographies. Moscow: Print-Shop of A.A. Levinson, 1915, 77 p.

6. Turaev, B.A. Rasskaz yegiptyanina Sinukheta i obraztsy yegipetskikh dokumentalnykh avtobiografiy. M.: Iz-vo skoropechatni A.A. Levinson, 1915, 77 p.

7. Florenskiy, P. The Works in 4 Volumes. Moscow: Mysl, 2000, Vol. 3(1), 622 p.

7. Florenskiy, P. Sochineniya v 4 tomakh. M.: Mysl, 2000, Vol. 3(1), 622 p.

8. Frank-Kamenetskiy, I.G. The Egyptian Religious Monuments in the Theban Age. Moscow: Print-Shop of A.A. Levinson, 1917, 82 p.

8. Frank-Kamenetskiy, I.G. Pamyatniki yegipetskoy religii v fivanskiy period. M.: Iz-vo skoropechatni A.A. Levinson, 1917, 82 p.

9. Shvidkovskiy, D.O. The Historical Path of the Russian Architecture and Its Connection with the Universal Architecture. Moscow: ARKHITEKTURA-S, 2016, 511 p.

9. Shvidkovskiy, D.O. Istoricheskiy put russkoy arkhitektury i ego cvyazi s mirovym zodchestvom. M.: ARKHITEKTURA-S, 2016, 511 p.

Nikolai L. Pavlov,
Prof., Doctor of Architecture. At present, he is the Professor of the Moscow Architectural Institute, the Advisor of the Russian Academy of Architecture and Construction Sciences, the Advisor of the Board of Governors at the Union of Architects of Russia, a member of the Board of Governors at the Union of Moscow Architects, an active member of the Russian Geographical Society, an Honorary Figure of Higher Vocational Education, his research interests are the theory and history of architecture and urban development

Light & Engineering
Vol. 27, No. 2, pp. 42–51, 2019 *https://doi.org/1o.33383/2018-043*

SIMULATION AND DESIGN STUDY FOR INTERIOR ZONE LUMINANCE IN TUNNEL LIGHTING

Mehmet Sait Cengiz

Department of Technical Vocational School, Bitlis Eren University, Turkey
E-mail: msaitcengiz@gmail.com

ABSTRACT

An optimal solution for tunnel lighting designs was determined using a computer software. The road tunnel under construction 14481 m in length was selected in order to get an optimal design solution for tunnel lighting.The lighting, luminaries, and road parameters were changed and the resulting scenarios were examined in a simulation environment. The proposed approach can be applied for the illumination of interior zones in tunnels of 10 km or longer with significant reduction in energy consumption. The optimal luminance values that affect vision comfort in the tunnel were calculated in a simulation environment. As a result, the most economic lighting system and luminaries were chosen among solutions conforming to technical standards for luminance values.

Keywords: tunnel lighting, luminance, glare, HPS lamp

1. INTRODUCTION

Tunnels are underground road constructions that are alternatives to over ground pedestrian ways, railways, highways, and channels, and they are used to enable urban or rural traffic flow. Vision comfort, speed, and safe traffic flow should be ensured in the tunnel just as in typical roads. When tunnels are not sufficiently lit, an approaching driver will experience a black hole effect during the daytime. A gradual lighting level decrease should be provided into the tunnel considering the time required for eyes to adapt to the dark to avoid vision loss during the daytime. The ideal condition is to light the tunnel to a typical road luminance level. However, such a solution cannot be applied in practice as both the installation and operating cost will be high. The main purpose of this study is to find a sufficient, economic, and optimal solution. When considering the adaptation of eyes to darkness, intense lighting in the first section of the tunnel and a gradual decrease in lighting will aid driver vision.

In this study, luminance levels from the technical report for tunnel lighting published by the International Commission on Illumination (CIE) in 1990 and 2004 were used [1,2].

2. LUMINANCE

Luminance is represented by L and has a unit of cd/m^2. L is the luminous intensity emitted in a certain direction from unit surface area. The luminance of the unit area at point M of a luminous surface at a normal direction and α angle of this surface is the limit of the ratio of the ΔI_α luminous intensity

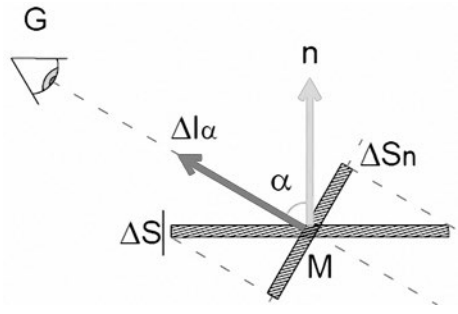

Fig. 1. The geometric state of glow from point *M* in the α direction

of the ΔS surface element involving point M in the ΔS_n apparent area of ΔS at a plane perpendicular to this direction [3]. The geometric state of the glow from point M of a surface in the α direction is illustrated in Fig. 1. The relative luminance calculation is presented in Equation 1.

$$L_\alpha = \lim_{\Delta S_n \to 0} \frac{\Delta I_\alpha}{\Delta S_n} = \frac{dI_\alpha}{dS_n}. \quad (1)$$

The surface can produce light itself or can reflect the light emitted from other sources. The levels of surfaces brightness with equal illumination but different reflection properties are different. For example, dull asphalt and bright asphalt have different glitter levels because of their reflection properties [3, 4–6].

3. TUNNEL ZONES AND CLASSIFICATION

When a driver travelling safely on an open road enters a tunnel, he/she continues to move on without experiencing a visual loss. Intense lighting is required in the first zone of the tunnel, so visual conditions do not go wrong for the driver entering the tunnel from daylight into darkness [7–9].

In tunnel lighting, there are differences between night time lighting that need to be established regardless of tunnel length and daytime lighting for tunnels longer than a critical length [10–12]. A tunnel can be illuminated at night similar to a typical road. However, the illumination level of the tunnel should be greater than open roads to make the tunnel safer and consider the noise in the tunnel. Previous studies demonstrate that a luminance level equal to 3cd/m^2 is sufficient throughout a tunnel in night time lighting even in long tunnels that have low traffic and a specific speed limit.

3.1. Tunnel Zones

Tunnel lighting is examined by classifying different luminance zones in order to ensure adaptation and provide economic solutions. Fig. 2 presents the zones of the tunnel.

The access zone is the area starting before the tunnel entrance (100–200) m and ending at the tunnel entrance. There are two factors affecting the adaptation luminance:

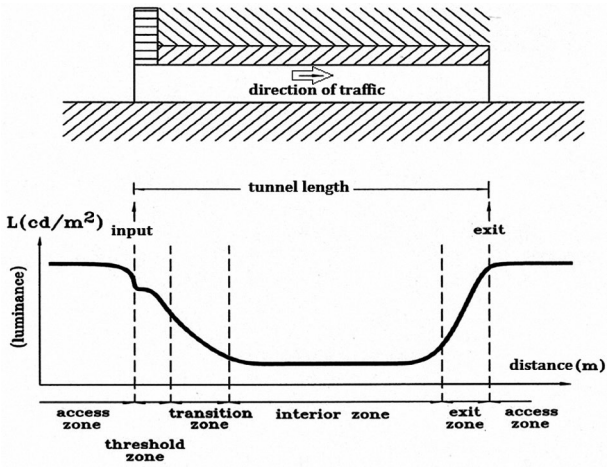

Fig. 2. Zones of the tunnel

- Around the tunnel entrance, "equivalent veiling luminance" (L_{seq}) formed by different luminance values;
- Luminance at the centre of the driver's field of view.

Equivalent veiling luminance is one of the most important factors in determining adaptation of the driver [1, 2, 13].

Entrance zone is the place where adaptation accurately starts from the tunnel entrance and continues to the interior zone of the tunnel. It is examined in two different zones:

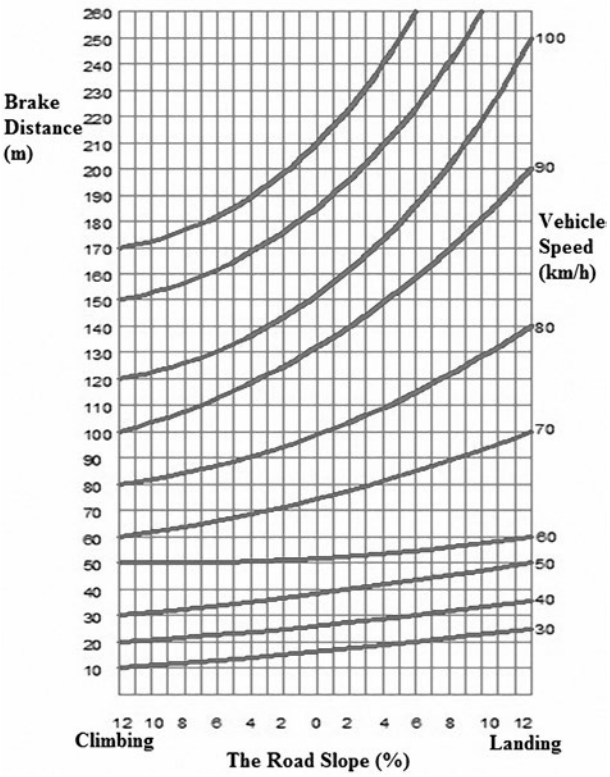

Fig. 3. Stooping distance based on speed [2, 13]

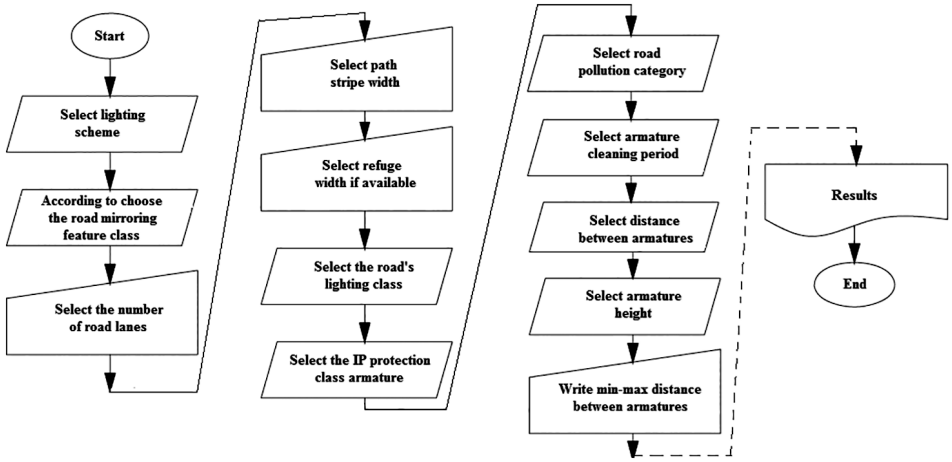

Fig. 4. The algorithm of the simulation program and data entered

– **Threshold zone**: limits of the zone starting from the tunnel entrance are determined on the basis that a critical object that may be dangerous in that zone can be seen by the driver in the approach at least from a distance equal to the stopping distance;

– **Transition zone**: after the threshold zone, the transition zone is where the luminance in the threshold zone is reduced to a luminance level in the interior zone. The length of the zone varies by the initial and final luminance value and the allowed speed limit.

Interior Zone: the constant luminance zone between entrance and exit zones of the tunnel.

Exit Zone: the zone from the end of interior zone to the exit that makes the adaptation easier to the zone with high luminance at the exit.

3.2. Stopping (Brake) Distance

The stopping distance or safe driving distance is the distance, from which the driver observes a dangerous object and can stop the vehicle safely. This distance depends on reaction time of the driver, stopping distance of the vehicle, allowed speed limit, inclination of the road, road pavement, and brake jamming ability of the vehicle. Fig. 3 presents a graphic for the stopping distance based on the speed considering the inclination of the road for the vehicle with moderately worn tires on a wet, clear road [2, 13].

4. LIGHT SOURCES

High-pressure sodium vapour (HPS) lamps are preferred under conditions of higher luminance level including under water tunnels, as HPS lamps have higher luminous flux and smaller dimensions than low-pressure lamps. As a result, less luminaries and area are required for lighting. Lighting efficiency (in terms of electricity consumption) of a similar lighting system increases up to 90 % with HPS lamps compared to fluorescent lamps based on results obtained from various tunnels with different structures that are open to vehicular traffic. The luminous efficiency is defined as the luminance level from the power required for the tunnel (for 1 m^2).

Previous studies on the photometric properties of HPS lamp armatures used in road lighting with LED light sources were performed. In the study designs, M3, M4, and M5 road lighting classes with 100 W and 150 W LED armatures could be achieved. M1 and M2 road lighting classes did not produce acceptable lighting magnitudes [14]. Since the road lighting class in this study is M2, LED lamps were not used as HPS lamps are widely used in road lighting [15–18]. Additionally, in Turkey, regulation studies, which were concluding in 2006, are requiring HPS lamps. As a result, this study simulation was performed accordingly with HPS lamps.

Since HPS lamps have more luminous flux than fluorescent lamps, glare can be prevented using reflection suitable for the direction of the driver. Sufficient luminance can be achieved by placing HPS lamps with proper power in a band-like order (correct line) at the entrance and transition zones. Since the lighting system is always band-like, problems concerning flickers and luminance uniformity are automatically addressed.

5. TUNNEL LIGHTING SYSTEM

Tunnel lighting is supposed to allow the driver travelling on a clear road with a certain comfort and

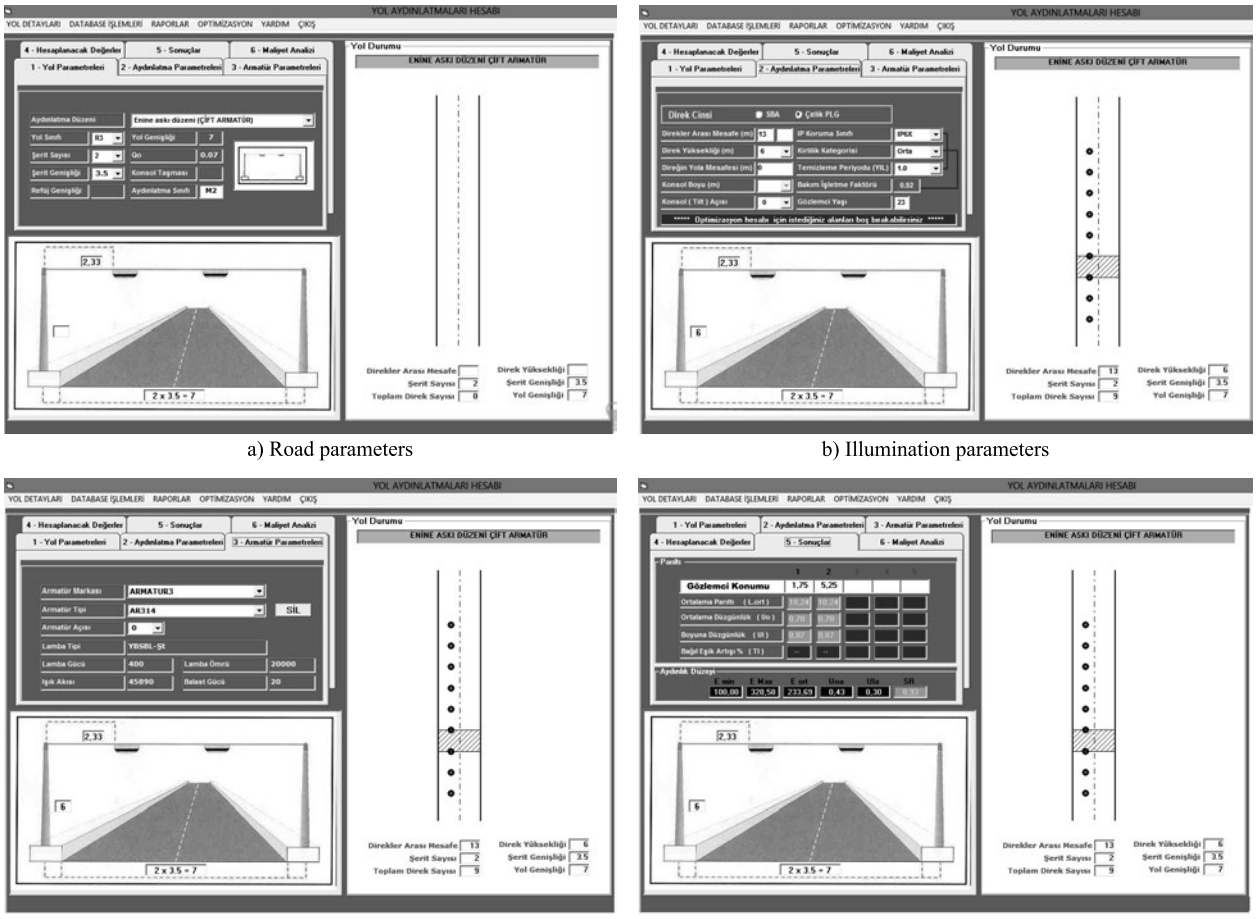

Fig. 5. Simulation program: a) road parameters, b) illumination parameters, c) luminary parameters, and d) results

safety without visual loss when moving into a tunnel. A tunnel entrance that is not illuminated sufficiently creates a "black hole" effect for a driver moving on a clear road, especially on a sunny day. The threshold zone constituting an important part of the tunnel lighting cost (the first entrance zone) depends on the luminance level of the access zone encountered while approaching the tunnel. For that reason, the first starting point of the most proper tunnel lighting, which is economic but provides the required conditions of view, is the accurate determination of the luminance level of the access zone in the tunnel approach zone.

There is an adverse condition for night time lighting compared to daytime lighting in terms of the technique of tunnel lighting. While outside the tunnel is brighter in daytime hours, the interior sections of the tunnel are brighter in night time hours. This condition eliminates the adaptation problems and the black hole effect from occurring in daytime. Since adaptation of eyes to low luminance takes more time than adaptation to high luminance, a luminance level of 3cd/m^2 should be ensured throughout the tunnel in night time lighting even in longer tunnels with low traffic and a certain speed limitation.

In tunnel lighting design, the vehicle speed limitation on a clear road approaching the tunnel should be considered. The tunnel design speed is the 90 km/h. The "stopping distance" of 130 m for a driver travelling with speed 90 km/h is to see a risky object and stops their car safely.

Tunnel lighting design calculations performed in this study are based on the recommendations involved in the technical report "Guide for the Lighting of Road Tunnels and Underpasses" CIE-1990 dated 2004 no-88.

5.1. Design and Planning Processes

Luminaries to be used in tunnel lighting should be chosen by taking into account glare level, luminance level of the road and walls, lighting uniformity and economy, and they should be determined

Table 1. Tunnel Road and Lighting Parameters

Tunnel road parameters	
Double armature, transverse arrangement	
Road class	R3
Number of lanes	2
Strip width	3.5 m
Road width	7 m
Q_o	0.07
Road lighting class	M2

*(*M2: *Speed of 90 km per hour can be* done the way)

Tunnel parameters of illumination	
Armature height	6 m
Fence distance	0 m
Console angle	0
IP protection	IP65
Pollution category	Middle
Annual clear period	1
Distance between armatures	13 m (400 W)
	17 m (250 W)
	15 m (150 W)
	17 m (100 W)
	15 m (70 W)

Table 2. Tunnel Lighting Parameters for HPS Lamps at Various Powers

Lamp type	Lamp power, W	Distance between armatures, m	$L_{average}$, cd/m^2	U_o	U_t	Number of luminaires (binary)	Current consumption, kW	Consumption situation
HPS	400	13	10.24	0.70	0.87	2208	883200	Over consumption
HPS	250	17	7.91	0.65	0.73	1688	422000	Over consumption
HPS	150	15	3.78	0.60	0.71	1912	286800	Over consumption
HPS	100	17	5.14	0.82	0.85	1688	168800	Suitable
HPS	70	15	2.46	0.65	0.75	1912	133840	Does not fit

in consequence of computer calculations according to the luminance method.

Even though lighting systems provide a good mean road surface luminance, there may be zones with low luminance where contrast is weak and small obstacles cannot be detected. The difference between minimum and mean road surface luminance into the field of view is expected to be lower than a certain value in order to obtain enough illumination at all points on the road. This obligation brings us to the overall uniformity (U_o) and longitudinal uniformity (U_l) values that are important secondary parameters.

Road types are defined in international technical reports and an optimal solution range is presented technically for these road types [19]. The required design calculations should be made through luminaries with known photometric characteristics, and the number and type of the luminaries should be determined according to these calculations.

Various choices are available for the road parameters in the simulation program. For the road parameters, the lighting system (bilateral, displaced, divided road, tunnel road with single luminary, tunnel road with two luminaries, etc.), road classes (R1, R2, R3, R4, N1, N2, N3, N4, etc.), number of lanes, lane width, refuge width, and road lighting classes (M1, M2, M3, M4, M5, M6, etc.) can be chosen. For the lighting parameters, features such as distance between the luminaries, height of the luminary, distance of the luminary from the road, console angle, IP protection class, pollution rate, cleaning period, and maintenance factor are chosen for post or hanger system lighting. For the luminary parameters, the name, angle of the luminary (angle relative to the road), power of the lamp used, lifetime, luminous flux, ballast power, and new lamps can be added into this simulation under the Database process at any time. As a result, it is possible to add any kind of lamp into the simulation [20–24]. An easy and accurate calculation is achieved in the

Table 3. Luminance Values According to the 1st and 2nd Observers under the 400 W HPS Lamps

$L_{average}$ = 10.24 cd/m² *Uo* = 0.70 *Ul* = 0.87									HPS-400 W	
1st observer, metre	**0.65 m**	**1.95 m**	**3.25 m**	**4.55 m**	**5.85 m**	**7.15 m**	**8.45 m**	**9.75 m**	**11.05 m**	**12.35 m**
0.583 m	8.70	10.82	13.08	14.82	15.84	16.08	15.09	14.93	12.90	9.17
1.750 m	8.86	9.00	9.02	9.49	9.78	9.63	9.03	9.54	10.24	9.26
2.917 m	8.01	8.11	7.40	7.61	7.88	7.90	7.18	7.52	9.08	8.39
4.083 m	8.12	8.23	7.64	7.86	8.08	8.03	7.32	7.71	9.20	8.47
5.250 m	9.07	9.31	9.58	10.12	10.46	10.14	9.33	9.82	10.52	9.44
6.417 m	8.57	10.72	12.99	14.82	15.83	16.21	15.08	14.85	12.92	9.10

2nd observer. metre	**0.65 m**	**1.95 m**	**3.25 m**	**4.55 m**	**5.85 m**	**7.15 m**	**8.45 m**	**9.75 m**	**11.05 m**	**12.35 m**
0.583 m	8.57	10.72	12.99	14.82	15.83	16.21	15.08	14.85	12.92	9.10
1.750 m	9.07	9.31	9.58	10.12	10.46	10.14	9.33	9.82	10.52	9.44
2.917 m	8.12	8.23	7.64	7.86	8.08	8.03	7.32	7.71	9.20	8.47
4.083 m	8.01	8.11	7.40	7.61	7.88	7.90	7.18	7.52	9.08	8.39
5.250 m	8.86	9.00	9.02	9.49	9.78	9.63	9.03	9.54	10.24	9.26
6.417 m	8.70	10.82	13.08	14.82	15.84	16.08	15.09	14.93	12.90	9.17

Table 4. Luminance Values According to the 1st and 2nd Observers under the 250 W HPS Lamps

$L_{average}$ = 7.91 cd/m² *Uo* = 0.65 *Ul* = 0.73									HPS-250 W	
1st observer, metre	**0.85 m**	**2.55 m**	**4.25 m**	**5.95 m**	**7.65 m**	**9.35 m**	**11.05 m**	**12.75 m**	**14.45 m**	**16.15 m**
0.583 m	7.49	8.81	7.97	8.77	9.29	10.75	11.31	11.18	11.20	7.87
1.750 m	7.40	7.28	6.43	7.09	7.48	8.15	8.16	8.38	8.82	7.71
2.917 m	7.05	6.11	5.13	5.67	6.01	6.24	6.21	5.83	6.98	7.38
4.083 m	7.27	6.30	5.34	5.99	6.29	6.44	6.37	6.04	7.15	7.58
5.250 m	7.77	7.69	6.98	7.81	8.13	8.85	8.74	8.79	9.22	8.06
6.417 m	7.24	8.61	7.74	8.58	9.22	10.66	11.34	11.10	11.10	7.71

2nd observer, metre	**0.85 m**	**2.55 m**	**4.25 m**	**5.95 m**	**7.65 m**	**9.35 m**	**11.05 m**	**12.75 m**	**14.45 m**	**16.15 m**
0.583 m	7.49	8.81	7.97	8.77	9.29	10.75	11.31	11.18	11.20	7.87
1.750 m	7.40	7.28	6.43	7.09	7.48	8.15	8.16	8.38	8.82	7.71
2.917 m	7.05	6.11	5.13	5.67	6.01	6.24	6.21	5.83	6.98	7.38
4.083 m	7.27	6.30	5.34	5.99	6.29	6.44	6.37	6.04	7.15	7.58
5.250 m	7.77	7.69	6.98	7.81	8.13	8.85	8.74	8.79	9.22	8.06
6.417 m	7.24	8.61	7.74	8.58	9.22	10.66	11.34	11.10	11.10	7.71

simulation results for the lighting system in which data is entered. Fig.4 shows the algorithm of the simulation program and the data entered.

The simulation and design study was performed for the New Zigana Mountain Tunnel (14481 m). As a result, the most economic and accurately calculated lighting data was achieved for a tunnel in which the lighting will be supplied. In the simulation, it was easier to calculate the most suitable luminance values, which is one of the most important problems in tunnels that need to be optimized.

Luminance values were first chosen. Luminaries were then chosen to provide the illumination level and they were placed to provide proper adaptation and safety conditions. This tunnel example requires daytime lighting because of its length and

Table 5. Luminance Values According to the 1st and 2nd Observers under the 150 W HPS Lamps

$L_{average}$ = 3.78 cd/m² *Uo* = 0.60 *Ul* = 0.71									HPS-150 W	
1st observer, metre	**0.75 m**	**2.25 m**	**3.75 m**	**5.25 m**	**6.75 m**	**8.25 m**	**9.75 m**	**11.25 m**	**12.75 m**	**14.25 m**
0.583 m	5.05	3.93	3.99	5.12	5.83	6.19	5.52	4.67	4.64	5.40
1.750 m	3.73	3.00	2.77	3.47	3.85	3.74	3.24	3.23	3.42	3.90
2.917 m	2.94	2.51	2.26	2.74	2.97	2.86	2.64	2.60	2.76	3.07
4.083 m	3.01	2.57	2.36	2.87	3.07	2.96	2.69	2.70	2.82	3.12
5.250 m	3.88	3.16	3.00	3.77	4.13	4.03	3.41	3.37	3.56	4.02
6.417 m	4.98	3.87	3.92	5.09	5.82	6.18	5.51	4.64	4.63	5.36

2nd observer, metre	**0.75 m**	**2.25 m**	**3.75 m**	**5.25 m**	**6.75 m**	**8.25 m**	**9.75 m**	**11.25 m**	**12.75 m**	**14.25 m**
0.583 m	4.98	3.87	3.92	5.09	5.82	6.18	5.51	4.64	4.63	5.36
1.750 m	3.88	3.16	3.00	3.77	4.13	4.03	3.41	3.37	3.56	4.02
2.917 m	3.01	2.57	2.36	2.87	3.07	2.96	2.69	2.70	2.82	3.12
4.083 m	2.94	2.51	2.26	2.74	2.97	2.86	2.64	2.60	2.76	3.07
5.250 m	3.73	3.00	2.77	3.47	3.85	3.74	3.24	3.23	3.42	3.90
6.417 m	5.05	3.93	3.97	5.12	5.83	6.19	5.52	4.67	4.64	5.40

Table 6. Luminance Values According to the 1st and 2nd Observers under the 100 W HPS Lamps

$L_{average}$ = 5.14 cd/m² *Uo* = 0.82 *Ul* = 0.85									HPS-100 W	
1st observer, metre	**0.85 m**	**2.55 m**	**4.25 m**	**5.95 m**	**7.65 m**	**9.35 m**	**11.05 m**	**12.75 m**	**14.45 m**	**16.15 m**
0.583 m	5.14	5.18	5.14	5.00	4.75	4.54	4.43	4.68	4.91	5.04
1.750 m	5.35	5.46	5.32	5.37	5.42	5.00	4.62	4.98	5.24	5.19
2.917 m	4.66	4.97	5.06	5.42	5.86	5.46	4.68	4.63	4.75	4.50
4.083 m	5.01	5.27	5.29	5.74	6.10	5.61	4.84	4.88	5.03	4.80
5.250 m	6.04	6.16	6.05	6.07	6.00	5.56	5.17	5.55	5.87	5.78
6.417 m	4.87	4.96	4.91	4.79	4.58	4.32	4.23	4.46	4.73	4.89

2nd observer, metre	**0.85 m**	**2.55 m**	**4.25 m**	**5.95 m**	**7.65 m**	**9.35 m**	**11.05 m**	**12.75 m**	**14.45 m**	**16.15 m**
0.583 m	4.87	4.96	4.91	4.79	4.58	4.32	4.23	4.46	4.73	4.89
1.750 m	6.04	6.16	6.05	6.07	6.00	5.56	5.17	5.55	5.87	5.78
2.917 m	5.01	5.27	5.29	5.74	6.10	5.61	4.84	4.88	5.03	4.80
4.083 m	4.66	4.97	5.06	5.42	5.86	5.46	4.68	4.63	4.75	4.50
5.250 m	5.35	5.46	5.32	5.37	5.42	5.00	4.62	4.98	5.24	5.19
6.417 m	5.14	5.18	5.14	5.00	4.75	4.54	4.43	4.68	4.91	5.04

a 90 km/h vehicle speed limitation in the clear road approaching the tunnel. The stopping distance of approximately 130 m for a driver travelling with speed 90 km/h is to see a risky object and stops their car safely. A symmetrical lighting system was preferred at night time lighting, which would continue through the threshold, transition, interior zones, and throughout the tunnel.

5.2. Features of the Tunnel Lighting System

The road pavement is asphalt, class R3. Additionally, Q_o = 0.07, the wall coating is concrete, the reflectivity is the 0.4, and the height of the luminary is the 6 m. The maintenance factor of the luminary is 0.92 and all calculated luminance values are corrected. The ratio of the smallest luminance

Table 7. Luminance Values According to the 1st and 2nd Observers under the 70 W HPS Lamps

$L_{average}$ = 2.46 cd/m² *Uo* = 0.65 *Ul* = 0.75									HPS-70 W	
1st observer, metre	**0.75 m**	**2.25 m**	**3.75 m**	**5.25 m**	**6.75 m**	**8.25 m**	**9.75 m**	**11.25 m**	**12.75 m**	**14.25 m**
0.583 m	2.72	3.06	2.73	2.64	2.49	2.58	3.06	3.36	3.49	2.77
1.750 m	2.59	2.65	2.37	2.28	2.17	2.15	2.48	2.85	2.87	2.61
2.917 m	2.11	1.96	1.80	1.68	1.66	1.59	1.72	1.96	2.01	2.14
4.083 m	2.18	2.02	1.89	1.77	1.73	1.66	1.78	2.05	2.07	2.20
5.250 m	2.77	2.85	2.59	2.50	2.36	2.35	2.64	3.00	3.02	2.74
6.417 m	2.68	3.02	2.69	2.61	2.48	2.56	3.05	3.35	3.49	2.75

2nd observer, metre	**0.75 m**	**2.25 m**	**3.75 m**	**5.25 m**	**6.75 m**	**8.25 m**	**9.75 m**	**11.25 m**	**12.75 m**	**14.25 m**
0.583 m	2.68	3.02	2.69	2.61	2.48	2.56	3.05	3.35	3.49	2.75
1.750 m	2.77	2.85	2.59	2.50	2.36	2.35	2.64	3.00	3.02	2.74
2.917 m	2.18	2.02	1.89	1.77	1.73	1.66	1.78	2.05	2.07	2.20
4.083 m	2.11	1.96	1.80	1.68	1.66	1.59	1.72	1.96	2.01	2.14
5.250 m	2.59	2.65	2.37	2.28	2.17	2.15	2.48	2.85	2.87	2.61
6.417 m	2.72	3.06	2.73	2.64	2.49	2.58	3.06	3.36	3.49	2.77

value to mean luminance value is greater than 0.4 in the calculations for tunnel lighting, ensuring that the rate of the smallest luminance value to the largest at the latitude coordinate of the observer is greater than 0.7 ($U_l \geq 0.7$). The luminance levels and uniformities of the tunnel walls are in accordance with relevant standards and that is very important for driving safety. All lighting luminaries were established in two lines 2.33 m from the tunnel walkways to the axis of the road and at a height of 6 m. The lighting in the tunnel will be supplied by the luminaries with symmetric light distribution. The contrast revealing coefficient, which is the most important criterion in the application of symmetric light distribution, is less than 0.2 and the flicker frequency of the interior zone is out of the 2.5–15 Hz range as mentioned in CIE-2004.

5.3. Simulation Study

The tunnel entrance lighting is approximately 130 m for a 90 km/h speed because of the stopping distance. The New Zigana Mountain Tunnel is 14481 m long, and the threshold zone has a length of 130 m, equal to the stopping distance. If 130 m of the road length is deducted from the whole road distance, 14351 m of the remaining road is the length of the transition, interior, and exit zones. There will be continuous lighting through 14481 m, all day. While the large part of the total power is consumed by the threshold zone in relatively short tunnels, consumption in the threshold zone is very low in a 14351 m long tunnel compared to the entire tunnel. In this study, lighting was established in a simulated environment with HPS luminaries for 400 W, 250 W and 150 W, 100 W and 70 W through the entire tunnel, excluding the threshold zone (130 m). Table 1 illustrates the tunnel road and lighting parameters.

Acceptable luminance values that do not disturb the vision comfort into the tunnel were calculated in the simulation performed with the values in the table. According to CIE-88 on 3.5 m wide road with two lanes, 1st observer stands at 1.75 m (transversal) and a 2nd observer stands at 5.25 m (transversal). Fig. 5 illustrates the simulation program and data entered for a 400 W HPS lamp. These processes are repeated at 250 W, 150 W, 100 W, and 70 W.

The simulation program written with Visual Basic is illustrating the optimum spacing between the two fittings, shown in Table 1 and with use of 400 W HPS lamps, is 13 m. 2x1104=2208 luminaries at 400 W were required for 14351 m of the remaining length of the tunnel, excluding the threshold zone. For the M2-type road lighting class, the desired criterions are, $L_{average} \geq 1.5\,\text{cd/m}^2$, $U_0 \geq 0.4$, $U_1 \geq 0.7$ and $TI \leq 10\%$, and all results obtained

from this study are available for the CIE31 standards. As a result of the simulation, the mean luminance of the road is the $L_{average} = 10.24\,cd/m^2$, the mean luminance uniformity is the U_0=0.7 and the longitudinal luminance uniformity is the U_1=0.87. This process is performed for 17 m with 250 W luminaries, 15 m with 150 W luminaries, 17 m with 100 W luminaries, and 15 m with 70 W luminaries. The chosen distances are optimal for luminance values based on the simulation. Table 2 illustrates the tunnel lighting parameters for HPS lamps at various powers (3 cd/m^2 or higher for highway tunnel lighting in Turkey).

According to simulation results, the 100 W HPS lamp is preferred as the most economic and optimal solution meeting the conditions. The M2-type road lighting class is available since *TI* is lower than 10 % in all regions in the tunnel.

5.4. Luminance Values

Table 3 presents the luminance values for the 1st and 2nd observers under 400 W HPS lamps in the tunnel according to simulation results.

Table 4 presents the luminance values for the 1st and 2nd observers under 250 W HPS lamps in the tunnel according to simulation results.

Table 5 presents the luminance values for the 1st and 2nd observers under 150 W HPS lamps in the tunnel according to simulation results.

Table 6 presents the luminance values for the 1st and 2nd observers under 100 W HPS lamps in the tunnel according to simulation results.

Table 7 presents the luminance values for the 1st and 2nd observers under 70 W HPS lamps in the tunnel according to simulation results.

5. RESULTS

The most accurate reference concerning tunnel road lighting and the selection of lamps to be used is international standards. The simulation tunnel road lighting was therefore adapted to the standards.

This simulation provided easier calculation of luminance values, which is very important in tunnel lighting.

The data of the desired lamp can be processed on the simulation compared to the Database option and the application results were observed.

This program is suitable for many tunnel lighting systems, such as single-sided from left, one-sided from right, displaced, bilateral, and double-sided from the refuge. According to CIE140, the luminance values for all points, mean luminance level, mean and longitudinal uniformity values were calculated for the observers.

Scenarios for HPS lamps meeting the desired conditions at various powers were examined by changing the luminary distance, height, and lamp power of the current tunnel lighting. Calculations were performed on simulations for 400 W, 250 W, 150 W, 100 W, and 70 W HPS lamps, and the 100 W HPS lamp was the most economic that met the minimum conditions conforming to the standards.

As shown in Table 2, the mean luminance value was greater than the 3 cd /m^2 value specified in the standards for the 100 W HPS lamp, which reached 5.14 cd /m^2 mean luminance. The 100 W HPS lamp provides sufficient luminance conditions. The 70 W HPS lamp luminance is equal to 2.46 cd /m^2 and that is less than the standard requirements.

When examining the instantaneous consumption values presented in Table 2, the 150 W HPS lamp consumed 1.7 times more energy than the 100 W HPS lamp, the 250 W HPS lamp 2.5 times, and the 400 W HPS lamp 5.23 times.

REFERENCES

1. International Committer On Illumination-CIE-88, Guide for the Lighting of Road Tunnels and Underpasses, 1990.

2. CIE Technical Report-88–2004. Guide for the Lighting of Road Tunnels and Underpasses [R], 2004.

3. Özkaya, M., Aydınlatma Tekniği, Birsen Yayınevi, İstanbul, 1994, 91.

4. Laurentin, C., Berruto, V., Fontynont, M. Effect of thermal conditions and light source type on visual comfort appraisal. Lighting Research & Technol., 2000. V32, #4, pp. 223–233.

5. CIE140, International Commission on Illumination, Road Lighting Calculations, Vienna-Austria, 33 (2000).

6. CIE61. Tunnel entrance lighting: a survey of fundamentals for determining the luminance in the threshold zone (E), 1984.

7. Veitch, J., Lighting and Health: issues for consideration, Light & Engineering, 2005, V13, #4, pp. 6–13.

8. Fuller, S., Carrasco, M., Exogenous attention and colour perception: performance and appearance saturation, Vision Research. 2006, 46, pp. 4032–4047.

9. Van Bommel, W., Van Den Beld, G., Van Ooyen M., Industrial light and productivity, Lighting & Engineering, 2003, V11, #1, pp. 14–21.

10. Iacomussi, P., Rossi, G., Soardo, P., Energy Saving and Environmental Compatibility in Road Lighting, Light & Engineering, 2012, V20, #4, pp. 55–63.

11. Peña-García, A., Gil-Martín, L.M., Study of pergolas for energy savings in road tunnels. Comparison with tension structures. Tunnelling and Underground Space Technology, 2013, 35, 172–177.

12. Gil-Martín, L.M., Gómez-Guzmán, A., Peña-García, A., Use of diffusers materials to improve the homogeneity of sunlight under pergolas installed in road tunnels portals for energy savings. Tunnelling and Underground Space Technology, 2015, 48, 123–128.

13. DIN-67524, Beleuchtung von Strassentunnelen und Unterführungen, 1972.

14. Onaygil, S., Güler, Ö., Erkin, E., Yol Aydınlatmalarında LED Kullanımı, V. Ulusal Aydınlatma Sempozyumu ve Sergisi, 2009.

15. Cengiz Ç., Kaynaklı M., Gencer G., Eren M., Yapici İ., Yildirim S., Cengiz MS., Selection Criteria and Economic Analysis of LEDs, Book of Abstracts, Imeset Int. Conf. Mult. Sci. Eng. Tech., October 27–29, 2017, Bitlis, Turkey.

16. UN Economic and Social Council, Economic Commission for Europe, Committee on Sustainable Energy, Steering Committee of the Energy Efficiency 21 Project, Final Report of Energy Efficiency Investment Project Development for Climate Change Mitigation, ECE/ENERGY/WP.4/ 2006/2, (21 March 2006).

17. Gencer G., Eren M., Yildirim S., Kaynaklı M., Palta O., Cengiz M.S., Cengiz Ç., Numerical Approach to City Road Lighting Standards, Book of Abstracts, Imeset Int. Conf. Mult. Sci. Eng. Tech., October 27–29, 2017, Bitlis, Turkey.

18. Yıldırım S., Yapıcı İ., Atiç S., Eren M., Palta O., Cengiz Ç., Cengiz M.S., Yurci Y., Numerical Analysis of Productivity and Redemption Periods in LED Illimunation. Imeset Book of Abstracts, Int. Conf. Mult. Sci. Eng. Tech.,, 12–14 July 2017, Baku.

19. CIE115, International Commission on Illumination, Recommendations far the Lighting of Roads for Motor and Pedestrian Traffic, Vienna-Austria, 1995, 25.

20. Onaygil S., TEDAŞ Genel Müdürlüğü Meslek İçi Eğitim Semineri, TEDAŞ Basımevi, Ankara, 2007, 1–70.

21. Onaygil S., 2007. TEDAŞ Genel Müdürlüğü Meslek İçi Eğitim Semineri-Gölbaşı Eğitim Tesisleri, Yol aydnlatma Semineri 23–24 Ocak 2007.

22. Cengiz MS., & Cengiz Ç., Numerical Analysis and An Application Study On Maintenance Factor In Tunnel Lighting, Journal of Engineering and Technological Sciences.(In press)

23. Onaygil, S., Yol aydınlatma projelerinde yol sınıfının belirlemesinin önemi, Kaynak Elektrik Dergisi, 1998, #12, 125–132.

24. Onaygil, S., "Determining the Luminance of the Threshold Zone in Tunnel Lighting", Ph.D. Thesis, Istanbul Technical University, 1990.

Mehmet Sait Cengiz had been the Director of Research and Development of Turkish Electricity Distribution Company in 2000–2010. In 2011, he completed his master degree in the field of Electrical and Electronics Engineering in Van Yüzüncü Yıl University. In 2016, he completed his doctorate degree in Inonu University, Institute of Science and Technology, Electrical and Electronics Engineering. At present, he works in the field of applied lighting at Bitlis Eren University

Light & Engineering
Vol. 27, No. 2, pp. 52–57, 2019 *https://doi.org/10.33383/2018-035*

RECONSTRUCTION OF ILLUMINATION DEVICES AT THE MOSCOW METRO

Leonid G. Novakovsky and Sergei A. Feofanov

Pharos-Alef (Moscow)
E-mail: pharos-alef@yandex.ru

ABSTRACT

To save the architectural appearance of cultural heritage stations is one of the main problems for the Moscow Metro. Development of station appearances is mainly connected to illumination devices that provide light to every station zone and define a comfort level to passengers and staff. They were designed in the first half of the 20th century. Now they do not meet any modern requirements. Many of these illumination devices are lost or replaced by more efficient illumination devices that totally misrepresent the original appearance of stations. Appearance of LED light sources allows to optimize luminous environments and to save the historical appearance of illumination devices and stations. This paper shows the ways of problem-solving in case of the entrance hall and the inter-escalator anteroom at *Krasnye Vorota* (station).

Keywords: metro, station lighting, architecture, luminous environment, cultural heritage, reconstruction, renewal, LEDs, energy saving, sconces

1. INTRODUCTION

Lighting upgrade of spaces at the first stations of the Moscow Metro that are considered to be cultural heritage sites is a complex, multi-variable, and contradictory task. The main problem is that the stations were designed in the early 1930s. The construction of illumination devices (chandeliers, sconces, torchères, platform lights) suggested incandescent lamps (IL) as light sources (LS) that were replaced to fluorescent lamps (FL) in the 1950s. With regard to solutions of that time, there were no restrictions of direct radiant influence on the human eye and they are not exist up to now, if it not related to light emitting diodes (LEDs) as we can conclude from modern lighting requirements for stations [1].

As a result, we see a situation where FL illumination devices (IDs) are used in the Moscow Metro (Fig. 1), which is significantly uncomfortable due to luminous flux pulsations and dazzle created by

Fig. 1. Exterior of IDs with a transparent diffuser and an FL

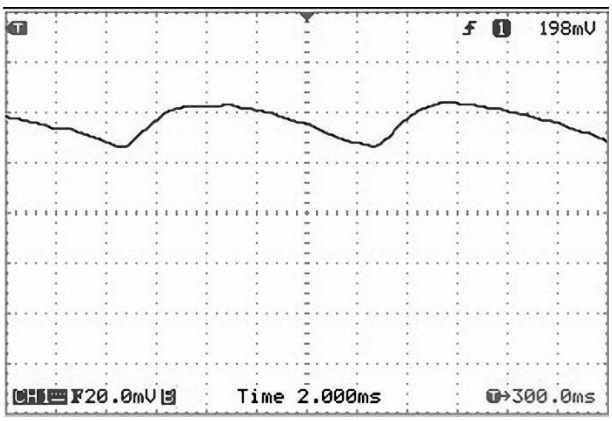

Fig. 2. Specific pulsation level of the FL luminous flux

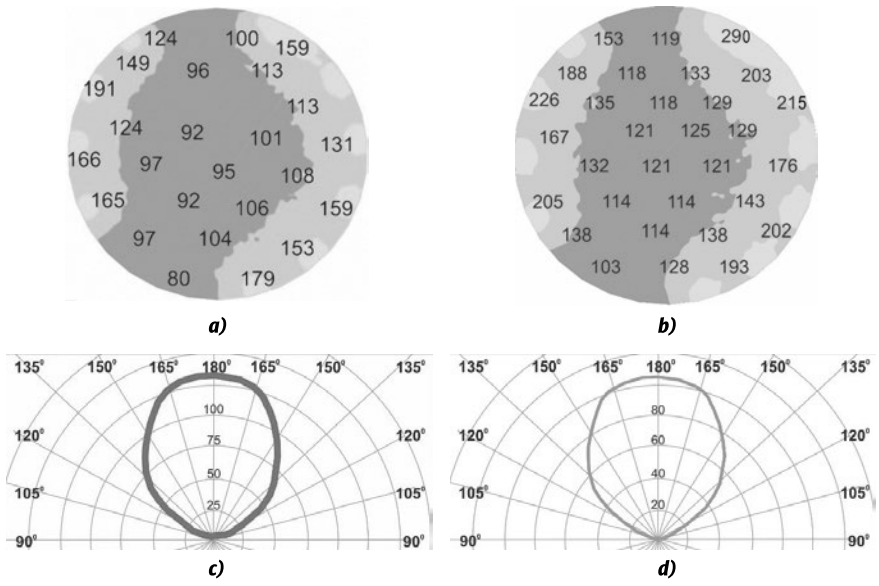

Fig. 3. Illuminance distribution (lx) on the floor of the entrance hall and the inter-escalator anteroom: *a*, *b* – E27 IL and CFL; *c*, *d* – bottle-shaped LIC of ID (sconce), with 100 W IL and 30 W CFL

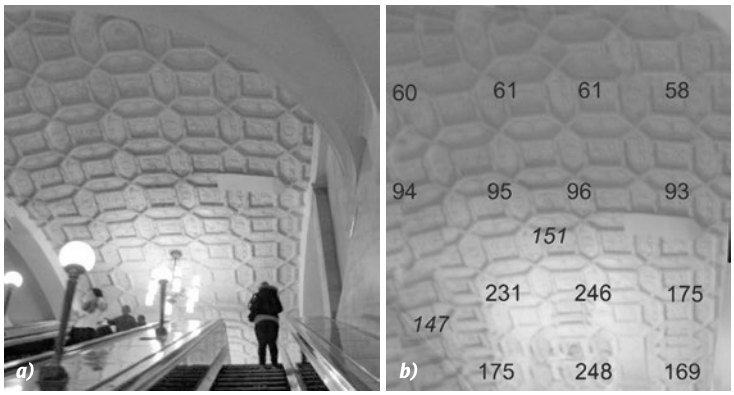

Fig. 4. Exterior of the ceiling in the entrance hall and its lighting principle before ID reconstruction: *a* – exterior; *b* – illuminance distribution

Fig. 5. IDs at *Krasnye Vorota* before reconstruction: *a* – sconce; *b* – chandelier

direct radiation of LSs from these devices on the visual sensory system (Fig. 2). Besides, the attempt to enhance the station lighting with traditional FLs and modern compact fluorescent lamps (CFLs) hardly improves the luminous environment. The Moscow Metro lighting mainly remains below the standard that is shown in Fig. 3, calculated with *DIALux evo 7.0*. The source data were the measured luminous intensity curves (LICs) of 100 W IL sconces and 30 W CFL sconces.

At the same time, the significant dimensions of a luminous element in FLs and CFLs devalue the role of glass diffusers (lamp shades) of these IDs that visually plays with relatively small dimensions of an IL filament. These IDs were designed with regard to such small dimensions [2]. The features of IDs that are mainly used now and especially in the 1930s are not enough for appropriate lighting of such architectural zones as ceilings. The lighting nature of IDs with traditional LSs is shown in Fig. 4.

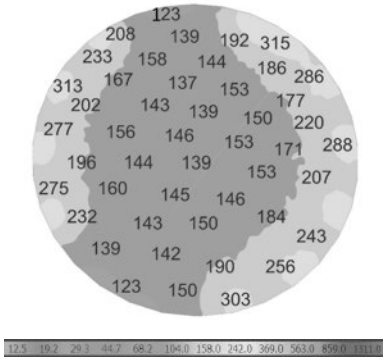

Fig. 6. Illuminance distribution (lx) on the floor of the inter-escalator anteroom with a luminous flux increase by 2000 lm

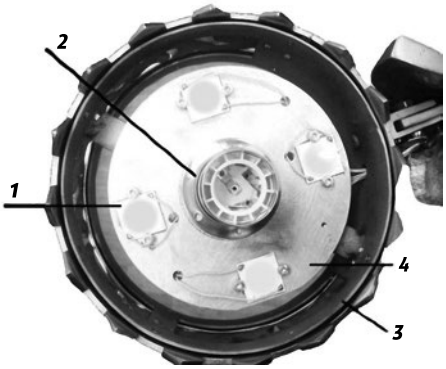

Fig. 8. Exterior of the LED module installed on the radiator: *1* – LED matrix; *2* – E27; *3* – decorative ring with attach fitting; *4* – radiator

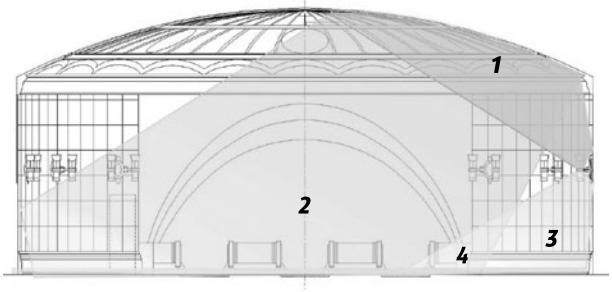

Fig. 9. Lighting layout of the inter-escalator anteroom – lighting distribution zones: main part of the ID luminous flux created with the LED module (*1*) and its reflection (*2*); part of the ID luminous flux created with an LED lamp (*3*); total of parts 2 and 3 (*4*)

Powerful white LEDs enable[1] to reconstruct and renew the given IDs.

As we solve these tasks, we should remember that lighting upgrade should be accomplished with a minimal stock list and with maximally unit-

[1] Their main disadvantage is blue light that extremely damages the human eye [3–6].

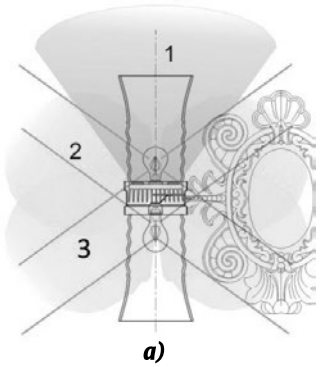

a)

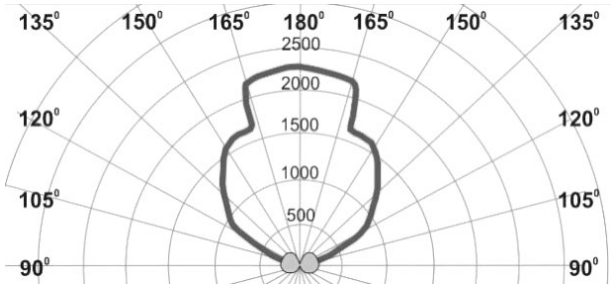

b)

Fig. 7. ID (sconce) engineering solution: *a* – layout for the zone division of the ID luminous flux, its part in zone 1 with an LED module, its parts in zone 2 and zone 3 with *Philips* LED filaments (E27); *b* – LIC of IDs with such light sources

ed LSs that allow for IDs to operate with regard to their service specifications. Development of a comfortable luminous environment can be more complete with concord of LS correlation in colour temperature to the human circadian biorhythm, e.g. from (4200–3700) K in the morning to (3200–2800) K in the evening [7, 8].

This complex task-solving should be accomplished while developing a common luminous environment that would meet the modern requirements of architectural lighting at a single station (in our case, *Krasnye Vorota* which is a cultural heritage site) and save the historical appearance of IDs presented in the original project of 1935.

2. RESULTS OF RESEARCH

The study subjects are IDs (chandeliers and sconces) with transparent glass diffusers or lamp shades (Fig. 5) that are installed at many stations of the Moscow Metro (with minor differences in their design and construction) such as *Prospekt Mira* (*Koltsevaya* line), *Komsomolskaya* (*Koltsevaya* line), *Kiyevskaya* (*Koltsevaya* line) and *VDNKh*.

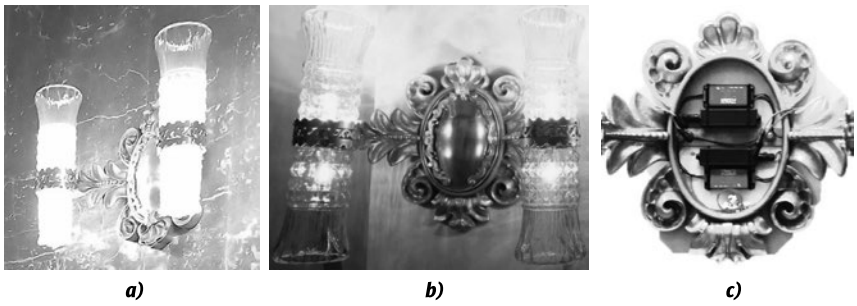

Fig. 10. Exterior of operational IDs (sconces): *a* – before reconstruction; *b* – after reconstruction; *c* – location of the power and control gear (for an LED module and standby lighting)

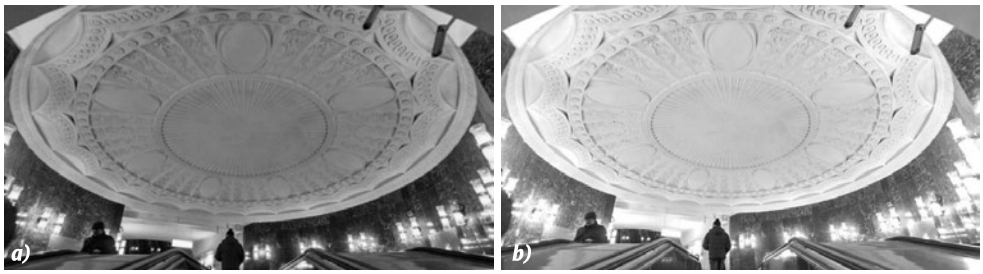

Fig. 11. Exterior of the illuminated ceiling in the inter-escalator anteroom: *a* – before reconstruction; *b* – after reconstruction (installation)

Their work is shown in the case of the entrance hall and the inter-escalator anteroom at *Krasnye Vorota*. According to the 1935 project, the inter-escalator anteroom is illuminated with 11 sconces with 4 prismatic cylindrical glass diffusers, first with 100 W ILs [9], then with 30 W CFLs.

The illumination level (Fig. 3) of these IL and CFL sconces does not meet any modern standards. The analysis shows that the growth of the luminous flux, e.g. by 2000 lm (Fig. 6), does not eliminate all specified disadvantages since the used lighting scheme plan for this station is not quite perfect[2]. So, another lighting scheme for the entrance hall and the inter-escalator anteroom was offered, which suggests the separation of the luminous flux for each ID (sconces, chandeliers) into 3 zones (Fig. 7). Zone 1 includes the 7000 lm luminous flux generated by an LED module with 4 LED matrices that are located at the bottom of a diffuser inside the ornamental ring of the ID in the way to avoid the radiant direction to get within the sight of passengers (Fig. 8). This flux is directed to the ceiling and is reflected from there (Fig. 9). The 800 lm luminous fluxes are formed in zone 2 and zone 3 by *Philips* LED filaments (6 pcs.) that are set at an angle that provides the desired effect of the light on the diffuser cutting and creates an illusion [10] of the main LS, illuminating the whole space without blinding any passengers because of a dull filament luminance. The rest of the ID luminous flux corresponds to the required lighting level of the wall and the floor (Fig. 9).

The offered method is obviously more expensive than just replacement of lamps. The price should be balanced by a decrease in maintenance costs which is possible due to a greater service life of LEDs.

The ID power and control gear is located on the main bracket under the decorative cover that saves the ID historical appearance (Fig. 10) and provides functions that match the modern requirements.

Only lower parts of the ID with appropriate LEDs are operating in a standby lighting mode. That provides the total illuminance of the floor at about 60 lx. The power source comes from a back-up circuit with a rated voltage of 100 V DC, and wherein the ID power and control gear feature is a separate polar input.

The offered ID construction totally excludes any discomfort [11] (the average UGR is about 10) and provides the appropriate lighting level and the

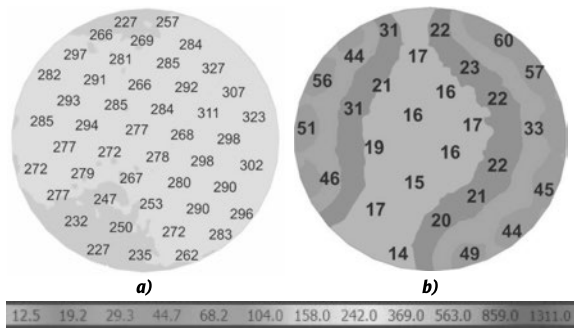

Fig. 12. Illuminance distribution on the floor of the inter-escalator anteroom after reconstruction in operating (*a*) and emergency (*b*) modes

[2] The lighting quality decreases: a bit brighter lighting of the floor causes hard visual discomfort (with non-illuminated ceiling) with increasing power consumption.

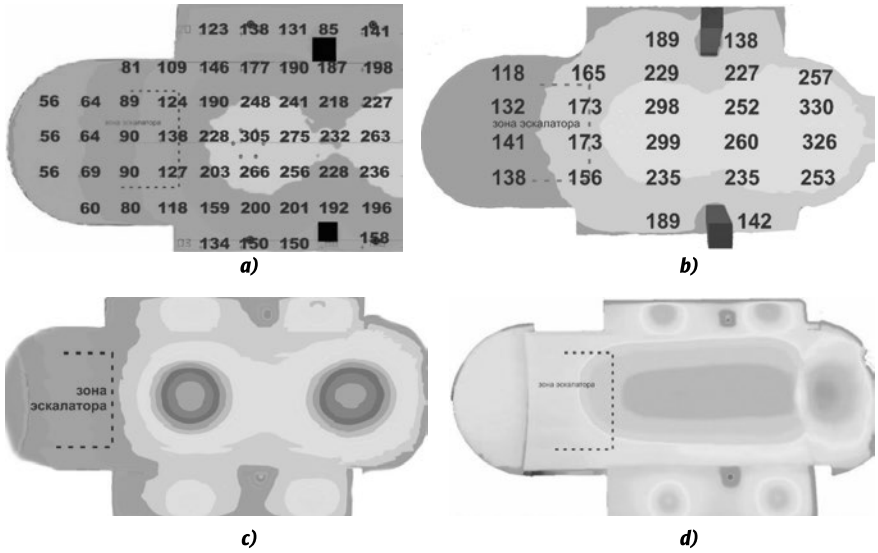

Fig. 13. Illuminance distribution (lx) on the floor and the ceiling of the entrance hall: *a* – on the floor before reconstruction; *b* – on the floor after reconstruction; *c* – on the ceiling before reconstruction; *d* – on the ceiling after reconstruction

necessary uniform illuminance distribution both on the art-treasured ceiling (Fig. 11) and on the floor (Fig. 12) with a decrease of total power consumption by 50 %.

While implementing the offered lighting scheme, the calculations of illuminance and UGR were conducted with *DIALux evo 7.0*, using results of the luminous intensity curves (LICs) of IDs (sconces) with the given LED module and the given LED lamps of 7.5 W (Fig. 12).

Lighting of the entrance hall is implemented in the same way. The only difference is that LED matrices (in an LED module) feature an additional cylindrical diffuser that spreads the light beam along the plasterwork to evenly illuminate the ceiling. The first torchère of the escalator (designed as per the solution described in [12, 13]) is used with the same purpose. The LS of the torchère provides additional illumination of the outer plasterwork.

We can see from the illuminance distribution of the ceiling and the floor in the entrance hall (Fig. 13) that the ceiling "works" after the implementation of the project. The floor is also fully illuminated (in total compliance with the requirements of [1]) with the necessary lighting level and the calculated UGR ≤ 20.

3. CONCLUSION

This work offered the methods for the Moscow Metro IDs with transparent diffusers (lamp shades) reconstruction by replacing weak LSs (ILs and FLs) with LED LSs, which ensure:

- Saving the ID historical appearance;
- Compliance with the illumination level requirements [1], no visual discomfort, energy consumption reduction, and compliance with the requirements for cultural heritage sites.

Unfortunately, during the 2017 renewal of *Krasnye Vorota*, the Moscow Metro has totally ignored the presented result of work. That is why the previous FL and CFL IDs remain at the renewed station with a pulsing luminous flux and a low colour quality that do not meet any modern requirements [1, 14].

REFERENCES

1. Sanitary and Epidemiological Rules SP 2.5.1337–03. Sanitary Rules of Metro Operation.

1. Sanitarno-epidemiologicheskiye pravila SP 2.5.1337–03. Sanitarnye pravila ekspluatatsii metropolitenov.

2. Gorbachov, N. V., Ratner, E.S. Lighting of the Moscow Metro: Preliminary Report // Svetotekhnika, 1935, No. 1, pp. 2–13.

2. Gorbachov, N. V., Ratner, E.S. Osveshcheniye moskovskogo metro: predvaritelnoye soobshcheniye // Svetotekhnika, 1935, No. 1, pp. 2–13.

3. Kaptsov, V. A., Deynego, V.N. Transport Lighting: Health Risks for Personnel and Passengers // Health Risk Analysis, 2016, No. 3, pp. 4–12.

3. Kaptsov, V. A., Deynego, V.N. Transportnaya svetotekhnika: riski zdorovyu personala i passazhirov // Analiz riska zdorovyu, 2016, No. 3, pp. 4–12.

4. Kaptsov, V. A., Deynego, V.N. Blue LED Light as a New Hygienic Problem // Health Risk Analysis, 2016, No. 1(13), pp. 15–25.

4. Kaptsov, V. A., Deynego, V.N. Siniy svet svetodiodov – novaya gigiyenicheskaya problema // Analiz riska zdorovyu, 2016, No. 1(13), pp. 15–25.

5. Kaptsov, V. A., Deynego, V.N. Disorders in the Melanopsin Effect of Pupil Constriction as a Risk Factor Causing Eye Diseases // Health Risk Analysis, 2017, No. 1, pp. 132–148.

5. Kaptsov, V. A., Deynego, V.N. Narusheniye melanopsinovogo effekta suzheniya zrachka – faktor riska zabolevaniya glaz // Analiz riska zdorovyu, 2017, No. 1, pp. 132–148.

6. Bizhak, G., Kobav, M. B. LED Spectra and Melatonin Suppression Function // Light & Enineering, 2012, No. 3, pp. 15–22.

7. Demidov, V. How We See What We See [3rd edition, republished and complemented], Berlin: Science & Technology. Rare Editions, 2010, 280 p.

7. Demidov, V. Kak my vidim to, chto vidim [izdaniye 3-e, pererab. i dop.]. Berlin: Ni T. Raritetnye izdaniya, 2010, 280 p.

8. Blatner, P. Luminous Environment for a Human: Science, Industry, and Law // Svetotekhnika, 2016, No. 1, pp. 45–49.

8. Blatner, P. Svetovaya sreda dlya cheloveka: nauka, promyshlennost i zakon // Svetotekhnika, 2016, No. 1, pp. 45–49.

9. GOST R52706–2007. Tungsten Incandescent Lamps for Everyday and Similar General Lighting. Operating Needs.

9. GOST R52706–2007. Lampy nakalivaniya volframovye dlya bytovogo i analogichnogo obshchego osveshcheniya. Ekspluatatsionnye trebovaniya.

10. Novakovskiy, L. G., Miras, J.-P. Illumination Tool for Creating a Light Beam // Utility Model No. 159921 RF.

10. Novakovskiy, L. G., Miras, J.-P. Svetovoy pribor dlya formirovaniya svetovogo puchka // PM No. 159921 RF.

11. GOST 33392–2015. Buildings and Structures. Test Method for Unified Glare Rating in Candlelight Conditions.

11. GOST 33392–2015. Zdaniya i sooruzheniya. Metod opredeleniya pokazatelya diskomforta pri iskusstvennom osveshchenii pomeshcheniy.

12. Novakovskiy, L. G., Kazakovskiy, N. I., Kanevskiy, A. V., Peselis, Yu.A. Light of the Metro Escalator Balustrade / Patent Decision No. 2017107716 dated March 2017 for a Utility Model.

12. Novakovskiy, L. G., Kazakovskiy, N. I., Kanevskiy, A. V., Peselis, Yu.A. Osvetitel eskalatornoy balyustrady metropolitena / Resheniye ot 03.2017 g. No. 2017107716 o vydache patenta na PM.

13. Novakovskiy, L. G., Feofanov, S. A. A Correct Illumination of an Esscalator is a Set of Radical Solutions // Light & Engineering, 2018, V. 26, #3, pp. 58–65.

14. GOST R54350–2015. Illumination Devices. Lighting Requirements and Test Methods.

14. Pribory osvetitelnye. Svetotekhnicheskiye trebovaniya i metody ispytaniy.

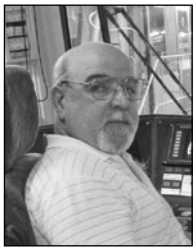

***Leonid G. Novakovsky*,**
Ph. D. in Technical Sciences, graduated from the Moscow State University of Mechanical Engineering in 1969. At present, he is the Director at *Pharos-Alef*

***Sergei A. Feofanov*,**
Ph. D. in Technical Sciences, graduated from the Moscow Automobile and Road Construction State Technical University in 2005. At present, he is the Senior Researcher at *Pharos-Alef*

Light & Engineering
Vol. 27, No. 2, pp. 58–66, 2019 *https://doi.org/10.33383/2018-040*

TECHNO-ECONOMIC ANALYSIS OF OFF-GRID PV LED ROAD LIGHTING SYSTEMS FOR ANTALYA PROVINCE OF TURKEY

A. Can Duman and Önder Güler

Istanbul Technical University, Istanbul, Turkey
E-mail: dumanan@itu.edu.tr; onder.guler@itu.edu.tr

ABSTRACT

In this study, a techno-economic analysis of off-grid PV LED road lighting systems is made for Antalya province of Turkey. DIALux software is used for road lighting calculations and HOMER software is used in modelling, sizing, and optimization of the energy systems. Calculations are made to determine whether maximum or minimum pole spacing options for both twin-bracket central and opposite lighting arrangements provide the optimal system design for off-grid PV LED road lighting systems under the *M3* lighting class in Antalya. The techno-economic analysis of the energy system in case of dimming LED luminaires after midnight is made. Since the payback periods of the systems are found to be above the system lifetime (20 years) with and without dimming, in addition to the current case, future projections, in which electricity unit prices increase and cost of PV system component and battery costs decrease, are examined.

Keywords: LED, road lighting, PV system, techno-economic analysis, dimming

1. INTRODUCTION

Renewable energy systems without giving rise to any greenhouse gas emissions unlike conventional energy sources have gained widespread support by governments, businesses and consumers in recent years. Photovoltaic (PV) and wind turbine technologies are among the most competitive renewable technologies, which provide a clean source of electricity and can replace traditional fossil sources by reducing CO_2 emissions. One of the sectors that consume energy is road lighting, and in recent years, the subject of meeting electricity energy demand of road lighting installations via off-grid renewable energy systems has gained an interest. Many studies have been evaluated in this area including the techno-economic feasibility of PV based lighting installations [1–5]. Under current economic conditions, off-grid lighting systems are feasible only in the rural areas, where electricity does not reach and new transmission lines are required to be installed. However, owing to the declining trend in LED luminaire and PV system component prices, the systems have a potential to become attractive in the rest of the world [6].

In the last seven years, PV costs reduced by more than 70 % due to the developments in the material technology and reached from 1.34 $/W to under 0.5 $/W [7, 8]. Beside the decreasing trend of PV prices, recent developments in LED technology have made it possible to switch from traditional lighting to energy efficient LED lighting. Apart from their cost benefit, LED luminaires with lower power requirements made it available to use smaller sized and thus cheaper PV panels and batteries, which led to investments in off-grid PV lighting installations at lower costs.

In this study, a techno-economic analysis of off-grid PV LED road lighting systems is made for Antalya, the fifth most populous province and tourism centre of Turkey being located at the south of the country with high solar irradiation and sunshine duration levels. DIALux software is used for road lighting calculations and HOMER software is

Table 1. Road Lighting Criteria for Selected Road Lighting Classes

Road Lighting Class	L_{avg} (cd/m²)	U_o	U_l	*TI* (%)	SR
M3	≥1.0	≥0.4	≥0.5	≤15	≥0.5

used in modelling, sizing and optimization of the PV energy systems. In the first part of the study, calculations are made to determine whether maximum or minimum pole spacing options for both twin-bracket central and opposite lighting arrangements provide the optimal system design in off-grid PV LED road lighting systems under the *M3* lighting class in Antalya. In case of meeting lighting criteria using maximum pole spacing, more durable, higher, and thus more expensive lighting poles mounted with higher capacity and costly PV system components and LED luminaires are required per kilometre. However, the number of poles to be built is lesser. On the contrary, in case of using minimum pole spacing, a higher number of lighting poles is required per kilometre whereas size, capacity and cost of the system components and length of the lighting pole decrease. In the second part of the study, a techno-economic analysis in case of dimming LED luminaires after midnight is made over the optimal design determined in the first part. Lighting calculations and energy system optimization is carried out once again over the optimal design. In addition to the current case, payback periods of the systems were calculated considering future scenarios for cases of 25 % increase in electricity tariffs, 25 % decrease in PV system component and battery costs, 50 % decrease in PV system component and battery costs, and 25 % increase in electricity tariffs with 50 % decrease in PV system component and battery costs.

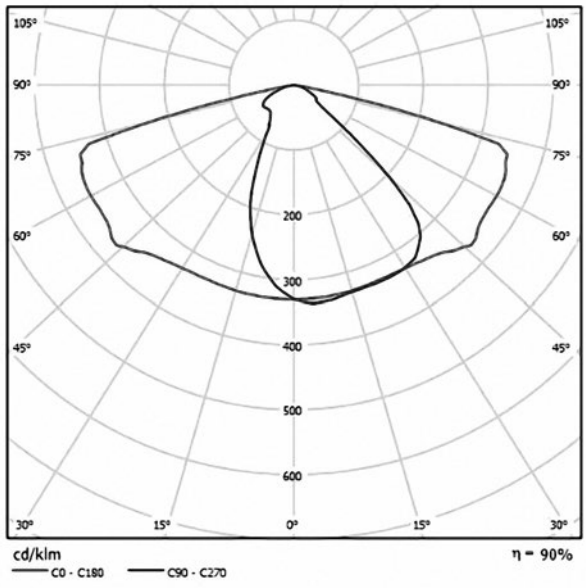

Fig. 1. The luminous intensity diagram of the luminaires

2. ROAD LIGHTING CALCULATIONS

Today, road lighting criteria are determined by the International Commission on Illumination (CIE) and the European Committee for Standardization (CEN) [9, 10]. Turkish Electricity Distribution Co. (TEDAŞ) holds the responsibility for the installation and maintenance of approximately 5 million lighting poles located in cities and rural areas in Turkey [11]. In 2016, according to Turkish Statistical Institute (TÜİK) data, electricity consumption in general lighting was 4161 GWh, which is 1.8 % of the total 231,204 GWh electricity consumption of Turkey [12].

In the study the *M3* road lighting class is selected, where relatively high-powered luminaires could be used without exceeding limited PV battery capacity that can be mounted on a lighting pole. Road lighting calculations are made for the twin-bracket central and opposite arrangements for a 4-lane road with a width of 14 meters. Median length is taken as 2 meters.

The road lighting calculations are performed according to TEDAŞ Technical Specification for LED Road Lighting Luminaires, Procedures, and Principles on the Usage of LED Luminaires in the General Lighting Scope, TS EN13201–3 and Technical Specifications for Road Lighting Luminaires TEDAŞ MYD-95–009.B [13–16]. The road lighting criteria need to be followed for the *M3* road lighting class are given in Table 1. The maintenance factor is set as 0.89 for the protection class of *IP66* that is guaranteed according to CIE154:2003 [17]. Road surface class is assumed to be *R3*.

The luminous intensity diagram of the luminaires used in the study is given in Fig. 1.

According to the TEDAŞ Technical Specifications for LED Road Lighting Luminaires, minimum pole spacings to be provided in the *M3* road lighting class are 30 m and 28 m for the twin-bracket central and opposite arrangements respectively [13]. There-

Table 2. Road Lighting Calculations for *M3* Road Lighting Class

Parameter	Arrangement			
	Opposite		Twin-bracket central	
Spacing (m)	28	51	30	49
Luminaire luminous flux (lm)	4641	9270	5642	9270
Luminaire power (W)	39	73	46	73
Luminous efficacy of luminaire (lm/W)	119	127	123	127
Height (m)	7	10	8	9.5
Boom length (m)	1	1	1.5	0.5
L_{avg} (cd/m^2)	1.01	1.00	1.09	1.02
U_o	0.47	0.42	0.53	0.40
U_l	0.76	0.53	0.78	0.51
TI (%)	10	13	10	14
SR	0.61	0.85	0.76	0.89

Table 3. Average Lighting Times and Durations for Antalya

Month	Daily average lighting time, h: min	Daily average lighting duration, h: min	Monthly average lighting duration, h
Jan	06:41 / 17:33	13:08	407.13
Feb	06:20 / 18:03	12:17	343.93
Mar	05:41 / 18:31	11:10	346.17
Apr	05:55 / 20:00	09:55	297.5
May	05:19 / 20:28	08:51	274.35
Jun	05:07 / 20:49	08:18	249
Jul	05:21 / 20:45	08:36	266.6
Aug	05:48 / 20:14	09:34	296.57
Sep	06:13 / 19:30	10:43	321.5
Oct	06:40 / 18:45	11:55	369.42
Nov	06:09 / 17:15	12:54	387
Dec	06:35 / 17:11	13:24	402
Total			3961.17

fore, in DIALux calculations, pole spacing ranged from 30 m to 55 m and 28 m to 55 m in 1 m increments, pole length ranged from 7 m to 10 m in 0.5 m increments and boom length ranged from 0 m to 1.5 m in 0.5 m increments with 0° boom angle.

In the study, to determine the most cost effective off-grid lighting installation for the *M3* road lighting class, the twin-bracket central and opposite arrangements are compared. Besides, maximum and minimum pole spacing options are compared in order to determine whether higher number of lighting poles with lower capacity luminaires, PV panels, and batteries or lower number of lighting poles with higher capacity luminaires, PV panels, and batteries give the most feasible result. Road lighting calculations according to the maximum and minimum pole spacing options for both twin-bracket central and opposite arrangements for the *M3* road lighting class are shown in Table 2.

3. CALCULATIONS

3.1. Modelling of Energy Systems

Energy system optimization is carried out using National Renewable Energy Laboratory (NREL)'s

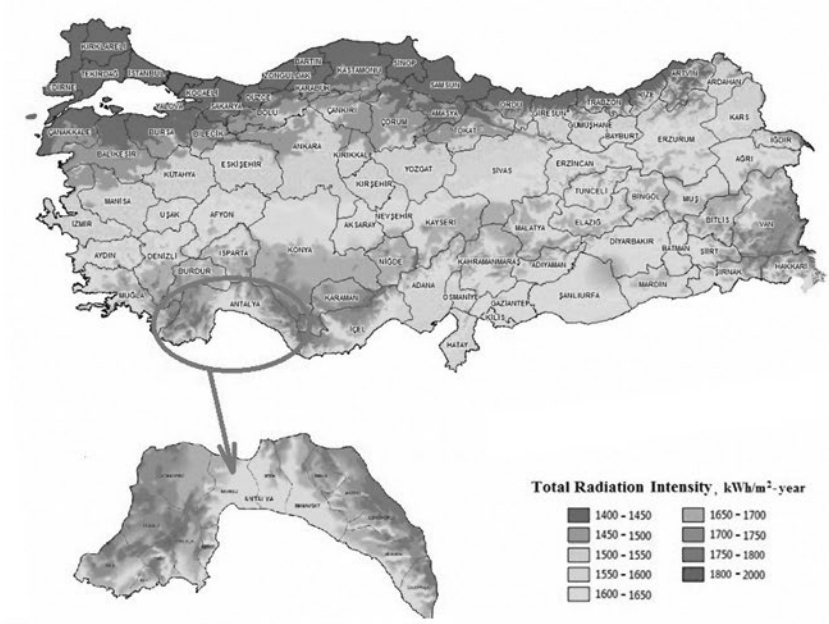

Month	Clearness index	Daily Radiation (kWh/m² per day)
January	0.521	2.485
February	0.548	3.371
March	0.568	4.585
April	0.572	5.658
May	0.604	6.710
June	0.660	7.638
July	0.668	7.533
August	0.670	6.855
September	0.682	5.828
October	0.640	4.225
November	0.553	2.774
December	0.524	2.277

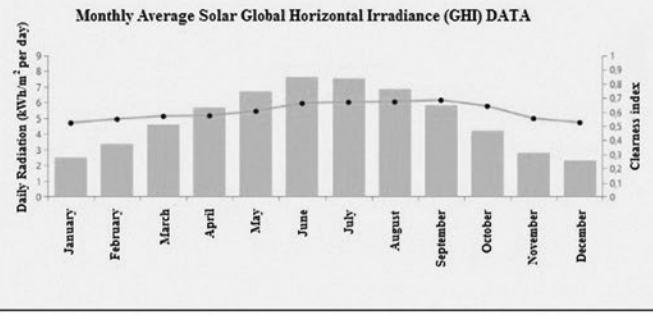

Annual Average (kWh/m² per day): 4.99

Fig. 2. Solar map of Turkey and global radiation and clearness index data of Antalya

micropower optimization model HOMER software. The lifetime of the energy systems to be installed is considered to be 20 years with 3 % real interest rate. Since lighting load demand must be supplied uninterruptedly throughout a year, no capacity shortage is allowed.

The PV panel capacity is searched in the range of (100–855) W for the twin-bracket central and in the range of (100–570) W for the opposite arrangements in 10 W increments with a lifetime of 20 years. The capital and replacement cost of a panel is taken as 0.52 $/W and operation and maintenance cost is taken as 7 $/year. Panels are tilted with a slope of 36.90º in respect to the latitude of the study area. The PV derating factor is assumed to be 90 %, and ground reflectance is set as 20 %. Solar irradiation data is extracted from the National Aeronautics and Space Administration (NASA) Meteorology and Solar Energy Database through HOMER. Batteries with nominal voltage of 12 V and nominal capacity varying between 33.3 Ah and 500 Ah are used. 30 % minimum state of charge (SoC) is allowed with round trip efficiency of 86 %. Battery prices varied between $117 and $997.5. Due to being installed on the same lighting pole, maintenance cost of the batteries are included in maintenance cost of the PV panels.

In the calculations, road lighting systems are assumed to be operating from dusk until dawn and out of operation during the daytime and civil twilight. Civil twilight is the time of the day, where the angle between the horizon and the Sun is less than 6º, the objects are identifiable, and people can perform daily tasks without any requirement of artificial lighting. Table 3 shows the daily and monthly average lighting durations for Antalya. As of the study date, daylight saving time is taken into account in the calculation of lighting durations.

Table 4. Optimization Results for Antalya under *M3* Lighting Class

Parameter	Arrangement			
	Opposite		Twin-bracket central	
	Min.	Max.	Min.	Max.
Pole spacing (m)	28	51	30	49
Luminaire power (W)	39	73	2x46	2x73
Battery capacity (V/Ah)	12/166.6	12/250	12/416.6	2x12/333.3
PV panel power (W)	240	540	530	800
PV tilt angle (°)	36.90			
Cost of energy ($/kWh)	0.258	0.228	0.227	0.225
Battery + PV initial cost ($)	490.05	790.80	1129	1829
Battery + PV net present cost ($)	594.19	977.51	1233	1933
Operation&maintenance cost ($)	104.14			
PV electricity production (kWh per year)	384	886	823	1227
Excess electricity production (kWh per year)	204.5	551.7	400.3	559.7
Excess electricity production / electricity production (%)	53.3	62.3	48.7	45.6
Load electricity consumption (kWh per year)	155	289	365	578
Unmet load (%)	0			
Autonomy (h)	79.13	63.66	83.84	84.86
CO_2 emission reduction (kg per year)	75.95	141.61	178.85	283.22

In the study, off-grid PV LED road lighting systems' contribution to the environmental sustainability is also taken into consideration, since one of the goals of the systems is to reduce CO_2 emissions. In CO_2 reduction calculations, the International Energy Agency (IEA) data are used, which determine the amount of CO_2 emission produced per kWh in Turkey as 490 g/kWh [18].

3.2. Optimization Results, Payback Periods, and Total Installation Costs per km

Turkey is situated between 36° – 42° North latitudes and 26° – 45° East longitudes and has the highest solar potential in Europe after Spain. According to the study carried out by the Electricity Affairs Survey Administration (EİE), Turkey has an average annual total sunshine duration of 2737 hours (daily total 7.5 hours) and the average total radiation intensity is 1527 kWh/m^2 per year (total 4.2 kWh/m^2 per day). Antalya is situated between North latitudes at 36° 07' – 37° 29' and East longitudes at 29° 20' – 32° 35'. Located in the Mediterranean Region of Turkey, Antalya is the tourism centre of Turkey and the fifth most populous province. The province has an average annual total sunshine duration of 3014 hours and the average total radiation intensity is 1650 kWh/m^2 per year [19]. The solar potential map of Turkey and the clearness index and global radiation data of Antalya province are shown in Fig 2. The data have been extracted from NASA's Surface Meteorology and Solar Energy Database through HOMER software.

Energy system configurations are simulated and optimized according to the lowest total net present costs (NPC) using HOMER. Detailed optimization results for single pole are given in Table 4.

Following the optimization stage, payback periods of PV energy systems and total cost of entire lighting installations per km are calculated. The electricity cost of 0.128 $/kWh for general lighting is used in the calculation of payback periods as of May 2016. As can be seen in Table 5, the lowest payback period and installation cost per km are found as 27.82 years and $62526.45 respectively with maximum pole spacing for the twin-bracket central arrangement whereas the highest payback period and installation cost per km is found to be

Table 5. Comparison of Payback Periods and System Installation Costs per km

Parameter	Arrangement			
	Opposite		Twin-bracket central	
	Min.	Max.	Min.	Max.
Pole spacing (m)	28	51	30	49
Luminaire power (W)	39	73	92	146
Pole length (m)	7	10	8	9.5
Battery + PV net present cost ($)	594.19	977.51	1233	1933
LED luminaire cost ($)	285	295.5	591	649.5
Charge regulator cost ($)	75	100	100	125
Payback period of the energy system (years)	33.73	29.13	28.53	27.82
Single pole system CoE ($/kWh)	0.258	0.228	0.227	0.225
Galvanized steel polygon lighting pole cost ($)	102.62	184.10	123.04	170.36
Boom cost ($)	7.35	7.35	10.09	4.60
Pole mounting cost ($)	54.47	97.72	65.31	90.43
Cable cost ($)	2.52	3.6	2.88	3.42
Cabling cost ($)	0.84	1.2	0.96	1.14
Total cost of single pole system ($)	1121.99	1666.98	2126.28	2977.45
Number of poles per km	36×2	20×2	34	21
Total installation cost per km ($/km)	80783.28	66679.2	72293.52	62526.45
Annual operation duration (h)	3961.17			
Annual electricity consumption per km (kWh)	11122.96	11566.62	12390.54	12144.95

33.73 years and $80783.28 respectively with minimum pole spacing for the opposite arrangement.

3.3. Calculation Results in Case of Dimming

According to the Procedures and Principles Regarding the Usage of LED Luminaires in the Scope of General Lighting [13] published by the Ministry of Energy and Natural Resources, it is obligatory to use dimmable luminaires in the LED lighting installations in order to reduce the illuminance levels. Dimming for the *M3* road lighting class is done by lowering the lighting class from *M3* to *M4*.

The calculations are carried out for the *M3* road lighting class using the twin-bracket central arrangement and dimming is applied from the *M3* to the *M4* road lighting class. The lighting hours of operation and load energy consumption during one year for the selected road are given in Table 6.

It is assumed that from the beginning of lighting operation until midnight illumination will be performed according to the *M3* road lighting class and from midnight until the end of lighting operation, lights will be dimmed and illumination will be performed according to the *M4* road lighting class. In this case, the lighting system will be under operation for 3961.17 hours annually and will illuminate for 1777.26 hours under the *M3* and 2183.91 hours under the *M4* road lighting class. Lighting calculations in case of dimming are given in Table 7.

In case of dimming, to switch from the *M3* lighting class to the *M4* lighting class after midnight, luminous flux of 73 W luminaire is reduced by 25 % and thus power consumption is decreased from 73 W to 51.1 W. In order to obtain new PV and battery capacity under dimming conditions, HOMER simulations are conducted once again. Comparison of detailed optimization results for normal case and dimming case are given in Table 8.

3.4 Payback Periods and Total Installation Costs under Current Conditions and for Future Scenarios

Following the optimization stage, payback periods of PV energy systems and total cost of entire

Table 6. The Lighting Hours of Operation and Load Energy Consumption (kWh) During One Year in Case of Dimming

Hour	Jan.	Feb.	Mar.	Apr.	May.	Jun.	Jul.	Aug.	Sep.	Oct.	Nov.	Dec.
0	0.102	0.102	0.102	0.102	0.102	0.102	0.102	0.102	0.102	0.102	0.102	0.102
1	0.102	0.102	0.102	0.102	0.102	0.102	0.102	0.102	0.102	0.102	0.102	0.102
2	0.102	0.102	0.102	0.102	0.102	0.102	0.102	0.102	0.102	0.102	0.102	0.102
3	0.102	0.102	0.102	0.102	0.102	0.102	0.102	0.102	0.102	0.102	0.102	0.102
4	0.102	0.102	0.102	0.102	0.102	0.102	0.102	0.102	0.102	0.102	0.102	0.102
5	0.102	0.102	0.07	0.094	0.032	0.011	0.036	0.081	0.102	0.102	0.102	0.102
6	0.07	0.034	0	0	0	0	0	0	0.022	0.067	0.015	0.015
There is no need for lighting between 7 and 17												
17	0.066	0	0	0	0	0	0	0	0	0	0.11	0.11
18	0.146	0.144	0.07	0	0	0	0	0	0	0.036	0.146	0.146
19	0.146	0.146	0.146	0	0	0	0	0	0.074	0.146	0.146	0.146
20	0.146	0.146	0.146	0.146	0.078	0.026	0.036	0.112	0.146	0.146	0.146	0.146
21	0.146	0.146	0.146	0.146	0.146	0.146	0.146	0.146	0.146	0.146	0.146	0.146
22	0.146	0.146	0.146	0.146	0.146	0.146	0.146	0.146	0.146	0.146	0.146	0.146
23	0.146	0.146	0.146	0.146	0.146	0.146	0.146	0.146	0.146	0.146	0.146	0.146

lighting installations per km are calculated in case of dimming under the *M3* lighting class according to the maximum pole spacing for the twin-bracket central arrangement. In addition to current conditions, payback periods of the energy system investments are also calculated considering future scenarios: 1) 25 % increase in electricity tariffs; 2) 25 % decrease in PV system components and battery costs; 3) 50 % decrease in PV system components and battery costs; 4) 25 % increase in electricity tariffs with 50 % decrease in PV system components and battery costs. The payback periods of the energy system investments and total installation costs per km under current conditions and for future scenarios are given in Table 9.

Table 7. Lighting Calculations with and without Dimming

Parameter	Lighting Class	
	M3	M4
Arrangement	Twin-bracket central	
Luminaire luminous flux (lm)	9270	6952.5
Luminaire power (W)	73	51.1
Luminous efficacy of luminaire (lm/W)	126.99	136.06
Spacing (m)	49	
Height (m)	9.5	
Boom length (m)	0.5	
L_{avg} (cd/m^2)	1.02	0.77
U_o	0.40	0.40
U_l	0.51	0.51
TI (%)	14	13
SR	0.89	

4. CONCLUSION

In this study, a techno-economic analysis of off-grid PV LED road lighting systems have been made for Antalya province of Turkey. In the first part of the study, optimal system design for off-grid PV LED road lightings systems under the *M3* lighting class in Antalya is obtained with the twin-bracket central arrangement using maximum pole spacing. In the second part of the study, over the determined optimal design, the techno-economic analysis of the energy system in case of dimming LED luminaires after midnight is made. In case of dimming, LED luminaire power is decreased from 2×73 W to 2×51.1 W after midnight and thus, required PV and battery size of the energy system to supply LED luminaires are decreased

Table 8. Comparison of Optimization Results for Normal Case and Dimming Case

Parameter	Normal case	Dimming case
Battery capacity (V/Ah)	2×12/333.3	12/500
PV panel power (W)	800	770
PV tilt angle (°)	36.90	
Levelized COE ($/kWh)	0.225	0.210
Battery + PV initial cost ($)	1829	1398
Battery + PV net present cost ($)	1933	1506
Charge regulator cost ($)	125	
Operation&maintenance cost ($)	104.14	
Load consumption (kWh per year)	578	483
Unmet electric load (%)	0	
Autonomy (h)	84.86	76.16
CO_2 emission reduction (kg per year)	283.22	236.67

Table 9. The Payback Periods of the Energy System Investments and Total Installation costs per km under current conditions and for future scenarios

Scenario	Case	Energy System Net Present Cost ($)	Load Electricity Consumption (kWh per year)	Payback Period (years)	Total Installation Cost per km ($)
Current conditions	Normal case	2058	578	27.82	62526.45
	Dimming case	1631	483	26.38	53559.45
25 % increase in electricity tariffs	Normal case	2058	578	22.25	62526.45
	Dimming case	1631	483	21.10	53559.45
25 % decrease in PV system component and battery costs	Normal case	1599	578	21.61	52887.45
	Dimming case	1280	483	20.70	46188.45
50 % decrease in PV system component and battery costs	Normal case	1144	578	15.46	43332.45
	Dimming case	929.87	483	15.04	38835.72
25 % increase in electricity tariff and 50 % decrease in PV system component and battery costs	Normal case	1144	578	12.37	43332.45
	Dimming case	929.87	483	12.03	38835.72

from 800 W to 770 W and from 2×12 V 333.3 Ah to 12 V 500 Ah respectively. LED luminaires operated 2183.91 hours dimmed and 1777.26 hours without dimming annually.

For both normal and dimming cases, payback periods of the systems are found to be between 28–26 years under current conditions and between 22–20 years when electricity tariffs increase by 25 % or PV system component and battery costs decrease by 25 %. While payback periods are above the system lifetime in the former scenarios, payback periods can go below 20 years and be reduced to 15 years in case of 50 % reduction in PV system component and battery costs, and moreover can be re-

duced to 12 years along with 25 % increase in electricity tariffs.

When dimming is applied, in current case the total NPC of the entire lighting installation per km decreases from $62 526.45 to $53 559.45 by 14.3 % and in the most favourable future scenario (25 % increase in electricity tariffs with 50 % decrease in PV system component and battery costs) the total NPC of the entire lighting installation per km decreases from $43 332.45 to $38 835.72 by 10.4 %.

REFERENCES

1. Wu M.S., Huang H.H., Huang B.J., Tang C.W., Cheng CW. Economic feasibility of solar powered led roadway lighting // Renew Energy, 2009, Vol. 34, pp. 1934–1938.

2. Liu G. Sustainable feasibility of solar photovoltaic powered street lighting systems // International Journal of Electrical Power & Energy Systems, 2014, Vol. 56, pp. 168–174.

3. Velaga R., Kumar A. Techno-economic evaluation of the feasibility of a smart street system: A case study of rural India // Procedia Social and Behavioral Sciences, 2012, Vol. 62, pp. 1220–1224.

4. Khalil A., Rajab Z., Amhammed M., Asheibi, A. The benefits of the transition from fossil fuel to solar energy in Libya: A street lighting system case study // Appl. Sol. Energy, 2017, Vol. 53, pp. 138–151.

5. Al-Kurdia L., Al-Masria R., Al-Salaymeh A. Economical Investigation of the Feasibility of Utilizing the PV Solar Lighting for Jordanian Streets // International Journal of Thermal & Environmental Engineering, 2015, Vol. 10, pp. 79–85.

6. Baurzhan S., Jenkins G.P. Off-grid solar PV: is it an affordable or appropriate solution for rural electrification in sub-Saharan African countries? // Renewable and Sustainable Energy Reviews, 2016, Vol. 60, pp. 1405–1518.

7. Feldman D., Barbose G., Margolis R., Bolinger M., Chung D., Fu R., Seel J., Davidson C., Wiser R. Photovoltaic System Pricing Trends Historical, Recent, and Near-Term Projections // National Renewable Energy Laboratory Publications, 2015.

8. EnergyTrend PV. PV Spot Prices, May 13, 2016. URL: https://pv.energytrend.com/pricequotes.html.

9. CIE115–2010. Lighting of Roads for Motor and Pedestrian Traffic, Central Bureau CIE, 2010.

10. EN13201:2003. Road Lighting. Part 2: Performance Requirements, CEN, Brussels EN, 2003.

11. Güler Ö., Onaygil S. Yol Aydınlatması Tesisatlarında Armatür Fotometrik Değerlerinin Önemi, IV [Importance Of Luminaire Photometric Values In Road Lighting Installations] // Ulusal Aydınlatma Sempozyumu, İzmir, 2017, p. 125–135.

12. TUIK. Distribution of net electricity consumption by sectors. May, 2016. URL: www.tuik.gov.tr/PreIstatistikTablo.do?istab_id=1579.

13. TEDAŞ. Technical Specification for LED Light Sourced Road Lighting Luminaires, 2015

14. Republic of Turkey The Ministry of Energy and Natural Resources. Procedures and Principles on the Usage of LED Luminaires in the General Lighting Scope, 2015.

15. EN13201:2004. Road lighting. Part 3: Calculation of Performance, CEN, Brussels EN, 2003.

16. TEDAŞ, Technical Specifications for Road Lighting Luminaires TEDAŞ MYD-95–009.B. 2008.

17. CIE154–2003. The Maintenance of Outdoor Lighting Systems, International Commission on Illumination, Wien, 2003.

18. ABB. Turkey Energy Efficiency Report, 2011.

19. General Directorate of Electrical Power Resources Survey and Development Administration. Turkey Solar Energy Potential Atlas of Turkey. May, 2016. URL: www.eie.gov.tr/MyCalculator/Default.aspx.

A.Can Duman,
M.Sc. He is an employee of Istanbul Technical University, Energy Institute

Önder Güler,
Ph.D. Prof. of the Istanbul Technical University, Energy Institute. Member of the Turkish National Lighting Commission and Society of electrical engineers. Research interests: road lighting, energy saving, energy consumption management in industry and buildings, wind energy, power quality

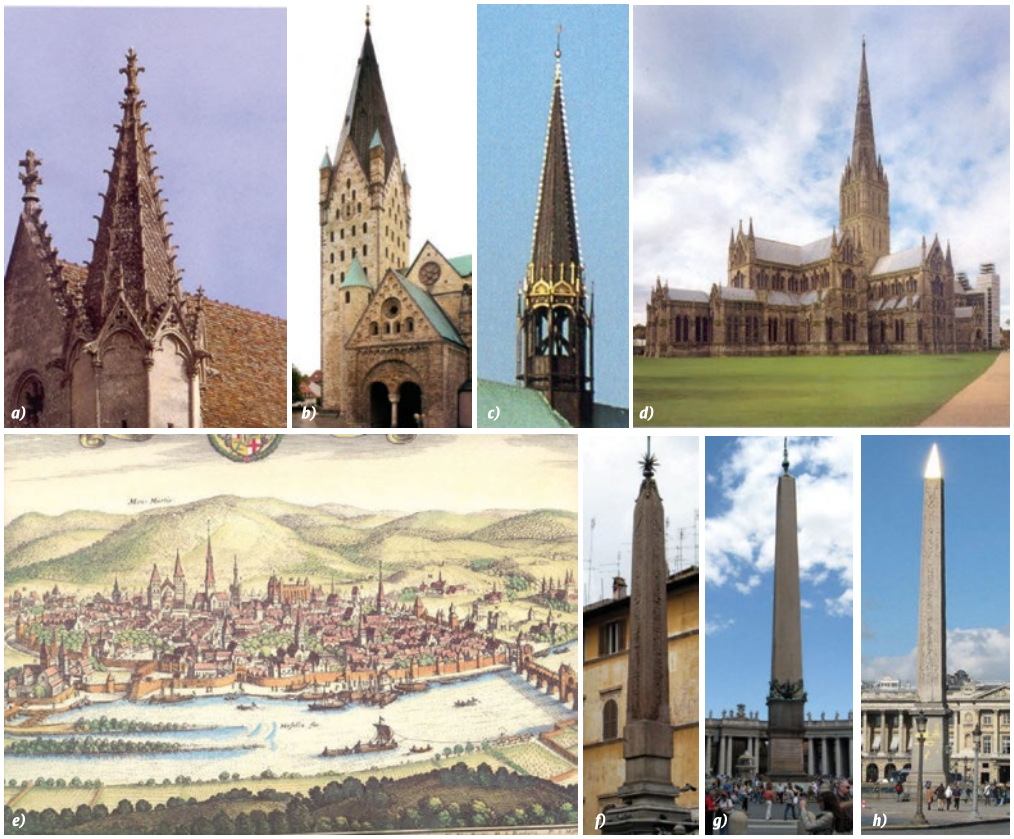

Fig. 6: *a* – the Church in Saint-Germer-de-Fly Abbey (France, 13th c.); *b* – the Church of Saint Patrokli, Soest (Germany, early 13th c.); *c* – the Saint Mary's Church, Lübeck (Germany, early 14th c.); *d* – the Cathedral Church of the Blessed Virgin Mary, Salisbury (England, 13th-14th c.); *e* – the tents and the spires in Trier (Germany); *f* – the Egyptian obelisk in front of the City Church, Rome (Italy); *g* – the Egyptian obelisk in the square in front of the Saint Peter's Basilica, Rome (Italy); *h* – the Egyptian obelisk in Place de la Concorde, Paris (France)

Fig. 7. The tents in the Russian architecture: *a* – the Trinity Church in Nyonoksa (early 18th c.); *b* – the Saints Zosima and Savvaty Church, the Trinity Lavra of Saint Sergius (early 17th c.); *c* – the Church of Ilya the Prophet, Yaroslavl (middle 17th c.); *d* – the Spasskaya Tower, Moscow (Kremlin); *e* – the tents on the Palace of Tsar Alexei Mikhailovich in Kolomenskoye near Moscow (middle 17th c.), watercolour by G. Quarenghi (18th c.); *f* – the tents on the Kremlin (engraving, 18th c.)

Fig.2. Trap of light in the transport interchange hub "Fulton Centre" (New York): a – general view of the building node; b – internal space with a mesh structure of the dome

Fig. 6. The system of sun protection in the office towers "Al Bahr" in Abu Dhabi: a – general view; b – modification of sun protection devices; c – transformation scheme panels

Fig. 7. Dynamic facade of the art centre in Shanghai (China): general view (transformation options)

Fig. 9. Architecture of natural light by Peter Zumthor: a – Museum, Cologne diocese of Columbus; b – St. Benedict chapel in Sumvitg

Fig. 11. The skyscraper “Walkie-talkie”, (London)

Fig. 12. Solar furnace in the Pyrenees (France)

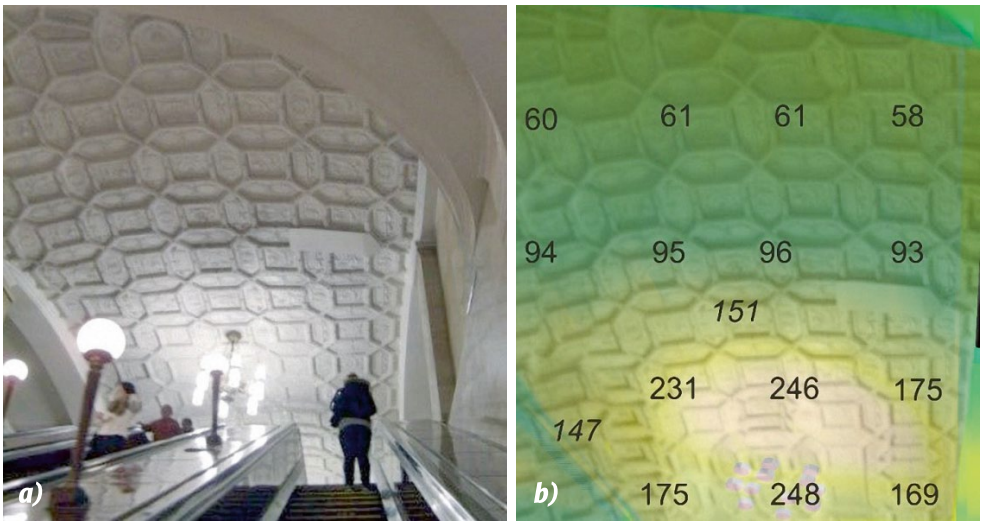

Fig. 4. Exterior of the ceiling in the entrance hall and its lighting principle before ID reconstruction: *a* – exterior; *b* – illuminance distribution

Fig. 5. IDs at *Krasnye Vorota* before reconstruction: *a* – sconce; *b* – chandelier

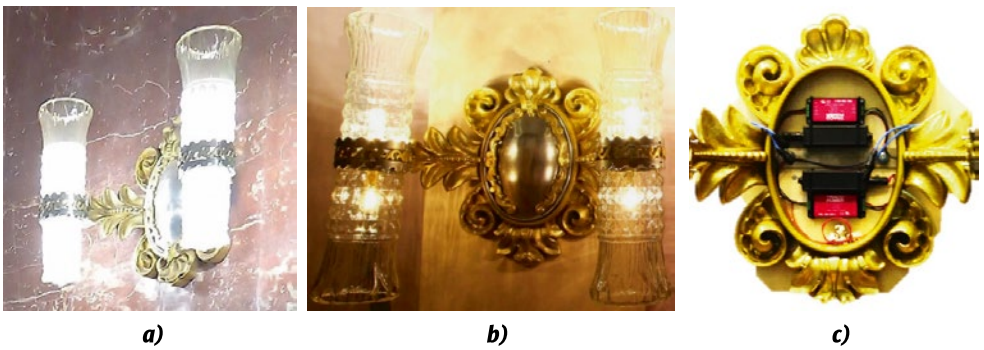

Fig. 10. Exterior of operational IDs (sconces): *a* – before reconstruction; *b* – after reconstruction; *c* – location of the power and control gear (for an LED module and standby lighting)

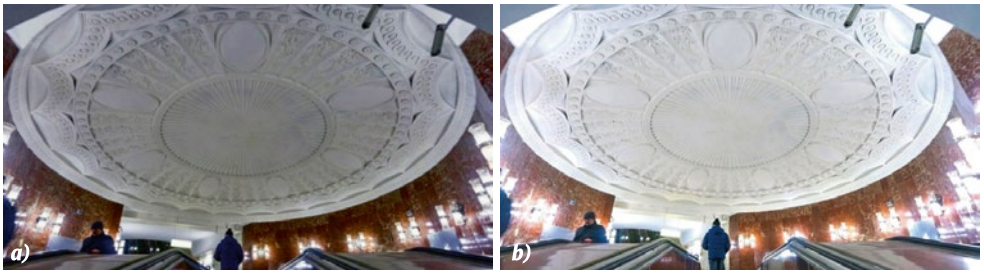

Fig. 11. Exterior of the illuminated ceiling in the inter-escalator anteroom: *a* – before reconstruction; *b* – after reconstruction (installation)

Light & Engineering
Vol. 27, No. 2, pp. 71–77, 2019 *https://doi.org/10.33383/2018-071*

POSSIBILITY OF USING IN RUSSIA THE EXPERIENCE OF LED LIGHTING APPLICATION AT THE USA AIRFIELDS

Vladimir V. Vorozhikhin*, Eugenia L. Moreva, Vladimir G. Starovoytov, and Igor G. Tyutyunnik

Financial University under the Government of the Russian Federation, Moscow
**Plekhanov Russian University of Economics, Moscow*
** E-mail: vorozhikhin@mail.ru*

ABSTRACT

The purpose of this paper is an investigation of LEDs illumination experience at US-based aerodromes with an assessment of its feasibility and its necessity in Russia.

The following methods were used: the analysis of aerodrome lighting requirements; the review and the analysis of development features in aerodrome LEDs illumination; the experience analysis of LEDs illumination of US-based aerodromes; the deductive analysis and the assessment synthesis of feasibility and necessity of US experience in LEDs illumination at Russian-based aerodromes.

The following results were achieved:

– The analysis of issues and opportunities was conducted for development of LEDs illumination at US-based aerodromes and of American experts' recommendations for its use;

– The cases were taken for use and assessment of development in LEDs illumination at US-based aerodromes;

– The review and the analysis were conducted in relation to a developing market of LEDs illumination at Russian-based aerodromes.

The main conclusion is that the US experience will improve quality and reliability of service provided in air transportation, comfort, and safety of Russian flights, as well as competitiveness of Russian-based airports and airlines (indirectly).

Keywords: LEDs illumination, airport network development, development features of aerodrome (airport) LEDs illumination, new market emergence for aerodrome (airport) LEDs illumination

1. INTRODUCTION

1.1. Aerodrome Lighting Requirements

The niche of air transportation in the international market of transport services is transportation of passengers, as well as of expensive, perishable, and hazardous goods, or of goods with small weight and dimensional values over long distances, with a high cost of payment per 1 kg of weight. Any non-scheduled delays, not to mention accidents and catastrophes, lead to significant and often irrecoverable damages [1]. That is why reliability of flight safety is so significant. Visual signals, including lighting equipment, are the most important part.

The aerodrome electrical lighting is included in the scope of airport activities [1, 2]. The international standards and the recommended practices are set out in the requirements for design and operation of aerodromes [2] and in the certification rules [3]. The system of visual lighting equipment includes:

- Funnel lighting system;
- Runway landing lights;
- Runway threshold lights;
- Runway end lights;
- Runway centre-line lights;
- Touchdown zone lights;
- Stop bars lights at taxi-holding points;

- Main taxi track lights and stop bars lights (excluding stop bars lights at taxi-holding points);
- Obstruction lights, etc.

The aerodrome lighting power network diagram is designed in such a way that, when a single section of the power network fails, the pilot does not lose any visual orientation and the luminance pattern does not become distorted. The properties of power networks for aerodrome lights and the rules for aerodrome lighting systems control are well known [2, 3].

Interacting with airlines, airports should provide comfort and safety of flights in accordance with the regulated service quality [4–6]. The importance of the infrastructure, which is a part of the aviation traffic safety system, requires its protection, which is governed by the airport security regulations (Decree of the Government of the Russian Federation dated 1 February 2011 No. 42 for Approval of the Security Rules for Airports and their Infrastructure).

In accordance with Article 48 of the Aviation Code of the Russian Federation [7], the equipment, including lighting equipment installed at civil aerodromes, joint civil/state aerodromes, and joint-use aerodromes, must meet the requirements for serviceability that are confirmed by an appropriate serviceability certificate [8, 9].

Multi-coloured lights (red, yellow, green, blue, and white signals) are used in US lighting systems, for which corresponding blackout curves are set (according to Engineering Brief No. 67D). White-yellow and red-yellow signal lights are used as well. The lights have various intensity rates: low (low-intensity lights), medium and high (high-intensity lights) [2, 3]. AC150/5340–30H provides replacement of three-stage regulators with a five-stage version. A variety of properties, as well as stiff requirements to luminance and reliability create the need for LEDs illumination and its intellectual management for airports. The narrow LEDs radiation spectrum also allows us to work with various optical systems, including infrared (IR) systems.

In addition to specified lights, the market sectors for LEDs illumination are lighting equipment of aircraft, buildings, structures, and environs [7]. Under such a use, LEDs become part of architectural and cultural design of modern airports. They ensure a comfortable stay of passengers in airport premises. They can support transmission of internet information with *Li-Fi* that allows for LEDs light to be used as an information carrier. Luminous carpets, being navigation and communication tools that show directions in multi-storey offices, airports, and shopping malls, are already widely used in the US. They feature arrows or text phrases to suggest directions for people and equipment. Smart light can provide security, transmit information about any accident or shot sounds to an appropriate service. Such a lighting system is already successfully operating not only at US-based airports, but also in streets of some cities (e.g. Los Angeles).

In Russia, for instance, integrated lighting systems are developed on the basis of street lights with Philips *RoadFlair* LEDs [10].

The need for development of home systems of electric and signal equipment in Russia was caused by rapid development of passenger flights and cargo flights in the 1970s and introduction of multi-seated jet aircrafts of the 2nd generation and of the 3rd generation such as TU-154, IL-62, IL-76, and IL-86. In 1971, the USSR joined the ICAO which developed standards and rules for unified properties and parameters of on-board equipment and ground equipment for flight operations at all weather conditions.

At that time, the airport equipment in the USSR did not meet the requirements of the ICAO, which significantly retarded development of international air transportation. Only few large airports were equipped with foreign equipment (from Czechoslovakia or Finland) which put civil aviation with joint air forces aerodromes (in particular cases) in a dangerous dependence on foreign suppliers [11].

The technical inferiority of Russia is repeated through a half of a century, demanding a strategic interaction of modern airport enterprises and airlines, innovative solutions (specifically, advanced LEDs illumination) to achieve competitiveness in the system of global air transportation [1].

1.2. Development of Smart LEDs Illumination Technologies for Airports

The advantages of LEDs illumination include the following: increased luminous efficacy, no hazardous substances, high durability features, extended service life, much smaller weight and size parameters [12–14].

In 2013–2016, a pilot project was implemented which introduced LEDs illumination at the largest international airport, PHL (Philadelphia, the US)

[15]. PHL employees, with the assistance of *GATEWAY* specialists from the US Department of Energy, first conducted a survey and an analysis of electrical energy consumption for lighting equipment in aircraft parking areas, apron areas, and passenger terminal areas. The expected energy savings reached almost 50 %.

The project implementation confirmed the calculations: the introduction of new lighting equipment allowed saving significant amounts of energy, optimizing the distribution of airport lighting levels for specific tasks of aircraft maintenance, ground equipment operation, passenger services, and flight safety [16, 17].

The practical use of new LED equipment prompted the Illuminating Engineering Society of North America (IESNA) to make changes to IESNA-RP-17–1987 (Airport Service Area Lighting) and IESNA-RP-14–1987 (Airport Road Automobile Parking Area Lights): they have been updated and merged into a single document, IES RP-37–15, which provides additional information on important advantages of LEDs illumination [18].

A brief overview of the standards of the Federal Aviation Administration of the United States (FAA) is given in [19] in terms of LEDs illumination and energy efficiency. FAA operations personnel controls lighting systems and visual indicators of approach flight tracks, and airport personnel controls runways, taxiways, and parking lights [20].

LEDs can provide enhanced colour rendering, which is important in determination of traffic route dye marking and, with high-efficient control devices, can switch on and off, instantly or gradually, at almost any temperature.

In December 2015, a 3 MW solar power plant was commissioned at the Minnesota International Airport (MSP) [21, 22]. During reconstruction and modernization of lighting equipment under the company's project on energy efficiency and renewable energy, 7,700 *Ameresco* halide lamps were replaced with energy-efficient LEDs which significantly reduced energy consumption. At the same time, this solar power plant currently provides almost 20 % of the total energy capacity for the airport, reducing greenhouse gas emissions by 6,813 tonnes per year. All this increases reliability and sustainability of airport lighting, saves significant amounts of energy, and allows them to build an airport lighting system with a high degree of independence from external sources of energy supply.

1.3. US-based Airports and Organizations that Explore LEDs Illumination Feasibility for Airport-associated Needs

There are about 5,000 US-based airports [23], 3,300 of which are part of the National Airports System and are eligible for federal development grants [25]. The Transportation Research Board (TRB), which offers innovative, research-based solutions to improve transport activities, is involved in air transportation development of the US. The TRB is jointly managed by the United States National Academy of Sciences, the United States National Academy of Engineering Sciences, and the United States Institute of Medicine.

The objective of this work is to study the experience of LEDs illumination at US-based aerodromes (airports) with an assessment of feasibility and necessity of LEDs illumination in Russia.

2. METHODS

Such scientific methods as analysis, synthesis, and deduction were applied during our study on modernization with an introduction of LEDs illumination at Russian airports based on the experience of the United States. The following analyses took place: the analysis of aerodrome lighting requirements; the review and the analysis of development features in aerodrome LEDs illumination; the experience analysis of LEDs illumination at US-based airports; the deductive analysis and the assessment synthesis of feasibility and necessity of the US experience in Russian LEDs illumination.

3. RESULTS

The aerodrome ground lighting (AGL) ensures visibility for runways and taxi tracks. Over the past decade, significant steps have been taken to support this activity at US-based aerodromes, and LEDs technologies have become more common in AGL (Figs. 1, 2).

Reconstruction of an AGL system requires development of high-quality project documentation. Acceptance testing and commissioning of AGL should be linked to each construction project and applicable regulations. In case of phased introduction of LEDs illumination, the issues of compatibility of LED lamps with existing energy infrastructure may arise at an airport. In order to ensure compatibility

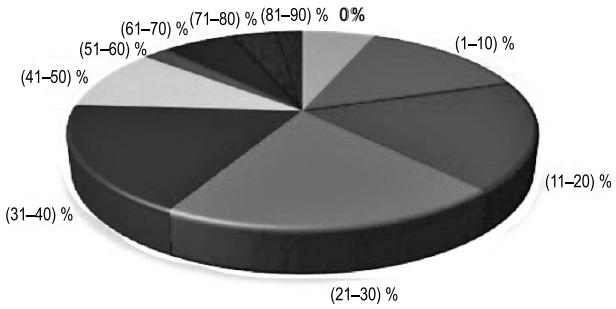

Fig. 1. The percentage for use of LED illumination devices at the surveyed aerodromes [25]

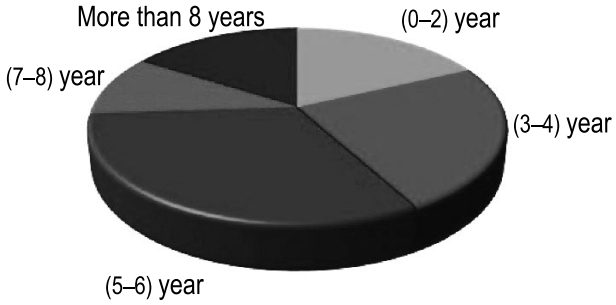

Fig. 2. The current duration for use of LEDs illumination at the surveyed aerodromes [25]

with existing equipment, design and installation of lamps should be coordinated [24].

Acceptance inspection of an aerodrome lighting system must include visual inspection and physical inspection of this system, electrical testing, photometric testing, and a systematic failure test [25].

LED lamps for various purposes (runway edge lights, runway centre-line lights, taxiway lights, obstruction lights, touchdown zone lights, lift-off zone lights, runway identification threshold lights, aerodrome signs, etc.) are used in various proportions in AGL [25].

Visual check identifies compliance of orientation and physical condition (including integrity and purity) with an energy supply system design (1 level, 3 levels, or 5 levels). It is recommended to check a 20 % random sample of lamps. If a defect is found, other 20 % of lamps should be opened and checked. All defective lamps should be repaired and rechecked.

Electrical testing ensures that minimum specified standards are met and provides basic data for service management. Circuit insulation resistance measurement (50 MΩ, according to AC150/5340–30H) ensures no current losses and is used to analyse dynamic properties of insulation processes and use environment. Measurements of impedance and power of system load should be carried out at regular intervals. Electrical equipment is non-resistant to dust and dirt which specifically contribute to overheating and premature failure of lamps.

Photometric testing (with lamps commissioning) includes standard photometric measurements that correspond to the type (purpose) of the tested lamp.

A systemic failure test allows you to detect substandard components (electronic components as a source of failure) during sweeping or so called burn-in. It is recommended to use a sweep period that is 5–10 times longer than the normal daily operating period which is usually 12 hours.

The system of acceptance tests is important for inventory management of lighting assets and for lighting system savings. The recommended warranty period is 4 years according to AC150/5345–43H, and the lamp replacement criteria are according to AC150/5340–26C. Airports should also check lamps at least twice a month. Lamps may have a higher failure rate due to vibration in the middle of the runway, on taxiways, or in touchdown zones. Modern LED lamps are much more reliable than their predecessors, requiring a much lower frequency of replacements. To manage warranty obligations, it is necessary to specify a lamp installation date and to develop a post-warranty strategy (e.g. including a service contract, an extended warranty period, or internal repair work).

The problem is equipment obsolescence due to rapid development of LED technologies, especially for small airports which cannot often receive any support from the FAA. The obsolescence problem is partially mitigated by adaptive electronics.

The typical empirical rule for spare parts is their 10 % share from the design quantity. However, with due regard to LEDs longevity, it can be reduced to 5 % (which also indicates LEDs advantage).

The savings of LEDs illumination depends on technical and operational properties of LED equipment. Decrease in expected operating costs for aerodrome LEDs illumination is confirmed by reduction in maintenance costs and a decrease in energy consumption of LED lamps.

Long-term operation (over 100,000 hours of continuous operation) is the main advantage of LED lamps that contain electrolyte-free capacitors in high-durable aluminium shells. At the same time, costs of special equipment are reduced (no crane trucks required for service of lamps up to 50 meters high).

4. DISCUSSION AND CONCLUSION

The article includes:

– The analysis of aerodrome lighting requirements, development features of aerodrome LEDs illumination, and experience of LEDs illumination at US-based aerodromes;

– The deductive analysis and the assessment synthesis of feasibility and necessity of the US experience in LEDs illumination of Russian-based aerodromes.

There is the number of on-line tools to compare estimated life-cycle values of various lighting systems [26], including in Russia:

1. The US Department of Energy (DOE) presents several methods to calculate energy savings and necessary costs for reconstruction of airport lighting systems (URL: http://www1.eere.energy.gov/femp/technologies/eep_eccalculators.html);

2. The New York State Energy Research and Development Authority (NYSERDA) offers an electronic worksheet to calculate life-cycle costs of commercial lighting systems. This worksheet can be adapted to estimate aerodrome lighting costs (URL: http://www.nyserda.ny.gov/Page-Sections/Business-Partners/Commercial-Lighting/Tок-Partners.aspx);

3. *General Electric Lighting* provides a number of simple tools to estimate energy costs and life-cycle costs (URL: http://www.gelighting.com/na/business_lighting/ education_resources/tools_software/toolkit);

4. The manufacturer of aerodrome lighting equipment, *ADB Airfield Solutions*, provides a tool for work with electronic worksheets to assess investment profitability and life-cycle costs for a number of types of LED illumination devices.

LEDs illumination costs became the greatest concern for personnel at the surveyed airports [25]. About 75 % of specialists said that LEDs illumination costs are a main barrier for aerodrome LEDs illumination. However, there is evidence that LEDs illumination, which is currently installed at aerodromes, provides (20–50)% of their general lighting in the majority of US-based airports [25]. Understanding the return on investment (ROI) required for adoption of LED technology helps decision makers select the best action plan for modernization of their airports. It is advisable to determine landing fees amounts for airlines at every aerodrome, with due regard to cost recovery for introduction of modern LEDs illumination [26, 27].

The following can be concluded based on the materials of the article:

- The state of the art for aerodrome (airport) LEDs illumination in Russia is lower than in the US;
- The experience of this LEDs illumination technology in the US is of undoubted interest for Russia since many of solved problems in the US can be taken into account when modernizing lighting systems of Russian airports;
- Russian organizations and institutions in fields of science, innovation, and operation of high-end equipment should participate in cross-professional discussion of various issues, and the scientific publications of the US, including the reports of the National Academy of Sciences of the United States, can be used to enhance this process;
- The US experience will improve quality and reliability of services provided in air transportation, comfort, and safety of Russian flights, as well as competitiveness of Russian-based airports and airlines (indirectly);
- It is advisable to use on-line tools in Russia that are recommended by US specialists to estimate life-cycle costs for LED lamps, with due regard to existing geographical and climatic factors.

REFERENCES

1. Pankratova, A.R. Evaluation of Strategic Interaction of Airport Enterprises and Airlines // Dissertation of Ph. D. in Economics. – Saint Petersburg: Federal State Budgetary Educational Institution of Higher Education – Saint Petersburg State University of Civil Aviation, 2017, 162 p.

1. Pankratova, A.R. Otsenka strategicheskogo vzaimodeystviya aeroportovykh predpriyatiy i aviakompaniy / Diss. … k-ta ekon. nauk. – SPb: FGBOU VO Sankt-Peterburgskiy gosudarstvennyy universitet grazhdanskoy aviatsii, 2017, 162 p.

2. Annex 14 to the Convention on International Civil Aviation. Aerodromes. Volume I – Aerodrome Design and Operations, 7th ed.: International Civil Aviation Organization (ICAO), 2016.

3. Aviation Regulations. Part 139: Certification of Aerodromes. Volume II – Aerodrome Certification Requirements, 2012, 163 p.

3. Aviatsionnyye pravila. Chast 139: Sertifikatsiya aerodromov. Tom II –Sertifikatsionnyye trebovaniya k aerodromam, 2012, 163 p.

4. GOST R56118–2014. Air Transportation. Aviation Operations Safety Management System. Safety Management System of the Equipment Suppliers Aviation Complex. Guidelines for Safety Management of Aviation Operations of Airport Complexes.

4. GOST R56118–2014. Vozdushnyy transport. Sistema menedzhmenta bezopasnosti aviatsionnoy deyatelnosti (SMB-AD). Sistema menedzhmenta bezopasnosti aviatsionnogo kompleksa postavshchikov obsluzhivaniya. Rukovodstvo po upravleniyu bezopasnostyu aviatsionnoy deyatelnosti aeroportovykh kompleksov.

5. GOST R55862–2013. Air Transportation. Aviation Operations Safety Management System. Safety Management System of the Equipment Suppliers Aviation Complex. Aviation Operations Safety Management System of Equipment Suppliers: Airlines, Airports, Air Traffic Management Organizations, Educational Institutions, Maintenance and Repair Organizations. General Provisions.

5. GOST R55862–2013. Vozdushnyy transport. Sistema menedzhmenta bezopasnosti aviatsionnoy deyatelnosti. SMB aviatsionnogo kompleksa (postavshchikov obsluzhivaniya). SMB aviatsionnoy deyatelnosti postavshchikov obsluzhivaniya: aviakompanii, aeroporty, organizatsii po organizatsii vozdushnogo dvizheniya, uchebnyye zavedeniya, organizatsii po tekhnicheskomu obsluzhivaniyu i remontu. Obshchiye polozheniya.

6. ICAO Doc 9859. Safety Management Manual, 8 Ed., (unedited advance version), 2018, 172 p.

7. Air Code of the Russian Federation dated 19 March 1997 No. 60-FZ (as amended on 03 August 2018) (as amended and supplemented, entered into force on 14 August 2018).

7. Vozdushnyy kodeks Rossiyskoy Federatsii dated 19 March 1997 No. 60-FZ (as amended on 03 August 2018) (as amended and supplemented, entered into force on 14 August 2018).

8. Register of Issued Certificates for Aerodrome Lighting Facilities, 2018, 2 p. URL: http://favt.ru/public/materials//3/2/6/f/7/326f7c66f5b664ec878773f8efcd5e44.pdf (reference date: 25 June 2018).

8. Reyestr vydannykh sertifikatov svetosignalnogo oborudovaniya aerodromov, 2018, 2 p. URL: http://favt.ru/public/materials//3/2/6/f/7/326f7c66f5b664ec878773f8efcd5e44.pdf (reference date: 25 June 2018).

9. Methodical Recommendations for Certification of Lighting Equipment installed at Certified Aerodromes Designed for Take-Off, Touchdown, Taxiing, and Parking of Civil Aircrafts (approved by Deputy Director of the Federal Air Transport Agency on 30 September 2017), 15 p. URL: http://www.favt.ru/public/materials//1/2/9/f/6/129f655b7a4ed5ae3b87e3961bbb34dd.pdf (reference date: 25 June 2018).

9. Metodicheskiye rekomendatsii provedeniya sertifikatsii svetosignalnogo oborudovaniya, ustanavlivayemogo na sertifitsirovannykh aerodromakh, prednaznachennykh dlya vzleta, posadki, ruleniya i stoyanki grazhdanskikh vozdushnykh sudov (approved by Deputy Director of the Federal Air Transport Agency on 30 September 2017), 15 p. URL: http://www.favt.ru/public/materials//1/2/9/f/6/129f655b7a4ed5ae3b87e3961bbb34dd.pdf (reference date: 25 June 2018).

10. Neverskaya, N. Lamps Give Us Light and Warmth, They Also Guard, Protect, and Grow. URL: http://www.forbes.ru/forbeslife/360381-chto-mozhet-svet-pyat-vozmozhnostey-sovremennyh-sistem-osveshcheniya (reference date: 25 June 2018).

10. Neverskaya, N. Svetilniki ne tolko svetyat i greyut, no i okhranyayut, zashchishchayut i vyrashchivayut. URL: http://www.forbes.ru/forbeslife/360381-chto-mozhet-svet-pyat-vozmozhnostey-sovremennyh-sistem-osveshcheniya (reference date: 25 June 2018).

11. Mayzenberg, S.I. Development of Electric Lighting Facilities for Civil and Special Aerodromes in 1972–1989 // Svetotekhnika, 2018, No. 3, pp. 84–91.

11. Mayzenberg, S.I. Sozdaniye kompleksov elektrosvetosignalnogo oborudovaniya dlya grazhdanskikh i spetsialnykh aerodromov v 1972–1989 godakh // Svetotekhnika, 2018, No. 3, pp. 84–91.

12. GOST R56231–2014/IEC/PAS62722–2–1:2011. Lamps. Part 2–1. Particular requirements for properties of LED lamps with LED light sources.

12. GOST R56231–2014/IEC/PAS62722–2–1:2011. Svetilniki. Chast 2–1. Chastnyye trebovaniya k kharakteristikam svetilnikov so svetodiodnymi istochnikami sveta.

13. GOST R55705–2013. Illumination devices with LED light sources.

13. GOST R55705–2013. Pribory osvetitelnyye so svetodiodnymi istochnikami sveta.

14. GOST R54815–2011/IEC/PAS62612:2009. LED lamps with an integrated control device for general lighting at over 50 V.

14. GOST R54815–2011/IEC/PAS62612:2009. Lampy svetodiodnyye so vstroyennym ustroystvom upravleniya dlya obshchego osveshcheniya na napryazheniya svyshe 50 V.

15. Terminal F Renovation and Expansion, Philadelphia Airport. URL: https://www.airport-technology.com/projects/terminal-f-renovation-and-expansion-philadelphia-airport (reference date: 25 June 2018).

16. SSL Evaluation: Philadelphia International Airport Apron Lighting // DOE/EE-1646. October, 2015, 2 p.

17. Philadelphia International Airport Apron Lighting: LED System Performance in a Trial Installation. Pacific Northwest National Laboratory, 2015, 34 p.

18. 2016 Guide to Airport Lighting. URL: https://www.specgradeled.com/2016-guide-to-airport-lighting/ (reference date: 25 June 2018).

19. Lepine, D. FAA Standards for LED Lighting and Energy Efficiencies, 2014, 22 p. URL: https://docplayer.net/32968558-Faa-standards-for-led-lighting-and-energy-efficiencies-dave-lepine.html (reference date: 25 June 2018).

20. Thurber, M. Airports. FAA Adapting to LED Lighting Push. URL: https://www.ainonline.com/aviation-news/aerospace/2015–01–15/airports-faa-adapting-led-lighting-push (reference date: 25 June 2018).

21. MSP Airport Solar PV and Energy Efficiency Project Overview – Presentation MSP&Ameresco, 2015, 18 p.

22. Minneapolis-St. Paul International Airport Powers Up Minnesota's Largest Solar Energy Project. URL: https://www.ameresco.com/minneapolis-st-paul-international-airport-powers-minnesotas-largest-solar-energy-project/ (reference date: 25 June 2018).

23. Airport Research Needs: Cooperative Solutions / Special Report. NAP, 2003, 116 p.

24. Issues with Use of Airfield LED Light Fixtures. NAP, 2012, 35(43) p.

25. LED Airfield Lighting System Operation and Maintenance / ACRP Report 148, 2015, 90 p.

26. Doc 9562. Airport Economics Manual. 3rd ed. – International Civil Aviation Organization, ICAO, 2013.

27. Doc 9082. ICAO's Policies on Charges for Airports and Air Navigation Services. 9th Ed. – International Civil Aviation Organization, ICAO, 2012.

Vladimir V. Vorozhikhin, Ph. D. in Economics, graduated from the Moscow Power Engineering Institute (MPEI) in 1979. He is the Leading Researcher of the Centre for Monitoring and Evaluation of Economic Security under the Institute for Economic Policy and Economic Security Issues at the Financial University

Eugenia L. Moreva, Ph. D. in Economics, graduated from the Lomonosov Moscow State University, faculty of economics. She is the Deputy Director of the Institute of Industrial Policy and Institutional Development at the Financial University. Her Research interests are innovation economics, regional integration, and intellectual capital

Vladimir G. Starovoytov, Doctor of Economics, graduated from the Moscow Aviation Institute (1979) and the Russian Academy of National Economy and Public Administration (2000). He is the Director of the Centre for Monitoring and Evaluation of Economic Security under the Institute for Economic Policy and Economic Security Issues at the Financial University. His research interests include strategic planning and management, economic security, contracting development in government and municipal procurement

Igor G. Tyutyunnik, lawyer, graduated from the Moscow New Law Institute, faculty of law. He is the researcher of the Institute of Industrial Policy and Institutional Development at the Financial University. His research interests include industrial policy, innovation activity, and economic crime

Light & Engineering
Vol. 27, No. 2, pp. 78–87, 2019 *https://doi.org/10.33383/2018-057*

DESIGN OF A CHIP ON BOARD (COB) LED BASED INDUSTRIAL LUMINAIRE WITH THERMAL SIMULATIONS

Seher Ates, Mustafa B. Yurtseven, and Sermin Onaygil

Istanbul Technical University, Istanbul, Turkey
E-mails: smete@itu.edu.tr; byurtseven@itu.edu.tr; onaygil@itu.edu.tr

ABSTRACT

As the technology advances, the efficiencies of Chip on Board (COB) LEDs are increasing. In this study, the utilization of COB LEDs in an industrial high-bay luminaire, which can be considered as a relatively high power application, has been investigated starting from the initial design process. For an industrial hall, single-chip LED based reference luminaires, which can provide the required lighting quality criteria have been identified. COB LED selection and photometric measurements are done, and the number of COB LEDs to be used has been calculated by targeting the luminous flux value of reference luminaires. The COB LED based luminaire prototype with a plate finned heat sink was modelled by using a CAD software and the computer aided thermal simulations were performed. Then the prototype was manufactured and experimentally analysed. The highest difference between the experimental analysis and the thermal simulation was found to be less than 7 %, which demonstrates the consistency of design and analyses. This study is an example of the steps to be followed in the manufacturing stage of a COB LED based luminaire. Additionally, it is aimed to provide a perspective to the use of COB LEDs in high power applications.

Keywords: COB LED, thermal simulation, experimental analysis

1. INTRODUCTION

Nowadays, Light Emitting Diodes (LEDs) are competing with conventional light sources in many areas through their advantages such as high luminous efficacy, long life-time expectations, and variety of white colour. On the other hand, high power LED light sources convert some percent of input electrical power to optical power, while the residual part is dissipated as heat [1–4]. If this heat energy is not removed steadily, the temperature of the structure increases. LED properties such as luminous flux, luminous efficacy, and efficiency are adversely affected from the increasing temperature [5]. The lifetime of an LED is also dependent on the temperature [6]. There are many studies about active and passive cooling systems in order to reduce the adverse effects of heat on the LEDs [7–11]. Passive cooling systems are more preferred in the market due to their advantages such as the ease of manufacturing, no maintenance need, no moving parts, no power requirement, the low cost, and the simple structure. Different type of metal fins are the most popular passive cooling solutions used by luminaire manufacturers.

With an appropriate cooling system, high power LEDs promise energy savings especially in power-intensive applications. One of these applications is industrial high-bay luminaires. In industrial high-bay luminaires, mostly single chip high power LEDs are used by combining large number of them together. COB LEDs, with their day-by-day increasing luminous efficacies, are also started to be used in industrial luminaires. Additionally, the number of light sources that has to be used for reaching a specified luminous flux value is less than single chip LED based luminaires. This situation can highlight COB LED based luminaires in terms of the mechanical design simplicity and the cost advan-

Table 1. Analyses Results of Single Chip LED Based Industrial High-bay Luminaires

Luminaire	Average illuminance [lx]	Uniformity	Luminous flux of luminaire [lm]	Electrical power [W]	Luminous efficacy [lm/W]	Number of luminaires	Energy consumption [W/m^2/100 lx]
A	315	0.722	25000	182	137.4	36	0.83
B	303	0.600	25000	200	125	36	0.95

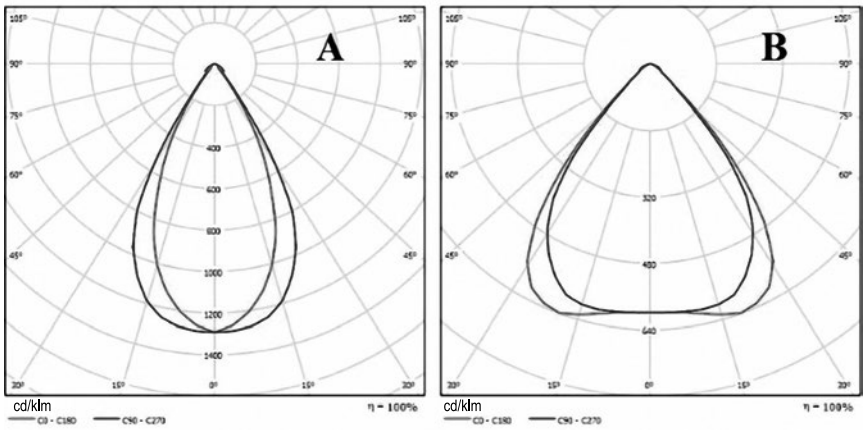

Fig. 1. Light distribution curves of reference single chip LED based industrial high-bay luminaires

tage. On the other hand, COB LEDs have a dense thermal power output from a small area, which indicates the importance of designing the cooling system to be used in the luminaire through thermal simulations and experimental analyses.

In this study, the procedure of designing a COB LED based luminaire is examined in detail. Selection of reference luminaires for benchmark, COB LED selection and measurements defining the number of COB LEDs, computer aided thermal simulations, experimental analyses and validation steps are followed, respectively. In addition, the thermal power value was determined by measurements rather than using a specific percentage of the electrical power, and then thermal simulations were performed according to these real measurement data.

2. LUMINAIRE BENCHMARK, SELECTION AND MEASUREMENTS OF COB LED

An industrial hall with the dimensions 50×50 m and 12 m ceiling height was used for analyses. The work plane height, boundary zone (distance between the walls and the calculation grid), the distance between the work plane, and the light emitting surface of the luminaires were 1 m, 1.5 m, and 9 m, respectively. The reflections of the ceiling, walls, and the floor were assumed as 70 %, 50 %, and 20 %. The maintenance factor was also taken as 0.80.

It was aimed to illuminate the selected industry hall according to the value of 300 lx average illuminance and 0.60 uniformity, which is given in the standard EN12464–1:2011 “Light and Lighting – Lighting of Work Places – Part 1: Indoor Work Places” for general machine works with the reference number 5.8.3 [12]. Maximum 5 % tolerance was allowed at the average illuminance for the determination of reference single LED chip based luminaires. DIALux, which is a lighting design software, was used in the analyses [13]. A large number of single chip-LED based industrial high-bay luminaires on the market were analysed, and two of them, which provided the aforementioned criteria,

Fig. 2. Temperature controlled Ulbricht Sphere and equipment

Table 2. Properties Obtained from the Measurements and Calculations

Driving Current, mA	Property	Cold Plate Temperature, °C					
		25	**35**	**45**	**55**	**65**	**75**
350	Solder temperature [°C]	29.3	38.7	48	57.5	66.7	76.3
	Voltage [V]	33.14	32.98	32.82	32.67	32.53	32.38
	Current [A]	0.35	0.35	0.35	0.35	0.35	0.35
	Luminous flux [lm]	1963	1940	1916	1891	1865	1837
	Optical power [W]	5.81	5.75	5.69	5.62	5.55	5.48
	CCT [K]	3859	3868	3881	3893	3908	3924
	CRI	83.6	83.6	83.5	83.5	83.5	83.4
	Electrical power [W]	11.60	11.54	11.49	11.43	11.38	11.33
	Thermal power [W]	5.79	5.80	5.80	5.81	5.83	5.86
	Efficiency [%]	0.50	0.50	0.50	0.49	0.49	0.48
	Luminous efficacy [lm/W]	169.2	168.1	166.8	165.4	163.8	162.1
700	Solder temperature [°C]	35.9	45.2	54.5	64	73.3	82.7
	Voltage [V]	34.39	34.22	34.05	33.89	33.73	33.59
	Current [A]	0.7	0.7	0.7	0.7	0.7	0.7
	Luminous flux [lm]	3695	3648	3598	3547	3492	3436
	Optical power [W]	10.95	10.82	10.69	10.55	10.4	10.25
	CCT [K]	3884	3895	3908	3922	3937	3957
	CRI	83.2	83.1	83.1	83.1	83.0	82.9
	Electrical power [W]	24.08	23.95	23.83	23.72	23.61	23.51
	Thermal power [W]	13.13	13.13	13.14	13.17	13.21	13.26
	Efficiency [%]	0.45	0.45	0.45	0.44	0.44	0.44
	Luminous efficacy [lm/W]	153.5	152.3	151.0	149.5	147.9	146.1
1050	Solder temperature [°C]	43.4	52.8	62.1	71.3	80.7	89.8
	Voltage [V]	35.40	35.22	35.05	34.88	34.73	34.58
	Current [A]	1.05	1.05	1.05	1.05	1.05	1.05
	Luminous flux [lm]	5236	5161	5082	5002	4918	4825
	Optical power [W]	15.57	15.35	15.15	14.91	14.68	14.42
	CCT [K]	3916	3925	3939	3956	3973	3998
	CRI	82.8	82.8	82.7	82.7	82.7	82.6
	Electrical power [W]	37.16	36.98	36.80	36.63	36.47	36.31
	Thermal power [W]	21.59	21.63	21.65	21.72	21.79	21.89
	Efficiency [%]	0.42	0.42	0.41	0.41	0.40	0.40
	Luminous efficacy [lm/W]	140.9	139.6	138.1	136.6	134.9	132.9

were selected as reference luminaires. The light distribution curves of selected reference luminaires and analyses results are shown in Fig. 1 and Table 1, respectively.

As it is seen from the Table 1, the luminous flux values of both reference luminaires are 25000 lm. This value was determined as the target for the design of COB LED based industrial high-bay luminaire. A COB LED light source, which is well documented and has a high luminous flux value, was selected and purchased from the market. The properties of COB LED for different currents and cold plate temperatures were measured using a 1-meter-diameter temperature controlled Ulbrich Sphere, which exists at the ITU, Energy Institute, Photometry and Radiometry Laboratory [14]. The temperature controlled Ulbrich Sphere and its equipment are shown in Fig. 2. Voltage, current, luminous flux, optical power, correlated colour temperature (CCT), and colour rendering index (CRI) were measured.

End of Table 2

Driving Current, mA	Property	Cold Plate Temperature, °C					
		25	35	45	55	65	75
1400	Solder temperature [°C]	51.9	60.9	70.3	79.4	88.7	98
	Voltage [V]	36.27	36.09	35.93	35.77	35.62	35.47
	Current [A]	1.4	1.4	1.4	1.4	1.4	1.4
	Luminous flux [lm]	6588	6486	6379	6260	6143	6017
	Optical power [W]	19.62	19.32	19.03	18.68	18.34	17.98
	CCT [K]	3948	3962	3979	3996	4018	4043
	CRI	82.5	82.5	82.4	82.4	82.3	82.3
	Electrical power [W]	50.78	50.53	50.30	50.08	49.86	49.65
	Thermal power [W]	31.16	31.21	31.27	31.40	31.52	31.67
	Efficiency [%]	0.39	0.38	0.38	0.37	0.37	0.36
	Luminous efficacy [lm/W]	129.7	128.4	126.8	125.0	123.2	121.2

Solder temperatures, which are the key parameters for the calculation of junction temperature, were also measured by the K type thermocouple. Electrical power, thermal power, efficiency, and luminous efficacy values were calculated from the Equations (1)–(4), respectively. Properties obtained from the measurements and calculations are given in Table 2.

$$\text{Electrical power}\left[W\right] = \\ = \text{Voltage}\left[V\right] \times \text{Current}\left[A\right]. \quad (1)$$

$$\text{Thermal Power}\left[W\right] = \\ = \text{Electrical Power}\left[W\right] - \\ - \text{Optical Power}\left[W\right]. \quad (2)$$

$$\text{Efficiency}\left[\%\right] = \\ = \frac{\text{Optical Power}[W]}{\text{Electrical Power}[W]} \times 100\%. \quad (3)$$

$$\text{Luminous Efficasy [lm/W]} = \\ = \frac{\text{Luminous Flux}[lm]}{\text{Electrical Power}[W]}. \quad (4)$$

As it is seen from Table 2, luminous flux, luminous efficacy, optical power, and efficiency values were adversely affected from the increasing temperature. Luminous efficacy and efficiency values were also decreased with increasing current steps. Correlated colour temperature (CCT) and colour rendering index values (CRI) were also changed with the temperature and the current. Considering the adverse effects of high currents on LED properties, 1050 mA current was selected to reach high luminous efficacy values and also to obtain a cost effective solution in terms of COB LED number. When the optical losses and driver efficiency are considered, the luminous efficacy value will also be lower than the measured values of COB LED.

The solder point temperature has been targeted as 60 °C for avoiding negative effects of high temperatures on COB LED properties and at the same time not to cause very large heat sink dimensions. The luminous flux at 1050 mA current and 60 °C solder point temperature was calculated as 5 100 lm by interpolating the luminous flux measurement values at 52.8 °C and 62.1 °C. The number of LEDs used in the COB LED based luminaire was calculated with the Equation (5) (luminous fluxes of reference luminaires were 25 000 lumens, the approximate efficiency value of the reflectors on the market was 85 %, the measured luminous flux value of COB LED at 1050 mA current and 60 °C solder point temperature was 5 100 lumens). From the Equation (5), the number of COB LEDs was calculated as 5.8 and the number of 6 was selected as an upper integer.

$$\text{Number of COB LEDs} = \frac{25\,000\,\text{lm}}{5100\,\text{lm} \times 0.85} = 5.8 \quad (5)$$

3. THERMAL SIMULATIONS AND EXPERIMENTAL ANALYSES

In this section, the computer aided thermal simulations and experimental analyses will be explained in detail.

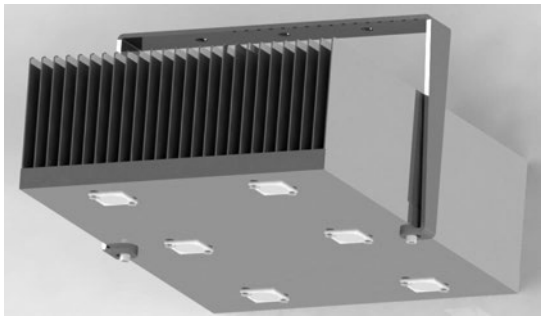

Fig. 3. 3D luminaire model with plate finned heat sink

3.1. Thermal Simulations

In this study, a commercial computational fluid dynamics program was used for thermal simulations. A plate finned heat sink with a pendant, which is expected to provide the targeted 60 °C solder point temperature, is designed with preliminary thermal simulations taking into account production possibilities. Selected dimensions of the base plate of the heat sink were 290×221×14 mm, the fin height was 76 mm, the fin thickness was 1 mm, and the number of fins was 26. In Fig. 3, the 3D model of the heat sink and mounted COB LEDs can be seen.

In detailed thermal simulations, material properties of the parts and thermal resistances were tried to define accurately in the software for the exact results. Materials of the parts and their thermal conductivities are listed in Table 3. For the simplicity of thermal simulations, the Printed Circuit Board (PCB) was assumed as one aluminium layer and the COB LED was assumed as two layers consisted of an LED chip and its coating. The thermal conductivity of LED top coating [15], pendant-stainless steel 304 [16] and heat sink-aluminium 1050 [17] were defined as 0.2 W/mK, 16.2 W/mK, and 222 W/mK, respectively.

The thermal resistance of the grease used between the PCB and the heat sink was defined approximately as 0.17 Kcm^2/W from the manufacturer catalogue at the supplied lowest pressure value (5 N/cm^2) [18]. The thermal resistance between the pendant and the heat sink was defined as 3.3 Kcm^2/W. The thermal resistance between the LED chip and the PCB was defined as 0.9 Kcm^2/W by considering the thermal resistance value, which is given in the datasheet of selected COB LED between the junction and solder points. In thermal simulations, the air temperature was defined as 24 °C. The thermal power of a COB LED was calculated from Table 2 at 1050 mA current and 60 °C solder point temperature and found as 129.84 W for 6 COB LEDs.

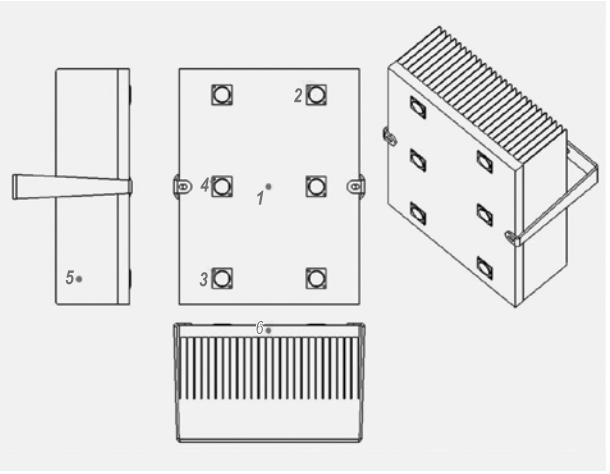

Fig. 4. Temperature measurement points

Mesh sensitivity analysis was performed for different mesh configurations, which are shown in Table 4. The maximum temperature was controlled according to the increasing number of mesh elements. The results of Mesh 4 were used in this study because after mesh 4 the maximum temperature did not change considerably.

Six temperature measurement points were specified on the thermal model (Fig. 4). From the temperature measurement points number 2, 3, and 4, which were the solder points of different COB LEDs, 59.7 °C, 59.7 °C, and 60.4 °C temperature values were obtained by the thermal simulation, respectively. The obtained thermal simulation results are consistent with the accepted 60 °C soldering point temperature used for determination of the luminous flux and the thermal power in the design beginning. The results of the thermal simulation will be compared and evaluated in the results and discussion section. The temperature distribution of the

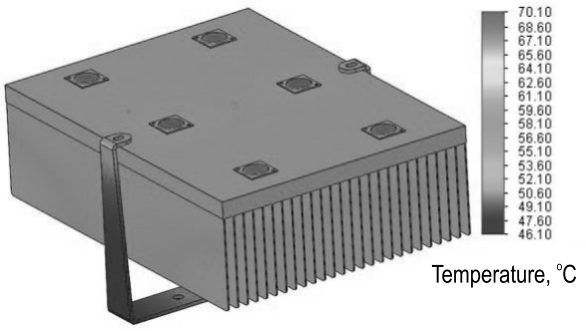

Fig. 5. Temperature distribution of the designed model

Table 3. Thermal Conductivity of the Parts Materials

Material	Thermal conductivity [W/mK]
Heat Sink – Al 1050	222
PCB – Al 5052	140 (at 273 K)
LED Chip – SiC	Between 150–126.6 (293 K – 473 K)
LED Top Coating	0.2
Pendant – 304 Stainless Steel	16.2

Table 4. Mesh Sensitivity Analysis

Mesh	The number of solid mesh elements	The number of total mesh elements	Maximum temperature of the system [°C]
1	273 705	753 648	68.9
2	403 717	1 188 612	69.4
3	520 764	1 492 682	70.0
4	663 822	1 864 318	70.1
5	1 170 087	3 271 968	70.1
6	1 683 470	4 615 745	70.1

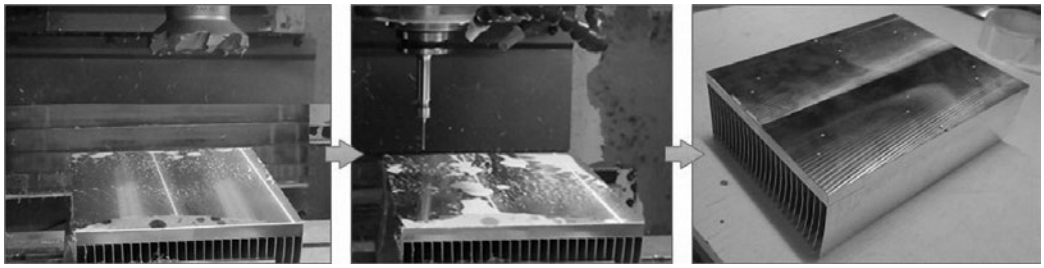

Fig. 6. Manufactured heat sink

designed model obtained from the thermal simulation is shown in Fig. 5.

3.2. Experimental Analyses

A prototype was manufactured and experimental analyses were carried out in order to determine the consistency of the method used in the design and thermal simulation of COB LED based industrial high-bay luminaire prototype. In the first stage of prototype manufacturing, a heat sink was produced from an aluminium block and the roughness of the surface, at which the LEDs will be mounted, was corrected. LED mounting holes were drilled. The manufactured heat sink is shown in Fig. 6.

Then the assembly steps were carried out in the following order (Fig. 7):

1. The surface was cleaned with isopropyl alcohol to remove residuals from production, which could adversely affect heat transfer;
2. The thermocouples were soldered to the solder point of the COB LEDs;
3. A thermal grease was applied between the PCB of COB LEDs and the heat sink to improve heat transfer;
4. COB LEDs were mounted on the heat sink;
5. The electrical and driver connections of the COB LEDs were made and the pendant of the prototype was mounted.

After manufacturing of the luminaire prototype, experimental analyses with laboratory measurements were done. The prototype was held in the air with the help of a pendant setup so that it was not touching anywhere as in computer-aided thermal simulations (Fig. 8). In the experimental analysis, the

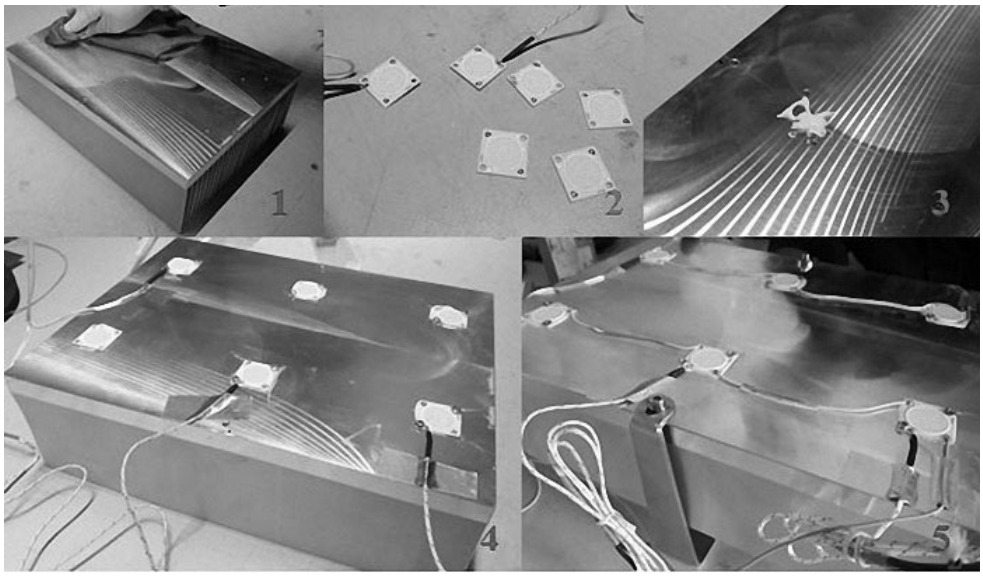

Fig. 7. Assembly steps of COB LED based luminaire prototype

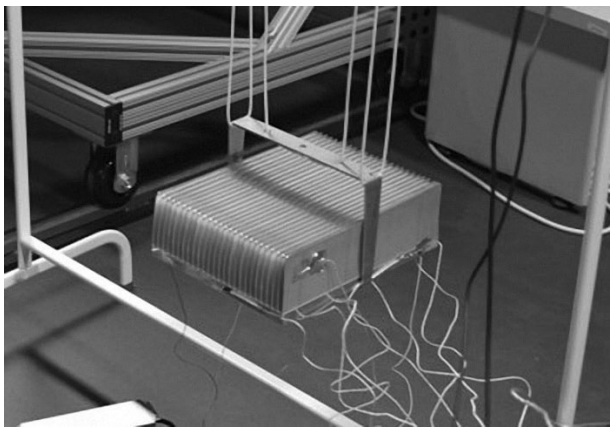

Fig. 8. Prototype pendant setup

speed and the temperature of air were controlled by measurement devices. Two air temperature sensors and one hot bulb speed sensor were used. The air temperature was between 24–24.5 °C and the air speed was below 0.04 m/s during measurements. The thermocouples were mounted on the points of the prototype, which are shown in Fig. 4 in order to compare the temperature values obtained from the experimental analysis and the thermal simulation. The temperature data were recorded with respect to time by using a digital multimeter. The sensors and the entire measurement system are shown in Fig. 9.

The temperature-time graph obtained as a result of the measurements is shown in Fig. 10. As it can be seen from the figure, the temperature increased with time and reached to thermal equilibrium. In the experimental analysis, the highest temperature values obtained from each thermocouple and the values obtained from the thermal simulation for the exact same points will be compared in the results and discussion section.

The luminous flux, optical power, CCT, and CRI properties were measured using a 2-meter-diame-

Table 5. The Results of Measurements and Calculations

Property	Value
Total electrical power supplied to drivers, W	246
Total electrical power supplied to LEDs, W	218.5
Driver efficiency, %	88.8
Optical power, W	94.8
Luminous flux, lm	31200
CCT, K	3923
CRI	82.42
Efficiency of LEDs,%	43.4
Luminous efficacy of LEDs, lm/W	142.8
Thermal power, W	123.7

Table 6. Comparison of the Temperatures Obtained from Experimental Analysis and Thermal Simulation for the Measurement Points

Number of thermocouple	Experimental analysis [˚C]	Thermal simulation [˚C]	Difference [%]
1	55.16	58.47	–6.0
2	56.20	59.67	–6.2
3	55.83	59.66	–6.9
4	57.05	60.37	–5.8
5	51.78	54.63	–5.5
6	54.25	57.52	–6.0

Table 7. Comparison of Properties for Prototype Measurement and COB LED Measurement Results

Property	Prototype measurement	Calculations from COB measurement	Difference [%]
Optical power [W]	94.8	91.2	3.8
Electrical power [W]	218.5	221	–1.1
Thermal power [W]	123.7	129.84	–5.0
Luminous flux [lm]	31200	30600	1.9
Efficiency of LEDs [%]	43.4	41.2	5.1
Luminous efficacy of LEDs [lm/W]	142.8	138.4	3.1
CCT [K]	3923	3936	–0.3
CRI	82.42	82.73	–0.4

ter Ulbricht Sphere after the prototype reached the thermal equilibrium (Fig. 11). For the prototype, electricity was supplied with two separate 1050 mA constant current drivers. The voltages applied to the LEDs were also measured for these two circuits, and the total electrical power supplied to the LEDs from the drivers was found by multiplying the current and measured voltages. Driver efficiency was found by dividing the electrical power given to the LEDs to the electrical power delivered to the drivers. Additionally, the efficiency, luminous efficacy, and thermal power of the LEDs were found using the Equations (3), (4), and (2), respectively. The results obtained by measurements and calculations are shown in Table 5. Results from experimental analyses and single COB LED measurements will be compared in the results and discussion section.

RESULTS AND DISCUSSION

In this study, the design of a COB LED based high-bay industrial luminaire was described step by step. The results obtained by the thermal simulation and experimental analysis from the temperature measurement points determined on the luminaire prototype are as shown in Table 6. The greatest difference between the thermal simulation and experimental analysis is –6.9 %, and these differences can be considered within acceptable limits. This situation demonstrates the consistency of the assumptions made and the thermal model.

The values obtained from the measurements made for one COB LED at the beginning of the design were used for six LEDs. The differences between the calculations from COB measurement and prototype measurements are given in Table 7. In this case, the differences between the thermal simulation and the experimental analysis, which are given in Table 6, can be explained by the difference between the single COB LED measured in the beginning of the initial design and the six COB LEDs used in the prototype. Already in the manufacturer catalogues, the properties of the LED products are given within certain tolerances (±7 % for the selected COB LEDs luminous flux).

The obtained results indicate the necessity of determining properties of the COB LED light source to be used in the beginning of the design process.

Fig. 9. Sensors and the entire measurement system

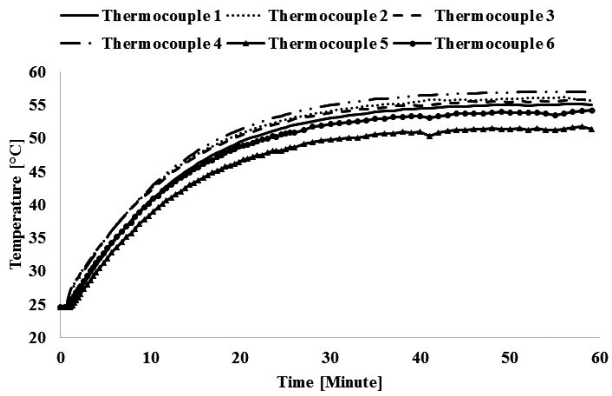

Fig. 10. Time dependent temperatures of the measurement points

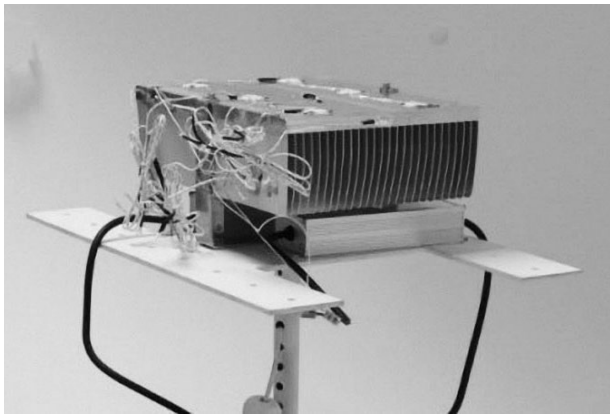

Fig. 11. Measurement of luminaire prototype using 2-meter-diameter Ulbricht Sphere

The thermal simulation should then be performed to ensure that the cooling system can provide the desired temperature values. Finally, the consistency of thermal simulation results should be checked with measurements on a prototype to be manufactured before mass production is started.

Another result of this study is, with a suitable thermal management system, COB LEDs can be used in high-power luminaires as an alternative to the single-chip LEDs, which are commonly used in the market. Thus, the number of LEDs used in luminaires as well as the mechanical design difficulty can be reduced. On the other hand, assuming an optical loss about 15 %, the COB LED based prototype, which was designed and experimentally analysed in this study, has a luminous efficacy of 108 lm/W. This value is lower than the luminous efficacy values of the single-chip LED based luminaires, which were selected for benchmarking in this study. But the main motivation of this study was to validate the thermal simulation results and experimental prototype measurement results of a COB LED based industrial high-bay luminaire starting from the single COB LED measurements. The validity of the method used in this study was verified with the analyses. It is also possible to apply this method starting from the first step for different design targets such as higher luminous efficacy etc.

This work was supported by the Research Fund of the Istanbul Technical University. Project Number: 39766.

REFERENCES

1. Yung K.C., Liem H., Choy H.S., Lun W.K. Thermal performance of high brightness LED array package on PCB // International Communications in Heat and Mass Transfer, 2010, Vol. 37, pp. 1266–1272.

2. Cheng T., Luo X., Huang S., Liu S. Thermal analysis and optimization of multiple LED packaging based on a general analytical solution // International Journal of Thermal Sciences, 2010, Vol. 49, pp. 196–201.

3. Ye H., Mihailovic M., Wong C.K.Y., van Zeijl H.W., Gielen A.W.J., Zhang G.Q., Sarro P.M. Two-phase cooling of light emitting diode for higher light output and increased efficiency // Applied Thermal Engineering, 2013, Vol. 52, pp. 353–359.

4. Deng X., Luo Z., Xia Z., Gong W., Wang L. Active-passive combined and closed-loop control for the thermal management of high-power LED based on a dual

synthetic jet actuator // Energy Conversion and Management, 2017, Vol. 132, pp. 207–212.

5. Yurtseven M.B., Mete S., Onaygil S. The effects of temperature and driving current on the key parameters of commercially available, high-power, white LEDs // Lighting Research & Technology, 2016, Vol. 48, pp. 943–965.

6. Bridges J. Extend the life of LEDs through thermal design – Part I (Magazine), 2015. URL: www.ledsmagazine.com/articles/print/volume-12/issue-4/features/developer-forum/extend-the-life-of-leds-through-thermal-design-part-i.html

7. Lu X., Hua T., Liu M., Cheng Y. Thermal analysis of loop heat pipe used for high-power LED // Thermochimica Acta, 2009, Vol. 493, pp. 25–29.

8. Liu Y. On Thermal Structure Optimization of a Power LED Lighting // Procedia Engineering, 2012, Vol. 29, pp. 2765–2769.

9. Li J., Ma B., Wang R., Han L. Study on a cooling system based on thermoelectric cooler for thermal management of high-power LEDs // Microelectronics Reliability, 2011, Vol. 51, pp. 2210–2215.

10. Deng Y., Liu J. A liquid metal cooling system for the thermal management of high power LEDs // International Communications in Heat and Mass Transfer, 2010, Vol. 37, pp. 788–791.

11. Chen I.Y., Guo M., Yang K., Wang C. Enhanced cooling for LED lighting using ionic wind // International Journal of Heat and Mass Transfer, 2013, Vol. 57, pp. 285–291.

12. EN12464–1: 2011. Light and lighting – Lighting of work places – Part 1: Indoor work.

13. Dialux. https://www.dial.de/en/dialux/ (accessed 01 April 2018).

14. Energy Institute. http://www.enerji.itu.edu.tr/en (accessed 10 April 2018).

15. Kolodeznyi E.S., Ivukin I.N., Serebryakova V.S., Bougrov V.E., Romanov A.E. Thermal Analysis of Phosphor Containing Silicone Layer in High Power LEDs // Materials Physics and Mechanics, 2014, Vol. 21, pp. 283–287.

16. Matweb – AISI Type 304 Stainless Steel, 2018. URL: http://asm.matweb.com/search/SpecificMaterial.asp?bassnum=mq304a.

17. Righton – Aluminium – 1050 H14. URL: http://www.righton.co.uk/PDF/Aluminium/Sheet%20 9010 %20White%20-%20693 %20Grey%20-%20 1050 %20H14.pdf (accessed 10 April 2018).

18. Kerafol – Keratherm Thermal Management Solutions, 2018. URL: www.kerafol.com/fileadmin/user_upload/Thermalmanagement/downloads/2017/Kerafol_Katalog_Keratherm_FINAL.pdf.

Seher Ateş,
graduated from Yildiz Technical University, Mechanical Engineering Department in 2009. She received M. Sc. degree from Istanbul Technical University in 2012. Between 2010–2018 she worked as a Research Assistant at Istanbul Technical University, Energy Institute, Energy Planning and Management Division and she is currently working on her Ph.D. Her research interests include thermal management of high power LEDs, thermal analyses of cooling systems, passive cooling methods and application of heat pipes in LED light systems

Mustafa B. Yurtseven,
graduated from Istanbul University, Mechanical Engineering Department in 2003. He got the M.Sc. degree in 2006 and Ph.D. degree in 2017 from Istanbul Technical University, Energy Institute. His research interests include photometric and radiometric measurements of LEDs, thermal management and statistical analyses

Sermin Onaygil,
obtained her M.Sc. degree in February 1983 and her Ph.D. in December 1990 both from Istanbul Technical University (ITU). Energy planning and management, intelligent building systems, energy economy, general illumination techniques as well as road and tunnel lighting, lighting automation, energy efficient measures in lighting can be listed within her basic working areas. She is the founder member of Turkish National Committee on Illumination and currently she is the President of the Committee. She represents Turkey in Division 4 of International Commission on Illumination entitled Transportation and Exterior Applications and actively takes part in various kinds of studies within this division as Vice Director. Sermin Onaygil works as an academic at the Energy Institute in Istanbul Technical University and she is the chairman of Energy Planning and Management Division within this Institute and she also directs master and Ph.D. thesis in these study field

Light & Engineering
Vol. 27, No. 2, pp. 88–96, 2019 *https://doi.org/10.33383/2018-034*

APPLICATION OF THE PHOTOMETRIC THEORY OF THE RADIANCE FIELD IN THE PROBLEMS OF ELECTRON SCATTERING

Victor P. Afanas'ev [1], Vladimir P. Budak [1], Dmitry S. Efremenko [2], and Pavel S. Kaplya [3]

[1] MPEI NRU, Moscow
[2] DLR, TU Munich, Germany
[3] Yandex LLC, Moscow
E-mail: budakvp@gmail.ru; efremenko@dlr.de; pavel@kaplya.com

ABSTRACT

The physical model of the radiance field is similar in some aspects to the elementary particle transport theory under the assumptions of the classical mechanics. Disregarding the differences in the used nomenclatures, it can be shown that the transport equations for the radiance field are identical to those for the particle flux density. Since the end of the 19th century, both theories have been developing in parallel, thereby enriching each other. In other words, a breakthrough, which has been made in one theory, readily contributes to the significant progress in another one. Nowadays the accuracy achieved in the experiments with particles is close to the limit, which allows validating the relationships derived within the light scattering theory. Besides, the experiments with particles are free from uncertainties in the scattering medium, which are typical for atmospheric remote sensing applications. In this paper, a new algorithm is described, which is derived by analogies between these theories. It is applied for calculating the electron flux elastically scattered by plane-parallel layers of a solid with the strongly forward peaked phase functions. The calculations are compared against the experimental angular distributions of electrons, which are elastically reflected by the two-layer solid samples.

Keywords: transport theory, small-angle approximation, light scattering, electron spectroscopy, invariant imbedding method

1. INTRODUCTION

The formulation of the transport theory for elementary particles is like the laws of the light beam propagation considered in the ray approximation framework. Moreover, these laws are valid for all classical particles, if they can be localized in space. The ray approximation can be regarded as a case of a more general quantum physical concept [1], in which a photon is considered as a small particle moving along a trajectory; the latter is referred to as a "ray." The density of the photon flux is associated with the radiance $L(\mathbf{r},\hat{\mathbf{l}})$ at the given point $\boldsymbol{r}$ in the direction $\hat{\mathbf{l}}$. Under this setup, the radiance field is given by the radiative transfer equation (RTE):

$$(\hat{\mathbf{l}},\nabla)L(\boldsymbol{r},\hat{\mathbf{l}}) = -\varepsilon L(\boldsymbol{r},\hat{\mathbf{l}}) + \frac{\sigma}{4\pi}\oint L(\boldsymbol{r},\hat{\mathbf{l}}')x(\hat{\mathbf{l}},\hat{\mathbf{l}}')d\hat{\mathbf{l}}', \quad (1)$$

here ε and σ are the extinction and scattering coefficients, respectively, while $x(\hat{\mathbf{l}},\hat{\mathbf{l}}')$ is the single scattering phase function. Initially, the RTE was introduced in [2] for a medium without scattering. In this case, for optically thin media, the RTE is reduced to the Bouguer law, i.e. exponential brightness attenuation along a ray.

The transfer equation for particles looks like Equation (1), namely,

$$(\hat{\mathbf{l}},\nabla)\psi(\boldsymbol{r},\hat{\mathbf{l}}) = -(\sigma_{el}+\sigma_{in})\psi(\boldsymbol{r},\hat{\mathbf{l}}) + \\ +\frac{\sigma_{el}}{4\pi}\oint\psi(\boldsymbol{r},\hat{\mathbf{l}}')x(\hat{\mathbf{l}},\hat{\mathbf{l}}')d\hat{\mathbf{l}}', \quad (2)$$

here $\psi(\mathbf{r},\hat{\mathbf{l}})$ is the particle flux density at the given point $\boldsymbol{r}$ along the direction $\hat{\mathbf{l}}$, σ_{el} is the elastic scattering cross-section, while σ_{in} is the inelastic scattering cross-section.

Equations (1) and (2) can be used to determine the flux density of photons and electrons reflected by multi-layered inhomogeneous media with the underlying surface. Essentially, they are the basis for the forward modelling in the Earth remote sensing retrieval codes and in the electron spectroscopy processing algorithms (describing the process of the electron lithography, determining the backscatter factor in the X-ray spectral analysis as well as analysing the X-ray photoelectron spectroscopy (XPS) and reflected electron spectroscopy (RES) data).

The description methodologies of both electron and optical scattering are based on the transport equations. Therefore, the methods designed for solving optical problems can be used in the problems related to atomic particle scattering in solids [3–5].

By using the electron spectroscopy framework, the problem of the quantitative composition analysis of samples can be readily solved. However, such an analysis of the experimental data typically requires a model of the multiple elastic and inelastic scattering of electrons in solids.

Retrieval of the component composition of multi-layered samples is an ill-posed problem. It incorporates the analysis of the energy spectra of emitted electrons and extracting the information of the interest. In this regard, there are additional requirements and constraints on the scattering signal modelling algorithms and their robustness.

The state-of-the-art methods of the XPS and the elastic peak electron spectroscopy (EPES) analysis are based on rather simplistic models, in which the process of multiple elastic scattering is neglected. One of the representatives of such models is the straight-line approximation (SLA) [6, 7]. The main advantage of SLA-like models consists in their simplicity. However, the SLA leads to a biased estimate of the scattered electron signal [8]. Essentially, the error of the SLA approach is because the elastic scattering cross-section σ_{el} in the situations, which are relevant for XPS, RES, and EPES, exceeds the inelastic scattering cross-section, i.e. $\sigma_{el} > \sigma_{in}$. Several techniques were developed in order to compensate the SLA bias. However, they are *ad hoc* and do not take rigorously into account all the factors that cause the methodological errors. Unlike in remote sensing applications, in the electron scattering spectroscopy, there are several independent methods for the layer-by-layer component analyses of samples. In its turn, it is possible to experimentally validate techniques, which describe the reflection processes from multi-layered inhomogeneous media. Besides, it is possible to control the composition of the sample under study, even at the stage of its preparation. In this regard, the layer-by-layer composition retrieval based on the analysis of electron spectra can be performed by using techniques provided by the radiative transfer theory. In this paper, it will be shown that the experimental data on angular distributions of elastically reflected electrons [9–11] is beneficial for validation of the radiation codes and models used in the Earth remote sensing operational algorithms [12–15]. The similar ideas were behind the verification study [16].

The invariant imbedding method was proposed by Ambartsumian in the 40s of the last century to describe the processes of radiation transfer in the atmospheres of stars and planets [17, 18]. Essentially, this method converts the RTE for the radiance into the equations for the reflection and transmission coefficients of a slab. The method was further developed in the works of Chandrasekhar, Sobolev, and others [19, 20], primarily, for spherical and Rayleigh single scattering phase functions [17–20]. In these cases, an iterative procedure appeared to be efficient. As the first approximation, a single scattering solution was used [18]. Typically, four iterations were enough to achieve the convergence. However, strongly forward peaked phase functions with the dominant small-angle scattering are of great practical importance. These are the cases relevant for the electron scattering in solids and the photon scattering in a turbid medium. In this paper, it will be shown that in the case of the dominant small-angle scattering it is possible to simplify the solution procedure since the nonlinear Chandrasekhar equations can be linearized.

The forward peaked phase functions were considered by Gaudsmith and Saunderson [21, 22] to solve the electron transport equation by using the small-angle approximation and the spherical harmonics method. Let us consider an infinite medium with the sources of light (or particles) placed

in the centre (the medium boundary is placed at $z = 0$); the source satisfies the following condition: $L(z = 0, \hat{\mathbf{l}}) = \delta(\hat{\mathbf{l}} - \hat{\mathbf{l}}_0)$. In [23] Scott developed a technique for solving transport equations by using the small-angle approximation. Dashen [3] applied the Ambartsumian equation, which solves the boundary problem of reflection from a semi-infinite medium, to describe the electron scattering process. Successful attempts to solve the linearized Ambartsumian and Chandrasekhar equations in the small-angle approximation were made in [4, 24]. Throughout the paper, the small-angle approximation is associated with the following small parameter

$$x(\pi) / x(0) \ll 1. \tag{3}$$

In this paper, the small-angle approximation is used to derive analytical expressions for radiation reflection processes both from a semi-infinite layer and from layers of finite thickness. The small-angle solutions of the Chandrasekhar equation for the transmission function will be given. It will be shown that the small-angle approximation can be used only for Chandrasekhar equations (written for the transmission function [19]), but not for the alternative formulation from [25]. An iterative procedure will be constructed that solves the problem of reflection from multilayer samples with an underlying surface at the bottom.

The main advantage of approximate analytical solutions consists in the high computational speed, which is a prerequisite for solving inverse problems by the fitting procedure. Note that the latter is the most robust approach to deal with the ill-posed problems of mathematical physics, namely, the remote sensing retrieval and quantitative composition analysis using the electron spectroscopy [26, 27].

The paper will present methods for the numerical solution of the Chandrasekhar equations. Currently, Monte-Carlo (MC) simulations [28, 29] are mainly used to describe the energy and angular spectra of electrons. However, MC codes require much computational time: e.g., on a standard laptop, this time ranges up to several minutes; whereas the same simulations, but based on the numerical solution of the Chandrasekhar equations presented in this paper, are performed within fractions of a second. Note, that the idea of using numerical methods to interpret the spectra of the electron spectroscopy is inherited from the radiative transfer theory.

The approbation of the approximate small-angle methods developed in this work is performed by using a comparison with exact numerical solutions as well as with the experimental data.

2. CHANDRASEKHAR EQUATIONS FOR REFLECTION AND TRANSMISSION FUNCTIONS, LINEARIZATION PROCEDURE, SOLUTION BY USING THE SMALL-ANGLE APPROXIMATION

The equation for the reflection function derived by Chandrasekhar [19] for a layer of finite thickness reads as follows:

$$\begin{aligned}
&\frac{\partial}{\partial \tau}\rho_m(\tau,\mu,\mu_0) + \left(\frac{1}{\mu}+\frac{1}{\mu_0}\right)\rho_m(\tau,\mu,\mu_0) = \\
&= \Lambda x_m(\mu,\mu') + \Lambda\int_0^1 x_m(\mu,\mu')\rho_m(\tau,\mu',\mu_0)\frac{d\mu'}{\mu'} + \\
&\quad + \Lambda\int_{-1}^0 \rho_m(\tau,\mu,\mu')x_m(\mu',\mu_0)\frac{d\mu'}{\mu'} + \\
&+ \Lambda\int_0^1\int_{-1}^0 \rho_m(\tau,\mu,\mu')x_m(\mu',\mu'')\rho_m(\tau,\mu'',\mu_0)\times \\
&\quad \times \frac{d\mu'}{\mu'}\frac{d\mu''}{\mu''},
\end{aligned} \tag{4}$$

where τ is the dimensionless layer thickness, m is the azimuthal expansion index, ρ is the reflection function, x is the single scattering phase function, $\Lambda = \sigma_{el} / (\sigma_{el} + \sigma_{in})$ is the single scattering albedo. Consider the azimuthal expansion

$$\begin{aligned}
&\rho(\tau,\mu,\mu_0,\varphi-\varphi_0) = \\
&= \sum_m \rho_m(\tau,\mu,\mu_0)\exp\left[im\left(\varphi-\varphi_0\right)\right],
\end{aligned} \tag{5}$$

with ϑ_0=arccos μ_0, φ_0 and ϑ=arccos μ, φ being the polar and azimuth angles of probing and viewing angles, respectively; the polar angles are defined with respect to the axis, which is perpendicular to the sample surface and looks towards the surface.

Similar to Equation (4), the equation for the transmission function $T(\tau,\mu, \mu_0,\varphi - \varphi_0)$ reads as follows (Eqn. 6):

$$\frac{1}{\mu}T_m(\tau,\mu,\mu_0)+\frac{\partial T_m(\tau,\mu,\mu_0)}{\partial\tau}=\Lambda\exp\left(-\frac{\tau}{\mu_0}\right)x_m(\mu,\mu_0)+\Lambda\int_0^1 x_m(\mu,\mu')T_m(\tau,\mu',\mu_0)\frac{d\mu'}{\mu'}+$$
$$+\Lambda\exp\left(-\frac{\tau}{\mu_0}\right)\int_0^{-1}\rho_m(\tau,\mu,\mu')x_m(\mu',\mu_0,\varphi'-\varphi_0)\frac{d\mu'}{\mu'}+ \quad (6)$$
$$+\Lambda\int_0^{-1}\int_0^1\rho_m(\tau,\mu,\mu')x_m(\mu',\mu'',\varphi'-\varphi'')T_m(\tau,\mu'',\mu_0,\varphi''-\varphi_0)\frac{d\mu'}{\mu'}\frac{d\mu''}{\mu''}.$$

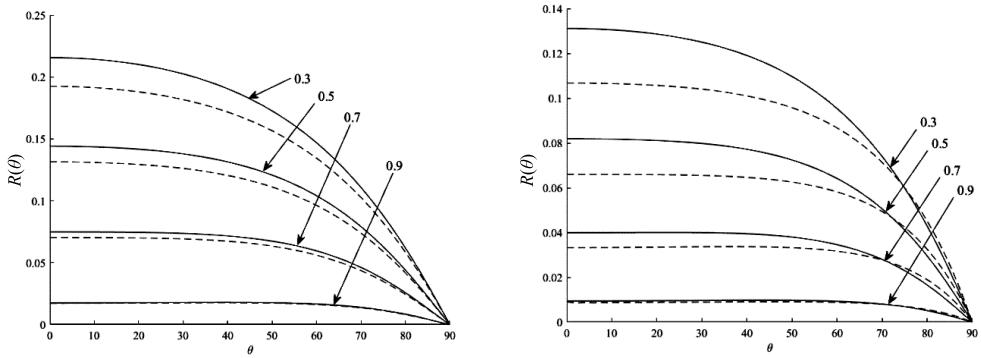

Fig. 1. The reflection functions for the semi-infinite medium. The normal angle of incidence. The calculations are performed for the Henyey-Greenstein phase function. Plot (a) shows the influence of the non-linear term on the reflection function. Plot (b) illustrates the increase of error of the small-angle approximation with the phase function smoothness. The solid line is the numerical solution (MDOM), the dashed line is the small-angle approximation. The normal angle of incidence. The single scattering albedo is 0.67. Numbers with arrows are the asymmetry parameters of the Henyey-Greenstein phase function

3. NUMERICAL SOLUTION FOR REFLECTION AND TRANSMISSION FUNCTIONS

We note that the methods discussed in this section were first developed for solving the problems of radiative transfer and significantly enriched the theory of electron transfer as well. To get the matrix form of Equation (1), the continuous dependency on μ' should be replaced with a discrete set of N values μ_i', while the integrals should be represented through the quadrature formulas. Then the reflection function S^m turns into a matrix of dimension $N\times N$, where s_i are the weights of the quadrature method, μ_i' are the quadrature nodes for the cosines of the incidence/observation angles, $w=\mathrm{diag}(s_i/\mu_i)$.

Bearing that in mind, Equation (4) takes the following form:

$$\frac{\partial}{\partial\tau}\rho^m(\tau)+A\rho^m(\tau)+\rho^m(\tau)A=$$
$$=C+\rho^m(\tau)D\rho^m(\tau), \quad (7)$$

with

$$A=\mathrm{diag}(1/\mu)-\Lambda x^{m+}w,\ C=\Lambda x^{m-},\ D=\Lambda w x^{m-}w.$$

The index "+" in the phase function is related to the process, in which the propagation direction after the scattering event is preserved, while the index "–" indicates that the upward propagation changes into downward one and *vice versa*.

Equation (7) is referred to as the differential algebraic Riccati equation [30, 31]. It can be solved numerically by several numerical techniques [31–34]. In this paper, we use the BDF (Backward Differential Formula) method [34]. The situation is somewhat simplified since the matrix x^{m+} is symmetric.

Having performed a similar discretization for particles elastically scattered inside a layer, we obtain the following matrix equation for the transmission function:

$$\frac{\partial}{\partial\tau}T_0^m(\tau)+A'T_0^m(\tau)=C, \quad (8)$$

with

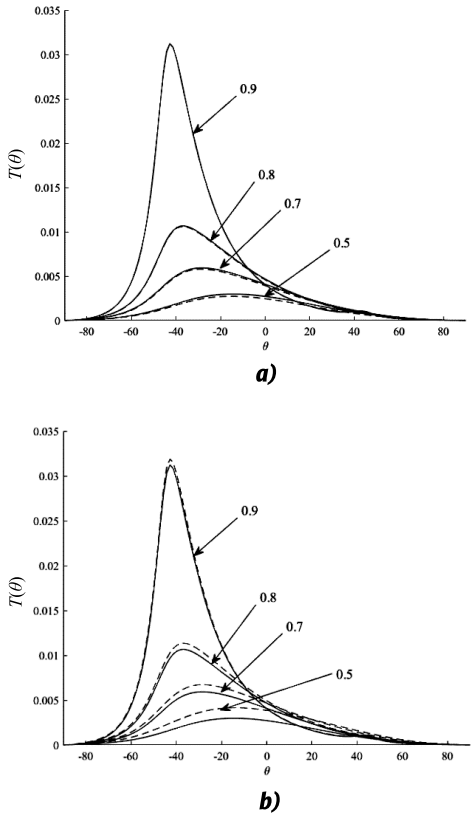

Fig. 2. The transmission functions for the layers of thickness 0.1 l_{tr}. Plot (a) shows the influence of the non-linear term. The solid line is the result with the non-linear term, while the dashed line shows the result without non-linear term taken into account. Plot (b) shows the increasing of the small-angle approximation error with the smoothness of the phase function. The solid line is the numerical solution (MDOM), the dashed line is the small-angle approximation. The angle of incidence is 45°, the single scattering albedo is 0.54. Numbers with arrows are the asymmetry parameters of the Henyey-Greenstein phase function

$$A' = \mathrm{diag}\left(\frac{1}{\mu}\right) - \Lambda x^{m+} w - \Lambda \rho_0^m(\tau) w x^{m-} w,\ C =$$

$$= \Lambda\left(x^{m+} + \rho_0^m(\tau) w x^{m-}\right)\mathrm{diag}\left(\exp\left(-\frac{\tau}{\mu}\right)\right).$$

Let us find the solutions of the equations obtained considering the nonlinear terms and the solutions of the linearized matrix equations based on the BDF method. For elastic scattering, we use the Henyey-Greenstein phase function, which is well-known in optics. The numbers in Figs. 1 and 2 show the value of the asymmetry parameter g, which determines the degree of elongation of the Henyey-Greenstein phase function:

$$x_{HG}(\mu) = \frac{1-g^2}{(1+g^2-2g\mu)^{3/2}} = \sum_{l=0}^{\infty}(2l+1)g^l P_l(\mu), \quad (9)$$

where P_l are the Legendre polynomials.

The solution of Equation (7) (and consequently, Equation (4)) is shown in Fig. 1 with solid lines, while the dashed line depicts the solution to Equation (7) with non-linear term neglected (i.e., the second term on the right-hand side). The plots in Fig. 1 reveal the increasing of the computation error of the linearized equations. That is quite an expected result since the phase functions with $g \le 0{,}5$ do not have a dominant small-angle scattering part. However, even in case of violation of condition (3), the linearized equations provide a result with an error less than 10%.

In Fig. 2, the solid lines represent the solution of Equation (8), the dashed line shows the solution of Equation (8) with neglected terms containing $\rho_0^m(\tau)$. In other words, this is a solution to Equation (6), in which the last two terms on the right-hand side are neglected.

4. ANALYTICAL SOLUTIONS OF LINEARIZED EQUATIONS FOR THE REFLECTION AND TRANSMISSION FUNCTIONS

The analysis performed on the basis of numerical solutions indicates that for strongly forward peaked phase functions (see condition (3)), the processes of reflection and transmission through the layer can be described by using the following equations:

$$\frac{\partial}{\partial\tau}\rho_m(\tau,\mu,\mu_0) + \left(\frac{1}{\mu}+\frac{1}{\mu_0}\right)\rho_m(\tau,\mu,\mu_0) =$$
$$= \Lambda x_m(\mu,\mu') + \quad (10)$$
$$+\Lambda\left(\frac{1}{\mu}+\frac{1}{\mu_0}\right)\int_0^1 x_m(\mu,\mu')\rho_m(\tau,\mu',\mu_0)\frac{d\mu'}{\mu'}$$

and

$$\frac{1}{\mu}T_m(\tau,\mu,\mu_0) + \frac{\partial T_m(\tau,\mu,\mu_0)}{\partial\tau} =$$
$$= \Lambda\exp\left(-\frac{\tau}{\mu_0}\right)x_m(\mu,\mu_0) + \quad (11)$$
$$+\Lambda\int_0^1 x_m(\mu,\mu')T_m(\tau,\mu',\mu_0)\frac{d\mu'}{\mu'}.$$

The method of spherical harmonics is based on the representation of functions through the Legendre polynomial series. However, to be able to apply the method of spherical harmonics (which is a standard procedure for analytic solution of Equations (10) and (11)), based on the orthogonality property of the Legendre polynomials within the domain [–1,1], it is necessary to perform the analytic extension of the integrands to the domain (0, –1). For Equation (10), this step is trivial since in the domain (0, –1) the integrand goes to zero due to condition (3); the analytical continuation for Equation (11) is not straightforward. There are several approaches to deal with this problem (see, e.g. [2]). The most efficient implementation is given in [35, 36].

The solution of Equation (11), in which the integration limits are extended into the range [–1, 1] in the integral term, can be found by using the idea of Goudsmit and Saunderson: namely, in the multiplier $1/\mu$ in the first term of the left-hand side of (11) and in the exponent in the first term of the right-hand side of (11) (with respect to τ / μ_0), the values μ, μ_0 are considered to be constants. This approximation means replacing the real path by the projective one. A significant error occurs if the transport path of a photon or electron $l_{tr} = n^{-1}\left(\sigma_{el} + \sigma_{in}\right)^{-1}$ and the average electron path between elastic collisions $l_{el} = 1/\left(n\sigma_{el}\right)$ are comparable. Note that in the case of the Henyey–Greenstein phase function we have

$$l_{tr} / l_{el} = \sigma_{el} / \left(\sigma_{el} + \sigma_{in}\right) = 1/\left(1-g\right). \qquad (12)$$

The error in this case does not exceed 5%, if $l_{tr} / l_{el} \gg 1$.

Considering the assumptions made after the substitution of the Legendre polynomial expansions into Equation (11), we obtain a system of separable differential equations; applying the boundary condition $T_{lm}(\tau) = 1$, the solution for the transmission function can be derived:

$$T(\tau,\mu,\mu_0) = \frac{\Lambda\mu\mu_0}{2}\sum_l \frac{2l+1}{2} x_l P_l\left(\mu_0 \to \mu\right) \times$$
$$\times\left[\frac{\mathrm{e}^{-\tau/\mu} - \mathrm{e}^{-(1-\Lambda x_l)\tau/\mu_0}}{\left(\mu-\mu_0\right)-\Lambda x_l\mu} + \frac{\mathrm{e}^{-\tau/\mu_0} - \mathrm{e}^{-(1-\Lambda x_l)\tau/\mu}}{\left(\mu_0-\mu\right)-\Lambda x_l\mu_0}\right]. \qquad (13)$$

Equation (10) is solved by the method of iterations, which provides the analytical extension in a systematic way. A detailed description of this procedure is given in [35, 36]. The final result is

$$\rho(\tau,\mu,\mu_0) = \frac{\mu\mu_0}{\mu+\mu_0}\sum_l \frac{2l+1}{2} x_l P_l\left(\mu_0 \to \mu\right) \times$$
$$\times\left[\begin{array}{l} E_1\left(\tau\dfrac{\mu+\mu_0}{\mu\mu_0}\right) - E_1\left(\left(1-\Lambda x_l\right)\tau\dfrac{\mu+\mu_0}{\mu\mu_0}\right) - \\ -\ln\left(1-\Lambda x_l\right)\end{array}\right], \qquad (14)$$

where $E_1(x) = \int_x^\infty t^{-1}e^{-t}dt$ is the integral exponent.

Figs. 1 and 2 illustrate the comparison between the exact numerical solution and the small-angle approximation model.

5. REFLECTION FROM MULTILAYER STRUCTURES

We consider reflection from multilayer structures using the angular distributions of electrons, elastically reflected from solids, as an example. In the literature, there are experimental data on the angular distributions of electrons reflected by homogeneous solids as well as by multilayer samples [9–10, 37–42].

Let us consider a two-layer sample (Fig. 3). In accordance with the described scheme, the reflection function for a two-layer sample can be represented as

$$R_{12m}\left(\tau_1,\tau_2,\mu_0,\mu\right) = R_{1m}\left(\tau_1,\mu_0,\mu\right) +$$
$$+\int_{-1}^{1} d\mu' \int_{-1}^{1} d\mu'' T_{1m}\left(\tau_1,\mu_0,\mu'\right) R_{2m}\left(\tau_2,\mu',\mu''\right) \times \qquad (15)$$
$$\times\, T_{1m}\left(\tau_1,\mu'',\mu\right) + \ldots$$

or, exploiting the one-speed approximation and the small angle approximation,

$$R_{12m}\left(\tau_1,\tau_2,\mu_0,\mu\right) = R_{1m}\left(\tau_1,\mu_0,\mu\right) +$$
$$+\int_{-1}^{1} d\mu' T_{1m}\left(\tau_1\left(1/\mu_0 + 1/\mu\right),\mu_0,\mu'\right) \times \qquad (16)$$
$$\times\, R_{2m}\left(\tau_2,\mu',\mu\right).$$

The computations for three-layer systems can be performed by using the relation, which is similar to Equation (16), namely,

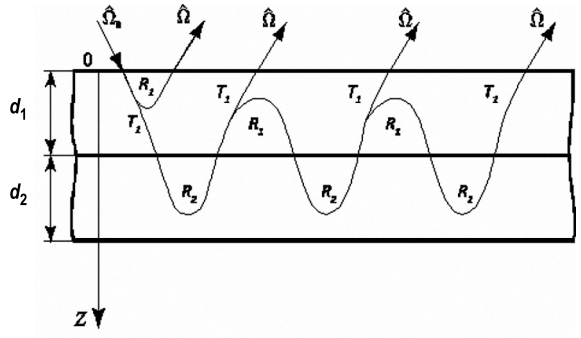

Fig. 3. The two-layer model of reflection. $\Omega = (\mu,\varphi)$, $\tau = d(\sigma_{in}+\sigma_{el})$, the curved line corresponds to the reflection function, while the straight line is associated with the transmission function

$$R_{123lm}(\tau_1,\tau_2,\tau_3) = R_{1lm}(\tau_1) + R_{23lm}(\tau_2,\tau_3)\times \\ \times\exp\left[-(1-\Lambda x_{lm})\tau_1\left(\mu^{-1}+\mu_0^{-1}\right)\right], \qquad (17)$$

here $R_{23lm}(\tau_2,\tau_3)$ is computed by using Equation (16) with the following index perturbation: $1\to 2;\ 2\to 3$.

Fig. 4 shows the angular distributions of electrons, elastically reflected by the two-layer systems (the layer of Be on the Au substrate), computed by using the exact numerical solutions and the small-angle solution (16).

6. CONCLUSION. MAIN RESULTS

The paper presents several analytical solutions that describe the radiance transmission and reflection in turbid media with the satisfactory accuracy. The derived solutions describe the radiation scattering in multi-layered inhomogeneous media. The approach developed in this work is based on the methods developed in radiative transfer for spherical and Rayleigh phase functions, as well as methods proposed by Ambartsumian, Chandrasekar, Sobolev, and other remarkable scientists, who solved the problems of light scattering in the atmospheres of stars and planets [17-20]. In the present work, it is shown that the methods designed in [17–20] are efficient in the problems, when the scattering phase functions are strongly forward peaked (condition (3)).

Analytical solutions such as (13) and (14) make it possible to perform calculations with the high speed and accuracy. Given that, the error of the models as a function of the most relevant parameters (namely, the asymmetry parameter and the single scattering albedo) can be analysed.

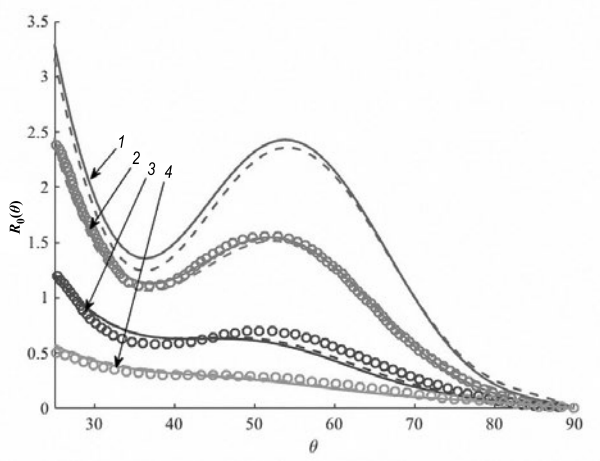

Fig. 4. Angular distributions of electrons, which are reflected by the gold samples with a beryllium layer on the top. The solid line corresponds to the exact numerical solution of Equations (7) and (8), dashed line show the results of the small angle approximation (Equations (13) and (14)), while the circles show the experimental data [10]. The computed Be layer thicknesses are: 1 – 0 nm, 2 – 0.5 nm, 3 – 2.5 nm, 4 – 3.8 nm

The computational speed is an essential factor in the inverse problem solution design. For example, when the reflection function from multilayer structures is considered, we need to determine the layer thickness. Typically, it is retrieved by using the fitting method, in which the direct problem is solved several times.

Due to the integration of numerical methods of the photometric light scattering theory into electron scattering problems for determining the hydrogen isotope profiles by the elastic peak electron spectroscopy (EPES), the sensitivity of the EPES technique has been increased by order of magnitude. In fact, the sensitivity has reached almost 10 % for hydrogen isotopes in plasma-faced materials [43].

Radiative transfer techniques applied for the physical interpretation of the effects of electron and ion scattering have brought the optical terminology (such as “brightness rotation” and “underlying surface”) into electron and ion spectroscopy [44]. The authors of this paper are confident that the presented small-angle solutions will be used for solving problems of light scattering in turbid media, as well as sea optics problems.

REFERENCES

1. Veklenko B.A. The nature of the photon and quantum optics // Light & Engineering, 2018, Vol. 26, # 2, pp. 4–13.
2. Beer A. Bestimmung der Absorption des rothen Lichts in farbigen Flüssigkeiten // Annal. Phys. Chem., 1852, Vol. 86, pp. 78–88.
3. Dashen R.F. Theory of electron backscattering // Phys. Rev., 1964, V.134, pp.1025–1032.
4. Afanas'ev V.P., Naujoks D. Backscattering of fast electrons // Phys. Stat. Sol., 1990, Vol. 164, pp. 133–140.
5. Borodyansky S. Effects of elastic scattering on energy spectra of emitted and backscattered electrons // Surf. Interface. Anal., 1993, Vol. 84, pp. 811–814.
6. Hofmann S. Auger- and X-Ray Photoelectron Spectroscopy in Materials Science // Springer, Berlin/Heidelberg, 2013, 528 p.
7. Powell C.J., Jablonski A. Progress in quantitative surface analysis by X-ray photoelectron spectroscopy: Current status and perspectives // J. of Electron Spectros. Relat. Phenom, 2010, Vol. 178–179, pp. 331–346.
8. Kaplya P.S. Sozdanie vy`sokotochny`x metodov analiza tvyordy`x tel na osnove rasshifrovki danny`x e`lektronnoj spektroskopii metodami invariantnogo pogruzheniya [Creating high-precision methods for analyzing solids on the basis of decoding electronic spectroscopic data by invariant imbedding methods] // Thesis for the degree of candidate physical and mathematical of sciences, 2016.
9. Bronstein I.M., Vasilyev A.A., Pronin V.P., Khinich I.I. Uprugoe otrazhenie e`lektronov srednix e`nergij ot neuporyadochenny`x metallicheskix poverxnostej [Elastic reflection of medium-energy electrons from disordered metal surfaces] // Izvestiya AN SSSR, Ser. Fizicheskaya, 1985, Vol. 49, # 9, pp. 1755–1759.
10. Bronstein I.M., Pronin V.P. Uprugoe rasseyanie e`lektronov srednix e`nergij metallicheskimi plyonkami [Elastic Scattering of Medium-Energy Electrons by Metal Films] // Fizika tvyordogo tela, 1975, Vol. 17, pp. 2431–2433.
11. Gergely G. Elastic backscattering of electrons: determination of physical parameters of electron transport processes by elastic peak electron spectroscopy // Prog. Surf. Sci., 2002, Vol.71, pp. 31–88.
12. Doicu A., Trautmann T. Discrete-ordinate method with matrix exponential for a pseudo-spherical atmosphere: Scalar case // J. Quant. Spectrosc. Radiat. Transfer, 2009, Vol. 110, pp. 146–158.
13. Spurr R.J.D., Kurosu T.P., Chance K.V. A linearized discrete ordinate radiative transfer model for atmospheric remote-sensing retrieval // J. Quant. Spectrosc. Radiat. Transfer, 2001, Vol. 68, #6, pp. 689–735.
14. Stamnes K., Tsay S.,C., Wiscombe W., Jayaweera K. Numerically stable algorithm for discrete-ordinate-method radiative transfer in multiple scattering and emitting layered media // Appl. Opt., 1988, Vol. 27, pp. 2502–2509.
15. Budak V.P., Korkin S.V. Complete matrix solution of radiative transfer equation for pile of horizontally homogeneous slabs // J. Quant. Spectrosc. Radiat. Transfer, 2011, Vol. 112, pp. 1141–1148.
16. Afanas'ev V.P., Budak V.P., Efremenko D.S., Lubenchenko A.V. Uglovy`e raspredeleniya e`lektronov i lyogkix ionov, uprugo otrazhyonny`x ot poverxnosti tvyordogo tela [Angular Distributions of Electrons and Light Ions Elastically Reflected from a Solid Surface] // Poverxnost`. Rentgenovskie, sinxrotronny`e i nejtronny`e issledovaniya, 2010, Vol. 4, #3, pp. 488–493.
17. Ambartsumyan V.A. Novy`j sposob raschyota rasseyaniya sveta v mutnoj srede [New method for calculating the scattering of light in a turbid medium] // Izv. AN Arm. SSR. Ser. geogr. i geofiz., 1942, #3, pp. 97–106.
18. Ambartsumyan V.A. K zadache o diffuznom otrazhenii sveta [To the problem of diffuse reflection of light] // Zhurnal e`ksperimental`noj i teoreticheskoj fiziki, 1943, Vol. 13, #9–10, pp. 323–334.
19. Chandrasekhar S. Radiative transfer // Oxford University Press, London, UK, 1950, 405 p.
20. Sobolev V.V. Rasseyanie sveta v atmosferax planet [The scattering of light in the atmospheres of the planets] // Nauka Publ., Moscow, 1972, 335 p.
21. Goudsmit S., Saunderson J.L. Multiple scattering of electrons // Phys. Rev., 1940, Vol. 57, pp. 24–29.
22. Goudsmit S., Saunderson J.L. Multiple scattering of electrons. II // Phys. Rev., 1940, Vol. 58, pp. 36–42.
23. Scott W. Theory of Small-Angle Multiple Scattering of Fast Charged Particles // Rev. of Modern Phys., 1963, Vol. 35, pp. 231–313.
24. Afanas'ev V.P. E`lementarny`e processy` i kinetika vy`sokotemperaturnoj neravnovesnoj plazmy` [Elementary processes and kinetics of high-temperature non-equilibrium plasma] // MPEI Publ., Moscow, 1988, 84 p.
25. Ambartsumyan V.A. K voprosu o diffuznom otrazhenii sveta mutnoj sredoj [On the diffuse reflection of light by a turbid medium] // Reports of the USSR Academy of Sciences, 1943, Vol. 38, #8, pp. 257–261.
26. Afanas'ev V.P., Golovina O.Yu., Gryazev A.S., Efremenko D.S., Kaplya P.S. Photoelectron spectra of finite-thickness layers // Journal of Vacuum Science & Technology B., 2015, Vol. 33, #3, 7 p.
27. Afanas'ev V.P., Gryazev A.S., Efremenko D.S., Kaplya P.S. Differential inverse inelastic mean free path and differential surface excitation probability retrieval from electron energy loss spectra // Vacuum, 2017, Vol. 136, pp. 146–155.
28. Werner W.S.M. Differential probability for surface adn volume electronic excitations in Fe, Pd and Pt // Surface Science, 2005, Vol. 588, pp. 26–40.
29. Werner W.S.M. Analysis of reflection electron energy loss spectra (REELS) for determination of the dielectric function of solids: Fe, Co, Ni // Surface Science, 2007, Vol. 601, #10, pp. 2125–2138.

30. Bellman R, Kalaba R, Wing G. Invariant imbedding and mathematical physics. I. Particle processes // J. Math. Phys., 1960, Vol. 1, pp. 280–308.

31. Flatau PJ, Stephens GL. On the fundamental solution of the radiative transfer equation // J. Geophys. Res, 1988, Vol. 93(D9), pp. 11037–11050.

32. Waterman P.C. Matrix-exponential description of radiative transfer // J. Opt. Soc. Am., 1981, Vol. 71, #4, pp. 410–422.

33. Efremenko D.S., Molina Garcia V., Gimeno Garsia S., Doicu A. A review of the matrix-exponential formalism in radiative transfer // J. Quant. Spectrosc. Radiat. Transfer., 2017, Vol. 196, pp. 17–45.

34. Pienado J., Ibañez J., Hernández V., Arias E. A family of BDF algorithms for solving Differential Matrix Riccati Equations using adaptive techniques // Procedia Computer Science, 2010, Vol. 1, pp. 2569–2577.

35. Afanas'ev V.P., Efremenko D.S., Kaplya P.S. Analytical and numerical methods for computing electron partial intensities in the case of multilayer systems // Journal of Electron Spectroscopy and Related Phenomena, 2016, Vol. 210, pp. 16–29.

36. Afanasyev V.P., Kaplya P.S., Lisitsyna E.Yu. Malouglovoe priblizhenie i model` Os`val`-da-Kaspera-Gauklera v zadachax otrazheniya e`lektronov ot tvyordy`x tel [Small-Angle Approximation and the Osvald-Kasper-Gaukler Model in the Problems of Electron Reflection from Solids] // Poverxnost`. Rentgenovskie sinxrotronny`e i nejtronny`e issledovaniya, 2016, #3, pp. 66–71.

37. Jablonski A., Hansen H.S., Jansson C., Tougaard S. Elastic electron backscattering from surfaces with overlayers // Phys. Rev.B., 1992, Vol. 45, pp. 3694–3702.

38. Jablonski A. Elastic electron backscattering from gold // Phys. Rev.B., 1991, Vol. 43, pp. 7546–7554.

39. Jablonski A., Jansson C., Tougaard S. Elastic electron backscattering from surfaces: Prediction of maximum intensity // Phys. Rev. B, 1993, Vol. 47, pp. 7420–7430.

40. Zommer L., Lesiak B., Jablonski A. Energy dependence of elastic electron backscattering from solids // Phys. Rev.B., 1993, Vol. 47, pp. 13759–13762.

41. Kuzovlev A.I., Kurnaev V.A., Remizovich V.S., Trifonov N.N. Refraction of the beam of charged particles during inclined transmission through a thin target // Nucl. Instrum. and Methods. Research Section B: Beam Interactions with Materials and Atoms, 1998, Vol. 135, pp. 477–481.

42. Bronstein I.M., Pronin V.P. Uprugoe otrazhenie e`lektronov srednix e`nergij pri napy`lenii Be na Au [Elastic reflection of medium-energy electrons during the deposition of Be on Au], XXVIII Herzen Readings. Physical and semiconductor electronics // LGPI of A.I. Herzen Publ. House, Leningrad, 1975, pp. 18–20.

43. Afanas'ev V.P., Gryazev A.S., Kaplya P.S., Köppen M., Ridzel O. Y., Subbotin N.Y., Hansen P. Investigation of Deuterium Implantation into Beryllium Sample by Electron Energy Loss Spectroscopy // IOP Conf. Series: Journal of Physics: Conf. Series, 2017, Vol. 891, 6 p.

44. Afanasyev V.P., Kaplya P.S. Funkciya propuskaniya. E`ffekt «povorota tela yarkosti» [Transmission function. The effect of "turning the body of brightness"] // Poverxnost`. Rentgenovskie, sinxrotronny`e i nejtronny`e issledovaniya, 2017, #12, pp. 66–75.

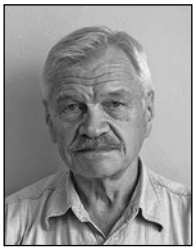

Viktor P. Afanas'ev,
Dr. of Phys. and Math. Science, graduated from the Moscow Power Engineering Institute (MPEI) in 1970. He works as a professor at the MPEI. In addition, he is a member of three dissertation councils and an expert of the Russian Academy of Science and the Federal Agency for Scientific Organizations

Vladimir P. Budak,
Prof., Dr. of Technical Science, graduated from the Moscow Power Institute in 1981, Editor in-chief of Svetotekhnika/ Light & Engineering Journal, Professor of the Light and Engineering Chair of the Moscow Power Institute NRU, Corresponding member of the Academy of Electro-technical Sciences of the Russian Federation

Dmitry S. Efremenko,
Dr. of Technical Science, graduated from the Moscow Power Engineering Institute (MPEI) in 2009. He works as a research scientist at the German Aerospace Center (DLR). He gives academic courses "Computational electrodynamics" and "Non-linear optimization" at the Technical University of Munich

Pavel S. Kaplya,
Ph.D. in Phys. and Math. Science, graduated from the Moscow Power Engineering Institute (MPEI) in 2012. He is an employee of Yandex LLC

Light & Engineering
Vol. 27, No. 2, pp. 97–104, 2019 *https://doi.org/10.33383/2018-018*

THE STATISTICAL EVALUATIONS OF TRANSMISSION CHARACTERISTICS, LIMITS OF RANGES AND SPEEDS OF TRANSMISSION OF INFORMATION VIA THE PULSED ATMOSPHERIC BISTATIC OPTICAL CHANNELS

Mikhail V. Tarasenkov[1], Egor S. Poznakharev[2] and Vladimir V. Belov[1]

[1] V.E. Zuev Institute of atmospheric optics, SB of RAS, Tomsk, Russia
[2] Tomsk state University, Tomsk, Russia
E-mail: belov@iao.ru; tmv@iao.ru

ABSTRACT

The simulation program by the Monte Carlo method of pulse reactions of bistatic atmospheric aerosol-gas channels of optical-electronic communication systems (OECS) is created on the basis of the modified double local estimation algorithm. It is used in a series of numerical experiments in order to evaluate statistically the transfer characteristics of these channels depending on the optical characteristics of an atmosphere plane-parallel model for wavelengths λ = 0.3, 0.5, and 0.9 μm at a meteorological visibility range S_M = 10 and 50 km. The results are obtained for a set of basic distances between the light source and the light receiver up to 50 km and for the angular orientations of the optical axes of a laser radiation beam and of the receiving system in a wide range of their values. The dependences of the pulse reactions maximum values over-the-horizon channels of the OECS on the variations of these parameters are established.

Keywords: atmosphere, scattered laser radiation, bistatic (over-horizon) optical communication, limit base distances, limit pulse transmission frequency

1. INTRODUCTION

Wireless optical communication through atmospheric channels develops in two directions: within the line of sight of the source by the receiver and outside it. The main advantage of the first type of communication is a high-speed data transmission. Disadvantages are interruption or impossibility of data transmission, associated with obstacles to the propagation of information signals and "running of the beam" on the input pupil of the receiver optical system, due to the turbulent pulsations of optical characteristics in the atmospheric communication channel. These disadvantages are deprived of optical communication out of the sight line, which allows it to be carried out at much greater distances.

In the foreign literature opto-electronic communication systems (OECS) are called "Non Line-of-Sight" ("NLOS"), and in the Russian literature they are called "over the horizon or bistatic OECS". There are much less works on these systems in the Russian and foreign press, than about the systems used within the line of sight. As it follows from [1–7], the over-horizon OECS can be divided into multicast optical communications at short and at long distances.

The first results of studies of some OECS bistatic channels characteristics are published in the article [5]. The studies were fulfilled in the Zuev Atmospheric optics Institute (AOI) of the Siberian branch of the Russian Academy of Sciences (SbRAS). The subsequent field experimental studies results of the transfer properties of these channels are considered in articles [6–8]. In particular in [8], it is reported that in the experiments the over-horizon communication at cloudless atmosphere at distances up to 70

km between the source of laser radiation with the wavelength λ = 510.6 nm and the receiver of radiation was realised. We have supplemented the experimental studies by the theoretical studies in order to predict the effect of a particular optical state of the atmosphere on the quality of communication and determine the optimal geometric scheme of its implementation.

The main results of our previous theoretical studies were published in articles [5, 9, 10]. The simulation of the response of the atmosphere as a linear system on the input of the Delta-pulse (i.e., the determination of the impulse response or the impulse response characteristics $h(t)$) and search (using this function) of the optimal communication patterns were their goal. In the framework of this problem in [9] the algorithm of the modified double local estimation of the Monte Carlo method of the nonstationary radiation transfer equation solution is proposed and considered [11]. The proposed algorithm makes a double local estimate at each point of collision in each possible time interval. The proposed algorithm [9] was taken as a basis in this work. In articles [9, 10] this algorithm is compared with the algorithms of statistical modelling of the function $h(t)$, proposed by other authors [12, 13]. Using the proposed algorithm, we have: 1) the analysis of ambient communication channels-scattered laser radiation, when the axis of the laser beam and the optical axis of the receiver lie in the same plane perpendicular to the earth's surface (flat model of the system atmosphere-land surface) and zenith angles of these axes are 85°; 2) the maximum communication range and the maximum of information transmission speed at λ = 0.5 μm and the characteristics of the receiving and transmitting system; 3) the comparison of transmission properties of channels on the wavelength λ = 0.3, 0.5 and 0.9 μm [14].

We considered here the general case, when restrictions on the position in space of the plane containing the axes of the laser beam and the receiving optical system, and on the zenith angles values of these axes orientation are removed.

2. THE PROBLEM STATEMENT

Knowing the response of the atmosphere (as a linear system) to the input Delta-pulse (impulse response) and the input signal, we can determine the received signal as a convolution integral of the form:

$$P(t) = S\int_0^\infty P_0(t')h(t-t')dt' = S\cdot p(t),$$

where S is the photodetector's receiving aperture area; $p(t)$ is the received radiation power, referred to the unit of the receiving aperture area; $P_0(t)$ is the power time function of the radiation source.

The atmospheric channel action of the OECS is considered as the action of a linear system (assuming the absence of nonlinear effects in the interaction of radiation with the medium in the communication channel). The definition of the impulse response of the atmospheric channel of OECS is performed as follows. We consider a plane system "atmosphere-Earth surface" without taking into account reflections from the earth's surface. The atmosphere is an aerosol-gas medium, which has the thickness about 100 km and is divided into 32 homogeneous layers, for every of which we use the optical parameters of the aerosol-gas atmosphere. The upper boundary of the first layer is set at an altitude of 0.1 km from the Earth surface, upper boundary of the second layer is set at an altitude of 0.5 km, and the boundaries of the layers from the third to the twenty third one have a step of 1 km. For subsequent layers, their thickness gradually increases from 2 to 30 km (the values of layer thickness are not given more detailed in this article, since they have little influence on the results of our calculations).

The geometric formation scheme of the communication channel is shown in Fig. 1. At the beginning of the coordinates on the Earth surface there

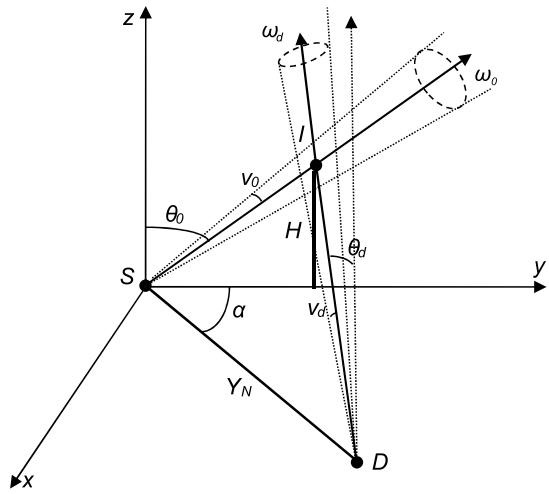

Fig. 1 Geometric scheme of atmospheric bistatic communication line

Table 1. Optical Parameters of the Near Ground Surface (0–0.1 km) Layer of the Atmosphere Used in the Calculations ($\sigma_{t,\,a}$ is aerosol attenuation coefficient, $\sigma_{s,\,a}$ is Aerosol Scattering Coefficient, $\sigma_{t,\,m}$ is Molecular Attenuation Coefficient, $\sigma_{s,\,m}$ is molecular Scattering Coefficient)

λ, μm	S_M, km	$\sigma_{t,\,a}$, km^{-1}	$\sigma_{s,\,a}$, km^{-1}	$\sigma_{t,\,m}$, km^{-1}	$\sigma_{s,\,m}$, km^{-1}
0.3	10	0.661	0.620	0.165	0.140
0.3	50	0.113	0.106	0.165	0.140
0.5	10	0.433	0.410	0.0166	0.0165
0.5	50	0.0739	0.0700	0.0166	0.0165
0.9	10	0.215	0.196	0.137	0.0015
0.9	50	0.0367	0.0334	0.137	0.0015

is a point source of radiation with the coordinates (0,0,0) with the beam divergence v_0 oriented in the direction ω_0 in the plane *Syz* at a zenith angle θ_0. At the base distance Y_N at an angle α from the *Syz* plane on the Earth surface there is the receiving system, which has the optical axis oriented to the point *I* on the axis of the source beam located at a height *H* from the Earth surface. The zenith angle of the receiving system optical axis is θ_d, and the angle of its field of view is v_d.

Let it be required to determine the pulse reaction of the OECS bistatic channel for the given conditions of its formation. The plane *Syz* is called the source plane, and the plane *SID* is called the plane of the receiver.

3. CALCULATION RESULTS

The program calculations based on the algorithm of the modified double local estimation [9] were performed under the following optical-geometric conditions: radiation wavelengths λ = 0.3, 0.5, and 0.9 μm; meteorological visibility ranges S_M = 10 and 50 km. The generator of optical models sets optical parameters of cloudless aerosol-gas atmosphere at the specified S_M on the basis of the program "LOWTRAN7" [15]. The values of optical factors for the above ground layer of the atmosphere are given in Table 1. At the same time θ_0 = 0°, 45°, and 85°; v_0 = 0.0034°; Y_N = 0.5–50 km; α = 0°, 10°, 30°, 60°, and 90°; $H = H_{min}$ = 0.1, 0.5, 1, 3, and 5 km; v_d = 2°; the maximum trajectory length l_{max} = 200 km (without Y_N). The H_{min} was taken as the height, at which θ_d = 85°. The total calculations were performed for 2412 variants of optical-geometric conditions. The calculation of one variant depended on the conditions of calculations and was about 40 minutes per computer with the performance 19.5 GFlops on the LIN-X test.

The average time interval error of the obtained results of calculations for S_M = 50 km was 0.1–6.2 % in all considered variants, and for S_M = 10 km it was 0.1–9 % with the exception of the variants with λ = 0.3 and 0.5 μm for $Y_N \geq 30$ km, in which the average time interval error lies within 0.16–34 %. Illustrations of some calculation results of the impulses maxima, which response for time intervals h_{max} when $H = H_{min}$ are shown in Fig. 2.

The dependence analysis of the h_{max} on optical-geometric conditions shows that for small base distances Y_N (2–3 km), other things being equal, h_{max} is maximal for λ = 0.3 μm. At large Y_N and at low atmospheric turbidity (S_M = 50 km), h_{max} is maximal for λ = 0.5 μm. At high atmospheric turbidity (S_M = 10 km), the behaviour of h_{max} is more complex. At small α (near 0°) at Y_N = 2–10 km, h_{max} is maximal for λ = 0.5 μm, and at Y_N > 10 km, h_{max} is maximal for λ = 0.9 μm (Fig. 2, (a)). However, at $\alpha \geq 10°$ and Y_N > 2 km, h_{max} is maximal for λ = 0.5 μm.

The reason for such dependence of the h_{max} values on the variable parameters is that at λ = 0.3 μm not only the radiation scattering is stronger, but also its attenuation (due to ozone absorption) is greater than at other λ; this greatly reduces the received signal power at large Y_N. The role of scattering and attenuation at λ = 0.5 is higher than at λ= 0.9 μm at high atmospheric turbidity and lower absorption (due to the presence of water vapour absorption at λ = 0.9 μm).

The calculations also show that, other things being equal, h_{max} at $H = H_{min}$ is higher than at any $H > H_{min.}$ This is due to the fact that when $H = H_{min}$ the length of the path *SID* and the scattering angles of the trajectories are minimal on the average.

Knowing the characteristics of the receiving and transmitting equipment and the pulse response of the atmospheric channel, it is possible to determine

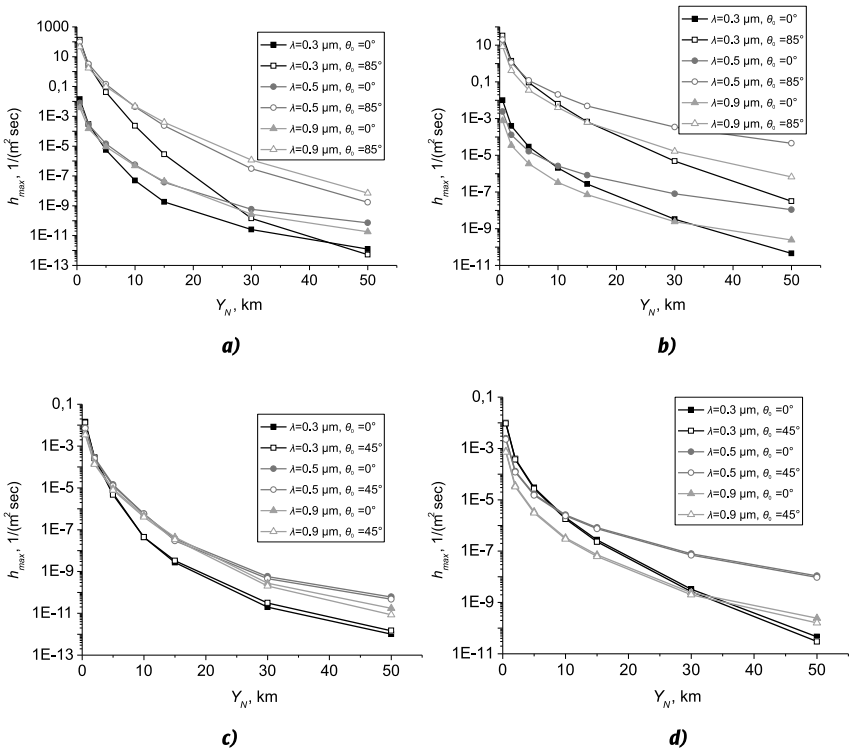

Fig. 2. Maximum impulse response h_{max} (Y_N) at:
S_M = 10 км, α = 0°, θ_d = 85° (*a*);
S_M = 10 км, α = 60°, θ_d = 85° (*c*);
$S_м$ = 50 км, α = 0°, θ_d = 85° (*b*);
S_M = 50км, α = 60°, θ_d = 85° (*d*)

the limit range of the communication line. As an appropriate example, we consider a laser with λ = 0.5 μm as a transmitting information system. Suppose that the laser pulse shape is rectangular, its duration Δt = 30 nsec and the average pulse power P_0 = 18 182 W. Let the amplifier element (PMT-17A) used as a part of an ideal receiving optical system. For the maximum range of communication for given α and θ_0, we take Y_N, in which the power level of the received radiation P matches the limit. For the upper bound of P we take the maximum P used under the given conditions.

With the growth of Y_N, the values of the impulse response are changed many times, so it makes sense to consider the value of the ratio P_0 to P reduced to decibels, η [2]:

$$\eta = 10\lg\left(P_0/P\right) = 10\lg\left(\frac{P_0}{pS}\right),$$

where p is the power of the received radiation per unit area of the aperture, S is the area of the aperture.

Then the limit Y_N will be the distance, at which

$$\eta > \eta_*,\ \eta_* = 10\lg\left(\frac{P_0}{P_*}\right),$$

where P_* is the limit of P_0.

As a limit, we take the power that satisfies the ratio [16–18]

$$\rho = \frac{F\Sigma_{\tilde{n}}M}{\sqrt{2e\Delta f[M^2 I_k(1+B)+\frac{2kT}{eR_i}(1+\frac{\mathrm{R}_e}{R_i})]}} = 1, \quad (1)$$

where

$$M = \frac{\Sigma_A}{\Sigma_c},\ \Delta f = \frac{1}{2R_iC_a},$$
$$I_k = \Sigma_c \cdot F + I_k + \Sigma_c \cdot F_b,\ I_k = j_T \cdot Q, \quad (2)$$

ρ is the signal-to-noise ratio; I_k is the mean value of the photocathode emission current; F is an average value of the luminous flux measured; Σ_c is the photocathode integral sensitivity; Σ_A is the anode sensitivity; R_e is the equivalent noise resistance; (1 + B) is the noise factor; T is the absolute temperature of the photomultiplier (PMT); M is the gain of the PMT; Δf is the frequency band; R_l is the load resistance; C_a is the capacitance between the anode output and the last cascade; F_b is the background illumination; I_{tk} is the current of the photocathode thermal emission; j_T is the thermoelectric current density; Q is the photocathode area.

Table 2. Constants of Approximation for the Calculation of η

λ, μm	S_M, km	C_1, dB	C_2, dB	C_3, dB/rad	N_0	C_4	C_5
0.5	10	114	–33.4	35.2	0.109	0.024	–0.016
0.5	50	120	–31.2	31.8	0.076	0.007	–0.003

The following values were used in the calculations (1) and (2) [6, 16–21]: Σ_c = 40 μA/lm [20, P. 134]; Σ_A =10 A/lm [20, P. 134]; $R_l = 10^8$ Ohm [18, P. 274]; $C_a = 10^{-11}$ F [18, P. 274]; $1 + B = 2.5$ [18, P. 274]; $T = 256$ *K* [6]; $R_e = 3.5 \cdot 10^6$ Ohm [20, P. 161]; $j_T = 10^{-15}$ A/cm^2 [16, P. 109]; $Q = 0.8$ cm^2 [19, P. 46]; $F_b = 0$ lm.

Our earlier estimates [14] for the PMT-17A showed that $F = 2 \cdot 10^{-11}$ lm in the conditions considered by us. For conversion from lm to W we have the equation

$$P = \frac{F}{C v(\lambda)},$$

where C = 683 lm/W; $v(\lambda)$ = 0.323 at λ = 0.5 μm [21, P. 23].

In this article, we consider a special case when $F_b = 0$ lm. The case of the presence of a solar background will be the subject of the following works. The algorithm of statistical modelling of the background radiation is developed and tested by us in the framework of [22].

For the maximum P and for cases, when $H = H_{min}$ (that corresponds to the best conditions for P), the ratio η was calculated. An approximation of its form was constructed for its description

$$\eta(\theta_0, Y_N, \alpha) = \left(\begin{array}{l} C_1 + C_2(1-\cos\theta_0) + \\ + C_3|\alpha|(1-\cos\theta_0) \end{array}\right)\left(\frac{Y_N}{0{,}5}\right)^{N_0 + C_4\theta_0 + C_5\theta_0|\alpha|}, \quad (3)$$

where C_1–C_5, N_0 are the approximation constants.

The applicability conditions of the formula (3) are: θ_d = 85° ($H = H_{min}$), –90° < α < 90°, 0° < θ_0 < 85°, and Y_N = 0.5–50 km. The values of the approximation constants are given in Table 2. The absolute approximation error at S_M = 50 km is 0.01–9.06 dB; the absolute approximation error at S_M = 10 km is 0.02–12.8 dB.

Using the approximation (3), the dependences η on the location of the receiving system and θ_0 for the situations, when η < 173 dB are constructed (Fig. 3). The figure shows that the obtained dependences are in full agreement with the conclusions obtained for the h_{max} dependencies.

Another factor that characterizes the quality of the communication channel is the limit number of pulses per unit of time, which can be transmitted and received through the communication channel. This characteristic is related to the speed of information transmission. Following the work [2], as the

Table 3. The Range of Variation of v_{max}

θ_0, °	α, °	v_{max} (0.5)	v_{max} (50)	θ_0, °	α, °	v_{max} (0.5)	v_{max} (50)
S_M = 10 km				S_M = 50 km			
0		4.53E+06	7.65E+03	0		4.61E+06	3.29E+04
45	0	1.04E+07	1.71E+04	45	0	1.05E+07	8.58E+04
45	10	1.03E+07	1.82E+04	45	10	1.03E+07	8.34E+04
45	30	9.06E+06	1.28E+04	45	30	9.15E+06	6.88E+04
45	60	6.45E+06	8.48E+03	45	60	6.55E+06	4.34E+04
45	90	4.34E+06	6.15E+03	45	90	4.44E+06	2.77E+04
85	0	1.99E+07	7.22E+04	85	0	1.99E+07	1.09E+06
85	10	1.87E+07	2.14E+04	85	10	1.88E+07	3.88E+05
85	30	1.22E+07	9.15E+03	85	30	1.24E+07	4.95E+04
85	60	2.72E+06	4.43E+03	85	60	2.89E+06	1.07E+04
$v_{max}(A) = v_{max}$ ($A = Y_N$)							

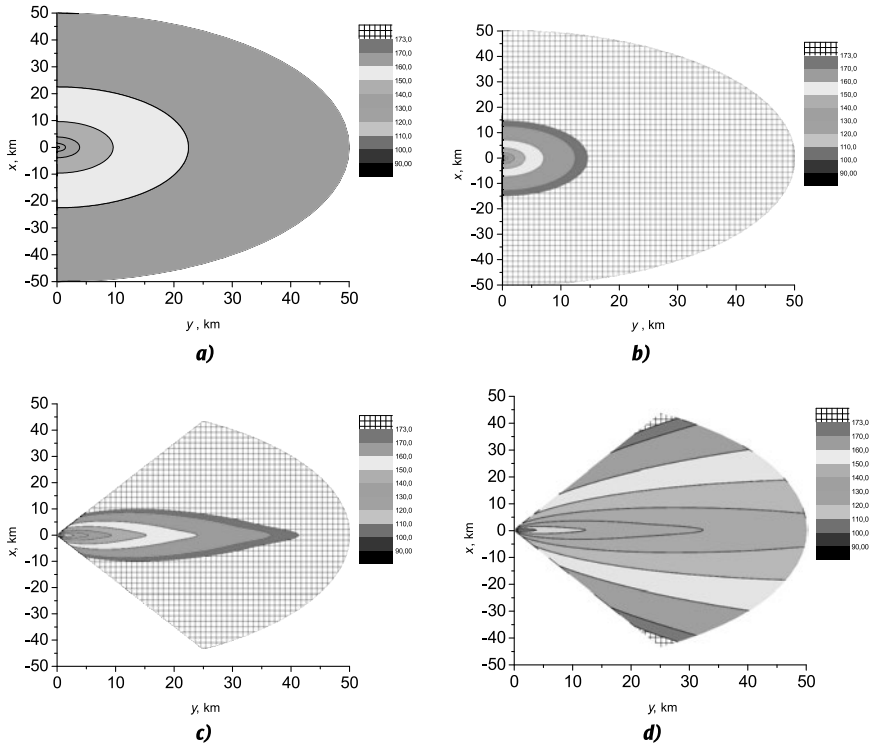

Fig. 3. Dependence $\eta(x, y)$ at $\lambda = 0.5$ μm at:
$S_M = 50$ km, $\theta_0 = 0°$ (a);
$S_M = 10$ km, $\theta_0 = 0°$ (b);
$S_M = 50$ km, $\theta_0 = 85°$ (c);
$S_M = 10$ km, $\theta_0 = 85°$ (d)

pulses transmission limit frequency v, which allows the communication channel, we can take the value of v_{max} defined implicitly as:

$$\frac{\left|F\left[P(t)\right](v_{max})\right|}{\left|F\left[P(t)\right](0)\right|} = 0.5,$$

$$F\left[P(t)\right](v) = \int_{-\infty}^{+\infty} P(t)e^{2\pi ivt}dt,$$

where $P(t)$ is the power distribution of the received radiation; F is the Fourier transform.

v_{max} values were calculated for the optical-geometrical conditions and characteristics of the receiving-transmitting equipment described above. Examples of calculation results are shown in Fig. 4, and Table 3 shows the range of v_{max} changes in the Y_N from 0.5 to 50 km and different values of θ_0 and α. The calculation results show that v_{max} decreases with the growth of Y_N and α. At small Y_N (up to 5 km) v_{max} weakly depends on the turbidity of the medium, and at large Y_N with increasing turbidity v_{max} decreases several times. From Table 3 it follows that v_{max} lies in the range from $4 \cdot 10^3$ to $2 \cdot 10^7$ Hz at $\Delta t = 30$ nsec and at the specified parameters of the transmitting-receiving communication system.

4. CONCLUSION

The simulation program by the Monte Carlo method of bistatic atmospheric aerosol-gas channels pulse reactions of OECS is created on the basis of the modified double local estimation algorithm [9, 10]. This program is used in a series of numerical experiments to statistically evaluate the transfer characteristics of these channels depending on the optical characteristics of an atmosphere plane-parallel model at $\lambda = 0.3$, 0.5, and 0.9 μm at a meteorological visibility range $S_M = 10$ and 50 km. The results are obtained for a set of basic distances (up to 50 km) between the radiation source and the radiation receiver and for the angular orientations of the optical axes of a laser radiation beam and of the receiving system in a wide range of their values. The dependences of the pulse reactions maximum values over-the-horizon channels of the OECS on the variations of these parameters are established.

The upper estimation of the limiting frequencies and the action ranges of the model optical-electronic communication system, which simulates the system already used in field experimental studies, is carried out [7, 8].

The main conclusions from the analysis of the results are as follows: 1) the maximum power of the received information pulse is maximum at $\lambda = 0.3$

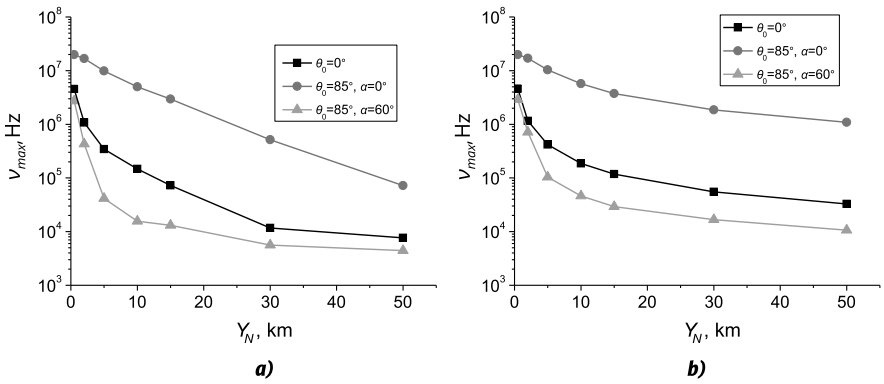

Fig. 4. Dependence of v_{max} (Y_N) at S_M =10 km (a) and 50 km (b)

μm at small base distances (2–3 km), other things being equal; 2) the maximum power of the received information pulse can be achieved for λ = 0.5 μm at large base distances (S_M = 50 km) and low turbidity; 3) it can be achieved for λ = 0.5 and 0.9 μm at high turbidity of the atmosphere (S_M = 10 km) depending on the basic distances and the orientation of the reception plane.

The limiting pulse transmission frequencies for bistatic communication optoelectronic systems depending on the optical state of the atmosphere and the geometrical parameters of the communication channel formation schemes lie in the range from $4 \cdot 10^3$ to $2 \cdot 10^7$ Hz.

The work was performed with financial support within the Priority direction II.10, project II.10.3.3. "Direct and inverse problems of sounding of the atmosphere and the Earth surface, atmospheric correction, and communication by optical-electronic systems using scattered laser radiation".

REFERENCES

1. Poller B.V., Britvin V.A., Kolomnikov J.D., Golovachev Yu.G., Konyaev S.I., Kusakina A.E., Shergunova N.A. Nekotory'e xarakteristiki rasprostraneniya lazerny'x signalov v usloviyax observatorii SO RAN "Kajtanak" na gornom Altae [Some of the characteristics of laser signals propagation in Observatory of the Russian Academy of Sciences of "Kaytanak" in mountain Altai] // Interexpo geo-Siberia, 2012, Vol. 2, #4, pp. 64–68.

2. Haipeng D., Chen G., Arun K., Sadler B.M., Xu Z. Modeling of non-line-of-sight ultraviolet scattering channels for communication // IEEE journal on selected areas in communications, 2009, Vol. 27, #9, pp. 1535–1544.

3. Han D., Liu Y., Zhang K., Luo P., Zhang M. Theoretical and experimental research on diversity reception technology in NLOS UV communication system // Optics express, 2012, Vol. 20, #14, pp. 15833–15842.

4. Elshimy M.A., Hranilovic S. Non-line-of-sight single-scatter propagation model for noncoplanar geometries // JOSA A., 2011, Vol. 28, #3, pp. 420–428.

5. Borisov B.D., Belov V.V. Vliyanie pogodny'x uslovij na parametry' korotkogo lazernogo impul'sa, otrazhyonnogo atmosferoj [Influence of weather conditions on the parameters of short laser pulses reflected from the atmosphere] // Optika atmosfery' i okeana, 2011, Vol. 24, #4, pp. 263–268.

6. Belov V.V., Tarasenkov M.V., Abramochkin V.N., Ivanov V.V., Fedosov A.V., Troitskiy V.A., Shiyanov D.V. Atmosferny'e bistaticheskie kanaly' svyazi s rasseyaniem. Chast' 1. Metody' issledovaniya [Atmospheric bistatic communication channels with scattering. Part 1. Research methods] // Optika atmosfery' i okeana, 2013, Vol. 26, № 4, pp. 261–267.

7. Belov V.V., Tarasenkov M.V., Abramochkin V.N. Bistaticheskie atmosferny'e optiko-e'lektronny'e sistemy' svyazi (polevy'e e'ksperimenty') [Bistatic atmospheric optoelectronic communication systems (field experiments)] // Pis'ma v ZhTF, 2014, Vol. 40, #19, pp. 89–95.

8. Abramochkin V.N., Belov V.V., Gridnev Yu.V., Kudryavtsev A.N., Tarasenkov M.V., Fedosov A.V. Optiko-e'lektronnaya svyaz' v atmosfere na rasseyannom lazernom izluchenii. Polevy'e e'ksperimenty' [Optical-electronic communication in the atmosphere on scattered laser radiation. Field experiments] // Svetotechnika, 2017, #4, pp. 24–30.

9. Belov V.V., Tarasenkov M.V. Tri algoritma statisticheskogo modelirovaniya v zadachax opticheskoj svyazi na rasseyannom izluchenii i bistaticheskogo zondirovaniya [Three algorithms of statistical simulation in tasks of optical communication for scattered radiation and bistatic sounding] // Optika atmosfery' i okeana, 2016, Vol. 29, #5, pp. 397–403.

10. Tarasenkov M.V., Belov V.V. Sravnenie trudoyomkosti algoritmov statisticheskogo modelirovaniya impul'snoj reakcii kanala bistaticheskoj lazernoj svyazi na rasseyannom izluchenii i bistaticheskogo lazernogo zondirovaniya [Comparison of complexity of algorithms of statistical simulation of the impulse response of the channel bistatic laser communication for scattered radiation and bistatic laser sounding] // Vy'chislitel'ny'e texnologii, 2017, Vol. 22, #3, pp. 91–102.

11. Marchuk G.I., Mikhailov G.A., Nazaraliev M.A., Darbinyan, R.A., Kargin B.A., Elepov B.S. Metod Monte-Karlo v atmosfernoj optike [Monte-Carlo in atmospheric optics] // Nauka, Siberian branch, Novosibirsk, 1976, 284 p.

12. Lotova G.Z. Modification of the double local estimate of the Monte Carlo method in radiation transfer theory // Russian Journal of Numerical Analysis and Mathematical Modeling, 2011, Vol. 26, #5, pp. 491–500.

13. Mikhailov G.A., Lotova G.Z. Chislenno-statisticheskaya ocenka potoka chasticz s konechnoj dispersiej [Numerical and statistical estimation of the particle flow with finite dispersion] // DAN, 2012, Vol. 447, #1, pp. 18–21.

14. Tarasenkov M.V., Belov V.V., Poznakhareva E.S. Modelirovanie processa peredachi informacii po atmosferny'm kanalam rasprostraneniya rasseyannogo lazernogo izlucheniya [Modeling of the process of information transfer in the atmospheric distribution of scattered laser radiation] // Optika atmosfery' i okeana, 2017, Vol. 30, #5, pp. 371–376.

15. Kneizys F.X., Shettle E.P., Anderson G.P., Abreu L.W., Chetwynd J.H., Selby J.E.A., Clough S.A., Gallery W.O. User Guide to LOWTRAN-7. ARGL-TR-86–0177. ERP 1010. Hansom AFB. MA 01731, 1988, 137 p.

16. Anisimov I.I., Glukhovskij, B.M. Fotoe'lektronny'e umnozhiteli [Photomultipliers] // Sov. Radio, Moscow, 1974, 61 p.

17. Aksenenko M.D., Baranochnikov M.L. Priyomniki opticheskogo izlucheniya: spravochnik [Optical radiation Receivers: Handbook] // Radio i svyaz', Moscow, 1987, 296 p.

18. Soboleva N.A. Melamid, A.E. Fotoe'lektronny'e pribory' [Photoelectronic devices] // Vy'ssh. shkola, Moscow, 1974, 376 p.

19. Vasiliev A.F., A.M. Chmutin. Fotoe'lektricheskie priyomniki izlucheniya [Photoelectric radiation detectors] // VolGU, Volgograd, Russia, 2010, 81 p.

20. Chechik N.O., Feinstein S.M., Lifshitz T.M. E'lektronny'e umnozhiteli. Pod red. D.V. Zernova [Electronic multipliers. Edited by D.V. Zernov] // GITTL, Moscow, 1957, 576 p.

21. Gurevich M.M. Fotometriya (teoriya, metody' i pribory') [Photometry (theory, methods and devices)] // Energoatomizdat, Leningrad, USSR, 1983, 272 p.

22. Belov V.V., Tarasenkov M.V., Piskunov K.P. Parametricheskaya model' solnechnoj dy'mki v vidimoj i UF-oblasti spectra [Parametric model of solar haze in the visible and UV region of the spectrum] // Optika atmosfery' i okeana, 2010, Vol. 23, #4, pp. 294–297.

Mikhail V. Tarasenkov, Ph.D. in Phys. and Math. Science. He graduated from the Tomsk State University (TSU) in 2007. Senior researcher at the Zuev Institute of atmospheric optics. Research interests: analysis of regularities of image formation through the atmosphere, atmospheric correction of images in the visible and UV radiation ranges, theoretical research on communication channels outside the line of sight

Egor S. Poznakharev, student of the TSU. Engineer of the Zuev Institute of atmospheric optics. Research interests: theoretical and experimental research on communication channels outside the line of sight

Vladimir V. Belov, Dr. of Phys. and Math. Science, Prof. He graduated from the TSU in 1971. Head of ROS laboratory of the Zuev Institute of atmospheric optics. Honored worker of science of Russia. Research interests: theory of optical radiation transfer in scattering and absorbing media, theory of laser sensing, theory of vision, atmospheric correction of aerospace images of the Earth surface, Monte Carlo method, multiple scattering

Light & Engineering
Vol. 27, No. 2, pp. 105–110, 2019 *https://doi.org/10.33383/2017-081*

MATRIX TRANSFORMATIONS FOR EFFECTIVE IMPLEMENTATION OF RADIOSITY ALGORITHM USING GRAPHIC PROCESSORS

Alexander S. Shcherbakov [1] and Vladimir A. Frolov [1, 2]

[1] Lomonosov Moscow State University, Moscow, Russia
[2] Keldysch Institute of Applied Mathematics, RAS, Moscow, Russia,
E-mail: alex.shcherbakov@graphics.cs.msu.ru; vladimir.frolov@graphics.cs.msu.ru

ABSTRACT

A method of form factors matrix transforming, which allows accelerating calculation of secondary illumination by the radiosity method is proposed. An adaptation of this method for graphic processors (graphics processing unit, GPU) is considered. In particular, it is proposed to use DXT textures to store form factors matrix and to reorder columns and lines of the matrix to reduce compression losses. The proposed optimisations increase the speed of radiosity algorithm work to ten times and reduce the GPU occupied memory volume to three times.

Keywords: radiosity, global lighting, GPU

1. INTRODUCTION

Global lighting of 3D scenes is a combination of the light source (LS) primary lighting and of the secondary lighting multiply reflected from the scene surfaces. The calculation of the secondary lighting is maximum complex as the illuminance integral dimension increases with each reflection. Therefore, in real time applications some methods of the approximate calculation are used.

2. A REVIEW OF THE EXISTING METHODS

2.1. Instant Radiosity Method

Instant Radiosity is one of the most popular methods due to its simplicity [1, 2]. To calculate the secondary lighting, secondary LSs are used, which are created by the ray tracing from primary LSs. Thus, the secondary lighting can be considered as the primary from secondary LSs. Reflective Shadow Maps (RSM) algorithm is a development of the Instant Radiosity method for GPU [3]. Instead of the ray tracing in the RSM, to create secondary LSs, the Shadow Maps are used. The main disadvantage of this method is its low accuracy.

2.2. Light Propagation Volumes Method

Light propagation method [4] creates secondary LSs, as well as the Instance Radiosity method, but the calculation of secondary lighting is made by means of the light propagation using a three-dimensional net. The main disadvantage of this method is the high memory consumption and low efficiency when calculating the light propagation through empty spaces.

2.3. Voxel Cone Tracing

Voxel Cone Tracing method [5] makes a "lighting collection" for each pixel by the several cones tracing from a set surface point imitating the Monte-Carlo ray tracing over a hemisphere. This method (just as the previous) uses a voxel net for a simplified geometry presentation, and the cone tracing is similar to the ray marching. The difference is that with the distance increase, the selection is made from more rough MIP-maps of the voxel net, due to which a geometrical cone appro-

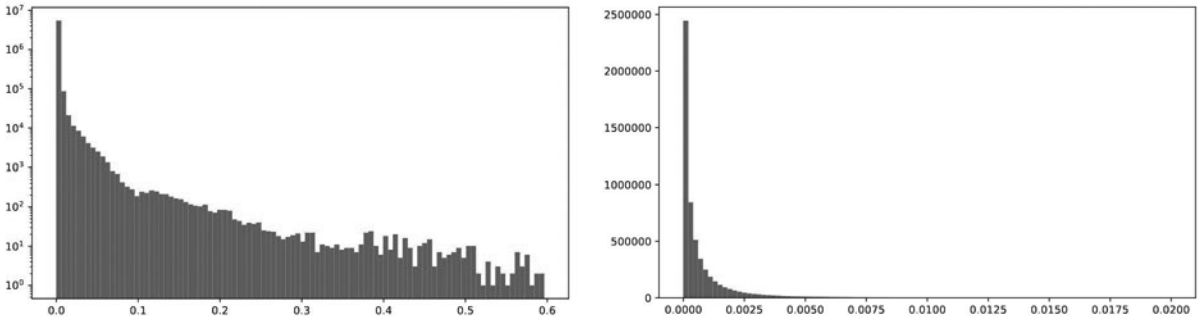

Fig. 1. Distribution of values in a form factor matrix (logarithmic and linear scales)

ximation occurs. A high calculation complexity and a calculation speed dependence on the resolution are the disadvantages of the algorithm.

2.4. Spherical Harmonics Method

Spherical harmonics method [6] is based on the expansion of complex illuminance functions into a sum of values, which are simpler to be calculated. For some surface points (as a rule, for top points) basis expansion coefficients of their lighting functions are calculated. Lighting functions from LSs are also expanded on the basis. As a result, the calculation of lighting in a point with the illuminance function expanded in it is reduced to a dot product of vectors consisting of illuminance function coefficients in this point and of lighting functions from LSs. This method is widely used when visualising open spaces, but it is less accurate than the radiosity method in case of closed rooms.

2.5. Radiosity Method

Radiosity method [7] allows obtaining high-quality images for closed rooms with diffuse surfaces, and in many respects, it is not worse than more modern methods. However, implementation time and required resources strongly depend on the scene. For the scenes containing hundreds of thousands triangles, a direct radiosity application is complicated because of the square complexity and of the memory consumption depending on the primitive numbers. Therefore, in practice, the radiosity algorithm is performed for a simplified scene (containing fewer surfaces) and the calculation result is transferred to the initial scene [8]. It should be noted that along with the spherical harmonics, the radiosity algorithm transfers the main computing complexity to a preliminary calculation stage, and due to this fact, a good accuracy and speed balance is reached in comparison with other methods.

3. KEY TERMS AND DEFINITITIONS

In the classical radiosity algorithm, the form factor matrix F of $n \times n$ size is used, where n is the number of scene sites. To calculate the illuminance m_i after reflection, this matrix is multiplied by n-component vector of initial luminous exitance $m_e^{(0)}$ containing the sites luminous exitance:

$$\overline{m}_i^{(1)} = F \cdot \overline{m}_e^{(0)}.$$

Multiplying the obtained vector by reflectance ρ of the sites, to which light has come, luminous exitance of the sites after reflection is calculated as follows:

$$\overline{m}_e^{(1)} = \overline{m}_i^{(1)} \cdot \rho. \quad (1)$$

Three-component vectors containing information on each colour channel are vector elements in these formulas, and real numbers from 0 to 1 are form factors matrix elements. The presented calculations can be repeated using vectors $m_e^{(n)}$ instead of the initial site luminous exitance to obtain light, which has come to the scene sites after an arbitrary reflection:

$$\overline{m}_i^{(n)} = F \cdot \overline{m}_e^{(n-1)}. \quad (2)$$

The full scene lighting after k reflections can be obtained by summation of vectors $m_i^{(n)}$:

$$\overline{I} = \sum_{n=1}^{k} \overline{m}_i^{(n)}. \quad (3)$$

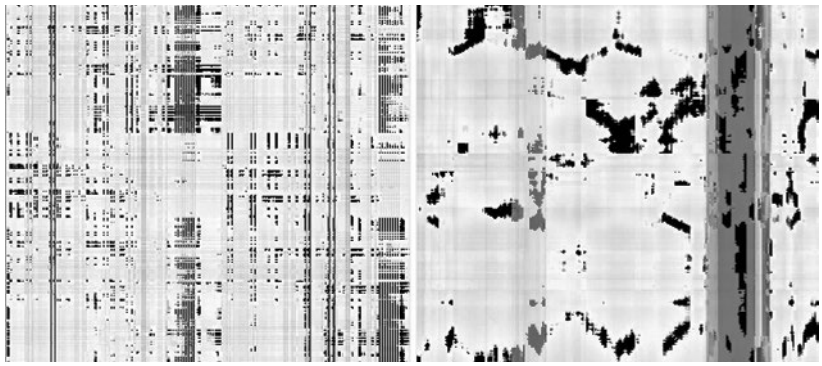

Fig. 2. A fragment of form factor matrix before selection (on the left) and after selection (on the right) of lines and columns. An increased fragment of form factor matrix

4. THE PROPOSED METHOD

4.1. Preliminary Calculation of Several Scene Reflections

The proposed modification is to use of the transformed form factor matrix. In the beginning, a "colour" form factor matrix is introduced:

$$F_{ij}^{C} = F_{ij} \cdot \rho_j,$$

where ρ_j is colour of j site. This matrix contains information on light transport between scene sites along each channel separately. Thus, its storage requires three times more memory. In this article, the use of the radiosity algorithm for the secondary scene lighting is considered. Therefore, the radiosity calculation begins not from the vector $m_i^{(1)}$ obtaining, but from the luminous exitance calculation after the first reflection $m_e^{(1)}$. One can consider that the vector $m_e^{(1)}$ is already calculated. We can transform the expression (2) using the formula (1) for an arbitrary index.

$$\begin{aligned} m_i^{(n)} &= F \cdot (\rho \cdot m_i^{(n-1)}) = \\ &= F^C \cdot m_i^{(n-1)} = (F^C)^{-1} \cdot m_i^{(1)}. \end{aligned} \quad (4)$$

The summation (3) can be transformed using (4):

$$\overline{I} = \left(\sum_{n=1}^{k} (F^C)^{n-1} \right) \cdot m_i^{(n)}.$$

The matrix polynomial in brackets does not depend on the primary scene lighting and depends only on the scene geometry and on surface materials. Therefore, it can be found at the preliminary calculation stage:

$$S = \left(\sum_{i=1}^{k} (F^C)^{i-1} \right).$$

Thus, the calculation of the secondary lighting by the radiosity method after k reflections is reduced to one multiplication of the vector by a matrix:

$$m_i^{(n)} = S \cdot m_i^{(1)}.$$

Using this type of matrix allows accelerating the calculation k times (where k is the number of reflections); however, it requires three times more memory.

To take into account all possible light reflections on a scene, it is necessary to calculate an infinite series

$$S = \left(\sum_{i=0}^{\infty} (F^C)^i \right).$$

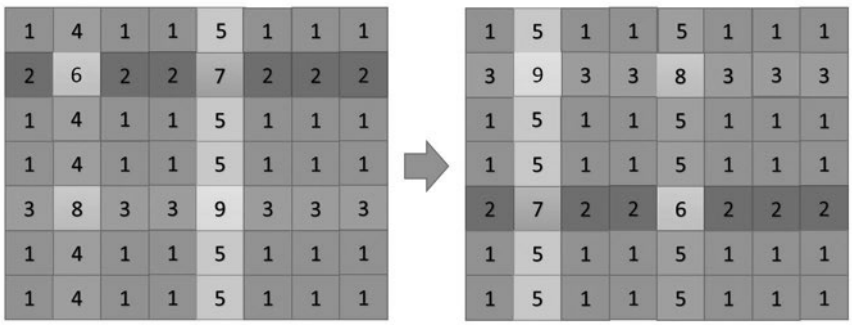

Fig. 3. Layout of lines and columns interchanging used by the authors when selecting

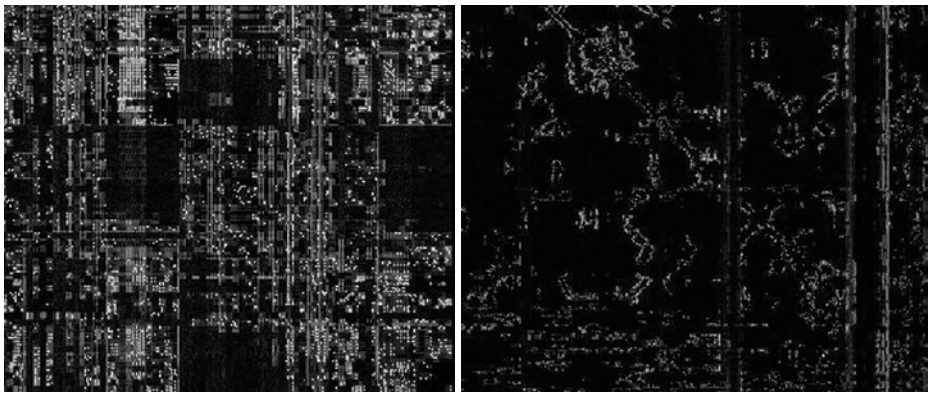

Fig. 4. Visualised difference between the compressed and uncompressed textures (an increased fragment) before (on the left) and after (on the right) lines and columns reordering

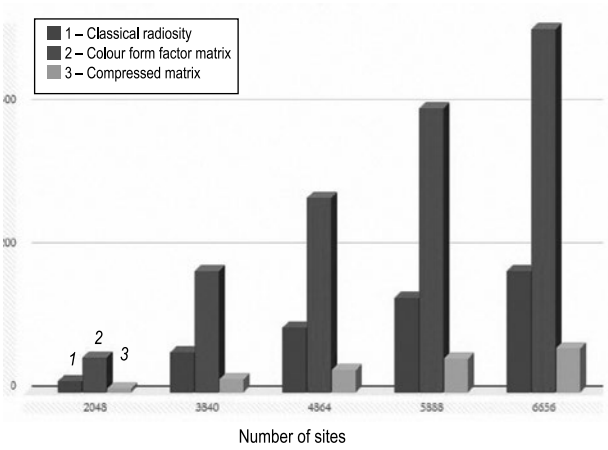

Fig. 5. Comparison of form factor files and matrices size, MB

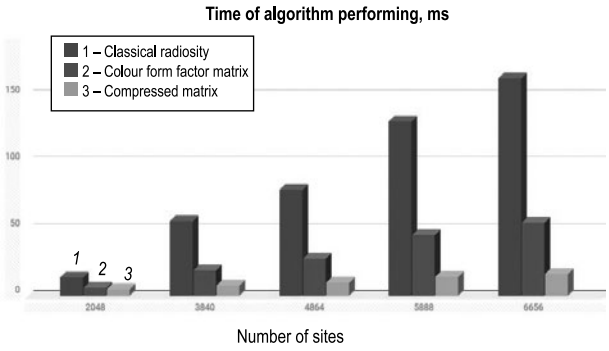

Fig. 6. Comparison of radiosity calculation speeds. (A compression increases the speed since the algorithm is limited by the memory access but not by calculations.)

Limit process. As the initial matrix is positively determined, all numbers in it are less than 1 and, moreover, sum of numbers in one line is less than 1, then the formula for the calculation of the geometrical progression sum is applicable to this series

$$S = F^C \cdot \left(I - F^C\right)^{-1}.$$

However, calculation of a reverse matrix is not always possible because of the solution instability. At the same time, the calculation of a series partial sum does not have such a disadvantage and allows taking into consideration large reflections number at the preliminary calculation stage.

4.2. DXT Compression

As the proposed algorithm modification requires a greater memory volume, a method of form factor matrix storage in the summary form was developed. As a storage format, DXT texture format supported by many GPUs was selected (a hardware decompression when reading is meant). For this format, all matrix values should be reduced to an interval of 0–255. Fig. 1 shows the value distribution in a form factors matrix. When scaling these numbers in the 0–255 interval, most of the numbers are set to zero. Therefore, large numbers, which make the basic contribution to the radiosity calculation, are stored separately of the rest matrix, and the following transformation is applied to the others:

$$value_i^{'} = \frac{\max\left(\log\left(\frac{value_i}{\max\limits_j value_j}\right) + shift, 0\right)}{shift} \cdot 255.$$

The texture, which is obtained as a result of a such transformation, is shown in Fig. 2, on the left.

However, the DXT compression is followed by losses. In order to minimise them when compressing, matrix lines and columns are sorted to reduce the difference between the neighbour values (Fig. 2, on the right). As the matrix is a relation of the scene sites for couples, lines and columns should change

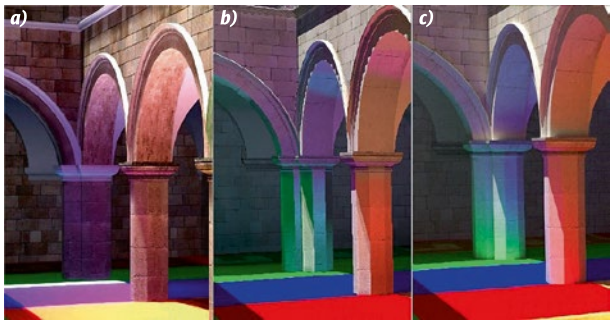

Fig. 7. Images obtained by the Light Propagation Volumes (a) and by the proposed (b) methods, as well as by the path tracing /reference/ (c). The Light Propagation Volumes and the proposed methods work with 40 frames/s frequency / (25 ms period), and the reference is obtained within 5 min.

positions simultaneously (Fig. 3). As a result, the root-mean-square error, when compressing, decreases to five times (Fig. 4).

4.3. Implementation Details

As modern 3D scenes contain hundreds of thousands of triangles and time of the radiosity algorithm implementation is unacceptable for a such scene site number, to calculate the secondary lighting, a simplified version of the same scene was selected using a simplification method based on the voxel net from the article [9].

Thus, the scene pre-processing is implemented according to the following schedule:

1. A simplified scene analogue is constructed based on the voxelisation;
2. Form factors are calculated for sites of the simplified scene;
3. A form factor matrix is calculated, which takes into consideration several light reflections;
4. The matrix numbers, which are bigger than the threshold value, are stored in a separate file, and zeroes are put on their places;

Fig. 8. An image obtained by the Light Propagation Volumes method (Unreal Engine 4)

5. Values in the matrix are reduced to the 0–255 interval;
6. An interchange of lines and columns is made;
7. The obtained matrix is stored as a DXT texture.

The visualisation occurs according to the following algorithm:

1. A shadow map is created;
2. Lighting of the simplified scene sites made by LSs is calculated;
3. The secondary lighting is calculated using the radiosity method by means of the form factor matrix stored as a texture;
4. The secondary lighting is transferred from the simplified scene to the initial.

4.4. Comparison of the results

The proposed algorithm modifications allow accelerating the radiosity algorithm in total to ten times (Figs. 5–7). The use of the form factor matrix, which is taking into consideration several reflections, increases the matrix file size three times, however, the use of the DXT compression allows reducing the required memory to three times in comparison with the initial form factor matrix

Fig. 9. An image obtained by the proposed method

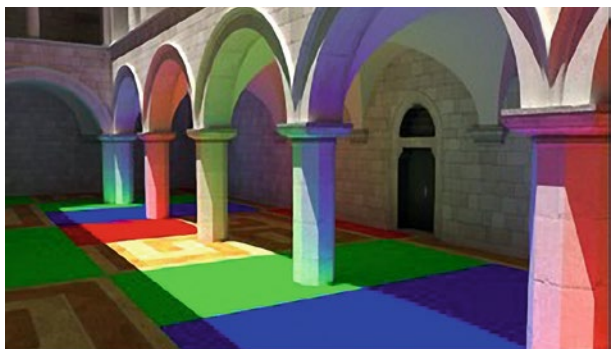

Fig. 10. An image obtained by path tracing (as a reference)

and with the classical radiosity algorithm (Fig. 5). We have carried out a comparison with the images obtained using the Light Propagation Volumes method of the Unreal Engine 4, the classical radiosity, and the ray tracing (reference). The proposed method shows a result comparable by accuracy with the classical radiosity. Based upon the images, it is closer to the reference than the Light Propagation Volumes method with the identical frame frequency (Figs. 7–10).

5. CONCLUSION

Unlike other widespread methods of solving the radiosity equation, the proposed method allows calculating the global lighting during $n^2+O(n)$ arithmetic operations and readings from the memory (where n is the number of scene sites) as it is reduced to the single multiplication of the matrix by the vector.

A similar result could be achieved solving a system of linear algebraic equations by means of LU expansion. However, an effective implementation of LU GPU expansion is nontrivial, and when using third-party libraries (for example, the CUBLAS), there is no possibility to use a compression. The latter, as noted above, is critical for the radiosity algorithms (Figs. 6, 7).

The work is supported by the grant 16–31–60048 mol_a_dk of the Russian Foundation for Basic Research.

REFERENCES

1. Keller A. Instant radiosity. Proc. 24th annual conf. on Computer graphics and interactive techniques (SIGGRAPH'97) // ACM Press/Addison-Wesley Publishing Co., New York, USA, 1997, pp. 49–56.

2. Budak V.P., Zheltov V.S., Kalakutsky T.K. Lokal'ny'e ocenki metoda Monte-Karlo v reshenii uravneniya global'nogo osveshheniya s uchyotom spektral'nogo predstavleniya ob''ektov [Local evaluations of Monte-Carlo method when solving equation of global illumination taking into account spectral object presentation] // Komp'yuterny'e issledovaniya i modelirovanie, 2012, V. 4, #1, pp. 75–84.

3. Dachsbacher C., Stamminger M. Reflective shadow maps. Proc. 2005 symp. on Interactive 3D graphics and games (I3D '05) // ACM, New York, USA, 2005, pp. 203–231.

4. Kaplanyan A., Dachsbacher C. Cascaded light propagation volumes for real time indirect illumination. Proc. 2010 ACM SIGGRAPH symp. on Interactive 3D Graphics and Games (I3D'10) // ACM, New York, USA, 2010, pp. 99–107.

5. Crassin C., Neyret F., Sainz M., Green S., Eiseman E. Interactive indirect illumination using voxel-based cone tracing: an insight. ACM SIGGRAPH 2011 Talks (SIGGRAPH '11) // ACM, New York, USA, 2011, Article 20, 1 p.

6. Lisle I.G., Tracy Huang S.-L. Algorithms for spherical harmonic lighting. Proc. 5th int. conf. on Computer graphics and interactive techniques in Australia and Southeast Asia (GRAPHITE '07) // ACM, New York, USA, 2007, pp. 235–238.

7. Goral C.M., Torrance K.E., Greenberg D.P., Battaile B. Modeling the interaction of light between diffuse surfaces. Proc. 11th annual conf. on Computer graphics and interactive techniques (SIGGRAPH'84) //SIGGRAPH, 1984, V. 18, #3, pp. 213–222.

8. Martin S., Einarsson P. A Real Time Radiosity Architecture for Video Games, SIGGRAPH, 2010. URL: http://www.geomerics.com/wpcontent/uploads/2014/03/radiosity_architecture.pdf.

9. Shcherbakov A., Frolov V. Avtomaticheskoe uproshhenie geometrii dlya raschyota vtorichnoj osveshhyonnosti metodom izluchatel'nosti [An automatic simplification of geometry for calculation of secondary illuminance by the radiosity method], Proceedings of the 26th International conference on computer graphics and sight, September 19–23, 2016, Nizhny Novgorod, pp. 34–38.

Alexander S. Shcherbakov, master student of the Faculty of Computational Mathematics and Cybernetics of the Lomonosov Moscow State University

Vladimir V. Frolov, Ph.D. Graduated from the Faculty of Computational Mathematics and Cybernetics of the Lomonosov Moscow State University. Research associate of the Lomonosov Moscow State University and of the Keldysch Institute of applied mathematics of the RAS

Light & Engineering
Vol. 27, No. 2, pp. 111–116, 2019 *https://doi.org/10.33383/2018-032*

THE ROLE OF THE SOLAR IRRADIATION PLATE FOR ESTIMATION OF THE INSOLATION REGIME OF URBAN TERRITORIES AND BUILDINGS

Adham Giyasov

National Research University of Civil Engineering, NRU MGSU, Moscow
E-mail: adham52@mail.ru

ABSTRACT

The article is devoted to the actual problems of modern urban planning – the development of an insolation (solar irradiation) plate and its wide application in the solution of town planning tasks for the summer warm period with the aim of creating a comfortable insolation, light and microclimatic environment in buildings and urban areas.

Keywords: insolation, insolation plate, illumination, solar radiation, buildings, buildings, microclimate, comfort of the environment

The purpose of the article is to develop the design of the insolation plate with the purpose of practical application for a qualitative and quantitative assessment of the insolation regime of premises and the territory of urban development for the summer warm period for different geographical latitudes.

Solar radiation has an extremely high biological and hygienic value, is a powerful health and preventive factor, having a positive psycho-physiological effect on a person. In this regard, regulatory documents determine the need to dose insolation of premises, territories and the human environment [1,2,3,4,5].

The effect of insolation on the life and activity of a person can be both positive (additional heating and lighting in cold weather, bactericidal action) and negative (overheating of the environment in the summer, uncomfortable lighting, glare, destroying effect of sunlight) [6,7].

Insolation causes a number of negative reactions on a person, in particular, causes the stress of a person's thermoregulatory apparatus, and leads to a weakening of local and systemic immune reactions, a violation of the cardiovascular system and exacerbation of herpetic infections.

In the summer months, with prolonged irradiation of buildings and the active surface of urban building, a superheating discomfort microclimate is formed indoors and in the building area, which determines the dosage of insolation and sun protection in the premises of residential, public buildings and urban areas [4].

In this regard, in the solution of town-planning tasks, in the process of developing a volume-planning structure of buildings, determining the height and orientation of buildings around the world, the size of the gaps between them, places for children's, economic and other sites, the requirements for the insolation environment must be taken into account, depending on the purpose of the buildings, territories and administrative area.

When developing a detailed design of micro-districts, urban areas, there is an intuitive approach for designing architectural and planning structures of construction, zoning of the territory of free micro-spaces, the formation of elements of landscaping, gardening and small architectural forms often occurs. For this reason, in the summer overheating period, the thermal discomfort of the human environment is created.

For the purpose of assessing the qualitative and quantitative indices of insolation of the summer

Table. Total Solar Irradiation, W/m^2

Orientation / hours	Horizontal plane	South	East	West
05	89	16	294	41
06	196	46	583	58
07	314	78	750	65
08	455	184	786	74
09	587	321	734	76
10	691	447	582	79
11	772	550	385	85
12	817	603	196	199
13	772	550	85	386
14	691	447	79	582
15	587	321	76	734
16	455	184	74	786
17	314	78	65	750
18	796	46	58	583
19	89	16	41	294
20	-	-	17	-

warm period, premises of buildings and territories with a complex space-spatial, architectural and planning solution, the design of an insolation plate is proposed. Insolation plate allows at the design stage to perform preliminary forecasting of the insolation regime and to identify architectural and construction and planning means for regulating the radiation and heat-wind conditions in urban micro-spaces.

Scientific developments in the issues of insolation of cities and buildings are widely conducted in our country and abroad. To this problem, such specialists as architects, hygienists, etc., show great interest, since insolation is the most important natural factor of urban development. A variety of graphs and plates have been developed to estimate the standard duration of insolation in accordance with the requirements for geographical areas [8–17].

The requirements for insolation and sun protection of building premises are carried out in accordance with the provisions of SanPiN and the Code of Rules. The boundaries of the zones in latitudes, the calculated days and the standard duration of insolation, sun protection of living quarters of the apartment, the territory of urban development are presented in the relevant regulatory documents [4,5,18–21].

Consideration of the role of the thermal effect of solar radiation as the determining factor of the overheating of the climatic environment is especially important in the architectural and structural design of buildings and urban micro-territories for the hot season. In connection with this SanPiN hygienic requirements for limiting the excessive thermal effect of insolation on the territory of residential development are defined.

At present, many methods for calculating the standard for the duration of insolation of rooms have been developed, for the insolation period, depending on the range of geographical latitudes established by SanPiN. They should be reduced to the following:

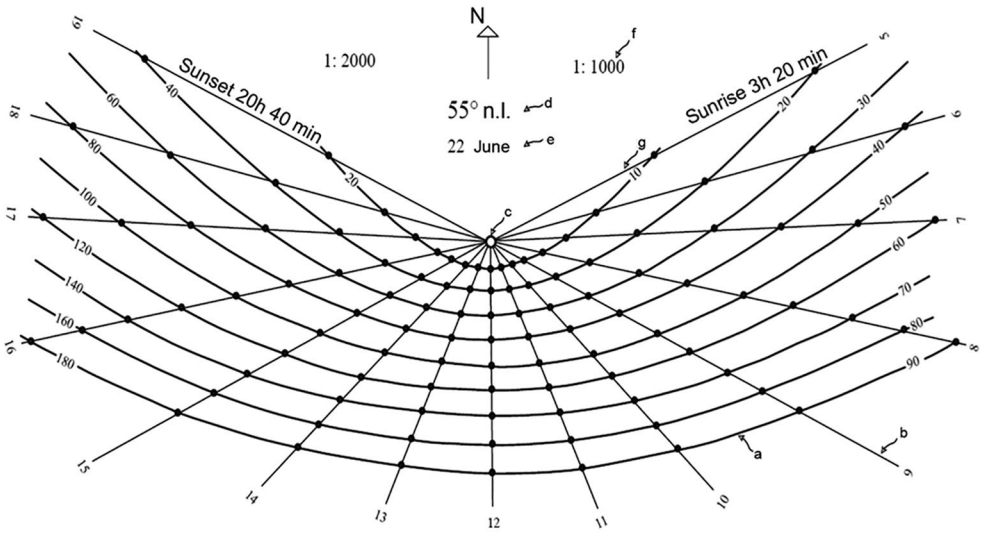

Fig. 1a. Insolation plate for the day's sun (main part)

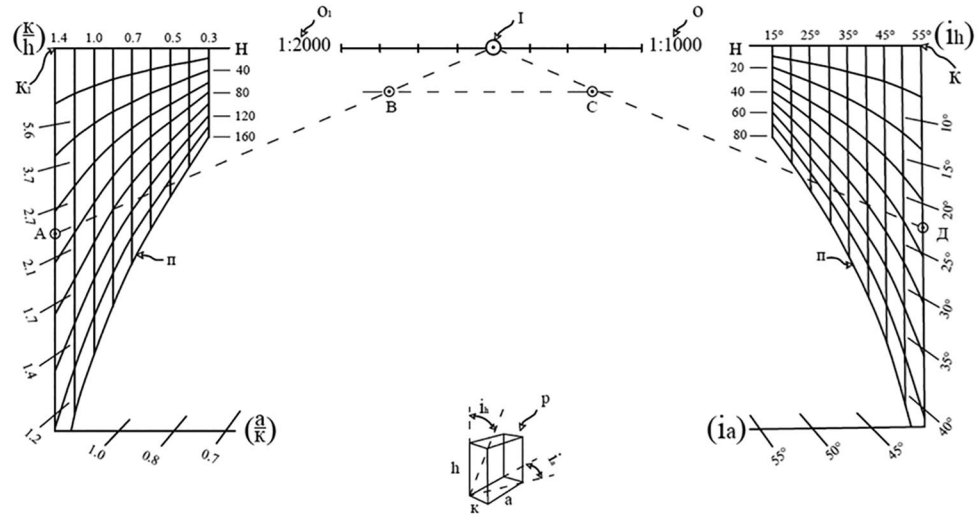

Fig.1b. Insolation plate (overlay part), insolation angle of the window

– A method of calculating insolation, which does not simulate the natural course of insolation on the building plan, and definition of qualitative and quantitative indicators is made by formulas and tables;

– A calculation method that does not simulate the natural course of insolation on the building plan, which gives insolation indices by means of charts, diagrams, graphs, and subsequent calculations by formulas and tables;

– A method of calculation, simulating the natural course of insolation in the building plan, which allows using instruments to determine the qualitative and quantitative indicators of the sun's energy, mainly for equal-floor buildings;

– Ways of calculation of insolation by computer programming, therefore, algorithms and computer programs that allow us to calculate only the qualitative characteristics of insolation have been developed.

Existing insolation plates, instruments and programs have a certain scope and are not universal for solving simultaneously a variety of architectural and spatial planning and voluminous spatial practical tasks in quantitative and qualitative estimation of insolation. Each of the instruments and techniques is acceptable at the boundary of the zones according to the geographical latitudes of the normalized period of the year, to predict the insolation regime in the relevant area of architectural and construction design, depending on the specific case of the spatial planning structure of urban buildings, such as the number of floors of buildings, the gap between them, orientation, zoning micro-territories, shading elements, landscaping and improvement.

It is also noted that the calculation of the qualitative and quantitative characteristics of insolation of

the warm period of the year in the above methods and instruments remained out of sight.

Along with the existing devices, the proposed practical application of the insolation plate allows to calculate both the qualitative and quantitative indices of insolation of the warm period of the year on the plotted layout of the multi-storey architectural and planning project at the design stage without complex graphic constructions.

The operating principle of the insolation device is determined by the laws of interaction of the visible movement of the sun in the sky and the position of the insolated object on the surface of the earth.

The insolation plate design kit for geographic latitudes is basing on solar geometry, i.e. the movement of the Sun in the sky in the summer warm months (Fig. 1a, b). The insolation plate was developed on the basis of astronomical tables, geographic data, reference nomograms and data of construction climatology SNiP and SP.

So, the insolation device of the plate type consists of two parts, the basic transparent fixed, characterizing the daylight course of the sun (Fig. 1a), and the overlay transparent moving around the central point, which determines the insolation angle of the window (Fig. 1b).

The main part of the device consists of a set of designs of individual transparent plates with an interval of 5° for the following latitudes 40°, 45°, 50°, 55°, 60° n.l., characterizing the daytime course of the sun (Fig. 1a). To the main part there is an overlay transparent part that takes into account the horizontal and vertical insolation angles of the window when calculating the qualitative and quantitative indices of indoor insolation (Fig. 1b).

Each insolation plate is acceptable in application for the geographical belt 5°, for example, a plate for 55° n.l. is used in the belt from 52°30[1] to 57°30[1]n.l.

The centred points **C** and **I** of the moving part of the plate are aligned with the inspected building object, made on a scale of 1: 1000 or 1: 2000.

Calculation of the duration of insolation of premises of buildings of different number of storeys, in hours, is made on the building plan by visual overlapping on the facade line of the building, fastened to the central points of both plates, coordinating the direction of the north sign of the insolation plate with the planning layout of the building. In this case, the quantitative characteristic of solar radiation of the insolation period, in W/m^2, using the data of the table attached to the main part of the plate is calculated.

Calculation of the duration of insolation of the territory of a multi-storey urban development is visually superimposed by the central point of the main part of the insolation plate to the point under study planning layout of the building, with the subsequent addition of the data of the table of arrival of solar radiation during the insolation period. The main part of the insolation device is to identify zones of active insolation of the territory of urban structures and to build an envelope of shadows from buildings of various-storey buildings, a shading area from greenery of various types in the hot extreme period of the year.

The design of the insolation plate is designed to assess the summer insolation regime of the facade and premises of buildings with different orientations, the presence and absence of a balcony, loggias, sun screens in a multi-height building, a building site with various means of sun protection and landscaping with large-scale plantings.

On the insolation plate, the insolation time is given by mean solar time.

Calculation of total solar radiation coming to the horizontal surface of the territory, roofs of buildings and vertical walls of buildings of different orientations for the insolation period is made according to the data of the table attached to the main part of the insolation plate.

In the design of an insolation plate, when calculating the quantitative and qualitative indices of the insolation of building premises, facade walls, building area, the intensity of total solar radiation, depending on the geographical latitude of the terrain, the time of the June day, the location and orientation of the surface, the height of the shading buildings, the state of the atmosphere and altitude above sea level are taken into account.

The data on the thermal solar radiation of the insolation period, determined from the table, are taken into account in the planning, building up of newly constructed and reconstructed micro-districts and cities, the orientation and arrangement of buildings, the shaping of buildings, the internal layout of buildings, the choice of dimensions, the type and arrangement of light barriers, the design of sunscreens, constructions for heat resistance, use of solar panels, landscaping, garderning, watering and sun protection of territories.

In the development and reconstruction of general plans for cities, settlements, as well as detailed planning projects and schemes for planning the organization of land and territories, the insolation plate allows to predict the qualitative and quantitative characteristics of the insolation regime of the urban area with the identification of zones and facades of buildings with active insolation, which allows us to estimate the comfort of the microclimate.

For practical purposes, at the stage of drawing up a detailed urban planning scheme aimed at improving the comfort of the microclimatic, light-climatic and bioclimatic environment, the insolation plate allows us to make practical design and research works according to the following scheme:

– An insolation chart is constructed for an urban building fragment plotted on a topographic base by means of an insolation plate, including an insolation graph with an isoline of 6, 8, 10, and 12 hours of insolation, and the intensity of arrival solar energy for these periods is calculated;

– An envelope of shadows is constructed with the identification of zones with the longest duration of insolation, shading and heating of the surface of the territory, insolation of facades and premises with the longest duration of insolation;

– A plot of shadows from large-scale tree plantations used to compile a dendrological plan is constructed, their location and density are determined taking into account the shading effect aimed at improving the microclimate;

– A purposeful functional zoning of the urban development area is carried out, depending on the insolation condition;

– When building planning, the orientation of buildings with the definition of gaps between them are correcting at the design stage.

The insolation plate has a wide application in the solution of town planning tasks for the summer warm period. Experts highlight the role of the insolation plate in calculating the duration of insolation of premises and the territory of buildings, the climate of buildings, assessing the energy efficiency of buildings, determining the thermal loads of the building's heat-and-cooling systems, calculating the heat resistance of the enclosing structures, assessing the microclimate of the premises, choosing effective protective measures to combat summer overheating in the premises and on the territories of building, the choice of the orientation of buildings and their window openings on the sides of the horizon, in solving problems in the field of light under different conditions of formation of interconnected zones of irradiation and shading in architectural planning and volumetric spatial formations of the city, in the design of solar protection systems and solar systems, as well as in the design and construction of ecological buildings and cities, planning, building, landscaping, gardering and watering of urban areas.

Summing up, it should be noted that the use of an insolation device of the plate type allows solving a number of scientific and practical town planning tasks by calculating and assessing the quantitative and qualitative characteristics of the insolation regime aimed at improving the ecological environment of urban buildings and buildings in the warm period of the year.

For the purpose of a wide application of the insolation plate, methodical instructions for describing the device, the principle of operation and application of the insolation plate in design practice have been compiled. The application of the insolation plate in practice was tested during the development of the general plan of the city of Buka in Uzbekistan and the reconstruction of the city of Dushanbe in Tajikistan, as well as in the preparation of graduation master's works.

REFERENCES

1. Humaner P.I. The Study of thermoregulation in hygiene and physiology of labour. M.: Medgiz, 1962, 231p.

2. Gubernskiy Yu. D., Litskevich V.K. Human Dwelling, M.: Stroyizdat, 1991, 227p.

3. Banhidi L. (translated from Hungarian) Thermal microclimate of premises (calculation of comfort parameters by human heat sensations), M: Stroyizdat, 1981, 247p.

4. Sanitary Rules: SanPiN. 2.2.1/2.1.1.1076–01: Hygienic requirements for insolation and sun protection of residential and public buildings and areas.

5. System of urban planning rules: SP 42.13330.2011. Planning and construction of urban and rural settlements (Updated version of SNiP 2.07.01–89*), Russian Ministry of Regional Development, 2010.

6. Eizenstat B.A., Lukina L.P. Bio-climate and microclimate of Tashkent. L.: Hydrometeoizdat, 1982, 128 p.

7. Markus T.A., Morris E.N. Buildings, climate and energy (translated from English), L: Hydrometeoizdat, 1985, 542 p.

8. Dunaev B.A. Insolation of the dwelling, M.: Stroyizdat, 1979, 102 p.

9. Dashkevich L.L. Methods of calculation of insolation in the design of industrial buildings, M: Gosstroiizdat, 1963, 526 p.

10. Maslennikov D.S. Basics and methods of calculation of the conditions of insolation in mass dwelling construction. The author's thesis of dissertation for Ph.D. M.: 1968, 28 p.

11. Obolensky N.B. Architecture and Sun, M.: Stroyizdat, 1988, 207 p.

13. Twarowski M. The Sun in Architecture (translated from Polish). M.: Stroyizdat, 1977, 288 p.

14. Architectural Physics: Textbook for universities: Special. "Architecture", by Litskevich V.K., L. I., Makarenko, I.V. Migalina, etc.; Under the editorship of N.V. Obolensky, M.: "Architecture-C", 2007, 448 p.

15. Olgyay V, Olgyay A. Solar Control and Shading Devices, Princeton University Press, New Jersey, 1957, 236 p.

16. Grimmond C.S.B. Progress in Measuring and Observing the Urban Atmosphere // Theoretical and Applied Climatology, 2006, Vol. 84, № .1–3, pp. 3–22.

17. Cocchia, A. Smart and Digital City: A Systematic Literature Review. R.P. Dameri and C. Rosenthal-Sabroux (eds.), Smart City, Progress in IS, Springer International Publishing Switzerland, 2014, pp.13–43.

18. SanPiN2.1.2.2645–10 " Sanitary and epidemiological requirements for living conditions in residential buildings and premises."

19. SP 54.13330.2011 Residential apartment Buildings.

20. SP 160.1325800.2014 Buildings and complexes multifunctional. Design rules.

21. SP 118.13330.2012* Public buildings and structures.

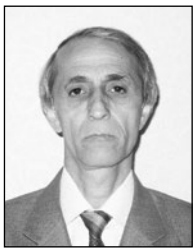

Adham Giyasov,

Prof. Dr. of Technical Sciences, graduated from the Tajik Polytechnic Institute in 1975. At present, he is engaged in scientific and pedagogical activities and works as a Professor of the Department of Design of Buildings and Structures at the University of Civil Engineering (NRU MGSU). His research interests are energy efficient buildings, architectural and construction physics, insolation, aerodynamics, urban ecology. More than 200 scientific, practical and methodical works have been prepared and published, and more than 10 textbooks for university students have been published

CONTENTS

VOLUME 27 **NUMBER 3** **2019**

LIGHT & ENGINEERING
(SVETOTEKHNIKA)